Linking glucocorticoid action and hypoxia: a novel mechanism driving an adverse metabolic phenotype?

by

Jonathan Mark Hazlehurst (The Queens'College)

A thesis submitted to The University of Oxford for the degree of

DOCTOR OF PHILOSOPHY

Oxford Centre for Diabetes, Endocrinology and Metabolism

Division of Medical Sciences

The University of Oxford, November 2018

Linking glucocorticoid action and hypoxia: a novel mechanism driving an adverse metabolic phenotype? Jonathan Hazlehurst, The Queen's College. DPhil MT 2018

Abstract.

Obstructive sleep apnoea (OSA) is characterised by repeated cycles of reduced and complete obstruction of air flow occurring in sleep. This can result in decreased oxygen levels (hypoxia). OSA and states of glucocorticoid excess are both associated with metabolic diseases including fatty liver disease. Whether increased glucocorticoids are a feature of OSA and may contribute to the increased metabolic risk seen in OSA is unknown.

In vitro, patient and healthy volunteer studies were employed to assess adipose response to hypoxia. Further metabolic effects of acute and chronic intermittent hypoxia (AIH and CIH) were examined in healthy volunteers and rodents respectively. The AIH study incorporated glucocorticoid receptor (GR) blockade. The patient study also examined the effect of OSA on glucocorticoid availability.

Adipocytes were sensitive to extreme hypoxia *in vitro* although this was not seen in adipose biopsies from patients with OSA or in assessment of adipose function in AIH. AIH in man and CIH in rodents resulted in increased *de novo lipogenesis* (DNL). Sham CPAP was associated with increased urinary glucocorticoids. GR blockade limited adipose tissue fatty acid mobilisation but did not affect the metabolic impact of AIH on DNL.

Intermittent hypoxia drives DNL. OSA is associated with increased glucocorticoids. Despite this GR blockade was not protective against the effects of intermittent hypoxia in this model and is unlikely to be a useful therapeutic target therefore in patients with OSA.

Acknowledgements

My supervisors have combined rigorous academic support with encouragement and support and demonstrate that it is possible to be a top academic and a caring mentor and I hope to take this forward in my own career. Thanks Jeremy and Leanne. Without Dr Laura Gathercole, Dr Nikolaous Nikolao, Dr Shelley Harris, Dr Marijana Todorcevic, Dr Ahmad Moolla, Dr Nathan Denton, Sandy and the OCDEM "runners" my DPhil and experience would have undoubtedly suffered. Diana Mantripp and the other OCDEM nurses were a constant source of encouragement and support and kept us all going across many a "clamp" with a kindness and attention to detail that is pivotal to well conducted human research. Catriona Charlton and Thomas Caunfield kept me and the GC and GC/MS going when we inevitably broke. When my father died suddenly with 3 months to go in the lab without them and Leanne and Jeremy I don't think I could have feasibly continued. The importance of their help and the kindness of the wider group in supporting me to complete this DPhil cannot be overestimated.

I should of course acknowledge the M40 who made much of this possible but who neither me nor my car (or its third clutch) miss.

This thesis is dedicated to the memory of my father Brian Hazlehurst who I miss very much. I am indebted to the support of the above people who started as colleagues but finished as friends plus the love of my family including my brilliant wife Jess and incredible son Toby.

Table of Contents

Abstract ..... **I**

Table of Contents ..... **III**

Table of Figures ..... **XI**

Table of Tables ..... **XVIII**

1. General Introduction **1**

1.1 Introduction **2**

1.2 An introduction to obstructive sleep apnoea (OSA) **2**

1.2.1 OSA: physiology 2

1.2.2 OSA: diagnosis and prevalence 4

1.2.3 OSA: the consequences of undiagnosed disease and current treatment 5

1.2.4 OSA: dyslipidaemia and glycaemic control 6

1.2.5 OSA: cardiovascular disease and mortality 8

1.3 The effects of OSA and hypoxia on key metabolic tissues **10**

1.3.1 The metabolic effect of hypoxia on adipose tissue *in vitro* 10

1.3.2 The metabolic effect of hypoxia on adipose tissue *in vivo* 13

1.3.3 The metabolic effect of hypoxia on hepatocytes *in vitro* 15

1.4 Mechanistic data from rodent studies linking OSA and metabolic disease 17

1.4.1 Insights from chronic intermittent hypoxia rodent studies: oxidative stress, glycaemic control and hepatic lipid handling 17

1.4.2. Insights from knock out rodent studies 22

1.4.3 Obstructive sleep apnoea and NAFLD.....26

1.5 Obstructive sleep apnoea and steroids..... 29

1.5.1 OSA and Aldosterone.....30

1.5.2 OSA and Testosterone.....33

1.5.3 OSA and the HPA axis.....35

1.5.4 Hypoxia and glucocorticoids.....39

1.5.5 The metabolic benefit from interruption in glucocorticoid signalling 40

1.6 Summary, hypotheses and aims 41

1.6.1 OSA and intermittent hypoxia have a direct effect on adrenal steroidogenesis.....42

1.6.2 The action of OSA and intermittent hypoxia is mediated via effects on adipose tissue.....42

1.6.3 OSA and intermittent hypoxia drive hepatic lipid accumulation.....43

1.6.4 Glucocorticoid receptor antagonism is metabolically beneficial and can protect against the metabolic effects of intermittent hypoxia 43

2. General Methods 44

2.1 RNA extraction and cDNA synthesis 45

2.2 Gene expression..... 47

2.3 Western blotting..... 47

2.4 Plasma analysis 48

2.5 Radioimmunoassay Insulin..... 48

2.6 Biochemical sample analysis..... 49

2.7 VLDL fraction isolation 49

2.8 Solid phase extraction of plasma and VLDL fraction samples. 49

2.9 Calculation of Ra NEFA and Rd NEFA 53

2.10 Deuterium plasma water analysis by Gas Bench and calculation of *de novo lipogenesis* 54

2.11 Glucose disposal and production..... 55

2.12 Isotopic enrichment of CO_2 in breath 58

2.13 Microdialysis 59

3. Adrenal steroidogenesis and adipose tissue responsiveness to OSA 61

3.1 Introduction..... 62

3.2 Materials and Methods..... 65

3.2.1 Research strategy.....65

3.2.2 Statement of contributions 65

3.2.3 Study design 66

3.2.4 Inclusion and Exclusion criteria 66

3.2.5 Urinary steroid profiling (GC/MS) 69

3.2.6 Plasma aldosterone and plasma cortisol 70

3.2.7 Statistical analysis of urinary steroid and plasma 71

3.2.8 Adipose tissue biopsy 71

3.2.9 Fluidigm 76

3.3 Results 86

3.3.1 The demographics and clinical characteristics of the patient cohort studied 86

3.3.2 The effect of CPAP withdrawal on the urinary steroid profile 91

3.3.3a Androgen metabolites 107

3.3.3b Cortisol metabolites 107

3.3.3c Mineralocorticoid metabolites 107

3.3.4 The effect of CPAP withdrawal on the plasma steroid profile 108

3.4 Discussion 114

4. Adipocytes are sensitive to hypoxic exposure 120

4.1 Introduction 121

4.2 Materials and Methods 122

4.2.1 Research strategy 122

4.2.2 Primary adipocyte tissue culture and hypoxic exposure 122

4.3 Results 124

4.3.1 Adipocyte sensitivity to hypoxia 124

4.4 Discussion 127

5. Glucocorticoid receptor antagonism offers metabolic benefit in man 131

5.1 Introduction 132

5.2 Materials and Methods 133

5.2.1 Research strategy 133

5.2.2 Statement of contributions 134

5.3 Results 137

5.3.1 Patient demographics 137

5.3.2 Safety and tolerability 138

5.3.3 Lipid metabolism 141

5.3.4 Insulin resistance 143

5.4 Discussion 144

6a. The metabolic effects of intermittent hypoxia in man 148

6a.1 Introduction 149

6a.2 Materials and Methods 150

6a.2.1 Research strategy 150

6a.2.2 Clinical Protocol 151

6a.2.3 ACTH and Cortisol ELISA 153

6a.2.4 Intermittent hypoxia protocol 154

6a.2.5 Statistical analyses 154

6a.3 Results 155

6a.3.1 Acute intermittent hypoxia 155

6a.3.2 Insulin resistance 155

6a.3.3 Fatty acid production and disposal 156

6a.3.4 Fatty acid mobilisation 157

6a.3.5 Fatty acid oxidation 158

6a.3.6 Fatty acid incorporation into VLDL TAG.....159

6a.3.7 De novo lipogenesis 160

6a.3.8 Cortisol and ACTH.....161

6a.4 Discussion 162

6b. Glucocorticoid receptor antagonism fails to protect against the metabolic effect of intermittent hypoxia 165

6b.1 Introduction 166

6b.2 Materials and Methods 167

6b.2.1 Research strategy.....167

6b.2.2 Statistical analysis 167

6b.3 Results 167

6b.3.1 Acute intermittent hypoxia 167

6b.3.2 Insulin resistance 168

6b.3.3 Lipid metabolism 169

6b.3.4 Hepatic de novo lipogenesis 171

6b.4 Discussion 172

7. Chronic intermittent hypoxia model in rats 174

7.1. Introduction 175

7.2. Materials and Methods 176

7.2.1 Research strategy 176

7.2.2 Statement of contributions 177

7.2.3 Protocol 177

7.2.4 Tissue weights and venous blood glucose 179

7.2.5 Liver histology 179

7.2.6 Liver gene expression 180

7.2.7 Measurement of liver TAG 181

7.2.8 Measurement of liver and plasma DNL 181

7.2.9 Measurement of liver 11βHSD1 activity 182

7.2.10 Statistical Analysis 182

7.3 Results 183

7.3.1 Tissue weights and animal behavioural monitoring.....183

7.3.2 Venous glucose 185

7.3.3 Liver histology 186

7.3.4 Liver gene expression.....187

7.3.5 Liver triacylglycerol.....189

7.3.6 Liver and plasma assessment of *de novo lipogenesis* 190

7.3.7 Liver 11βHSD1 expression and activity 191

7.4 Discussion 191

8. Final conclusions and future directions.....195

8.1 Final conclusions 196

8.1.1 Adipose tissue plays a comparatively minor role in the metabolic response to hypoxia and OSA 196

8.1.2 Intermittent hypoxia increases hepatic *de novo lipogenesis* 197

8.1.3 OSA is associated with changes in steroid levels though the functional consequences of this are not clear.....198

8.2 Future thoughts..... 199

9. References 201

Table of Figures

FIGURE 1-1 THE NON-ANATOMICAL CAUSES OF OSA. THIS FIGURE IS ADAPTED FROM THE EXCELLENT REVIEW BY ECKERT (3). 4

FIGURE 1-2 THE POTENTIAL MECHANISMS BY WHICH HYPOXIA COULD DRIVE HEPATIC LIPID ACCUMULATION IN PATIENTS WITH OSA. (FFA=FREE FATTY ACIDS; TAG=TRIACYLGLYCEROL; DNL=DE NOVO LIPOGENESIS). 26

FIGURE 1-3 STEROID METABOLITES MEASURED FROM URINE USING GAS CHROMATOGRAPHY MASS SPECTROMETRY. (THE STEROID IN BLACK ARE THE TRADITIONAL NAMES AND ARE FOUND WITHIN THE PLASMA, THE RED ANNOTATIONS ARE THE METABOLITES MEASURED WITHIN THE URINE) THIS FIGURE WAS GENERATED BY A COLLABORATOR DR ANGELA TAYLOR AT THE UNIVERSITY OF BIRMINGHAM 30

FIGURE 1-4 THE EFFECT OF GLUCOCORTICOIDS MODULATING LIPID METABOLISM IN THE LIVER AND ADIPOSE TISSUE IN THE FASTING AND FED STATE. (GCS=GLUCOCORTICOIDS; ⇧=INCREASED; ⇩=DECREASED; # = RODENT AND CELL LINE DATA; *= HUMAN DATA (ALL REFERENCES INCLUDED IN ABOVE TEXT). 37

FIGURE 3- 1 THE EXPERIMENTAL SET UP AND ASSESSMENT SCHEDULE FOR THE CPAP WITHDRAWAL STUDY. (OSA= OBSTRUCTIVE SLEEP APNOEA; CPAP=CONTINUOUS POSITIVE AIRWAY PRESSURE) 69

FIGURE 3- 2 THE STANDARD CURVES OF THE ALDOSTERONE AND CORTISOL ELISAS. 71

FIGURE 4- 1 THE EFFECT OF HYPOXIA ON ADIPOSE GENE EXPRESSION OF GENES KNOWN TO BE OXYGEN SENSITIVE. DATA IS PRESENTED AS ARBITRARY UNITS (AU) (MEAN ± SE). 125

FIGURE 4- 2 THE EFFECT OF HYPOXIA ON ADIPOSE PROTEIN EXPRESSION OF HIF1A PROTEIN IN RESPONSE TO DIFFERENT OXYGEN TENSIONS (0.1, 1, 5 AND 21%). DATA SHOWN FOR ADIPOCYTES FROM TWO DIFFERENT PRIMARY ADIPOSE SOURCES. 126

FIGURE 4- 3 THE EFFECT OF HYPOXIA ON ADIPOSE GENE EXPRESSION OF GENES KNOWN TO BE GLUCOCORTICOID SENSITIVE. DATA IS PRESENTED AS ARBITRARY UNITS (AU) (MEAN ± SE). 127

FIGURE 5- 1 THE TIMELINE AND WORK FLOW OF THE GR ANTAGONISM STUDY.....135

FIGURE 5- 2 THE PLASMA ACTH AND CORTISOL OF PATIENTS RANDOMISED TO EITHER NO TREATMENT OR RU486 600MG OD FOR 7 DAYS. (ACTH=ADRENOCORTICOTROPHIN; ***P<0.001). DATA PRESENTED AS MEAN±SD. PRE REFERS TO PRE-RANDOMISATION TO EITHER NO TREATMENT OR RU486 AND POST REFERS TO AFTER 1 WEEK OF EITHER NO TREATMENT OR RU486. 139

FIGURE 5- 3 SAFETY MONITORING BLOODS OF PATIENTS RANDOMISED TO EITHER NO TREATMENT OF RU486 600MG OD FOR 7 DAYS (ALT: ALANINE AMINOTRANSFERASE; AST: ASPARTATE TRANSAMINASE; *P<0.05, ***P<0.001). DATA PRESENTED AS MEAN±SD. PRE REFERS TO PRE-RANDOMISATION TO EITHER NO TREATMENT OR RU486 AND POST REFERS TO AFTER 1 WEEK OF EITHER NO TREATMENT OR RU486.....140

FIGURE 5- 4 THE EFFECT OF RU486 ON CHOLESTEROL AND HDL CHOLESTEROL. (*P<0.05). DATA PRESENTED AS MEAN±SD. PRE REFERS TO PRE-RANDOMISATION TO EITHER NO TREATMENT OR RU486 AND POST REFERS TO AFTER 1 WEEK OF EITHER NO TREATMENT OR RU486. 141

FIGURE 5- 5 THE EFFECT OF RU486 ON TRIACYLGLYCEROL (TAG) AND VERY LOW DENSITY LIPOPROTEIN (VLDL) TAG AND DE NOVO LIPOGENESIS WITHIN THE PLASMA TAG AND VLDL TAG FRACTION (*P<0.05). DATA PRESENTED AS MEAN±SD. PRE REFERS TO PRE-RANDOMISATION TO EITHER NO TREATMENT OR RU486 AND POST REFERS TO AFTER 1 WEEK OF EITHER NO TREATMENT OR RU486.....142

FIGURE 5- 6 THE EFFECT OF RU486 ON MEASURES OF LIPOLYSIS AND ADIPOSE INSULIN RESISTANCE (ADIPO-IR). AS WELL AS FATTY ACID OXIDATION MEASURED BY OHB (NEFA=NON-ESTERIFIED FATTY ACIDS; OHB=B-HYDROXYBUTYRATE; *P<0.05; **P<0.01). DATA IS PRESENTED AS MEAN±SD. PRE REFERS TO PRE-RANDOMISATION TO EITHER NO TREATMENT OR RU486 AND POST REFERS TO AFTER 1 WEEK OF EITHER NO TREATMENT OR RU486. 143

FIGURE 5- 7 THE EFFECT OF RU486 ON FASTING PLASMA GLUCOSE, INSULIN, ADIPOSE-INSULIN RESISTANCE (ADIPO-IR) AND HOMA2 (HOMEOSTATIC MODEL OF ASSESSMENT OF INSULIN SENSITIVITY 2). (*P<0.05, **P<0.01). DATA PRESENTED AS MEAN±SD. PRE REFERS TO PRE-RANDOMISATION TO EITHER NO TREATMENT OR RU486 AND POST REFERS TO AFTER 1 WEEK OF EITHER NO TREATMENT OR RU486. 144

FIGURE 6A-1 SCHEMATIC OVERVIEW OF THE INTERMITTENT HYPOXIA STUDY. (DNL=DE NOVO LIPOGENESIS; TAG=TRIACYLGLYCEROL; IH=INTERMITTENT HYPOXIA). 153

FIGURE 6A-2 A TRACE SHOWING THE INTERMITTENT DESATURATIONS ACHIEVED USING THE INTERMITTENT HYPOXIA PROTOCOL. THE TIME SHOWN IS AN HOUR INTERVAL. 154

FIGURE 6A-3 THE EFFECT OF INTERMITTENT HYPOXIA ON MEASURE OF INSULIN SENSITIVITY ASSESSED ACROSS A HYPERINSULINAEMIC-EUGLYCAEMIC CLAMP. A. M-VALUE RELATES TO THE RATE OF GLUCOSE INFUSION REQUIRED TO MAINTAIN EUGLYCAEMIA IN HYPERINSULINAEMIC CONDITIONS. B. M/I SHOWS THE M-VALUE ADJUSTED FOR MEASURED PLASMA INSULIN. C. GLUCOSE PRODUCTION WAS QUANTIFIED USING THE APPEARANCE OF ISOTOPICALLY LABELLED GLUCOSE ([^{2}H]-GLUCOSE) MEASURED PRIOR TO INSULIN INFUSION. D. GLUCOSE DISPOSAL WAS QUANTIFIED ISOTOPICALLY FOLLOWING THE INFUSION OF INSULIN AT THE COMPLETION OF THE HYPERINSULINAEMIC-EUGLYCAEMIC CLAMP. DATA IS PRESENTED AS MEAN±SD. 156

FIGURE 6A-4 THE EFFECT OF INTERMITTENT HYPOXIA ON NEFA APPEARANCE AND DISPOSAL. THIS WAS QUANTIFIED BY MEASURING THE APPEARANCE AND DISPOSAL OF

ISOTOPICALLY LABELLED PALMITATE ([U^{13}C]-PALMITATE) WITHIN THE NEFA TOTAL PALMITATE ISOLATED FROM THE PLASMA FRACTION MEASURED USING GAS CHROMATOGRAPHY MASS SPECTROMETRY. DATA DISPLAYED INCLUDES THE TIME PERIODS OF THE HYPERINSULINAEMIC-EUGLYCAEMIC CLAMP IMMEDIATELY PRIOR TO INSULIN INFUSION (LABELLED PRE-INSULIN) AND IMMEDIATELY PRIOR TO THE CESSATION OF INSULIN INFUSION (LABELLED POST-INSULIN). (NEFA=NON-ESTERIFIED FATTY ACIDS; AUC=AREA UNDER THE CURVE; OPEN BARS=AIR; CLOSED BARS=INTERMITTENT HYPOXIA. P<0.05*). DATA IS PRESENTED AS MEAN±SD. 157

FIGURE 6A-5 THE EFFECT OF INTERMITTENT HYPOXIA ON LIPOLYSIS EXPRESSED AS PLASMA NEFA (A), GLYCEROL (B) AND SUBCUTANEOUS ABDOMINAL ADIPOSE INTERSTITIAL FLUID GLYCEROL (C). DATA DISPLAYED INCLUDES THE TIME PERIODS OF THE HYPERINSULINAEMIC-EUGLYCAEMIC CLAMP IMMEDIATELY PRIOR TO INSULIN INFUSION (LABELLED PRE-INSULIN) AND IMMEDIATELY PRIOR TO THE CESSATION OF INSULIN INFUSION (LABELLED POST-INSULIN) (NEFA=NON-ESTERIFIED FATTY ACIDS; AUC=AREA UNDER THE CURVE; OPEN BARS=AIR; CLOSED BARS=INTERMITTENT HYPOXIA. P<0.05*). DATA IS PRESENTED AS MEAN±SD. 158

FIGURE 6A-6 THE EFFECT OF INTERMITTENT HYPOXIA ON FATTY ACID OXIDATION MEASURED AS THE INCORPORATION OF ^{13}C, FROM ^{13}C-PALMITATE INTO CO_2 AND THE PLASMA CONCENTRATION OF B-HYDROXYBUTYRATE. DATA DISPLAYED INCLUDES THE TIME PERIODS OF THE HYPERINSULINAEMIC-EUGLYCAEMIC CLAMP IMMEDIATELY PRIOR TO INSULIN INFUSION (LABELLED PRE-INSULIN) AND IMMEDIATELY PRIOR TO THE CESSATION OF INSULIN INFUSION (LABELLED POST-INSULIN). (NEFA=NON-ESTERIFIED FATTY ACIDS; AUC=AREA UNDER THE CURVE; OHB= B-HYDROXYBUTYRATE; OPEN BARS=AIR; CLOSED BARS=INTERMITTENT HYPOXIA. P<0.05*). DATA IS PRESENTED AS MEAN±SD. 159

FIGURE 6A-7 THE ESTERIFICATION OF ^{13}C-PALMITATE INTO VLDL TAG. THIS WAS MEASURED VIA QUANTIFICATION OF THE INCORPORATION OF [U^{13}C]-PALMITATE INTO THE TOTAL PALMITATE ISOLATED FROM THE VLDL TAG FRACTION USING GAS CHROMATROGRAPHY

MASS SPECTROMETRY. DATA DISPLAYED INCLUDES THE TIME PERIODS OF THE HYPERINSULINAEMIC-EUGLYCAEMIC CLAMP IMMEDIATELY PRIOR TO INSULIN INFUSION (LABELLED PRE-INSULIN) AND IMMEDIATELY PRIOR TO THE CESSATION OF INSULIN INFUSION (LABELLED POST-INSULIN) (AUC=AREA UNDER THE CURVE; VLDL=VERY LOW DENSITY LIPOPROTEIN; TAG=TRIACYLGLYCEROL; OPEN BARS=AIR; CLOSED BARS=INTERMITTENT HYPOXIA. P<0.05*). DATA IS PRESENTED AS MEAN±SD. 160

FIGURE 6A-8 THE EFFECT OF INTERMITTENT HYPOXIA ON PLASMA TAG, VLDL TAG AND DNL MEASURED IN THE PLASMA AND VLDL TAG FRACTIONS. (A) TAG WAS MEASURED WITHIN THE PLASMA AND (B) ISOLATED VLDL FRACTIONS. SIMILARLY, DNL WAS MEASURED IN THE PLASMA TAG (C) AND VLDL TAG FRACTIONS (D). DNL WAS MEASURED VIA QUANTIFICATION OF DEUTERATED WATER INTO THE ISOLATED PALMITATE TAG FRACTION EITHER FROM WHOLE PLASMA (C) OR THE LIVER SPECIFIC VLDL FRACTION (D). (AUC=AREA UNDER THE CURVE; VLDL=VERY LOW-DENSITY LIPOPROTEIN; TAG=TRIACYLGLYCEROL; DNL=*DE NOVO LIPOGENESIS*; OPEN BARS=AIR; CLOSED BARS=INTERMITTENT HYPOXIA. P<0.05*, P<0.001**). DATA IS PRESENTED AS MEAN±SD.161

FIGURE 6A-9 THE EFFECT OF INTERMITTENT HYPOXIA ON PLASMA ACTH AND CORTISOL (ACTH=ADRENOCORTICOTROPIC HORMONE; OPEN BARS=AIR; CLOSED BARS=INTERMITTENT HYPOXIA). ACTH AND CORTISOL WERE MEASURED USING COMMERCIALLY AVAILABLE ELISA AT THE BEGINNING OF THE STUDY PROTOCOL T=0, PRIOR TO THE INSULIN INFUSION T=240 MINUTES AND AT THE END OF THE INSULIN INFUSION T=360 MINUTES. DATA IS PRESENTED AS MEAN±SD. 162

FIGURE 6B- 1 THE EFFECT OF INTERMITTENT HYPOXIA AND INTERMITTENT HYPOXIA AND RU486 ON MEASURES OF INSULIN SENSITIVITY MEASURED ACROSS A HYPERINSULINAEMIC-EUGLYCAEMIC CLAMP. A. M-VALUE RELATES TO THE RATE OF GLUCOSE INFUSION REQUIRED TO MAINTAIN EUGLYCAEMIA IN HYPERINSULINAEMIC CONDITIONS. B. M/I SHOWS THE M-VALUE ADJUSTED FOR MEASURED PLASMA INSULIN. C. GLUCOSE PRODUCTION WAS QUANTIFIED USING THE APPEARANCE OF ISOTOPICALLY

LABELLED GLUCOSE ([^{2}H]-GLUCOSE) MEASURED PRIOR TO INSULIN INFUSION. D. GLUCOSE DISPOSAL WAS QUANTIFIED ISOTOPICALLY FOLLOWING THE INFUSION OF INSULIN AT THE COMPLETION OF THE HYPERINSULINAEMIC-EUGLYCAEMIC CLAMP.....168

FIGURE 6B- 2 THE EFFECT OF INTERMITTENT HYPOXIA AND RU486 COMPARED TO THE EFFECT OF INTERMITTENT HYPOXIA ALONE ON TAG, VLDL TAG AND DNL MEASURED IN THE PLASMA AND VLDL TAG FRACTIONS. (A) TAG WAS MEASURED WITHIN THE PLASMA AND (B) ISOLATED VLDL FRACTIONS. SIMILARLY, DNL WAS MEASURED IN THE PLASMA TAG (C) AND VLDL FRACTIONS TAG (D). DNL WAS MEASURED VIA QUANTIFICATION OF DEUTERATED WATER INTO THE ISOLATED PALMITATE TAG FRACTION EITHER FROM WHOLE PLASMA (C) OR THE LIVER SPECIFIC VLDL FRACTION (D). (AUC=AREA UNDER THE CURVE; VLDL=VERY LOW-DENSITY LIPOPROTEIN; TAG=TRIACYLGLYCEROL; DNL=*DE NOVO LIPOGENESIS*; OPEN BARS=INTERMITTENT HYPOXIA; CLOSED BARS=INTERMITTENT HYPOXIA AND RU486.) DATA IS PRESENTED AS MEAN±SD. 171

FIGURE 7- 1THE EXPERIMENTAL DESIGN OF THE RODENT CHRONIC INTERMITTENT HYPOXIA (CIH) EXPOSURE. 179

FIGURE 7- 2 BODY WEIGHTS AND TISSUE WEIGHTS FROM ADULT MALE WISTAR RATS EXPOSED TO ROOM AIR (N=8) OR CHRONIC INTERMITTENT HYPOXIA (IH) (N=8).....184

FIGURE 7- 3 BODY WEIGHTS AND TISSUE WEIGHTS FROM ADULT MALE WISTAR RATS EXPOSED TO ROOM AIR (N=8) OR CHRONIC INTERMITTENT HYPOXIA (IH) (N=8).....185

FIGURE 7- 4 THE FASTING VENOUS GLUCOSE AT COMPLETION OF PROTOCOL. IH=INTERMITTENT HYPOXIA.....186

FIGURE 7- 5 NO HISTOLOGICAL CHANGES WERE OBSERVED BETWEEN LIVERS SECTION FROM CONTROL (A 4X MAGNIFICATION; C 20X MAGNIFICATION) AND INTERMITTENT HYPOXIA EXPOSED RATS (B 4X MAGNIFICATION; D 20X MAGNIFICATION). 187

FIGURE 7- 6 LIVER MRNA EXPRESSION OF GENES KNOWN TO BE OXYGEN SENSITIVE (N=8 CONTROLS; N=7 INTERMITTENT HYPOXIA). DATA IS EXPRESSED AS MEAN±SD. (*P<0.05) 188

FIGURE 7- 7 LIVER MRNA EXPRESSION OF KEY GENES OF LIVER LIPID METABOLISM. (N=8 CONTROLS; N=7 INTERMITTENT HYPOXIA). DATA IS EXPRESSED AS MEAN±SD. (*P<0.05) 189

FIGURE 7- 8 LIVER TAG CONTENT NORMALISED TO MG OF TISSUE. TAG=TRIACYLGLYCEROL. (N=8 CONTROLS; N=7 INTERMITTENT HYPOXIA) 190

FIGURE 7- 9LIVER AND PLASMA ASSESSMENT OF DE NOVO LIPOGENESIS. DNL WAS MEASURED BY THE RATIO OF PALMITATE LABELLED WITH DEUTERATED WATER TO UNLABELLED PALMITATE WITHIN THE LIVER TISSUE (A) AND WITHIN PLASMA TOTAL LIPID FRACTION (B). THIS WAS MEASURED USING GAS CHROMATOGRAPHY MASS SPECTROMETRY (DNL=DE NOVO LIPOGENESIS; 271/270 IS THE INCORPORATION OF DEUTERATED WATER IN TRIACYLGLYCEROL. (N=8 CONTROLS; N=7 INTERMITTENT HYPOXIA)) DATA IS EXPRESSED AS MEAN±SD. 190

FIGURE 7- 10 LIVER MRNA EXPRESSION AND EXPLANT ACTIVITY OF 11B-HYDROXYSTEROID DEHYDROGENASE (11B-HSD1). (N=8 CONTROLS; N=7 INTERMITTENT HYPOXIA). DATA IS EXPRESSED AS MEAN±SD. (*P<0.05) 191

Table of Tables

TABLE 2-1 THE DILUTIONS REQUIRED TO MAKE STANDARDS FOR GCMS ANALYSIS OF D2 GLUCOSE 55

TABLE 3-1 THE CONCENTRATIONS OF RNA AND RNA QUALITY INDICES FROM THE SUBCUTANEOUS ABDOMINAL ADIPOSE OF PATIENTS WITH OSA WHO WERE COMPLIANT WITH CPAP TAKEN AT BASELINE (A) OR AFTER 2 WEEKS OF RANDOMISATION TO EITHER SHAM OR CONTINUED CPAP THERAPY (B). 72

TABLE 3-2 THE CUSTOM DESIGNED ASSAYS FOR THE FLUIDIGM OF THE ADIPOSE BIOPSY RNA FROM THE CPAP WITHDRAWAL STUDY 78

TABLE 3-3 BASELINE CHARACTERISTICS OF THOSE IN THE CPAP WITHDRAWAL STUDY 87

TABLE 3-4 THE EFFECT OF SHAM AND CONTINUED CPAP ON THE OXYGEN DESATURATION INDEX (ODI) AND BLOOD PRESSURE (BP) 88

TABLE 3-5 THE EFFECT OF SHAM CPAP ON THE URINARY STEROID PROFILE OF PATIENTS WITH OSA. STATISTICALLY SIGNIFICANT VALUES ARE HIGHLIGHTED IN GREY. STATISTICAL SIGNIFICANCE IS TAKEN AS $P<0.05$. VALUES ARE EXPRESSED IN µG EXCRETED/12 HOURS. DATA IS PRESENTED AS MEAN ±SD. WHERE DATA IS NOT NORMALLY DISTRIBUTED IT IS MARKED AS†. 92

TABLE 3-6 THE EFFECT OF SHAM CPAP ON THE URINARY STEROID RATIOS OF PATIENTS WITH OSA. STATISTICALLY SIGNIFICANT VALUES ARE HIGHLIGHTED IN GREY. WHERE DATA IS NORMALLY DISTRIBUTED IT IS EXPRESSED AS MEAN ± STANDARD DEVIATION. WHERE DATA IS NOT NORMALLY DISTRIBUTED IT IS MARKED AS† 101

TABLE 3-7 THE EFFECT OF SHAM CPAP THERAPY ON EARLY MORNING FASTED PLASMA ALDOSTERONE (PG/ML) AND CORTISOL (NG/ML). THIS WAS A RETROSPECTIVELY

PLANNED ANALYSIS AND NOT ALL PATIENTS HAD AVAILABLE PLASMA (N, NUMBERS AS PRESENTED). WHERE DATA IS NOT NORMALLY DISTRIBUTED IT IS MARKED AS†.....108

TABLE 3-8. THE EFFECT OF CPAP WITHDRAWAL ON THE GENE EXPRESSION OF SUBCUTANEOUS ABDOMINAL ADIPOSE TISSUE. DATA IS PRESENTED IN ARBITRARY UNITS ± STANDARD DEVIATION. THE SIGNIFICANT VALUES ARE HIGHLIGHTED IN GREY. (*P<0.05) 109

TABLE 5-1 THE DEMOGRAPHICS AND BIOCHEMICAL PROFILES OF THE PARTICIPANTS. DATA MARKED† IS NOT NORMALLY DISTRIBUTED. 137

TABLE 6B 1 A COMPARISON OF THE EFFECT OF INTERMITTENT HYPOXIA (IH) AND IH + RU486 ON LIPID METABOLISM (NEFA=NON-ESTERIFIED FATTY ACIDS; TTR=TRACER:TRACEE RATIO; AUC=AREA UNDER THE CURVE) 170

TABLE 7-1 THE ANIMAL AND TISSUE WEIGHTS FOR ALL ANIMALS FOLLOWING COMPLETION OF THE STUDY PROTOCOL. DATA IS PRESENTED AS MEAN±SD. SC=SUBCUTANEOUS. 183

Abbreviations

3T3L1: a mouse-derived cell line that can be differentiated to take on the appearance and phenotype of an adipocyte

3α5βTHALDO: 3α5β-tetrahydroaldosterone

5αTHA: 5α-tetrahydrocorticosterone

11βHSD1: 11β-Hydroxysteroid dehydrogenase type 1

11βHSD2: 11β-Hydroxysteroid dehydrogenase type 2

11DHC: 11 dehydrocorticosterone

18OHTHA: 18-hydroxycorticosterone

AASM: American Academy of Sleep Medicine

ACC1: acetyl-CoA carboxylase 1

ACTB: β-actin

ACTH: adrenocorticotropic hormone

Adipo-IR: adipose tissue insulin resistance

AE: adverse events

AFLD: alcoholic fatty liver disease

AHI: apnoea-hypopnoea index

AIH: acute intermittent hypoxia

ALT: alanine aminotransferase

AMPK: 5'AMP-activated protein kinase

ApoB: apolipoprotein B

ARNT: aryl hydrocarbon Receptor Nuclear Translocator

AST: aspartate aminotransferase

ATP: adenosine triphosphate

AUC: area under the curve

BMI: body mass index

BP: blood pressure

CD36: fatty acid translocase

cDNA: complimentary deoxyribonucleic acid

C/EBPα: CCAAT/enhancer-binding protein α

CE: cholesterol ester

CIH: chronic intermittent hypoxia

CO_2: carbon dioxide

COPD: chronic obstructive pulmonary disease

CPAP: continuous positive airway pressure

CPT-1: carnitine palmitoyltransferase I

CRH: corticotrophin releasing hormone

Dec1: differentiated embryo chondrocyte gene 1

DNL: de novo lipogenesis

DUSP1: dual specificity phosphatase 1

ECG: electrocardiogram

EEG: electroencephalogram

ELISA: enzyme-linked immunosorbent assay

EOG: electrooculogram

ER: endoplasmic reticulum

FAS: fatty acid synthase

FibroMax: a non-invasive score which is combination of measures of steatosis, steatohepatitis and fibrosis

FiO_2: the oxygen concentration of inspired gas

FLI: fatty liver index

G6Pase: glucose-6-phosphatase

GC: gas chromatography

GC/C/IRMS: gas chromatograph-combustion-isotope ratio mass spectrometer

GC/MS: gas chromatograph/mass spectrometry

GILZ: glucocorticoid-induced leucine zipper

GLUT1: glucose transporter 1

GR: glucocorticoid receptor

HADH: hydroxyacyl-coenzyme A dehydrogenase

HbA1c: glycated haemoglobin

HDL: high density lipoprotein

HepG2: a human liver cancer cell line

HIF: hypoxia-inducible factors

HOMA-IR: homeostatic model assessment of insulin resistance

HOMA2: homeostatic model of assessment 2

HPA: hypothalamic-pituitary-adrenal

HRP: horse radish peroxidase

H6PD: Hexose-6-phosphate dehydrogenase

IBM SPSS:

IH: intermittent hypoxia

IL-6: interleukin 6

IPGTT: intra-peritoneal glucose tolerance test

IQR: interquartile range

IRS1:insulin receptor subunit 1

IRS2: insulin receptor subunit 2

ITT: insulin tolerance test

IVC: individually ventilated cage

IVGTT: intravenous glucose tolerance test

KO: knock-out

LDL: low density lipoprotein

LDL-R: low density lipoprotein receptor

LPL: lipoprotein lipase

MAPK: mitogen-activated protein kinase

MHRA: medicines and healthcare products regulatory authority

MI: myocardial infarction

MOL%: % by molarity

mRNA: messenger ribonucleic acid

NADPH: Nicotinamide adenine dinucleotide phosphate

NAFLD: non-alcoholic fatty liver disease

NAS: NAFLD activity score

NASH: non-alcoholic steatohepatitis

NEFA: non-esterified fatty acid

NF-κB: Nuclear factor-κB

NHS: National Health Service

NR3C1: glucocorticoid receptor

NTC: non-tissue controls

O_2: oxygen

OCDEM: the Oxford Centre for Diabetes, Endocrinology and Metabolism

OD: once a day

ODI: oxygen desaturation index

OGTT: oral glucose tolerance test

OHB: β-hydroxybutyrate

OSA: Obstructive sleep apnoea

PA: primary aldosteronism

PaO_2: arterial partial pressure of oxygen

$PaCO_2$: arterial partial pressure of carbon dioxide

PGC-1α: peroxisome proliferator-activated receptor gamma coactivator 1-alpha

PEPCK: Phosphoenolpyruvate carboxykinase

PHD: prolyl hydroxylase domain enzyme

PKLR: pyruvate kinase 1

PPARγ: peroxisome proliferator activated receptor γ

PCR: polymerase chain reaction

Ra: the rate of appearance

RAT: respiratory arousal threshold

RCT: randomized controlled trial

Rd: the rate of disposal

RDI: respiratory disturbance index

RU486: Mifepristone

SaO_2: the oxygen saturation measured via capillary oxygen saturation monitoring

SCD-1: stearoyl-CoA desaturase-1

SGK1: serum/glucocorticoid regulated kinase 1

SPE: solid phase extraction

SREBF1: sterol regulatory element binding factor 1

STOP-BANG: questionnaire used to screen individuals for OSA

TG: triglyceride

TAG: triglyceride

THE: tetrahydrocortisone

THF: tetrahydrocortisol

TNFα: tumour necrosis factor α

TTR: tracer to tracee ratio

VEGFA: vascular endothelial growth factor A

VHL: Von Hippel-Lindau

VLDL: very low density lipoprotein

WT: wild type

1. General Introduction

1.1 Introduction

1.2 An introduction to obstructive sleep apnoea (OSA)

1.2.1 OSA: physiology

The signs, symptoms and consequences of obstructive sleep apnoea (OSA) are described by the American Academy of Sleep Medicine as "*a direct result of the derangements that occur due to repetitive collapse of the upper airway: sleep fragmentation, hypoxemia, hypercapnia, marked swings in intrathoracic pressure, and increased sympathetic activity*" (1). The collapse of the upper airway is the dominant step resulting in increasing hypoxia and hypercapnia with a resultant partial arousal from sleep and a gasping breath before the cycle of intermittent collapse of the upper airway repeats. The driver of the partial arousal is multifactorial and though this in part protective it further exacerbates sleep fragmentation (2). Although much of the upper airway is a rigid structure the muscular segment between the hard palate and the larynx (pharynx) is susceptible to occlusion. The muscles of the pharynx hold the upper airway open and relax during sleep making the upper airway susceptible to this occlusion (3, 4). The anatomical and therefore functional dynamic nature of the pharynx is necessary for speech and swallowing. This upper airway occlusion results in termination of air flow (apnoea) whilst partial occlusions results in reduced flow (hypopnoea). Those with OSA often have narrower upper airways than controls (5) as a result at least in part by increased adiposity of the soft tissue around the neck and this partially explains the significant association between OSA and obesity.

However, this very anatomically driven explanation of OSA pathogenesis is increasingly recognised to be an oversimplification with other phenotypes now implicated in

OSA (4). These include: ineffective upper-airway dilator muscles; unstable ventilatory control; and low respiratory arousal threshold (4) (Figure 1-1).

The upper-airway dilator muscles relax during sleep and their function is controlled by a combination of chemo- and mechanoreceptor input. The chemoreceptors are thought to be less responsive to deviations in PaO_2 and $PaCO_2$ during sleep (6) although the responsiveness may be exaggerated in patients with OSA compared to controls further driving sympathetic arousals (7) which may further fragment sleep architecture with potential metabolic consequences.

The unstable ventilatory control refers to the ventilatory response to a given ventilatory disturbance. This is also referred to as loop gain. In high loop gain a small change in breathing would result in a large respiratory correction. In OSA the loop gain has been shown to be elevated (8) which contributes to the frequent oscillations in respiratory function across sleep.

A low respiratory arousal threshold (RAT) is associated with increased disruption of sleep duration and architecture as well as normalising airflow prior to the change in chemo- and mechanoreceptor signalling necessary to determine adequate ventilatory response (4). A low RAT is often a feature of more severe OSA although ethnic differences occur (9). OSA can occur across the different stages of sleep though increasingly it is recognised that disruption of rapid eye movement sleep is most relevant for the metabolic consequences of OSA including hypertension (10).

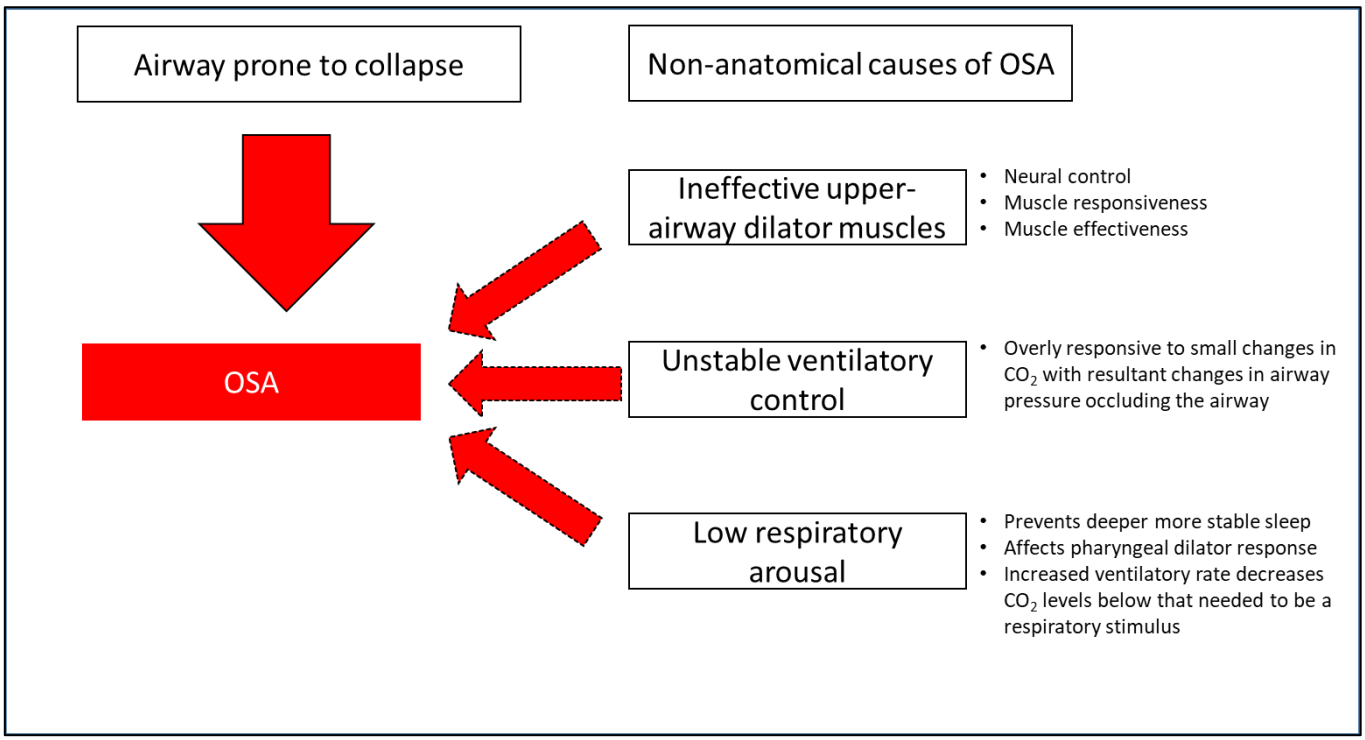


Figure 1-1 The non-anatomical causes of OSA. This figure is adapted from the excellent review by Eckert (3).

1.2.2 OSA: diagnosis and prevalence

The prevalence of OSA (defined as an AHI (apnoea-hypopnoea index) or RDI (respiratory disturbance index) ≥ 5) in the general adult population (age ≥ 18 years) is 13-33% for men and 6-19% for women (11). Additionally it is increasingly accepted that there is a significant burden of previously undiagnosed OSA even in young (18-30 years) lean individuals (BMI 18-25 kg/m^2) without established cardiometabolic disease further highlighting that OSA is a common problem that can easily be overlooked as a diagnosis (12).

The diagnosis of obstructive sleep apnoea relies on a sleep study. This is either in the form of a full laboratory sleep study (polysomnography) or limited channel polysomnography in the patient's home using an approved device (13). A full laboratory sleep study includes an electroencephalogram (EEG), electrooculogram (EOG), chin electromyogram, airflow

measurement, oxygen saturation, respiratory effort and an electrocardiogram (ECG) (13). Limited home sleep studies include measurement of oxygen saturations, heart rate, nasal air flow and chest movement. The criteria required for diagnosis is the apnoea hypopnoea index (AHI) which is a combination score that incorporates apnoea and hypopnoea episodes per hour. NICE reports that a score of ≥ 15 (diagnostic of moderate OSA) in association with sleepiness is an indication for treatment with continuous positive airway pressure (CPAP) or a score of ≥ 5 accompanied by symptoms that affect quality of life having also failed to benefit from lifestyle modification or other relevant treatment options (14). The American Academy of Sleep Medicine (AASM) defines apnoea as the complete cessation of air flow lasting ≥ 10 seconds whilst the current hypopnoea definitions are either i) a respiratory event lasting ≥ 10 seconds with a ≥ 30% reduction in thoracoabdominal effort or nasal airflow and ≥ 3% reduction in oxygen saturation that may or may not be associated with an arousal or ii) a ≥ 50% reduction in nasal pressure signal and a ≥ 3% reduction in desaturation or arousal. It is also deemed acceptable to diagnose hypopnea according to the above if there is a ≥ 4% reduction in desaturation where arousal data is not available (https://aasm.org/aasm-clarifies-hypopnea-scoring-criteria/).

1.2.3 OSA: the consequences of undiagnosed disease and current treatment

Since the recognition that OSA was a significant risk factor for cardiovascular disease nearly 30 years ago (15) treatment strategies have not changed significantly. In addition to the individual's risk of cardiovascular disease, OSA is associated with a two-fold increase in the risk of a work-related accident (16) or a road traffic collision (17). Despite the risks that untreated OSA poses to the individual and the wider community, a significant disconnect persists between areas of the UK with a higher OSA prevalence and the provision of sleep

centres capable of diagnosing and managing OSA (18). A report by the British Lung Foundation estimates that further investment in OSA assessment and management could save the NHS £28million pounds and prevent 40,000 round traffic collisions annually (19). The current treatment consists of lifestyle advice aimed at losing weight and CPAP therapy in those who meet eligibility criteria (14). CPAP is a tight-fitting positive pressure mask worn during the sleep that increases the airway pressure within the patient's upper airways to reduce their collapsibility. As well as being noisy many patients find CPAP therapy claustrophobic and data suggests that over 30% of patients advised to use CPAP never start and 15% abandon its use within a year whilst the remaining individuals who persist with CPAP often use it less than the minimally recommended 4 hours per night (20). However, it is important to note that although a figure of <50% compliance is commonly cited compliance be even lower as much of this data relies on self-reporting (20, 21).

1.2.4 OSA: dyslipidaemia and glycaemic control

There is now a significant body of work identifying OSA as an independent risk factor for dyslipidaemia and diabetes risk across cohorts of different ethnicity. Although the severity of OSA can be stratified by several methods the commonest is by using the AHI (Apnoea-Hypopnoea Index) as discussed in the previous section.

In a Japanese cohort, of 275 working aged men (mean age 44), the respiratory disturbance index (formula quantifying respiratory events taken from polysomnography) was positively correlated with fasting plasma triglyceride concentrations (22). Similarly in a large Brazilian cohort study of over 1000 people (male and female; aged 20-80 years) the AHI>15 and time spent with nocturnal saturation <90% were independently associated with fasting

plasma triglycerides (TG) and homeostatic model of assessment of insulin resistance (HOMA-IR) (23). These findings were echoed in a large meta-analysis that included over 18,000 patients, with AHI found to be an independent predictor of elevated low-density lipoprotein cholesterol (LDL) and TG (24) supporting a potential mechanistic link between OSA and cardiovascular disease secondary to changes in lipid profiles. The same group performed a meta-analysis examining the effect of CPAP (continuous positive airway pressure) therapy on dyslipidaemia and found improvements in plasma LDL, total cholesterol and high-density lipoprotein cholesterol (HDL) but no change in TG concentrations (25). However, the duration of CPAP in the included studies ranged from 2 days to 1 year therefore the full extent of metabolic improvements with CPAP therapy may have been masked. In a recent study of long term (~1 year) CPAP use in non-obese individuals treatment had no effect on measures of glucose homeostasis following an oral glucose tolerance test (OGTT) (26), although at baseline nocturnal time spent <90% oxygen saturations was correlated with insulin resistance. Whilst an earlier meta-analysis of studies assessing the effect of CPAP (duration 1-24 weeks) on HOMA-IR in non-diabetic individuals showed an improvement (27). In those with type 2 diabetes 1 week of effective CPAP therapy (in sleep laboratory for 1 week; compliance of >8hrs) was sufficient to improve fasting glucose and the dawn phenomenon (increase in glucose in the early hours of the morning) (28).

Randomised controlled trials (RCTs) investigating the effect of CPAP on HbA1c in patients with OSA and type 2 diabetes have yielded conflicting results. Forty-two men with type 2 diabetes (HbA1c mean 8.5%) and newly diagnosed OSA were randomised to three months of CPAP or placebo CPAP. CPAP had no effect on HbA1c, HOMA% or measures of insulin sensitivity across a euglycaemic-hyperinsulinaemic clamp (29). A separate larger

randomised open-label (298 patients with diabetes (HbA1c 6.5-8.5%) and newly diagnosed OSA) study also showed no improvement in HbA1c following 6 months of CPAP, however there were reductions in diastolic blood pressure as well as indices of sleepiness and quality of life (30). Variations in conclusions may be secondary to study duration or baseline HbA1c. Previously published studies have shown that OSA is associated with worse glycaemic control in those with diabetes (31–34). In a study of 131 patients with type 2 diabetes the presence of moderate-severe OSA (AHI≥15) was associated with an increased risk of diabetes associated complications including renal disease and this increased risk appeared to be driven by increased rates of hypertension (35). It seems therefore that the presence of OSA is associated with dyslipidaemia and dysglycaemia and that CPAP therapy may be associated with improvements in lipid profile although the effects on glycaemic control in patients with diabetes are yet to be conclusively demonstrated.

In a human model of acute intermittent hypoxia (AIH) 5 hours of 24 desaturations/hour resulted in insulin-resistance measured with an intravenous glucose tolerance test (IVGTT) conducted between hours 5-8 as the intermittent hypoxia protocol continued (36). The results showed a reduction in indices of glucose disposal and insulin sensitivity (36). The effect on lipid metabolism was not studied. In a separate study employing the same intermittent hypoxia protocol 3 hours of IH was sufficient to cause a rise in plasma glucose though there was no effect on an OGTT performed following the exposure (37).

1.2.5 OSA: cardiovascular disease and mortality

In a prospective study of over 1000 individuals, OSA was an independent risk factor for stroke and all-cause mortality, after correction for possible confounders, and despite a

relatively short follow-up of just over 3 years (38). However, although an AHI of 5 was used as the cut-off for OSA the mean AHI of the patients was actually over 30 thus this risk was associated with particularly severe OSA (38). Additionally, a high proportion of the OSA patients in this cohort had either achieved 10% weight loss or received positive airway pressure treatment which could not be reasonably adjusted for (38). In a smaller study that included 638 untreated patients, OSA severity was associated with an increased risk of all cardiovascular outcomes and mortality following a stroke (39). In a separate smaller study that used an AHI of 15 as the diagnostic cut-off, OSA was associated with increased 10-year mortality in those who had presented for rehabilitation post stroke (40); however this study only included 23 patients with OSA which limits its extrapolation. Similarly, cardiovascular related outcomes post myocardial infarction (MI) were found to be worse in those with OSA (AHI $\geq$ 15) with nocturnal hypoxaemia a particular risk factor (41) in the 15 months following MI. In a meta-analysis of individuals undergoing primary percutaneous coronary angiography following MI an AHI $\geq$ 15 was an independent risk factor for further cardiovascular events (42). In a prospective study with a 20 year follow up, moderate-severe OSA (defined by the respiratory disturbance index (RDI)) was associated with an increased risk of stroke, all-cause mortality, cancer incidence and cancer mortality but not cardiovascular disease (43). However, in this study no data was given about whether the patients were treated with CPAP and as such any cardiovascular risk may have been masked.

In a large meta-analysis of over 7000 patients, CPAP was not associated with a risk reduction in cardiovascular outcomes including myocardial infarction, stroke and cardiovascular death (44). However, two of the studies included in the analysis were of patients with central sleep apnoea and it has been commented previously that there was

considerable heterogeneity of OSA severity in the included studies, as well as comparatively poor compliance with CPAP that may have limited the power of the meta-analysis to detect any benefit form CPAP (45). In smaller studies using CPAP in high risk individuals who have already had a stroke (46) or myocardial infarction (47) there was an improvement in cardiovascular outcomes. In a large study of 2717 individuals (SAVE trial) with moderate-severe OSA and confirmed cardiovascular or cerebrovascular disease, participants were randomised to receive either CPAP or no CPAP in addition to standard care. CPAP treatment did not result in a reduction in cardiovascular events however, the mean nocturnal compliance with CPAP in this study was only 3.3 hours despite a strategy prior to randomisation to attempt to ensure good compliance (48).

From the data summarised above it is evident that OSA is indeed a risk factor for cardiovascular/cerebrovascular disease as well as worse clinical outcomes in those who have had either an MI or stroke. Variable compliance with CPAP and the heterogeneity of the cohorts studied, particularly in the larger series, limits firm conclusions regarding the effect of CPAP on primary prevention however in small studies of high-risk patients there does seem to be an advantage of CPAP in secondary prevention.

1.3 The effects of OSA and hypoxia on key metabolic tissues

1.3.1 The metabolic effect of hypoxia on adipose tissue *in vitro*

OSA is a complex condition that includes changes in sympathetic activation, intra-thoracic pressure and intermittent hypoxia which all occur during sleep thus resulting in a fragmented sleep pattern. Each of these components of OSA is likely to be relevant in a

clinical setting. Much of the relevant *in vitro* and animal work focuses on the metabolic effect of hypoxia.

Adipocytes are sensitive to hypoxic exposure in tissue culture experiments. Much of the published literature involves hypoxic exposure of FiO_2 (1%) for 24 hours of two-dimensionally cultured proliferating or differentiated adipocytes, which may explain some of the differences in findings between *in vitro* cellular studies and *in vivo* studies which are summarised in the following sections.

Mature adipocytes are derived from mesenchymal stem cells initially via *determination* whereby the fate of the stem cell to become an adipocyte is initiated and then via *terminal differentiation* whereby the immature pre-adipocyte takes on the biological functionality of a mature adipocyte (49). Increasingly *in vitro* data supports a role for hypoxia in controlling both determination and subsequent terminal differentiation. Bone marrow derived mesenchymal stem cells preferentially differentiate into adipocytes in conditions of extreme hypoxia (0.2% oxygen) rather than osteocytes in a manner dependent on hypoxia inducible factor-1 α (HIF-1α) (50). Whilst in the same cell type the opposite finding was shown at a slightly higher oxygen tension (2%). A separate study compared the differentiation of human derived pre-adipocytes in more physiological oxygen tensions (5% and 10%) and compared the effect *vs* the traditional cell culture oxygen tension (21%). Whilst the authors point out that, adiponectin secretion and isoproterenol induced lipolysis are increased in adipocytes cultured at the lower oxygen tensions suggesting a closer biological equivalent to the *in vivo* adipose tissue, the traditional markers of adipose differentiation peroxisome proliferator activated receptor γ (PPARγ) and CCAAT/enhancer-binding protein α (C/EBPα)

were unchanged (51). It seems therefore that the oxygen tension of cultured cells is relevant to adipose differentiation and subsequent biology although the optimal oxygen concentration required for culture is debated. Moreover, the biological *in vivo* environment of cells cultured *ex vivo* is also likely to be crucial since it has been shown that visceral adipose tissue-derived multipotent mesenchymal cells from individuals without the metabolic syndrome were able to undergo healthy proliferation and angiogenesis compared to those from patients with the metabolic syndrome (52).

The effect of hypoxia on the various physiological functions of adipose tissue/adipocytes, including lipogenesis and lipolysis has also been studied. Much of this functional work has used the murine cell line 3T3L1 which are fibroblast-like cells that can be differentiated to become phenotypically similar to lipid-laden adipocytes (53). Whilst gene expression profiles of 3T3L1 cells closely mirror white adipose under certain experimental conditions they can take on beige or brown adipose gene expression profiles which may limit their application in the study of human adipose tissue (53). Differentiated 3T3L1 adipocytes cultured for 1 week at 5% O_2 had reduced levels of TG and droplet size, compared to cells cultured at 21% O_2; this effect appeared to be mediated by a reduction in glucose uptake and lipogenesis and increased lipolysis (54). In contrast, when 3T3L1 cells were differentiated in hypoxic conditions (4% O_2) there was increased lipogenesis and droplet size as well as adipocyte specific markers (55). Therefore, the effect of hypoxic exposure may also depend on whether the cell is a mature adipocyte or in the process of differentiating. Clearly *in vivo* adipose tissue is composed both of mature and differentiating adipocytes as well as additional cell types that further contribute to the microenvironment of the adipocyte.

1.3.2 The metabolic effect of hypoxia on adipose tissue *in vivo*

There is debate around optimal conditions to investigate the role of hypoxia on adipose tissue biology *in vitro* and this is reflected by the divergent findings from human studies.

It has been hypothesized that as adipose tissue expands, due to caloric excess, the tissue becomes hypoxic as the relative distance from the capillary blood increases. It is therefore postulated that as adipose tissue expands it becomes hypoxic and that this represents a trigger for inflammation and adipose dysfunction leading to metabolic disease (56). However, this hypothesis is contested. It is clear that the arterial saturations of patients with obesity are inversely proportional to adiposity thus potentially exposing tissue to hypoxia, yet the oxygen consumption of subcutaneous abdominal adipose has been shown to decrease across obesity (57). Furthermore, selective venous catheterization of abdominal adipose tissue did not show the anticipated changes in the lactate:pyruvate ratio (a marker of cytosolic redox state) with obesity arguing against a hypoxic adipose tissue environment (57). When studies have directly measured the oxygen tension within adipose tissue across obesity there has been debate about whether the tissue is hypoxic or even hyperoxic. Work by Goossens *et al* used adipose tissue microdialysis incorporating a method of continuous measurement of tissue oxygenation optochemically and found increased oxygen levels in the subcutaneous abdominal adipose tissue of individuals with obesity. The authors explained this by the finding of reduced adipose tissue blood flow and oxygen consumption in obesity (58). This is in direct contrast to a previous study using a Clarke electrode directly inserted into the abdominal adipose tissue which showed that in obesity abdominal adipose had lower oxygenation; however this study failed to show activation of the hypoxia mediated vascular endothelial growth factor A (VEGFA) signalling (59) These discrepant findings have been

partially explained by the different methods used, the large range of oxygen tensions seen in the groups studied and differing levels of insulin resistance in the subjects (60). Despite these differences it has been shown that adipose tissue uses very little oxygen (2-4 μmol.100g^{-1}tissue.min^{-1}) compared to more metabolically active tissue like skeletal muscle (57) and that even when the tissue is thought to be exposed to comparatively low oxygen levels there is no overt metabolic signal in response to the hypoxic exposure (57).

Although there is continued debate about the hypoxic conditions of adipose across obesity there is some useful data from research in patients with chronic lung conditions that can provide insight into the possible relationship between systemic hypoxia and the effects on adipose tissue. Chronic obstructive pulmonary disease (COPD) is a chronic progressive lung condition that encompasses emphysema and chronic bronchitis. Work in patients with severe COPD who required long term oxygen therapy had their oxygen treatment suspended and an assessment made of their adipose tissue function by direct sampling using adipose tissue microdialysis in conditions of systemic hypoxia and again after reintroduction of normoxia using supplemental oxygen (61). Basal lipolysis and pharmacologically stimulated lipolysis were increased in hypoxic conditions with no apparent change in adipose blood flow. However there was no change in plasma non-esterified fatty acid (NEFA) concentrations suggesting that the changes observed locally in the abdominal adipose tissue may not be mirrored systemically (61). In a recent paper, subcutaneous abdominal adipose tissue oxygenation (measured by Clarke type electrode) and gene expression were studied in 16 men with OSA before and after 4 months of compliant CPAP therapy and compared with BMI matched controls. Oxygen levels in adipose tissue were no different between controls and patients and CPAP therapy had no effect on adipose tissue oxygenation. Gene expression data

from this study suggested that the OSA adipose tissue was mildly inflamed compared to that of controls but this was not altered by CPAP therapy (62). These findings are supported by another recent study, which compared the abdominal adipose tissue of those with OSA and well-matched controls, and no difference was observed in serum cytokines or adipose mRNA profiles of inflammatory and endoplasmic reticulum (ER) stress genes (63). In this study however, modest changes were seen with 24 weeks of CPAP therapy. However the CPAP was in association with a weight loss intervention and the group that were adherent to CPAP lost more weight, so it remains unclear if the effects seen were CPAP or weight-loss mediated (63).

The limited impact of the contribution of the intermittent hypoxia of OSA on abdominal adipose tissue is supported by work employing an acute intermittent hypoxia protocol in otherwise healthy males (64) . The experimental design enabled assessment of the effect of intermittent hypoxia on abdominal adipose tissue lipoprotein lipase (LPL) activity following a lipid rich meal. Although intermittent hypoxia was associated with an increase in plasma NEFA there was no post-prandial increase in TG or LPL activity (64). This is likely to suggest that the effect on NEFA was not a result of changes to insulin resistance in abdominal adipose tissue since the anticipated effects were not seen in the fed state.

1.3.3 The metabolic effect of hypoxia on hepatocytes *in vitro*

As the human liver is not easily biopsied or imaged in real time during hypoxic conditions much of the *in vivo* data that is directly relevant to this thesis has come from animal studies and is discussed below (section 1.4.1)

There is a small amount of literature from *in vitro* studies that is directly relevant to the presented work undertaken in this thesis. *In vitro*, hepatocytes exposed to hypoxic conditions undergo increased intracellular lipid accumulation which could either be mediated by a reduction in fatty acid β-oxidation or changes to fatty acid synthesis, uptake or export. 1% O_2 for 18 hours causes a doubling of intracellular TG, however this was accompanied by a reduction in the expression of genes involved in fatty acid synthesis (fatty acid synthase (FAS)); sterol regulatory element-binding protein 1c (SREBP-1c); stearoyl-CoA desaturase-1 (SCD-1) alongside a reduction of regulators of fatty acid β-oxidation (Peroxisome proliferator-activated receptor gamma coactivator 1-alpha (PGC-1α)); Carnitine palmitoyltransferase I (CPT-1)) (65) suggesting that TG accumulation is likely mediated by changes to fatty acid β-oxidation rather than lipogenesis. Furthermore these changes seemed to be mediated by HIF-1α and HIF-2α as silencing of either gene abrogated these effects (65). The finding of increased intracellular TG accumulation in response to hypoxia has been demonstrated previously (66) with fatty acid β-oxidation appearing to have the predominate effect since hydroxyacyl-coenzyme A dehydrogenase (HADH) activity (which is a surrogate measure of fatty acid β-oxidation) decreased in hypoxic culture at 1% for 24 hours (66); although silencing HIF-2α reduced hepatocyte lipid accumulation in response to hypoxia there was no effect on HADH activity or on genes involved in fatty acid β-oxidation. This is in contrast with findings from the rodent experiments discussed above whereby the constitutive action of HIF-2α drives steatosis via reduced fatty acid β-oxidation (67). The hypoxic response of lipid laden hepatocytes may be impaired leading to an inflammatory pro-apoptotic environment. Hepatocytes pre-treated with fatty acids prior to exposure to hypoxia do not upregulate HIF-1α to the same extent and have lower cellular adenosine triphosphate (ATP)

and reduced cell viability (68) such that the increased TG in hypoxia may result in a rapid acceleration to inflammation and cell death. Some of the effects of hypoxia on lipid metabolism may be insulin mediated since *in vitro* work has demonstrated that IH interrupts insulin-signalling and gluconeogenesis (69).

Most published data employ sustained hypoxia exposure protocols (18-24 hours) which may limit its relevance in OSA which involves an oscillating oxygen tension between normoxia and hypoxia multiple times per hour. Based on the evidence from animal/cell studies it seems that hepatocytes are oxygen sensitive and that cellular hypoxia contributes to hepatic lipid accumulation although this is yet to be demonstrated in human *in vivo* models.

1.4 Mechanistic data from rodent studies linking OSA and metabolic disease

1.4.1 Insights from chronic intermittent hypoxia rodent studies: oxidative stress, glycaemic control and hepatic lipid handling

As discussed, the pathophysiology of OSA includes chronic nocturnal intermittent hypoxia; recurrent sympathetic arousal and disturbed sleep as well as changes in thoracic pressure with resultant effects on venous return. Much of the mechanistic data published thus far focuses on the link between hypoxia and metabolic disease.

There is an oxygen gradient in healthy liver tissue. Oxygenated blood arrives via the hepatic artery in the portal triad and deoxygenated blood leaves via the central hepatic vein such that the oxygen tension in the peri-portal area is 60-65 mmHg reducing to 30-35 mmHg in the peri-venous area (70). This results in established zonal differences in lipid metabolism with increased lipid oxidation in the peri-portal area and increase lipogenesis and re-esterification of exogenous fatty acids in the peri-venous area (71). Early rodent work

supports the modulation of this gradient resulting in changes to lipid metabolism with rats exposed to hypoxia showing increased hepatic TG content (72).

In a rat model of chronic intermittent hypoxia (CIH) 12 weeks of CIH resulted in increased insulin secretion which was accompanied by pancreatic lesions and inflammation as well as increased signalling via the mitogen-activated protein kinase (MAPK) pathway (73). Additionally, it has been reported that even comparatively mild CIH protocols are sufficient to cause insulin resistance as measured by insulin tolerance test (ITT) in rodent models (74). It was found that insulin receptor expression and phosphorylation decreased in muscle and adipose but not in liver in this study (74). As well as insulin resistance, measured by HOMA-IR and ITT a more recent study identified widespread reduced insulin induced phosphorylation across the signalling cascade in skeletal muscle, white adipose tissue and liver (75). Of interest in this study, they found that despite insulin resistance whole-body glucose tolerance as measured by an intraperitoneal glucose tolerance test (IPGTT) was actually improved by CIH in a manner that seemed to be mediated by 5'AMP-activated protein kinase (AMPK) activation in skeletal muscle (75). A direct effect on insulin signalling in hepatocytes *in vitro* has been demonstrated with IH inhibiting downstream phosphorylation within the insulin signalling pathway (69).

In support of tissue-specific effects of CIH, rats with streptozocin induced diabetes were exposed to chronic intermittent hypobaric hypoxia and it was observed that there was upregulation in HIF-1α and components of the insulin signalling cascade as well as improvements in hepatic steatosis and insulin resistance (76). This finding of metabolic improvement clearly opposes the other studies discussed herein and is likely the result of a

different hypoxic exposure protocol as hypobaric hypoxia (simulating an altitude of 5000m) was induced for 6 h/day (76) rather than a chronic intermittent hypoxia (CIH) of repeating desaturations throughout the day; the former is likely to reflect the key metabolic differences seen since the metabolic advantages of living at altitude are widely accepted (77).

The upregulation of hepatic HIF-1α in response to IH has been seen in previous studies and it has been postulated that changes to hepatic lipid uptake might be via effects on hepatic LDL-receptor (LDL-R) expression supporting the *in vitro* finding that antagonism of HIF-1α abrogates the hypoxic induction of LDL-R (78). In addition to effects on hepatic lipid uptake, it has been reported that CIH reduces plasma TG clearance by different adipose tissue depots (including epididymal, omental, subcutaneous, and retroperitoneal WAT) by lipoprotein lipase activity. This is partially dependent on upregulation of angiopoietin-like protein 4 (79). This may result in increased lipid availability contributing to hepatic lipid accumulation as well as plaque formation in coronary arteries. Further work has suggested that the increase in plasma TG in hypoxia is a result of reduced plasma clearance rather than increased hepatic TG secretion (80) however the study that suggested this employed a sustained acute hypoxia protocol and that the method used to assess TG secretion relied on the assumption that all measured TG was hepatic in origin.

In addition to changes in TG clearance, CIH for 12 weeks has been shown to increase the expression of genes that regulate hepatic lipid synthesis including SREBF1 and ACC1, as well as hepatic TG and phospholipid levels (81). These findings have also been seen with more acute exposure (5 days of IH) in lean mice (82). Hepatic lipid accumulation may also be secondary to the effects of CIH on nitrogen metabolism since CIH is associated with increases

the hepatotoxic metabolites trimethylamine, dimethylamine and methylamine which all contribute to a reduction in VLDL synthesis and excretion (83). This same study demonstrated a reduction in choline (83). Choline deficiency is a commonly studied animal model of NAFLD (84).

Changes in hepatic TG and liver injury are not reported in all rodent CIH studies. In a separate rat model of CIH, CIH alone had no effect on plasma cholesterol, TG, glucose, or insulin concentrations although there was an additional deleterious effect when CIH was employed in obese (fa/fa Zucker rats) (85). Notably, CIH in lean animals resulted in increased markers of liver inflammation measured as hepatic expression of cytokines IL-6, TNFα and NF-κB (85) mirroring the study by Quintero et al that showed even modest intermittent hypoxia exposures were sufficient to increase hepatic NF-κB (86). Whether adipokine profiles change in response to CIH is less clear with divergent findings reported (85, 87). Similarly CIH in lean mice for 4 weeks had no effect on measures of insulin sensitivity, although insulin independent glucose disposal was impaired (88). In diabetic animals (streptozotocin model) the effect of CIH on improved glycaemic control may be mediated through increased muscle glycogen storage (89); however, this study employed a model of hypobaric hypoxic which as discussed above may explain these differences.

There is also evidence that oxidative stress may connect CIH and metabolism as antagonism of NADPH oxidase 4 attenuated the increase in blood pressure seen in animals exposed to CIH (90). In the most detailed evaluation of hepatic oxidative stress in response to CIH changes in NF-κB, aconitase/fumarase activity and lipid peroxides paralleled the increase seen in hepatic TG (86). This finding of hepatic stress in rodents exposed to CIH has also been

demonstrated by elevation in plasma markers of liver inflammation including ALT and AST as well as histologically with hepatocyte ballooning (91). The lipid peroxidation seen in animals models is a likely driver of the inflammatory response to intermittent hypoxia with resultant inflammation and tissue necrosis (92).

CIH exposure has been reported to increase plasma and renal artery catecholamines as well as driving impaired glucose metabolism and hepatic lipid accumulation (93). This finding directly links CIH with increased sympathetic tone. The mechanistic relevance of this is supported by the observation that adrenal medullectomy reduces fasting plasma glucose and insulin levels in mice treated with IH (88). However, in this study IH did not result in insulin resistance on intravenous glucose tolerance test (IVGTT). The association of increased sympathetic tone and IH may be particularly relevant in OSA patients with established cirrhosis. In a rodent model of cirrhosis CIH resulted in endothelial dysfunction which manifested as reduced relaxation and hyper responsiveness to vasodilating and vasoconstricting agents, respectively (94). This is likely to be of particular significance in patients who develop portal hypertension.

The clinical data linking OSA and NAFLD is covered in subsequent sections. Any potential mechanism linking OSA and NAFLD has not been fully elucidated although CIH has been shown to cause increase lipid peroxidation, lobular inflammation and fibrosis in a mouse model of diet induced steatosis (91) suggesting CIH may be the cardinal feature of OSA associated with NAFLD. Much of the data linking CIH to metabolic disease and in particular NAFLD also involves rodents receiving an obesogenic diet and data concerning the isolated effect of intermittent hypoxia is lacking. Furthermore, the models employed by most

studies are severe (often more than 30 desaturations/hour) and cover a more substantial portion of a 24-hour period than a typical night's sleep in a patient with OSA (rodent studies typically involve 8-10 hours of CIH/day). It is also important to note that as highlighted above some of the studies employ models of hypobaric hypoxia which may not be directly comparable to patients with OSA.

Additional mechanistic detail linking OSA/CIH with NAFLD will be covered in the section below.

1.4.2. Insights from knock out rodent studies

HIF consist of a stable β-subunit and an α-subunit. In normoxic conditions the α-subunit is hydroxylated at one or both of two conserved prolyl domains by members of the PHD family. This identifies it for polyubiquitination by a complex containing von Hippel-Lindau protein (VHL). In hypoxic conditions α and β subunits dimerize and translocate to the nucleus where they act as transcription factors.

There is conflicting data as to the contribution of HIF in regulating the changes to lipid metabolism which may relate to the models used. Liver specific knock out of HIF-1α was shown to worsen hepatic lipid accumulation in a mouse model of alcoholic fatty liver disease (AFLD) in a manner dependent on differentiated embryo chondrocyte gene 1, (*Dec1*) (95). Conversely, another group showed that liver specific knockout of HIF1α was protective from lipopolysaccharide and ethanol induced model of liver injury with a reduction in hepatic lipid accumulation (96). However, in over-feeding models, which better align with the clinical pathogenesis of human NAFLD, the data is more consistent. HIF-1 α KO mice are partially protected from hepatic fibrosis induced by 6 months of a high trans-fat diet and *ex vivo*

hepatocytes from KO animals exhibited reduced collagen cross-linking on exposure to hypoxia (1% 24 hours) in culture (97). It should be noted that in this study hepatic TG content was not different between WT and KO animals which may be a feature of the extent of hepatic steatosis induced by 6 months of such a diet, alternatively HIF-1 α may activate hepatic fibrosis independent of the classic pathogenesis (98) pathway of non-alcoholic steatohepatitis (NASH) progression initiated by hepatic lipid accumulation. In an *in vitro* study, using the HepG2 hepatocyte cell line, fatty acid induced hepatocyte apoptosis was actually reduced with HIF-1 α over expression (99). This opposing finding may represent a cell-culture phenomenon in an immortalized cell line not previously exposed to high levels of circulating fatty acids and thus may differ from the previously discussed rodent studies.

Mice engineered to express HIF-1α and HIF-2α that are not degraded by hydroxylation have increased hepatic lipid accumulation as well as hepatic neovascularization with the livers histologically similar to VHL knockout animals (100). In a study examining a series of VHL knockout mice (+/- HIF-1α and/or HIF-2α knockouts) it was shown that HIF-2α is the major determinant of severe hepatic steatosis and inflammation (67). In this study, constitutive action of HIF-2α was associated with a reduction in fatty acid oxidation along with the regulatory genes of lipogenesis (including sterol regulatory element binding factor 1 (SREBF1)) suggesting that increased lipogenesis may not be the major determinant of HIF mediated hepatic steatosis. A separate murine study including a liver microarray profile identified HIF-2α dependent increased expression of genes involved in lipogenesis and fatty acid uptake and a reduction in the expression of genes involved in fatty acid oxidation and a concomitant increase in proinflammatory or profibrotic genes as the likely underlying mechanism linking HIF-2α expression to the development of steatohepatitis (101). The

differing findings in respect to the expression of genes involved in lipogenesis between these two studies may be a result of temporal changes as the authors of the 2nd cited study found that the induction of these genes increased at 3 days and fell by 14 days (101). Neither study employed a functional assessment of lipogenesis.

Although small molecule HIF-2α antagonists are now available as yet there are no human or animal studies examining their application in NAFLD. There is only limited data implicating HIF in human NAFLD although in one study HIF-1α liver expression was reduced in those with NASH (102). This differs from some animal data whereby HIF-1α liver expression was increased in advanced NASH that was induced using the methionine-choline deficient diet model (103).

In a rat model of diet induced NAFLD although antagonism of HIF1α had a protective effect on steatosis and fibrosis there was no benefit upon indices of insulin resistance (104). Similarly in obese mice anti-sense HIF-1α treatment resulted in lowered plasma glucose levels, and hepatic gluconeogenesis and steatosis (105). Supporting data is drawn from the HIF factor prolyl hydroxylase 1 (PHD1) knock out mice which develop hepatic steatosis and measures of hepatic insulin resistance (measured as reduced insulin mediated phosphorylation of protein kinase B) even when fed a non-obesogenic diet (106). In this study they examined the hepatic gene expression of key glycolytic enzymes and found in knockout mice increased expression of PKLR (Pyruvate kinase 1) which is the rate limiting enzyme. Conversely, others have examined the effect of specific PHD2 knock-out and found increased HIF-2α liver mRNA and improved glucose tolerance and hepatic steatosis (107). This finding is augmented by the observation in mice with constitutively active HIF-2α which have induction of insulin

receptor substrate-2 (IRS2) and reduced hepatic steatosis and gluconeogenesis (108). In conditional hepatic $VHL^{-/-}$ mice which have increased levels of all HIFs there is increased hepatic glucose uptake and storage (109, 110). In a cellular model using desferrioxamine to stabilize HIF there was upregulation of insulin receptor substrate-1 (IRS1) and increased glucose uptake (111). Taken together it is plausible that the class of PHD is relevant for the subsequent action of HIFs on hepatic glucose metabolism however, the effects of PHD1 knockout were only seen in mice fed a low-fat diet; there was no demonstrated additive effect in animals on a high-fat diet (106). The PHD2 effects were reproducible across normal chow and high-fat diets and could be pharmacologically copied with a specific antagonist (112).

Liver biopsies from patients with NAFLD show that HIF-2α is over expressed and liver-specific HIF-2α knock-out mice are protected from developing progressive NAFLD when on a pro-inflammatory diet (113). Liver-specific HIF-2α over-expressing mice develop progressive steatohepatitis and fibrosis with gene expression array data suggesting the mechanism is mediated by increased hepatic fatty acid uptake and synthesis offset by a reduction in β-oxidation (114). Additionally, HIF-2α is likely to have indirect effects on NAFLD progression since individuals with obesity have higher intestinal HIF-2α (which was shown to correlate with markers of liver inflammation) and mice with disruption of intestinal HIF-2α are protected from diet-induced steatosis (115). In further support of a role for HIF in the progression of diet induced NAFLD, that is outside of the context of hypoxic exposure, it has been shown that PHD3 and VHL knock out mice develop severe steatosis (116). Less data exists on the role of the β-subunit (also referred to as aryl hydrocarbon receptor nuclear translocator (ARNT)). Liver-specific deletion of ARNT was associated with increased serum TG as well as impaired fasting and post-prandial glucose concentrations although there was

actually a reduction in the liver TG in fasting animals (117) supporting a role for the HIF dimer in driving hepatic TG accumulation.

Although there are apparent contradictions within the summarised literature taken together there seems to be a role for HIF in the context of diet-induced NAFLD which is likely to be mediated predominantly by changes in hepatic lipid metabolism. This may modulate hepatic lipid metabolism by distinct biological processes (**Figure 1-2**).

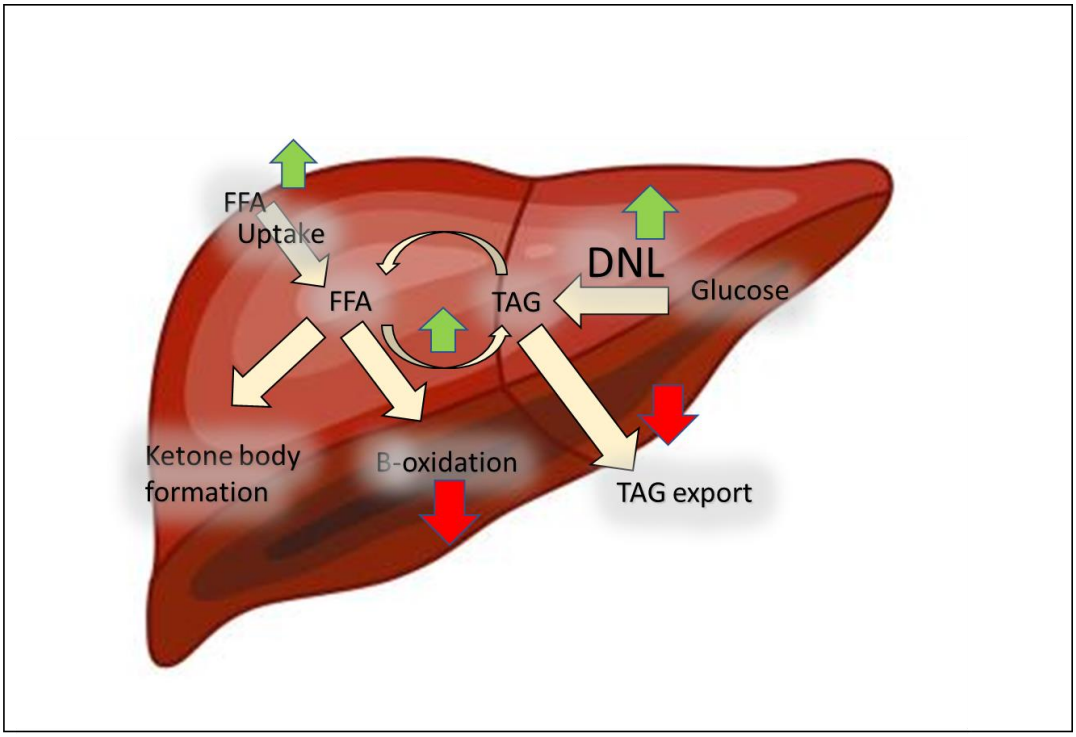


Figure 1-2 The potential mechanisms by which hypoxia could drive hepatic lipid accumulation in patients with OSA. (FFA=free fatty acids; TAG=triacylglycerol; DNL=de novo lipogenesis).

1.4.3 Obstructive sleep apnoea and NAFLD

There is an increasing clinical literature demonstrating an association between OSA and NAFLD. However, many of the published studies are limited by failure to adjust for

confounders including BMI and diabetes status which is particularly necessary given the heterogeneous nature of NAFLD and OSA. Furthermore, given the variety of methods used to diagnose and stratify the severity of NAFLD direct comparisons between studies are difficult.

In a cohort drawn from the Taiwan National Health Insurance database individuals with OSA were divided by whether they received CPAP or not. Individuals treated with CPAP had a lower cumulative incidence of NAFLD and cirrhosis for each of the time periods studied including up to 9 years (9.77% non-CPAP vs 6.78% CPAP, $P<0.001$) (118). Although the individuals within the two groups were matched for age and gender and comorbidities no data concerning the severity of OSA was provided. Therefore it remains possible that rather than CPAP treatment being associated with a reduction in incidence of liver disease it may be a surrogate for more severe OSA leaving the unlikely possibility that in individuals with OSA increasing severity may protect from NAFLD (118). A previous study which has some statistical limitations argues against this (119). It was shown that the severity of NAFLD (stratified on the basis of the hepato-renal index on ultrasound) was associated with the severity of obstructive sleep apnoea. However, no attempt was made to adjust for body mass index or other potential confounders (119). In a separate study those identified by the STOP-BANG questionnaire as being at high risk of OSA were more likely to have significant liver fibrosis after adjustment for confounders (120). In one bariatric surgery cohort the severity of OSA (defined by either AHI, mean SaO_2 or nadir SaO_2) was not associated with adverse liver histology at time of intra-operative biopsy (121). However, in a separate larger bariatric surgery cohort the presence of OSA was independently associated with a range of liver histological parameters including the NAFLD activity score (NAS score) and fibrosis (122). Another study addressed the same question in a non-bariatric cohort using the fatty liver index

(FLI) and found the severity of NAFLD was associated with severity of OSA across these same parameters (123). Furthermore in a cohort of individuals without obesity the nadir saturations of individuals with OSA were positively associated with NAFLD presence and severity (124). In a paediatric cohort of individuals who had liver biopsies as well as polysomnography, NAFLD severity was increased in those with OSA and markers of oxidative stress (F(2)-isoprostanes) were also associated with NAFLD severity (125). In a meta-analysis including over 2000 patients drawn from 18 studies OSA was associated with an increased odds ratio of NAFLD including advanced fibrosis (126). It seems that across multiple cohorts there is a direct association between OSA and NAFLD presence and severity.

The FibroMax test is a combination score measuring features of steatosis, steatohepatitis and fibrosis based on 10 measured biomarkers that can be used as an alternative to liver biopsy for the staging of liver disease (127). In a recent pooled analysis of data from three randomized controlled trials comparing sham and effective CPAP, treatment did not affect the FibroMax test. However, the duration of treatment was only 6-12 weeks and levels were high at baseline with significant rates of likely NASH (128). In a meta-analysis of five studies, CPAP treatment (duration: 1 day-3 years) was associated with a reduction in plasma ALT and AST (129). However, in this analysis there was no data provided as to the cause of the deranged liver enzymes or of any control cohorts. In a more recent study that was retrospective in design NAFLD was defined as a raised ALT without a known cause of chronic liver disease. CPAP use (>3 months) was associated with an improvement in plasma ALT and AST concentrations (130). As with the previous meta-analysis the design limits the conclusions that can be drawn regarding the impact of CPAP on NAFLD. In a small paediatric study of children with biopsy confirmed NAFLD, CPAP therapy for 3 months was associated

with a reduction in ALT and a urinary marker of oxidative stress (F2-isoprostane) (131). Overall, it seems that OSA is associated with NAFLD but the data regarding any liver specific benefit from CPAP is less conclusive.

1.5 Obstructive sleep apnoea and steroids

It is increasingly recognised that OSA is associated with changes in steroidogenesis and the key studies as well as their relevance to metabolism are outlined in the following sections. The assessment of steroid metabolism can be determined by urinary gas chromatograph/mass spectrometry (GC/MS) which allows an accurate assessment of the steroids themselves as well as the measurement of their precursors and metabolites which is particularly informative as biological action is not limited to the steroid product (**Figure 1-3**). Although this method is technically demanding and slow it provides a comprehensive assessment of a wide panel of steroid metabolites and is a powerful tool in hypothesis

generating research (132).

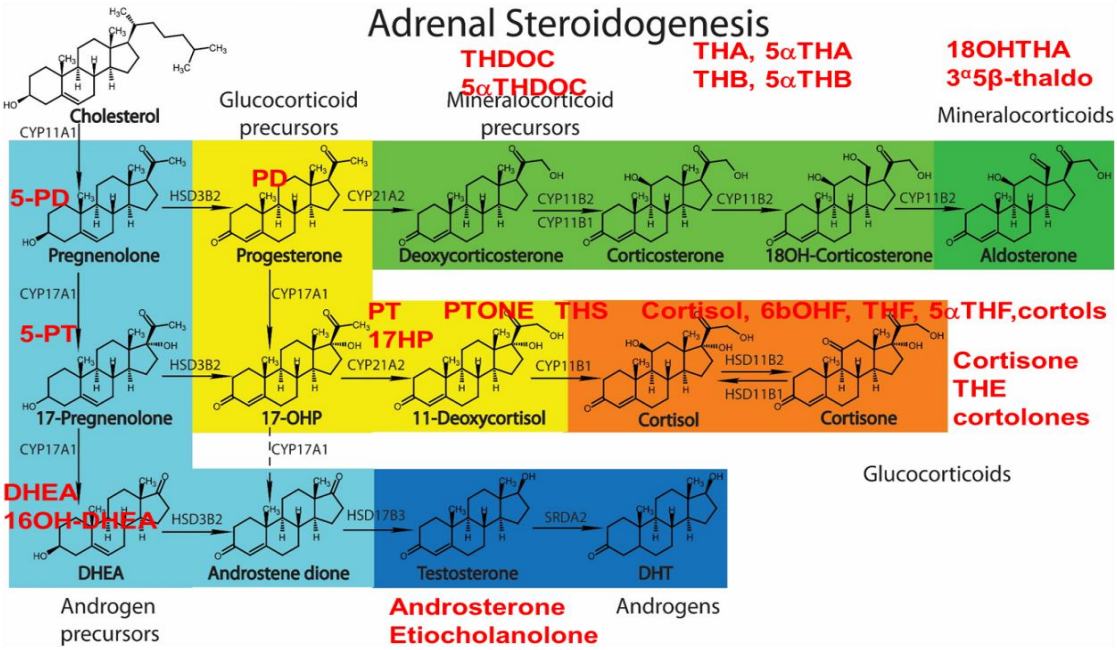


Figure 1-3 Steroid metabolites measured from urine using gas chromatography mass spectrometry. (The steroid in black are the traditional names and are found within the plasma, the red annotations are the metabolites measured within the urine) This figure was generated by a collaborator Dr Angela Taylor at the University of Birmingham

Much of the current literature regarding OSA and steroidogenesis involves the simple measurement of plasma levels of circulating steroids typically performed in early morning samples, however given that OSA is likely to be seen during sleep, it is likely that overnight or 24hour urine collections would provide more informative data.

1.5.1 OSA and Aldosterone

Aldosterone is the major mineralocorticoid hormone. The simplified or classical explanation of its function and regulation is that it is produced and released by the zona

glomerulosa cells of the adrenal cortex under the regulation of the renin-angiotensin-aldosterone system in response to reductions in osmotic pressure or plasma sodium or increases in plasma potassium. The resultant effect is the increased reabsorption of sodium and water at the expense of potassium within the kidney (133).The more recently described non-genomic effects of aldosterone or its role in metabolic signalling outside of renal epithelial cells are not discussed here but have been examined elsewhere (134).

Several publications have linked obstructive sleep apnoea with increased levels of the mineralocorticoid aldosterone. Given the established association between OSA and hypertension a perturbation in mineralocorticoid signalling may represent a potential underlying mechanism and has been the target of interventional studies discussed below.

In a small study of 20 patients with normal blood pressure and newly diagnosed OSA and well-matched non-OSA controls there was no difference in morning aldosterone concentrations (135). A separate study supports these findings in individuals without co-existent cardiovascular disease and also showed the preservation of the diurnal variation in renin-aldosterone activity (136). In a recently published meta-analysis of 13 studies there was no difference in aldosterone levels in individuals with OSA on initial analysis. After the removal of a study with a small sample size there was an apparent increase in aldosterone levels in those with OSA compared to those without although this was not statistically significant (137). Furthermore when hypertensive patients with and without OSA were compared it was shown that plasma aldosterone concentrations were higher in those with OSA (137). In a previous analysis of individuals with resistant hypertension and OSA urinary aldosterone and plasma aldosterone correlated with the severity of OSA in individuals found

to have concomitant primary aldosteronism as the cause of their resistant hypertension. In the remaining individuals with normal levels of aldosterone only urinary aldosterone correlated with OSA severity (138). This supports the finding of high prevalence of primary aldosteronism (PA) in individuals with OSA and hypertension (139) and PA may need to be excluded when these conditions co-exist if there are other supporting features (e.g. low potassium). In a recent study, treatment of PA either medically or surgically was associated with an improvement in markers of OSA severity (140).

In a recent meta-analysis of 8 studies CPAP, of a minimum duration of 1 month, was not associated with a reduction in plasma aldosterone concentrations (141) despite reportedly good compliance with treatment. Furthermore, when the three RCTs were examined separately there was no change in plasma aldosterone. However, this meta-analysis included those with resistant hypertension raising the possibility of patients within the data set having unrecognized PA. In another meta-analysis that excluded studies of patients with resistant hypertension treatment with CPAP was associated with a reduction in plasma aldosterone (142). In a study that post-dates these meta-analyses individuals with OSA and resistant hypertension were randomized to either CPAP or no treatment for 6 months with a resultant modest decrease in urinary aldosterone (143).

The mineralocorticoid antagonist spironolactone has been trialled in individuals with OSA and resistant hypertension. One study showed an improvement in blood pressure in the spironolactone group as well as in nadir nocturnal saturations and the apnoea-hypopnoea index (AHI) (144). Similar findings occurred in a study examining the use of eplerenone (145) although the findings from both studies are limited by a lack of an appropriate placebo control

group. In a systematic review and meta-analysis of the three available studies it has been shown that antagonism of the mineralocorticoid receptor is associated with an improvement in indices of OSA severity (146) suggesting a bi-directional relationship between aldosterone and OSA severity. This hypothesis is further supported by the finding of increased prevalence of OSA in individuals found to have hyperaldosteronism with an odds ratio of OSA of 1.8 in those with biochemically confirmed hyperaldosteronism (147). This may be mechanistically explained in part by fluid retention within the upper airway in those with OSA (148).

It seems, therefore, that there is a high prevalence of undiagnosed PA in individuals with OSA and hypertension and that this may well skew some of the findings presented above. In small well-defined cohorts, CPAP treatment is associated with a reduction in aldosterone levels whilst OSA per se in the absence of hypertension does not seem to be associated with raised indices of aldosterone. Whether there is a direct effect of hypoxia on renal expression of the mineralocorticoid receptor is less clear though one study suggests that hypoxia might result in down regulation of this receptor (149).

1.5.2 OSA and Testosterone

The association between low levels of testosterone and OSA have been the subject of research for some time, however many of the studies include patients with a spectrum of testosterone levels including eugonadal individuals which may limit some of the study findings. In one small study comparing 10 individuals with newly diagnosed OSA and 7 matched controls although morning salivary testosterone concentrations were similar, the evening levels were found to be significantly lower in the OSA group (150). In two small studies by the same group nocturnal testosterone and luteinizing hormone levels were found to

be significantly lower in individuals with OSA compared to well-matched controls when measured serially across sleep (151, 152). In a separate study there was found to be a negative correlation between oxygen desaturation index and nadir SaO_2 and testosterone (153). In a large study of 1312 men who had a testosterone level measured and who had a subsequent sleep study those with lower testosterone levels were associated with increased nocturnal awakenings and a higher AHI as well as lower nocturnal oxygen saturations (154). Furthermore, CPAP treatment for 3 months had no impact on testosterone levels (155). Whilst a meta-analysis that included 232 patients drawn from 7 studies found that CPAP therapy (duration 1-9 months) was not associated with changes in testosterone levels (156). However, most of the patients included in the analysed studies had normal testosterone levels at baseline which may have masked any potential advantage of CPAP in hypogonadal patients. Patients with co-existent OSA and diabetes have also been studied and CPAP appears not to impact testosterone levels (157).

There are concerns about prescribing testosterone in individuals with OSA. However, increasingly it has been shown that although testosterone therapy worsens markers of OSA severity for approximately 7 weeks this deterioration does not persist at 18 weeks (158, 159). Longer studies are needed to clarify this and patients must be counselled about this. Furthermore, testosterone replacement has been shown to increase the risk of developing OSA compared to well matched controls (160). In an RCT of men with obesity with OSA, testosterone therapy improved sexual desire but only those with the lowest level of baseline testosterone had a generalized sense of improved vitality (161).

Severe OSA does seem to be associated with low levels of testosterone which appear to be unaffected by CPAP therapy. In those individuals who are deemed likely to benefit from testosterone therapy it is important to realize that the individuals OSA may initially deteriorate, but this is likely to be transient. The mechanism linking testosterone to a deterioration in OSA is ill-defined but seems to be independent of upper airway calibre (162).

1.5.3 OSA and the HPA axis.

Cortisol secretion by the zona fasciculata cells of the adrenal glands is under the control of adrenocorticotropic hormone (ACTH). ACTH is secreted by the corticotrope cells of the pituitary in response to corticotropin releasing hormone (CRH) from the hypothalamus. Glucorticoids whether produced endogenously or administered medicinally are major regulators of metabolism. It is increasingly recognised that their action is dependent on insulin action with some effects differing between the fed and fasted state (163, 164). Systemically glucocorticoids cause insulin resistance across most tissue types whilst some of my previously published data from human *in vivo* studies suggests a synergistic effect with insulin in adipose tissue (163). We have previously postulated a role for endogenous glucocorticoids in driving NAFLD (165). The potential mechanisms underlying this are likely mediated by direct effects on the liver as well as indirectly via the adipose tissue. In brief glucocorticoids drive hepatic fatty acid uptake via increased expression of fatty acid translocase (CD36) (166) which then undergoes increased rates of esterification (167) and reduced hepatic export as VLDL TG (163). Although glucocorticoids in the fasted state do not appear to drive *de novo* lipogenesis (DNL) (163) in the fed state the presence of glucocorticoids drives DNL which may well be an insulin-mediated effect (163, 168). This is accompanied by increased gluconeogenesis (169) providing additional substrate for DNL. The increased accumulation of hepatic lipid in

response to glucocorticoids is exacerbated by a reduced secretion of TG from the liver (163) and reduced β-oxidation (170, 171). Increased levels of adipose tissue lipolysis in the fasted state provide further substrate for hepatic lipid accumulation (163) (Figure 1-4).

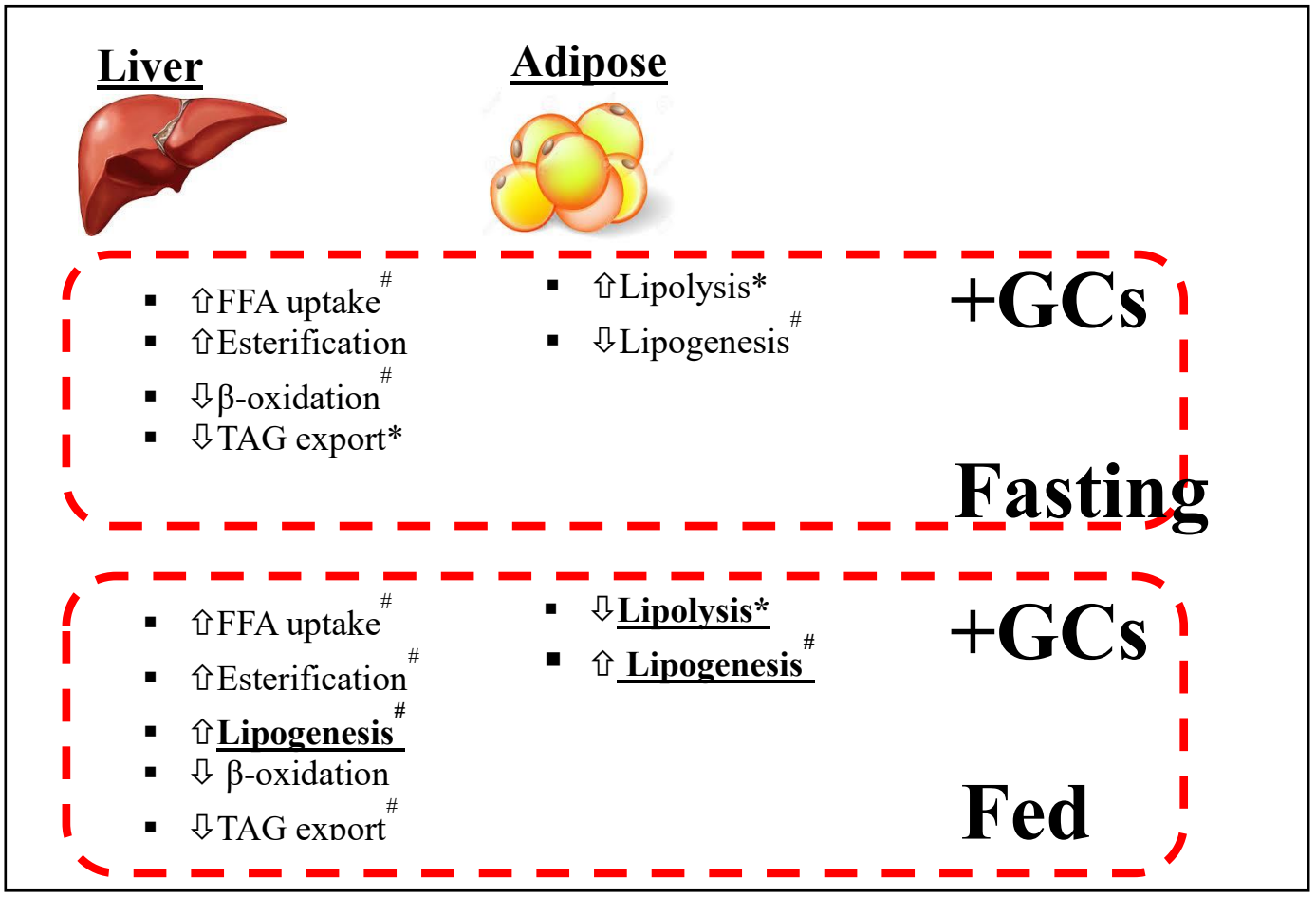


Figure 1-4 The effect of glucocorticoids modulating lipid metabolism in the liver and adipose tissue in the fasting and fed state. (GCs=glucocorticoids; ⇧=increased; ⇩=decreased; # = rodent and cell line data; *= human data (all references included in above text).

Much has been written about altered cortisol levels and OSA. In a study of 56 men with moderate-severe OSA those with severe OSA had lower morning cortisol levels than those with moderate OSA or control subjects; there was a significant negative correlation between morning cortisol and AHI (172). However, in a study of 72 individuals who did not have obesity but who did have OSA and underwent blood sampling hourly, 24 hour levels of cortisol were significantly higher than in 37 matched controls (173). Furthermore, in the same study 2 months of CPAP therapy was shown to reduce cortisol levels when compared to

sham-CPAP (173). In a study of laboratory supervised CPAP therapy 1 week of effective CPAP had no effect on 24 hour cortisol profiles (28). A separate study examining 14 days of CPAP therapy also showed no effect on cortisol levels, however this study was limited by poor compliance with treatment (174). In a three month study with high participant compliance to CPAP therapy, there was a reduction in 24 hour ACTH and cortisol profiles (175). A larger study of 38 patients with OSA treated with CPAP for 3 months showed a reduction in evening cortisol levels (176). The finding of increased cortisol in OSA patients has also been extended to paediatric patients who have been shown to have higher salivary levels of cortisol throughout the day than controls (177). However the potential derangement of the HPA axis in patients with OSA may affect the axis response to a given stressor since those with OSA have a reduced response to a 1µg adrenocorticotropic hormone (ACTH) test (178). In a meta-analysis of 7 studies there was no apparent difference in cortisol levels between controls and patients with OSA although the authors cite heterogeneity of cortisol assessment methods and the statistical tests used as likely confounders (179). In a rodent study intermittent hypoxia was shown to increase plasma corticosterone (the rodent equivalent of cortisol) as well as the production of corticosterone by the adrenal zona fasciculata-reticularis cells in response to ACTH in an *ex vivo* assay providing biological plausibility to the effect seen in some of the human cohort studies (180).

In a large prospective study of 1612 patients with Cushing's syndrome and well-matched controls, those with Cushing's had a 2.82-fold higher risk of developing OSA (181). In a study of 30 females with newly diagnosed Cushing's syndrome (endogenous cortisol excess) there was a high prevalence of previously undiagnosed OSA compared to age and BMI matched controls (182). However, it is important to note that in a separate study

there was a high false positive response in those with OSA undergoing overnight dexamethasone suppression tests that normalized after CPAP therapy for a few days (183). This finding has been shown previously wherein nasal CPAP for 3 months resulted in reduced morning cortisol levels post dexamethasone suppression test (184). As with all CPAP studies variable compliance may affect results and one alternative to CPAP intervention studies is to study CPAP withdrawal. In the only study examining CPAP withdrawal, one night of CPAP withdrawal did not cause an acute stress response in terms of levels of ACTH or cortisol (185). Taken together, the data supports the conclusion that cortisol levels overnight and across the day are higher in those with OSA and that CPAP treatment is associated with a reduction in cortisol levels.

1.5.4 Hypoxia and glucocorticoids

In addition to the association between OSA and circulating levels of cortisol within individual tissues there may be a direct effect of hypoxia either on the pre-receptor metabolism of cortisol or a direct effect on the glucocorticoid receptor. The local bioavailability of cortisol is mediated by the enzyme 11β-Hydroxysteroid dehydrogenase type 1 (11β-HSD1) which reduces the inactive cortisone to cortisol in a manner dependent on the availability of Nicotinamide adenine dinucleotide phosphate (NADPH) as an electron donor. NADPH is itself produced by the enzyme hexose-6-phosphate dehydrogenase (H6PD).

11β-HSD1 has been shown to be induced in adipocytes *in vitro*, in a manner dependent on the transcription factor NF-κB (186). The same paper showed a reduction in adipose expression in diet-induced obesity that corresponded to an increase in angiogenic factors. Furthermore, it has also been shown that 11β-HSD1 knockout mice are protected from

adipose tissue hypoxia and have improved angiogenesis and reduced adipose tissue fibrosis in a model of diet-induced obesity (187). Taken together it seems likely that the hypoxic induction of 11β-HSD1 may be detrimental to expanding adipose tissue limiting the angiogenic response. The regulation of 11β-HSD by hypoxia has also been shown in cardiac myocytes were hypoxia upregulates the 11β-HSD2 isoform resulting in inactivation of cortisol to cortisone (188).

Emerging data from my collaborators also shows a direct role for hypoxia on the glucocorticoid receptor in the liver including activating phosphorylation of the GR and nuclear trafficking of the receptor (Wilson *et al* unpublished). In the published literature it has been shown that hypoxia upregulates the GR in renal proximal tubular epithelial cells as well as potentiating the action of exogenous steroid at the GR. Additionally over expression of HIF1α was shown to upregulate the GR even in the context of normoxia (189).

It seems likely that in addition to the effect of OSA upregulating the HPA axis there may be a direct effect of hypoxia on tissues, increasing cortisol bioavailability via 11β-HSD1 as well an increase in glucocorticoid mediated signalling either via direct effects on the receptor or via potentiation of the action of steroids. These effects may well contribute to the metabolic phenotype seen in OSA.

1.5.5 The metabolic benefit from interruption in glucocorticoid signalling

There is little data about the impact of glucocorticoid receptor (GR) antagonism outside of Cushing's. In one study of patients with type 2 diabetes, antagonism of the GR in combination with inhibition of glucocorticoid synthesis for one week was associated with improvements in insulin sensitivity, gluconeogenesis and improvements in insulin mediated

suppression of glycerol and fatty acid suppression (190). RU486 (also known as Mifepristone) and is a non-selective competitive inhibitor of several steroid receptors including the glucocorticoid receptor, mineralocorticoid receptor, progesterone receptor and androgen receptor. The glucocorticoid receptor antagonist RU486 has been trialled in post-menopausal women with a resultant improvement in total cholesterol and HOMA-IR (191). RU486 has also been used to try to prevent metabolic complications in patients treated with antipsychotic agents (risperidone and olanzapine) with some improvement in lipid profile, glycaemic control and weights (192, 193). In these studies which used RU486 at a dose of 600mg for 6 weeks the medication was well tolerated with low rates of reported AEs (192, 193). RU486 has not been studied in patients with OSA or in the context of human or animal models of intermittent hypoxia.

1.6 Summary, hypotheses and aims

The contribution of OSA to metabolic disease has only been partially defined. Recent work from both animal and human studies suggests that OSA may play an important role in the pathogenesis of NAFLD. The mechanisms linking these two diseases are comparatively poorly understood. Whether the action of OSA to contribute to NAFLD is via a direct effect on the liver or via an intermediary metabolic tissue such as subcutaneous abdominal adipose tissue is unknown. Given the existing data linking OSA and the hypothalamo-pituitary-axis a role for glucocorticoids driving this metabolic phenotype is plausible, though it has not been previously examined. Furthermore, the methodologies used previously to study steroidogenesis in OSA have been limited. The work undertaken in this doctoral thesis aims to address some of the current discrepancies in the literature as well as some of the remaining

mechanistic questions with a translational body of work including *in vivo* and *ex-vivo* human studies, an animal model and *in vitro* cell-based work.

1.6.1 OSA and intermittent hypoxia have a direct effect on adrenal steroidogenesis.

To test this hypothesis, I aim to:

- Examine the full urinary steroid profile of patients with OSA who are established on CPAP treatment and are then randomised to either receive sham treatment or continue CPAP (Chapter 3).

- Examine the plasma steroids in healthy volunteers exposed to intermittent hypoxia (Chapter 6a).

1.6.2 The action of OSA and intermittent hypoxia is mediated via effects on adipose tissue

OSA and hypoxia have been postulated to cause an inflammatory adipose phenotype that could contribute to the development of metabolic disease however much of the experimental work involves non-physiological conditions. To test this hypothesis, I aim to:

- Examine the gene expression profile of subcutaneous abdominal adipose of patients who are established on CPAP treatment and are then randomised to either review sham treatment or continue CPAP using a high-throughput gene expression technique called a Fluidigm® (Chapter 3).

- Examine the gene expression profile of primary subcutaneous abdominal adipocytes cultured in different oxygen tensions to determine whether adipose tissue is oxygen sensitive at a range of physiological oxygen tensions (Chapter 4).

- Examine the metabolic effect of intermittent hypoxia on adipose tissue metabolism in healthy volunteers using a combination of a hyperinsulinaemic-clamp and stable isotopes (Chapter 6a).

1.6.3 OSA and intermittent hypoxia drive hepatic lipid accumulation

To address this hypothesis I will:

- Examine the metabolic effect of intermittent hypoxia on hepatic lipid metabolism in healthy volunteers using a combination of a hyperinsulinaemic-clamp and stable isotopes (including deuterated water) (Chapter 6a).

- Examine whether hepatic lipid synthesis is increased in rats exposed to intermittent hypoxia (Chapter 7).

1.6.4 Glucocorticoid receptor antagonism is metabolically beneficial and can protect against the metabolic effects of intermittent hypoxia

To evaluate this hypothesis I will:

- Examine the baseline metabolic data of healthy volunteers treated for 1 week with the glucocorticoid receptor antagonist (RU486) (Chapter 5).

- Study whether a glucocorticoid receptor antagonist (RU486) modulates the metabolic action of intermittent hypoxia in healthy volunteers (Chapter 6b)

2. General Methods

2.1 RNA extraction and cDNA synthesis

The method detailed below was used for the CPAP withdrawal study (Chapter 3), tissue culture (Chapter 4) and rodent work (Chapter 7).

Snap frozen tissue (**Chapter 3 and 7**) was subsequently transferred to 1ml of Tri Reagent® (SigmaAldrich, UK) and homogenized mechanically before being transferred to a new Eppendorf. Tissue culture samples (cultured adipocytes) (**Chapter 4**) were lysed in 1ml of Tri Reagent®. The protocol for both tissue and cultured adipocytes is then as follows. Samples were then centrifuged (10 min; 885g; 4˚C). 200 µl of chloroform was added and the samples were agitated for 1 minute before being allowed to stand at room temperature for 15 minutes. Samples were then centrifuged and the aqueous phase was transferred into a new Eppendorf. A further 500 µl Tri Reagent® and a further 100 µl of sample was added to the original tube. This was then agitated, allowed to stand and centrifuged as before prior to adding this aqueous phase to the aqueous phase collected in the previous step. To these combined aqueous phases 750 µl of isopropranol and 1 µl of GlycoBlue (Thermo Fisher Scientific, UK) was added and the samples were kept at -20˚C overnight. Samples were centrifuged for 30 mins and the supernatant was discarded. The pellets were then washed in 80% ethanol before further centrifugation. This washing step was repeated once. The pellet was then dissolved in RNAse free water prior to quantification on a NanoDrop (ND1000, ThermoScientific, Wilmington, DE, USA). The RNA was diluted to a concentration of 50ng/µl before being used for cDNA synthesis.

For cDNA synthesis the components of the kit (BD Biosciences, Berkshire, UK) were allowed to reach room temperature and briefly vortexed before preparing the master mix

solution on ice. The components of the master mix included 10X RT buffer, 25XdNTP Mix, 10XRT Random Primers, Multiscribe^{TM} Reverse Transcriptase, RNase inhibitor and Nuclease-free H_2O. 10µl of the 2X RT master mix was added to 10µl of the RNA sample prior to sealing, centrifugation and thermal cycling. The thermal cycler ran at 4 steps (25°C 10 min; 37°C 120 min; 85°C 5min; hold step at 4°C).

1µl of each sample was pooled together and diluted with TrisHCL to make a dilution series between 1:10 to 1:320. The reaction included 4µl of 2 X Taqman Universal PCR Master mix (KapaBiosystems, Massachussets, USA), 0.4 µl of A qPCR was then run on the Corbett RotorGene qPCR (ThermoFisher, UK) to ensure the reverse transcription step had worked and to determine the desired dilution prior to qPCR. The cDNA was diluted 1:20 in TrisHCL. The cDNA was then used for conventional qPCR except for in the case of the CPAP withdrawal study which employed a custom designed fluidigm assay to quantify changes in gene expression (**Chapter** 3). The details of the fluidigm are found within **Chapter 3**.

2.2 Gene expression

Conventional real-time PCR was used to determine mRNA expression of the key genes within both human adipocyte (**Chapter 4**) and rodent liver tissue (**Chapter 7).** mRNA expression levels were determined using an ABI 7900HT sequence detection system (Perkin-Elmer Applied Biosystems, Warrington, UK). All reactions were carried out in 6µl final volume in reaction buffer, containing 3µl of 2 X Taqman Universal PCR Master mix (KapaBiosystems, Massachussets, USA), probe-primer mix for gene of interest (0.3 µl) and 2.7µl cDNA. All adipocyte data gene expression was standardised against RNA polymerase II (POL2RA). Many of the typically chosen housekeeping genes in adipocyte biology (GAPDH, PPIA etc) are differentially regulated in hypoxia whilst POL2RA expression is known to be stable in hypoxia (194) and was stable in the current work. Rodent liver tissue gene expression was standardised against β-actin which was stably expressed. Data were expressed as the cycle number at which logarithmic PCR plots crossed a calculated threshold line (Ct values) and used to determine Δct values [Δct=(ct of target gene)-(ct of housekeeping gene)]. Arbitrary units were calculated using the formula (1000*2-Δct). All statistics were performed on Δct values.

2.3 Western blotting

Isolation of protein from human AT and western blot for HIF1A

Frozen adipocytes were homogenized in a urea/SDS buffer supplemented with complete protease inhibitor (Roche Applied Science) and protein concentrations were quantified and normalised (Pierce^{TM} BCA Protein Assay, Thermofisher). Western blotting was performed by chemiluminescent method using the ChemiDoc MP system (BioRad, Hertfordshire, UK).

Criterion XT Bis-Tris Gels and the Trans-Blot® Turbo™ system transfer pack (both BioRad, Hertfordshire, UK) were used. The antibodies used were rabbit anti- HIF-1 antibody (10006421) (diluted 1:100) (Cayman, Cambridge, UK) and the secondary was HRP-IgGs (Agilent Dako, Cheshire, UK) (diluted 1:2500). HRP-conjugated anti-β-actin was used as a control (Abcam, Cambridge, UK). HRP action was measured using ECL detection (BioRad, Hertfordshire, UK). Densitometry was performed using ImageJ.

2.4 Plasma analysis

Whole blood was collected throughout the study according to the sampling protocol described above. Blood was collected into heparinised syringes (Starstedt, Leicester) and centrifuged for 10 minutes at 825g 4°C (Eppendorf Centrifuge 5702R, Stevenage, UK) to isolate plasma for subsequent analysis.

2.5 Radioimmunoassay Insulin

Plasma insulin was measured using a human-specific insulin radioimmuno assay (HI-14K, EMD Millipore, St. Louis, Missouri, USA) according to the manufacturers protocols. In this assay a fixed concentration of radio-labelled tracer antigen (^{125}I-labeled Human Insulin) is incubated with a fixed concentration of antiserum. The addition of unlabelled antigen (from the plasma sample) causes competition for the antibody binding sites on the antibody. As such the amount of radiolabelled tracer bound to the antibody decreases with increasing concentration of insulin in the samples of interest. Free tracer can then be washed off and the concentration of insulin can be calculated against established insulin standards. All samples were measured in duplicate. The co-efficient of variation between the duplicates was <10% otherwise samples were repeated.

2.6 Biochemical sample analysis

Plasma samples were run on our in-house laboratory clinical analysers (iLab 600/650) for the quantification of plasma TG, NEFA, 3-hydroxybutyrate and glucose. The analyser uses a photometric method with detection of colour changes at appropriate wave lengths for each given method. The samples were analysed according to established in-house standard operating procedures. Each method requires a specific calibration series and associated quality controls that are required to be within pre-determined parameters prior to running the plasma samples.

2.7 VLDL fraction isolation

Separation of the VLDL-rich fraction (Svedberg floatation rate (S_f) 20-400) was achieved using density gradient ultracentrifugation. Ultracentrifugation was performed in a floor standing centrifuge (SW40 Ti, Beckman Instruments, Palo Alto, CA, USA) swinging bucket rotor at 284061g and 15°C for 16 hours. This method enabled isolation of the VLDL fraction. At which point apoB and TG concentrations were analysed using a commercially available laboratory analyser (iLab 600/650). The VLDL fraction was then further processed to isolate the TAG and NEFA fractions as detailed below.

2.8 Solid phase extraction of plasma and VLDL fraction samples.

This method describes the extraction of lipid methyl esters from different plasma lipid fractions: VLDL TAG and NEFA; and plasma TAG and NEFA.

The extraction of total lipid from plasma and VLDL fractions was performed via Folch extraction with subsequent separation of lipid fractions (TG and NEFA) and then preparation

of fatty acid methyl esters as we have described previously (195). The full method is detailed below.

The determination of the lipid composition of each fraction is dependent on the following calculations which result in the final figure expressed as Mol%. The Mol% is the percentage by molarity that each individual lipid (identified by carbon chain length) contributes to the total pool of lipid within that fraction (e.g. TAG or NEFA fractions). The calculations immediately below to calculate Mol% are ultimately used to calculate the production (Ra) and disposal of NEFA (Rd). The calculation of Ra and Rd NEFA are detailed in the following section.

The calculations that result in this Mol% are as follows:

1. Concentration (µmol/L)=((GC/MS Area of desired peak/GC/MS Area of internal standard)*Molecular weight of internal standard)/Molecular weight of desired peak*((1/volume of sample)*1000)/3
2. Mol%=(Concentration of desired peak/Total concentration of all peaks)*100

The calculations above are dependent on the presence of an internal standard which is added to the samples prior to the extraction process. Although the external standard does not contribute to the calculations of the data it is used to calculate the recovery of the sample processing which is a marker of efficiency of the Folch extraction. The external standard is added to the GC vials after extraction prior to running the samples on the GC/MS. The method for the extraction is detailed below.

500µl of sample or blank (saline) was added to each tube as well as 5 ml of 2:1 (v:v) chloroform:methanol solution as well as 20µl of internal standard. The samples were mixed on the rotary mixer to ensure prior to the addition of 1ml of 1M NaCl to each tube. The samples were mixed again prior to centrifugation for 10 minutes at 1296g at 14 (±4) °C (Beckman J6 floor-standing centrifuge, Palo Alto, CA, USA). The aqueous phase was discarded and the solvent phase was transferred into a new tube before being evaporated to dryness in at 50 (±10) °C under Nitrogen (freestanding evaporator Zymark).

Sample separation using SPE columns to extract different lipid fractions

The remaining method for lipid extraction involves three stages: two extraction stages and one methylation stage.

Stage I

The dry lipid extract was then dissolved in 1ml of chloroform. The subsequent extraction relies on the principle that different lipid fractions are soluble in different solvents and undissolved lipid fractions are retained in the lipid columns till they are eluted with the appropriate solvent. Initially the columns were pre-washed with 2 x 1ml of acetone then with 2 x 1ml of chloroform collecting the solvent into the waste container. The samples were added to the columns and allowed to drip through into the cholesterol ester/TG (CE/TG) collection tubes. The remainder of the CE/TG fraction was eluted with a further 2 ml of chloroform. The samples were then dried down in the Zymark as before. The samples were retained for subsequent elution of the TG fraction in stage II. Fresh tubes were placed under the columns

and the NEFA fraction was eluted with the addition of 2ml of diethyl ether with 2% acetic acid. The NEFA samples were dried down in the Zymark as before.

Stage II

New columns were preconditioned with 4 x 1 ml of hexane. The CE/TG fraction from stage I was dissolved in 1 ml hexane and added to the columns and allowed to drip through into the waste collection. The CE fraction was further eluted with 2 ml of hexane into the waste collection. The waste collection was then replaced with sample collection tubes and the TG fraction was eluted with 2 x 1 ml of hexane: chloroform: methanol (100:5:5). This TG fraction was then dried down in the Zymark as before and returned for methylation.

Methylation

400µl of toluene-BHT solution was added (10mg butyl hydroxytoluene/100ml toluene) to the dried fraction and vortexed. 800 µl of 1.5% H_2SO_4 was added (made in methanol) to the above. The tubes were capped and vortexed before being placed in the water bath for methylation for 1 hour. The samples were then allowed to cool. 2ml of neutralising solution was added ((25g $KHCO_3$ (0.125M) + 34.6g $K2CO_3$ (0.125M) made up to 500ml with distilled water). Diluted stock 1 in 5 for use) 2 ml of cyclohexane was then added. The samples were subsequently placed on the rotary mixer prior to centrifugation as before (10 minutes at 1296g at 14 (±4) °C (Beckman J6 floor-standing centrifuge, Palo Alto, CA, USA)). The upper solvent phase was transferred to a new tube and dried down in Zymark. 20 µl of external standard was added to each gas chromatography vial. 190 µl chloroform was added to the dried down samples and vortexed. The contents of these tubes were then

transferred to the gas chromatography vials using a glass pipette. Inserts were used for the NEFA samples within the GC vials. The STDB and RM6 standards were prepared into GC vials by adding 100 µl of stock solution and 900 µl of chloroform. These standards were run with the samples on the and were made fresh every 2 weeks and subsequently on the GC/MS.

The GC allowed for identification of the areas (or relative amounts) of the individual fatty acid within the isolated lipid fraction (ie either NEFA or TG) whilst the GC/MS allowed for the identification of the amount of labelled isotope relative to the unlabelled metabolite (tracer to tracee ratio (TTR). In the present study this was either the labelling of palmitate (either in the NEFA or TG fraction) with ^{13}C-palmitate or the labelling of palmitate (within the TG or VLDL-TAG) fraction with deuterated water ($^{2}H_2O$).

2.9 Calculation of Ra NEFA and Rd NEFA

The calculation of whole body Ra and Rd NEFA is reliant on knowing the ^{13}C-Palmitate TTR corrected for background (i.e. prior to the infusion of stable isotope) (A). It is also reliant on knowing the NEFA concentrations for each sample (µmol/L) (D). The Mol% detailed above is also required (E).

Ra palmitate (B) (per kg body weight) = infusion rate (µmol/kg body weight/min) / A

Ra palmitate (C) (whole body) = B * participants weights (kg)

Ra NEFA whole body (F) (µmol/min) = C / (E/100)

Rd NEFA whole body (µmol/min) = F / D

2.10 Deuterium plasma water analysis by Gas Bench and calculation of *de novo lipogenesis*

In addition to the GC and GC/MS TG and VLDL TG data the calculation of *de novo lipogenesis* relies upon the deuterium enrichment of the plasma water fraction. Deuterium plasma water quantification is necessary for the quantification of *de novo lipogenesis* according to the calculation ($\Delta\ ^{2}H/^{1}H$ ratio in palmitate methylester/($\Delta\ ^{2}H/^{1}H$ ratio in water pool*22))*100, where 22 is the number of water molecules incorporated into palmitate via DNL.

Preparation of standards

The plasma water samples were run on the gas bench having first run a set of standards to allow subsequent calculation of plasma water deuterium enrichment. A series of standards was prepared. The initial stock solution (standard 1000) w as prepared by weighing 0.80g of 99.8% deuterium and dissolving in 5L of deionised water. The remaining standards (standard 750, 500 and 250) were prepared via onward dilution of the standard 1000.

The gas bench was first calibrated using the previously prepared standards prior to running the samples. The method for the calibration followed that of the samples which is detailed below.

Samples

The Gas bench II mode was used throughout. After calibration, the samples were then prepared. Thawed plasma samples were spun at 1296g for 10 minutes at 4^{o}C. Standards 0, 250

and 500 allowed to reach room temperature. For all sequences there were 1x deionised water, 2xStandard 0 and 2x standard 500 run at the start of each sequence, 2xstandard 0 and 2x standard 500 run between the first set and duplicate set of samples and 1x 250, 2x diluent, 2x standard 0 and 2x standard 500 run at the end of each sequence. There was a standard 250 run after every 5-6 samples. For all standards 500ul of standard was pipetted into exetainer tubes. For the diluent samples 500ul of diluent (DI water) was pipetted into two tubes.

All samples were weighed for correction values: the empty tube was weighed first and the weight recorded, the DI water (diluent) was then added and the weight recorded then the plasma was added and the weight further recorded. For all enriched plasma samples, they were diluted 1:50 (490µl deionised water and 10µl plasma). For all unenriched (background) samples they were diluted as follows: 200µl of deionised water and 300µl of plasma. All enriched samples were run in duplicate. Samples were then vortexed. One catalyst was added to each tube. The samples were placed into the sample block (23^{o}C). Having ensured that the first set of standards were within in-house parameters the samples were run.

2.11 Glucose disposal and production

The analysis of D2 glucose by GC/MS was dependent on accurate standards and controls which required dilution in deionised water. Unlabelled glucose (D0) was made to a working stock concentration of 100 µg/ml. Isotopically labelled glucose (D2) was made to two working dilutions (Dilution 1= 10 µg/ml; Dilution 2= 1 µg/ml). The subsequent dilutions to make the appropriate standards are detailed below.

Table 2-1 The dilutions required to make standards for GC/MS analysis of D2 glucose

Standard	D2 dilution stock	D2 Volume (ul)	Do Volume (ul)	Approx TTR
1		0	200	0
2	2	10	200	0.00051
3	2	20	200	0.00103
4	2	100	200	0.00514
5	1	20	200	0.01028
6	1	50	200	0.02570
7	1	100	200	0.05141
8	1	150	200	0.07711
9	1	175	200	0.08997
10	1	220	200	0.11310

Having thawed the samples, they were then briefly vortexed before centrifugation at 2026g for 10 minutes at 4ºC. 50ul was pipetted into a LP4 tube before the addition of 500ul ethanol at which point the samples were vortexed prior to further centrifugation at 2026g for 5 minutes at 4ºC. The supernatant was transferred into 4.5ml tubes and dried down in a centrifugal evaporator for 45 minutes. 100ul of 2% methylhydroxamine hydrochloride in pyridine (2% w/v so 0.02g/1ml) was prepared and was added to all samples. Samples were then capped, vortexed and placed in a heating block at 90ºC for 2 hours. Samples were cooled then 50ul of BSTFA+1%TMCS (N,O-Bis(trimethylsilyl)trifluoroacetamide + 1%

Trimethylchlorosilane) was added. Samples were capped, vortexed and placed back in the heating block at 120ºC for 15 minutes. Samples were again cooled then dried in the centrifugal evaporator. 500µl decane was added and samples vortexed. 50µl of sample was pipetted into GC vial containing 500µl decane. GC vials were capped, vortexed then run on the GC/MS to identify the enrichment of glucose with isotopically labelled glucose ([^{2}H]-glucose).

The calculations required to ascertain the Ra and Rd of glucose are derived from the Steele equation (196) and are detailed below. The 321/319 ratio is the tracer/tracee ratio of [^{2}H]-glucose labelled to unlabelled glucose.

1. Average TTR = ((TTR 321/319-background TTR) + (TTR 321/319 for proceeding measurement))/2
2. dTTR/dt = ((TTR-background TTR) - (TTR-background TTR for proceeding measurement))/time interval between the measurements in minutes)
3. Total glucose infused during the clamp (mg/min) = rate of the 20% Dextrose infused
4. Total glucose infused during the clamp (µmol/min/kg) = above*1000/(Molecular weight of glucose*weight of the participant in kg)
5. mg/min of labelled ([^{2}H]-glucose) via the 20% Dextrose = step 3*TTR of the infusate (which here is the 20% Dextrose)
6. total mg/min labelled ([^{2}H]-glucose) = step 5 + infusate rate of [^{2}H]-glucose within the Normal Saline
7. Glucose value of plasma (mg/l) = glucose measured in mmol/l*180

8. Total Ra (mg/min) = ((infusate rate of [^{2}H]-glucose within the Normal Saline *0.99/step 1) - ((0.65*plasma volume of patient* Average (step 7, proceeding step 7)*step 2)/step 1))+(step 5/step 1)

   0.65 is the distribution fraction of glucose taken from the original Steele calculations

   The distribution volume of the patient is calculated by weight of patient (kg) x 0.22

9. Total Ra (µmol/min/kg) = step 8*1000 / (180*weight of patient in kg)

   180 is molecular weight of glucose

10. Endogenous Ra (µmol/min/kg) = step 9-step 4
11. dG/dt = (step 7-proceeding step 7) / (time between two values (in minutes))
12. Rd (mg/min) = step 9-step 11*distribution volume*distribution factor + step 6
13. Rd (µmol/min/kg) = step 12*1000 / (180*weight of patient in kg) where180 is molecular weight of glucose

2.12 Isotopic enrichment of CO_2 in breath

The ^{13}C enrichment of CO_2 in breath from the infused ^{13}C-palmitate was employed for the quantification of fatty acid oxidation.

Expired breath was collected hourly throughout the study and was stored at room temperature prior to measurement and analysis. The CO_2 was separated from the other gases using a capillary column (CP-PoraPLOTQ; Variant Ltd, Oxford, United Kingdom) using the GC-combustion-isotope ratio mass spectrometer (GC/C/IRMS). The splitless injection mode

with an injection volume of 10 µl and an injector temperature of 110ºC were used. The oven temperature was maintained at 35ºC. The run time per sample was 10 min. The column flow was held constant at 1.2 mL/min. The results ($\delta^{13}C\ ^{0}/_{00}$) were only accepted if the background enrichment was in accordance with the anticipate range of natural enrichment. The tracer to tracee ratio (TTR) ($^{13}C{:}^{12}C$) ratio was calculated according to the previously published calculation (197):

$$TTR\ (^{13}C{:}^{12}C) = [(\delta^{13}C\ ^{0}/_{00}/1000)+1] \times 0.0112372$$

The rate of expiration was calculated by multiplying the TTR (tracer-to-tracee ratio) of $^{13}CO_2$ to $^{12}CO_2$ by the $\dot{V}CO_2$ (mmol/min) (197). The $\dot{V}CO_2$ was calculated based on the subjects' basal metabolic rate which itself was estimated by body composition measurement (TANITA®,Amsterdam-Zuidoost, Netherlands). The calculation is as follows:

$$=(((((KJ/(15.913/0.85)+5.207))/24)/60))*(1000/22.4)$$

Where KJ is the basal metabolic rate in kilojoules, 15.913 is the energy expenditure per litre of O_2 consumed (198), 0.85 is the respiratory quotient, 5.207 is energy expenditure per litre of CO_2 (198) produced, 24 is the hours in a day, 60 is the minutes in an hour and 1000/22.4 is the conversion from litres/min to mmol/min.

2.13 Microdialysis

Subcutaneous abdominal adipose microdialysis was used as we have described previously (163, 199). This method allows the measurement of urea, glucose, pyruvate and lactate from the adipose interstitial fluid as a measure of metabolism directly from

subcutaneous abdominal adipose tissue. A single microdialysis catheter (Linton Instrumentation, Norfolk, UK) was inserted under local anaesthetic (1-2 ml of 1% lidocaine) into the subcutaneous adipose tissue 5-10 cm to one side of the umbilicus. Using the microdialysis pump, a microdialysate solution (physiological sterile saline solution) was introduced into the catheter (perfusion rate = 0.3µl/minute). Microdialysis took place over the duration of the hyperinsulinaemic clamp and basal phase. Samples were taken every 30 minutes throughout the study period and at the end of the sampling period the catheter was removed. Microdialysate fractions were stored at -80°C and subsequently analysed by automated analyser (ISCUS flex) for glycerol, glucose, lactate and pyruvate according to manufacturer's instructions. Paired samples (i.e. samples from air and then from hypoxia) from an individual were always processed sequentially.

Samples were collected into the microdialysis vials as described above. The microdialysis samples were then stored at -80°C prior to analysis on the ISCUS Clinical Microdialysis Analyser. The Analyser was first calibrated using pre-prepared calibrators (Reagent Set A, Linton Instrumentation, UK). Samples were then run sequentially. The samples from each participants' visit 3 and visit 5 were run consecutively after the same calibration. Results that were not consistent with the time points pre and post the potentially anomalous sample were re-run.

3. Adrenal steroidogenesis and adipose tissue responsiveness to OSA

3.1 Introduction

3.1.1 OSA and adrenal steroidogenesis

OSA is associated with changes in steroidogenesis and CPAP has been shown to modulate this. The published studies rely on the measurement of plasma steroids typically from early morning fasted samples and no previous studies have assessed steroidogenesis using urinary GC/MS from overnight urine collections (i.e. from when OSA is most clinically relevant). Adrenal steroidogenesis is often classified as sex steroids, mineralocorticoids and glucocorticoids as outlined previously (**Chapter 1, Figure 1-3**). The effect of CPAP on plasma steroid levels has been studied though these studies are typically limited by variable CPAP compliance. CPAP withdrawal offers a comparatively "cleaner model" for the study of CPAP effect.

The major sex steroid in men is testosterone. Nocturnal testosterone is typically lower in those with OSA (150) and a low testosterone level is associated with an increased risk of OSA (154) as well as OSA severity (153). CPAP therapy (duration 1-9 months) is not associated with changes in testosterone levels (156).

Plasma aldosterone is significantly higher in patients with OSA and hypertension compared to control patients with hypertension but not OSA although maybe unchanged in normotensive patients (137). In another meta-analysis that excluded studies of patients with resistant hypertension treatment with CPAP was associated with a reduction in plasma aldosterone (142). Given the association between aldosterone and OSA severity (138) as well as the finding that treatment of primary aldosteronism improves OSA there is a clear reciprocal relationship between aldosterone and OSA (140).

The available meta-analysis of 7 studies, which showed no difference in cortisol levels between controls and patients with OSA, was limited by heterogeneity of cortisol assessment methods and statistical tests used (179). In the largest published series, 72 non-obese individuals with OSA underwent blood sampling hourly and 24 hour levels of cortisol were significantly higher than in 37 matched controls (173). Furthermore, in the same study 2 months of CPAP therapy was shown to reduce cortisol levels when compared to sham-CPAP (173) a finding reproduced (175, 176). One study examined the effect of one night of CPAP withdrawal and did not show a change in ACTH or cortisol (185). However, a previous study showed a negative correlation between morning cortisol and AHI as well as lower morning cortisol in those with severe OSA compared to moderate OSA or control patients (172)

We hypothesise that CPAP withdrawal is associated with activation of the HPA axis which we intend to demonstrate using GC/MS urinary steroid profiles in a randomised controlled study of CPAP withdrawal.

3.1.2 OSA and adipose tissue

Adipose tissue uses very little oxygen (2-4 μmol.100g^{-1}.min^{-1}) compared to more metabolically active tissue like skeletal muscle (57). Whilst debate exists around adipose oxygenation across obesity as discussed in chapter 1 it seems reasonable to conclude that the adipose tissue of patients with hypoxia associated respiratory disease will be comparatively hypoxic. Two previous studies show only a modest effect of CPAP initiation on subcutaneous abdominal adipose gene expression and have been discussed within chapter 1 (62, 63).

The key advantages of the current work are:

- CPAP withdrawal model means that patients serve as their own controls circumventing some of the heterogeneity in previously studied cohorts comparing those with OSA to controls
- CPAP withdrawal models protect against the variable compliance seen in CPAP initiation models.

The key disadvantage of the model may be that it is not directly possible to extrapolate these data to a CPAP intervention study at least in part because of effects of CPAP on the upper airway musculature.

For these reasons, despite varied results in CPAP initiation studies we think that the CPAP withdrawal model represents a useful experimental system to study the relationship between OSA and steroidogenesis as well as OSA and subcutaneous abdominal adipose gene expression.

We hypothesise that OSA has a direct effect on adrenal steroidogenesis which we will assess using GC/MS of overnight urine collections from patients in a CPAP withdrawal study as well as measuring morning plasma steroid levels. We also hypothesise that OSA has a direct effect on the transcriptional profile of subcutaneous abdominal adipose which we will assess using a high-throughput gene expression technique called a Fluidigm® from patients in this CPAP withdrawal study.

3.2 Materials and Methods

3.2.1 Research strategy

In this chapter, we will examine the effect of CPAP withdrawal on adrenal steroidogenesis as well as on adipose tissue gene expression. The CPAP withdrawal model will be achieved by randomising patients established on CPAP therapy for confirmed OSA to either sham therapy or continued CPAP. Overnight urine collections pre and 2 weeks post randomisation will be analysed by GC/MS to analyse the steroid profile and fasted morning subcutaneous abdominal adipose biopsies taken at the same time points will be analysed to study the effect on gene expression.

We will test the hypotheses that (1) OSA has a direct effect on adrenal steroidogenesis and that (2) OSA has a direct effect on the subcutaneous abdominal adipose tissue.

3.2.2 Statement of contributions

The patient facing components of this clinical study were conducted by Professor John Stradling, Dr Chris Turnbull and staff at the Oxford Centre for Respiratory Medicine, Oxford, UK (REC Reference: 12/SW/0254) (200). Urine, plasma and adipose tissue were provided from the study for our analysis. Urinary steroid measurement was conducted by Prof Wiebke Arlt and Miss Beverley Hughes at the University of Birmingham, UK. The urine and plasma statistical analysis was conducted by myself and Dr Turnbull. Adipose and plasma analysis was conducted by me (Dr Jonathan Hazlehurst) under the supervision/advice of Dr Laura Gathercole and Dr Marijana Todorcevic (both colleagues at the time at OCDEM, University of Oxford).

3.2.3 Study design

This study included 23 individuals with proven obstructive sleep apnoea who were already established on CPAP therapy. There were 23 participants included in this study as that was the subset of patients recruited in Oxford that was part of a larger multi-centre study. Patients were recruited from within the respiratory clinic at the Churchill Hospital. Individuals were randomised to receive sham or continued CPAP. Sham (sub therapeutic CPAP) was established using the ResMed Autoset machine by setting the CPAP machine to the lowest pressure (<1cm H_2O), insertion of a flow-restricting connector at the machine outlet, and insertion of six extra holes in the collar of the main tubing at the end of the mask to allow air escape and to prevent rebreathing of CO_2. This CPAP withdrawal model is well validated and it has been shown that 2 weeks of CPAP withdrawal is sufficient to cause a return of ODI and AHI to pre-treatment levels as well as changes to blood pressure and objectively measured sleepiness (201). CPAP withdrawal as a model of OSA rather than CPAP initiation has the additional advantage that the patients are well characterized and are established on CPAP therapy whilst in CPAP initiation studies poor compliance further complicates study design.

Prior to commencing the study patients undertook an overnight timed urine collection which was repeated on the final night of the study. Additionally, on the morning prior to starting the study and at the end of the 2 weeks patients had a fasted blood sample collected in heparinised tubes from which plasma was isolated by centrifugation (10 mins; 885g). At these same time points participants had abdominal adipose tissue biopsies (full details below) (Figure 3-1).

3.2.4 Inclusion and Exclusion criteria

Inclusion

- Objectively confirmed obstructive sleep apnoea defined on conventional criteria (at the time of original diagnosis) also with an oxygen desaturation index (ODI, ≥4% dips) of >20 (this threshold excludes participants with borderline OSA, in whom there may be little experimental effect).

- Currently >20/h oxygen desaturations (≥4% dips) returning during an ambulatory nocturnal pulse oximetry performed at the end of a 4-night period without CPAP, prior to entry into the study.

- Treated with CPAP for more than 12 months, minimum compliance 4h per night, AHI <10 with treatment (derived from CPAP download data).

- Written informed consent.

Exclusion Criteria:

- Previous ventilatory failure (awake resting arterial oxygen saturation <93% or arterial PCO_2 > 6kPa) or severe respiratory disorders other than OSA.

- Unstable, untreated coronary or peripheral artery disease, severe arterial hypertension (>180/110mmHg), severe arterial hypotension (<90/60mmHg).

- Previously diagnosed with Cheyne-Stokes breathing.

- Current professional driver.

- History of any sleep-related driving or other accident.

- Age <20 or >75 years at trial entry.

- Acute upper respiratory infection.

- Mental or physical disability precluding informed consent or compliance with the protocol

- Non-feasible trial follow-up (for example, distance from follow-up centre, physical inability).

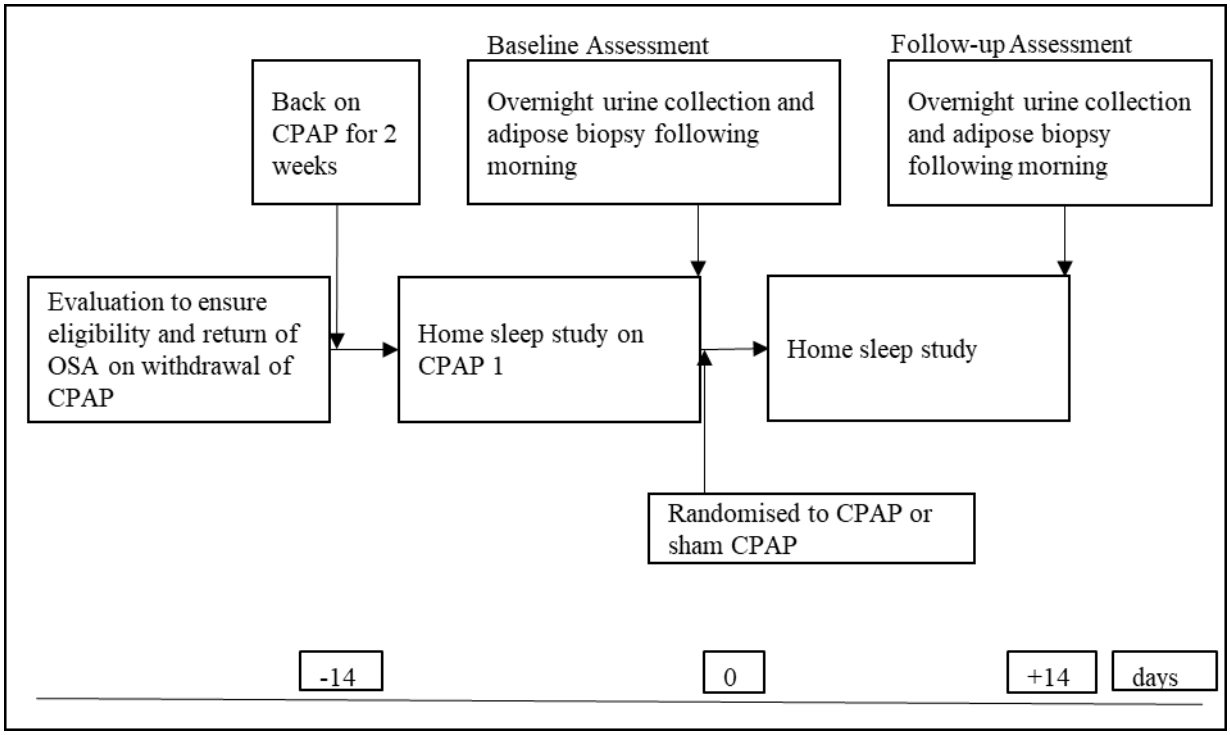


Figure 3- 1 The experimental set up and assessment schedule for the CPAP withdrawal study. (OSA= obstructive sleep apnoea; CPAP=continuous positive airway pressure)

3.2.5 Urinary steroid profiling (GC/MS)

Timed overnight urine collections were obtained from the patients in the CPAP withdrawal study. The volume and duration of collection was recorded. Analysis of the samples was performed by a blinded assessor. Quantification of 32 distinct adrenally derived steroids and 17 subsequent steroid ratios was carried out by GC/MS. The analytes measured are typically not the steroids or precursors themselves but compounds derived from hepatic or renal oxido-reduction and glucuronide or sulphate conjugation. Urinary steroid profiles were then compared pre and post 2 weeks of either continued therapy or sham CPAP. The method is as described previously (202) and in brief conjugated and free steroids were extracted from 1ml aliquots of urine by solid-phase extraction. The extraction process has five stages: 1). The initial solid phase extraction of free and conjugated steroids; 2) Enzyme hydrolysis of steroid conjugates; 3) Solid phase extraction

of free steroids; 4) Chemical derivatisation; and 5) Liquid/liquid extraction. The final derivative (in cyclohexane solution) which is injected into the GC/MS is termed a methyloxime-trimethylsilyl ether.

GC/MS used was an Agilent 5973 instrument operating in selected-ion-monitoring (SIM) mode to achieve sensitive and specific detection and quantification. The Agilent instrument separates the analytes by gas chromatography using fused-silica columns. The steroids are ionized in the mass spectrometer and specific ions formed from individual metabolites are detected and quantified. A single ion of defined mass/charge (m/z) ratio is designated for the detection of each compound and an internal standard added for quantification.

3.2.6 Plasma aldosterone and plasma cortisol

Plasma aldosterone and cortisol were measured by commercially available enzyme-linked immunosorbent assay ELISAs (R&D, Abingdon, UK). In this retrospectively planned analysis plasma was not available for all patients (details in results). As a result we were not able to measure renin and aldosterone was measured in a seated position. In brief plates with pre-coated antibody are loaded with sample and standard and the substance of interest competes for binding sites with HRP-peroxidase labelled substance which is subsequently read on a spectrophotometer at 450 nM with correction at 540 nM. The concentration of samples is then calculated from a standard curve with a logarithmic x-axis of the concentrations of the standards and a linear y-axis of the absorbance. The intra-assay co-efficient of variation of the aldosterone ELISA was 16% and the cortisol ELISA was 13%.

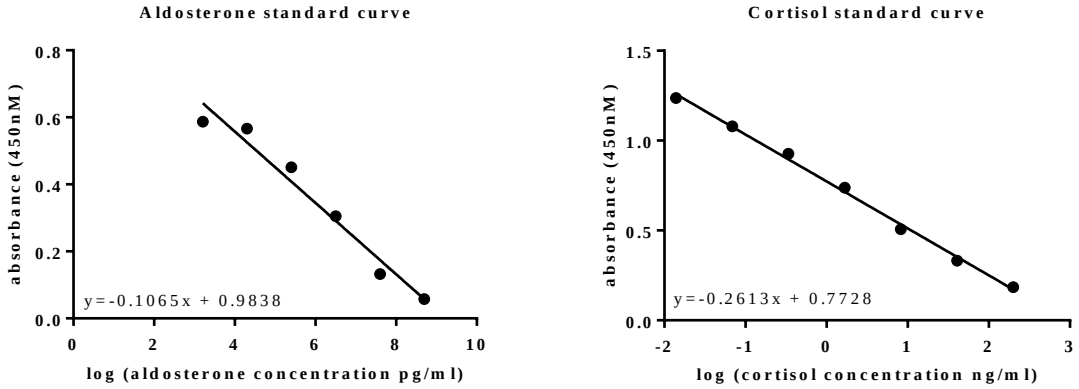


Figure 3- 2 The standard curves of the aldosterone and cortisol ELISAs.

3.2.7 Statistical analysis of urinary steroid and plasma

The data was analysed using IBM SPSS. A fixed effect ANOVA model was employed for analysis of the urinary steroid and plasma data with follow-up blood/urine steroid level as the dependent variable. For the unadjusted analysis the binary treatment was (CPAP=0 and sham=1) and the baseline blood/urine steroid level were employed as predictors. The unstandardised beta for binary treatment and corresponding p value were reported. In the adjusted analysis adjustments were made for gender, age, BMI and screening ODI. Statistical significance was defined with a two-sided alpha as $p<0.05$. These data were exploratory and hypothesis generating and are therefore p values were not corrected for multiple comparisons.

3.2.8 Adipose tissue biopsy

Abdominal adipose tissue biopsies were taken in the early morning in the fasted state at the beginning of the study and then again after 14 days of either continued CPAP or sham CPAP. Abdominal adipose tissue biopsies were taken 10 cm lateral to the umbilicus having first cleaned the skin with iodine solution and anaesthetized the area with 5 ml of 1% lidocaine. Biopsies were taken making a small incision (1-2 cm) with a scalpel and removing approximately 100mg of adipose tissue. The incision was then closed with a

single suture. Adipose biopsies were snap frozen in liquid nitrogen. RNA extraction and cDNA synthesis are detailed in the general methods section.

Patient two and patient thirteen were not included in the analysis as there were only two females in this section of the study (patient 1 also a female did not provide an adipose biopsy) therefore it was felt that this would introduce significant heterogeneity into the data.

Table 3-1 The concentrations of RNA and RNA quality indices from the subcutaneous abdominal adipose of patients with OSA who were compliant with CPAP taken at baseline (A) or after 2 weeks of randomisation to either sham or continued CPAP therapy (B).

Sample ID	ng/ul	A260	A280	260/280	260/230
2A	72.7	1.818	0.949	1.91	0.95
2B	156.44	3.911	1.944	2.01	1.07
3A	80.78	2.02	1.008	2	0.54
3B	217.64	5.441	2.822	1.93	0.94
4A	351.06	8.776	4.509	1.95	1.61
4B	90.95	2.274	1.222	1.86	1.16
5A	119.37	2.984	1.565	1.91	0.55

Sample ID	ng/ul	A260	A280	260/280	260/230
5B	148.73	3.718	1.951	1.91	0.88
6A	59.92	1.498	0.823	1.82	0.18
6B	105.18	2.63	1.396	1.88	1.16
7A	46.46	1.162	0.626	1.86	0.25
7B	80.71	2.018	1.138	1.77	0.27
8A	409.95	10.249	5.217	1.96	0.7
8B	204.03	5.101	2.682	1.9	0.44
9A	51.42	1.286	0.675	1.9	0.18
9B	248.75	6.219	3.166	1.96	0.87
10A	338.24	8.456	4.354	1.94	1.7
10B	322.42	8.061	4.05	1.99	1.65
11A	417.84	10.446	5.349	1.95	1.61

Sample ID	ng/ul	A260	A280	260/280	260/230
11B	289.99	7.25	3.786	1.91	1.78
12A	70.44	1.761	0.958	1.84	1.22
12B	387.95	9.699	4.838	2	1.48
13A	303.31	7.583	3.886	1.95	1.47
13B	237.64	5.941	3.112	1.91	1.4
14A	64.99	1.625	0.792	2.05	0.73
14B	293.35	7.334	3.735	1.96	1.51
15A	106.32	2.658	1.517	1.75	0.53
15B	90.59	2.265	1.325	1.71	0.41
16A	88.65	2.216	1.245	1.78	0.89
16B	95.97	2.399	1.359	1.77	0.41
17A	151.11	3.778	2.094	1.8	0.73

Sample ID	ng/ul	A260	A280	260/280	260/230
17B	85.54	2.139	1.231	1.74	1.27
18A	122.78	3.069	1.721	1.78	0.8
18B	160.83	4.021	2.188	1.84	1.03
19A	141.46	3.536	2.01	1.76	0.59
19B	130.12	3.253	1.762	1.85	1.67
20A	71.7	1.793	1.035	1.73	0.8
20B	183.21	4.58	2.433	1.88	1.54
21A	188.57	4.714	2.517	1.87	1.8
21B	165.61	4.14	2.22	1.87	1.59
22A	87.85	2.196	1.25	1.76	1.32
22B	113.7	2.843	1.409	2.02	2.44
22B	137.21	3.43	1.852	1.85	1.47

Sample ID	ng/ul	A260	A280	260/280	260/230
23A	90.71	2.268	1.264	1.79	0.99
23B	145.27	3.632	1.97	1.84	0.91

3.2.9 Fluidigm

Delta gene assays were designed by Fluidigm to a custom designed list of genes relevant to adipose tissue metabolism and oxidative stress. The EvaGreen® dye method was used to determine expression. In total 85 genes were measured and 3 housekeeping genes (18S ribosomal RNA (RN18S1), low density lipoprotein receptor-related protein 10 (LRP10) and peptidylprolyl isomerase A (PPIA)). There are four steps: preparation of the reverse transcription; preamplification; preparation of the samples and assays and running the IFC 96.96 chip Fluidigm on the BioMark HD System. In brief, the reverse transcription mix includes per reaction 1µL Reverse Transcription Master Mix (Fluidigm); 3 µL RNase-free water; 1µL RNA (50ng/µL). A standard thermal cycler was used (25˚C 5min; 42˚C 30min; 85˚C 5min; 4 ˚C hold). The preamplification reaction included 1µL PreAmp Master Mix (Fluidigm); 0.5µL of a pooled DELTAgene Assay Mix (1µL per assay made up to 200µL total volume with DNA suspension buffer (10mM Tris, pH 8.0, 0.1mM EDTA (TEKnova)) 2.25µL of RNase-free water and 1.25µL of cDNA. The preamplification was performed on a standard thermal cycle (95˚C 2min; 10 cycles of 95˚C 15s and 60˚C 4min; 4 ˚C hold). Unincorporated primers were then removed by treatment with Exonuclease I. To each preamplification reaction 1.4µL RNase free water;

0.2µL ExoNuclease I Reaction Buffer and 0.4µL of ExoNuclease I at 20 units/µL (New England BioLabs). This was incubated on a thermal cycle (37˚C for 30min; 80˚C for 15min; 4˚C hold). The final products were diluted 10-fold by adding 43µL of TE buffer (10mM Tris-HCL, 1mM EDTA (TEKnova)). To 2.7µL of the Preamplification and Exonuclease I treated sample was added 3µL of 2X SsoFast EvaGreen Supermix with low ROX (Bio-Rad) and 0.3µL of 20X DNA Binding dye sample loading reagent (Fluidigm). The assays were then prepared and to 0.3µL of assay was added 3µL of 2X Assay loading reagent and 2.7µL of DNA suspension buffer. To the 96.96 Dynamic Array IFC chip, 150µL of control line fluid was added to each accumulator. The chip was then primed on the IFC Controller HX. When primed 5µL of each prepared assay and 5µL of each prepared sample into the chip inlets. The chip was then loaded using the IFC Controller HX.

The real-time PCR was then run on the BioMark HD system with the linear derivative baseline correction method and auto global Ct threshold method. The data were expressed in arbitrary units having been corrected for the geometric mean of the selected housekeeping genes.

The genes were chosen on the basis of their functional relevance to a number of adipose specific and general cell metabolic pathways. Further genes were chosen as potential indicators of oxidative and endoplasmic reticulum stress as well as inflammation. The data presented (Table 3-8) does not include the female patients in the study. As there were only 3 females in the study and one did not consent to a fat biopsy the other two were excluded from this analysis to minimise heterogeneity within the sample particularly because of some of the steroid metabolism and action genes measured. However, the analysis was re-run (data not show) with the two females included and was unchanged. 3

further patients (6,7 and 17) were also removed from the analysis as the cDNA was of low yield and the CT values did not meet quality control criteria when run on the BiomarkHD. The data is expressed as relative gene expression in arbitrary units. The gene expression data has been further grouped in according with the metabolic pathway involving the gene of interest. In this hypothesis generating high throughput assay the initial statistical assessment employed were Student's t-tests (GraphPad Prism 5.0).

Table 3-2 The custom designed assays for the Fluidigm of the adipose biopsy RNA from the CPAP withdrawal study

Target Name		Fluidigm Assay ID	Exon Junction
Lipid Metabolism			
ABHD5	Abhydrolase Domain Containing 5	GEA00023960	4-5 NM_016006
ACACA	Acetyl-CoA Carboxylase Alpha	GEA00032308	47-48 NM_198837
ADIPOQ	Adiponectin	GEP00057388	3-4 NM_001177800
CIDEC	Cell Death Inducing DFFA Like Effector C	GEP00066952	5-6 NM_022094
DGAT1	Diacylglycerol O-Acyltransferase 1	GEA00031283	2-3 NM_012079

Target Name		Fluidigm Assay ID	Exon Junction
FABP3	Fatty Acid Binding Protein 3	GEA00018537	1-2 NM_004102
FABP4	Fatty Acid Binding Protein 4	GEP00059740	1-2 NM_001442
FABP5	Fatty Acid Binding Protein 5	GEA00019064	1 NM_001444
FASN	Fatty Acid Synthase	GEA00032375	11-12 NM_004104
LEP	Leptin	GEP00056370	2-3 NM_000230
LIPE	Lipase E	GEA00026729	8-9 NM_005357
LPL	Lipoprotein Lipase	GEA00026344	7-8 NM_000237
MGLL	Monoglyceride Lipase	GEA00024359	7-8 NM_007283
PER1	Period Circadian Regulator 1	GEA00032274	8-9 NM_002616
PER2	Period Circadian Regulator 2	GEP00059503	3-4 NM_022817
PLIN1	Perilipin 1	GEP00058591	2-3 NM_002666
PLIN2	Perilipin 2	GEA00024586	7-8 NM_001122

Target Name		Fluidigm Assay ID	Exon Junction
PNPLA2	Patatin Like Phospholipase Domain Containing 2	GEP00066953	5-6 NM_020376
PPARA	Peroxisome Proliferator Activated Receptor Alpha	GEP00057488	5-6 NM_005036
Cell metabolism			
AKT2	AKT Serine/Threonine Kinase 2	GEA00012963	10-11 NM_001626
AQP7	Aquaporin 7	GEP00056193	2-3 NM_001170
CLOCK	Clock Circadian Regulator	GEA00030717	18-19 NM_004898
CREB1	CAMP Responsive Element Binding Protein 1	GEA00013568	5-6 NM_004379
G6PD	Glucose-6-Phosphate Dehydrogenase	GEP00061380	6-7 NM_000402
GAPDH	Glyceraldehyde-3-Phosphate Dehydrogenase	GEP00055153	4-5 NM_002046
GLUL	Glutamate-Ammonia Ligase	GEA00024249	6-7 NM_002065
IRS1	Insulin Receptor Substrate 1	GEP00056368	1-2 NM_005544
IRS2	Insulin Receptor Substrate 2	GEP00061382	1-2 NM_003749

Target Name		Fluidigm Assay ID	Exon Junction
JAK2	Janus Kinase 2	GEA00013040	17-18 NM_004972
MAPK1	Mitogen-Activated Protein Kinase 1	GEA00012736	4-5 NM_002745
NPR3	Natriuretic Peptide Receptor 3	GEP00066955	7-8 NM_001204375
PGK1	Phosphoglycerate Kinase 1	GEA00005544	7-8 NM_000291
PDHA1	Pyruvate Dehydrogenase E1 Alpha 1 Subunit	GEP00060947	2-3 NM_001173455
PDK4	Pyruvate Dehydrogenase Kinase 4	GEA00028131	4-5 NM_002612
PDP1	Pyruvate Dehyrogenase Phosphatase Catalytic Subunit 1	GEA00015086	2 NM_018444
PIK3CA	Phosphatidylinositol-4,5-Bisphosphate 3-Kinase Catalytic Subunit Alpha	GEP00056385	18-19 NM_006218
PPARG	Peroxisome Proliferator Activated Receptor Gamma	GEA00005569	7-8 NM_138711

Target Name		Fluidigm Assay ID	Exon Junction
PRKAA1	Protein Kinase AMP-Activated Catalytic Subunit Alpha 1	GEA00026243	6-7 NM_206907
SLC2A1	Solute Carrier Family 2 Member 1	GEP00056173	9-10 NM_006516
SLC2A4	Solute Carrier Family 2 Member 4	GEA00027378	10-11 NM_001042
WNT5A	Wnt Family Member 5A	GEP00055829	4-5 NM_003392
Cellular remodelling			
BMP4	Bone Morphogenetic Protein 4	GEA00013531	3-4 NM_130851
BMP7	Bone Morphogenetic Protein 7	GEA00013535	2-3 NM_001719
COL1A1	Collagen Type I Alpha 1 Chain	GEA00004461	23-24 NM_000088
COL3A1	Collagen Type I Alpha 3 Chain	GEA00030417	26-27 NM_000090
CTNNB1	Catenin Beta 1	GEP00055724	7-8 NM_001098210
FGFR1	Fibroblast Growth Factor Receptor 1	GEP00056764	5-6 NM_023110

Target Name		Fluidigm Assay ID	Exon Junction
ICAM1	Intercellular Adhesion Molecule 1	GEP00056359	3-4 NM_000201
LOX	Lysyl Oxidase	GEA00012358	2-3 NM_002317
MMP1	Matrix Metallopeptidase 1	GEP00057273	5-6 NM_001145938
MMP2	Matrix Metallopeptidase 2	GEA00013719	3-4 NM_004530
MMP3	Matrix Metallopeptidase 3	GEP00056035	7-8 NM_002422
MMP9	Matrix Metallopeptidase 9	GEA00013721	2-3 NM_004994
PLAT	Plasminogen Activator, Tissue Type	GEP00056386	7-8 NM_000930
SERPINE1	Serpin Family E Member 1	GEP00056400	4-5 NM_000602
Steroid metabolism and action			
ADRB2	Adrenoceptor Beta 2	GEP00057483	1 NM_000024
ARNT	Aryl Hydrocarbon Receptor Nuclear Translocator	GEP00062415	12-13 NM_001668
DUSP1	Dual Specificity Phosphatase 1	GEA00018877	3-4 NM_004417

Target Name		Fluidigm Assay ID	Exon Junction
HSD11B1	Hydroxysteroid 11-Beta Dehydrogenase 1	GEA00012713	5-6 NM_181755
NR3C1	Nuclear Receptor Subfamily 3 Group C Member 1	GEP00056354	5-6 NM_001018077
SGK1	Serum/Glucocorticoid Regulated Kinase 1	GEP00060290	9-10 NM_001143676
SRD5A1	Steroid 5 Alpha-Reductase 1	GEA00012776	1-2 NM_001047
GILZ	Glucocorticoid-Induced Leucine Zipper	GEA00016810	2-3 NM_004089
Oxidative stress			
ANGPTL4	Angiopoietin Like 4	GEA00023241	6-7 NM_139314
CAT	Catalase	GEA00023106	10-11 NM_001752
GPX1	Glutathione Peroxidase 1	GEA00014011	1 NM_201397
GPX3	Glutathione Peroxidase 3	GEA00020250	2-3 NM_002084
HIF1A	Hypoxia Inducible Factor 1 Alpha Subunit	GEA00012495	6-7 NM_001530

Target Name		Fluidigm Assay ID	Exon Junction
MTOR	Mechanistic Target Of Rapamycin Kinase	GEA00029978	15-16 NM_004958
NOX4	NADPH Oxidase 4	GEA00031712	2-3 NM_001143836
SIRT1	Sirtuin 1	GEA00013147	6-7 NM_012238
SOD1	Superoxide Dismutase 1	GEP00060586	2-3 NM_000454
UCP2	Uncoupling Protein 2	GEA00024727	3-4 NM_003355
VEGFA	Vascular Endothelial Growth Factor A	GEA00012311	2-3 NM_001025366
Endoplasmic reticulum stress			
ATF6	Activating Transcription Factor 6	GEA00029249	6-7 NM_007348
EIF2AK3	Eukaryotic Translation Initiation Factor 2 Alpha Kinase 3	GEA00030327	8-9 NM_004836
ERN1	Endoplasmic Reticulum To Nucleus Signaling 1	GEA00032340	6-7 NM_001433
Inflammation			

Target Name		Fluidigm Assay ID	Exon Junction
CCL2	C-C Motif Chemokine Ligand 2	GEP00055652	1-2 NM_002982
CCL28	C-C Motif Chemokine Ligand 28	GEA00016507	2-3 NM_148672
CD36	CD36 Molecule	GEA00028331	4-5 NM_001001547
IFNG	Interferon Gamma	GEA00012368	1-2 NM_000619
IL10	Interleukin 10	GEA00012369	4-5 NM_000572
IL6	Interleukin 6	GEA00012521	4-5 NM_000600
IL8	Interleukin 8	GEA00012363	2-3 NM_000584
NFKB1	Nuclear Factor Kappa B Subunit 1	GEP00056435	5-6 NM_001165412
TNF	Tumour Necrosis Factor	GEP00059924	2-3 NM_000594

3.3 Results

3.3.1 The demographics and clinical characteristics of the patient cohort studied

Twenty-three patients were included in the study. Of the 23 patients studied there was a male predominance with an average age of 60.8±8.4 years and a BMI of 36.9±7.4

kg/m^2 and an oxygen desaturation index of 38.2±16. There were 4 patients with type 2 diabetes, all of whom had all been randomised to continue CPAP (**Table 3-3).**

Table 3-3 Baseline characteristics of those in the CPAP withdrawal study

	Sham CPAP group (n=12)	Continued CPAP group (n=11)
	Mean ± SD, median (IQR) or number (%)	Mean ± SD, median (IQR) or number (%)
Age	62.0 ± 9.1	59.7 ± 7.9
Male gender	10 (83%)	10 (91%)
BMI	37.1 ± 7.8	36.8 ± 7.4
Original ODI at diagnosis	54.1 ± 22.9	53.1 ± 14.5
Screening ODI off CPAP	33.7 (24.8, 51.0)	35.2 (23.7, 53.3)
Current smoker	1 (9%)	1 (9%)
Cardiovascular disease	2 (18%)	1 (9%)
Hypertension	7 (64%)	3 (27%)
Diabetes mellitus	0 (0%)	4 (36%)
Hormonal medication	1 (9%)	0 (0%)

Table 3-4 The effect of sham and continued CPAP on the oxygen desaturation index (ODI) and blood pressure (BP)

	Sham CPAP		Continued CPAP		Unadjusted analysis			Adjusted analysis		
	Baseline	Follow-up	Baseline	Follow-up						
	Mean ± SD or median (IQR)	Mean ± SD or median (IQR)	Mean ± SD or median (IQR)	Mean ± SD or median (IQR)	Treatment effect	95% CI	p value	Treatment effect	95% CI	p value
ODI	5.3 ± 4.9	49.6 ± 26.2	7.1 ± 6.5	6.5 ± 4.8	43.8	26.3, 61.1	<0.001*	47.8	31.8, 63.8	<0.001*
Office systolic BP	132.5 ± 16.9	134.6 ± 14.5	135.4 ± 17.5	137.3 ± 16.5	-0.7	-9.1, 7.8	0.87	-1.3	-10.2, 7.6	0.76
Office diastolic BP	83.1 ± 10.0	86.1 ± 9.7	81.9 ± 11.7	83.3 ± 11.5	1.8	-2.6, 6.2	0.41	2.1	-3.0, 7.1	0.40

	Sham CPAP		Continued CPAP		Unadjusted analysis			Adjusted analysis		
	Baseline	Follow-up	Baseline	Follow-up						
	Mean ± SD or median (IQR)	Mean ± SD or median (IQR)	Mean ± SD or median (IQR)	Mean ± SD or median (IQR)	Treatment effect	95% CI	p value	Treatment effect	95% CI	p value
Office heart rate	66.8 ± 9.6	67.0 ± 10.5	65.6 ± 8.6	63.8 ± 8.5	2.2	-2.6, 7.0	0.36	3.3	-1.9, 8.5	0.20
Home systolic BP	127.3 ± 13.5	127.3 ± 13.9	135.4 ± 17.5	132.9 ± 14.0	-1.5	-12.0, 9.1	0.77	-0.6	-12.0, 10.9	0.92
Home diastolic BP	81.7 ± 10.8	83.0 ± 12.0	81.9 ± 11.7	78.7 ± 12.7	4.6	-3.7, 12.9	0.26	6.2	-2.4, 14.7	0.14

	Sham CPAP		Continued CPAP		Unadjusted analysis			Adjusted analysis		
	Baseline	Follow-up	Baseline	Follow-up						
	Mean ± SD or median (IQR)	Mean ± SD or median (IQR)	Mean ± SD or median (IQR)	Mean ± SD or median (IQR)	Treatment effect	95% CI	p value	Treatment effect	95% CI	p value
Home heart rate	67.4 ± 9.0	68.8 ± 9.9	65.6 ± 8.6	66.7 ± 9.5	0.3	-6.4, 7.0	0.92	0.4	-7.5, 8.3	0.91

Those randomised to sham CPAP had their OSA unmasked as demonstrated by their oxygen desaturation index (ODI) increasing (5.3 ± 4.9 to 49.6 ± 26.2 ($p<0.001$ in unadjusted and adjusted analysis) whilst those who continued CPAP had no change in their ODI (7.1 ± 6.5 to 6.5 ± 4.8). This demonstrates that 2 weeks of sham CPAP therapy is sufficient to cause a return of OSA. In the present study there were no changes in either home or office blood pressure recordings after sham CPAP (**Table 3-4**).

3.3.2 The effect of CPAP withdrawal on the urinary steroid profile

Patients collected an overnight urine collection pre and 2 weeks post randomisation to either sham or continued CPAP therapy as outlined in **Figure 3-1**. Of the 23 patients in the study, 22 provided paired urine collections. Of these 22 patients, 1 was excluded from the final analysis as the urine was not properly collected. Of the 34 distinctly measured urine steroid metabolites and 17 steroid ratios several were altered in those randomised to sham CPAP (**Table 3-5**).

Table 3-5 The effect of sham CPAP on the urinary steroid profile of patients with OSA. Statistically significant values are highlighted in grey. Statistical significance is taken as p<0.05. Values are expressed in µg excreted/12 hours. Data is presented as mean ±SD. Where data is not normally distributed it is marked as†.

Steroid	**Sham CPAP**		**Continued CPAP**		**Unadjusted analysis**			**Adjusted analysis**		
	Baseline	**Follow-up**	**Baseline**	**Follow-up**						
	Mean ± SD or median (IQR)	**Mean ± SD or median (IQR)**	**Mean ± SD or median (IQR)**	**Mean ± SD or median (IQR)**	**Treatment effect**	**95% CI**	**p value**	**Treatment effect**	**95% CI**	**p value**
Androgen Pathway										
5-PD	189.8 ±119.8	183.6 ± 134†	146.5 ± 87.6	149.4 ±64.0	-1.8	-56.7, 53.0	0.95	-9.5	-67.5, 48.6	0.73
Pregnadienol	55.5 ± 56.8†	48.6 ± 53.1†	45.4 ± 38.2	45.7 ± 34.2†	-5.8	-19.5, 7.9	0.39	-8.6	-22.6, 5.4	0.21

Steroid	**Sham CPAP**		**Continued CPAP**		**Unadjusted analysis**			**Adjusted analysis**		
	Baseline	**Follow-up**	**Baseline**	**Follow-up**						
	Mean ± SD or median (IQR)	**Mean ± SD or median (IQR)**	**Mean ± SD or median (IQR)**	**Mean ± SD or median (IQR)**	**Treatment effect**	**95% CI**	**p value**	**Treatment effect**	**95% CI**	**p value**
5-PT	60.9 ± 35.3	67.4 ± 45†	65.6 ± 39.0	66.8 ±30.2	4.6	-16.2, 25.3	0.65	4.1	-19.1, 27.2	0.71
DHEA	64.0 ± 81.8†	94 ± 151†	90.1 ± 164†	73.5 ± 75†	36.7	-44.6, 118.0	0.36	39.3	-52.6, 131.3	0.38
16a OH DHEA	126.7 ± 129†	176.7 ± 1188†	134.9 ± 144†	124.7 ±112.1	60.4	-0.1, 120.8	0.05	56.9	-2.4, 116.2	0.06
ANDROS	335.6 ± 171.7	354.4 ± 163.0	507.9 ± 291.3	548.5 ± 231.6	-82.6	-207.0, 41.7	0.18	-77.0	-215.4, 61.4	0.25

Steroid	**Sham CPAP**		**Continued CPAP**		**Unadjusted analysis**			**Adjusted analysis**		
	Baseline	**Follow-up**	**Baseline**	**Follow-up**						
	Mean ± SD or median (IQR)	**Mean ± SD or median (IQR)**	**Mean ± SD or median (IQR)**	**Mean ± SD or median (IQR)**	**Treatment effect**	**95% CI**	**p value**	**Treatment effect**	**95% CI**	**p value**
11b-OH-ANDRO	187.0 ± 116.9	207.3 ± 137†	169.6 ± 89.4	181.3 ± 67.7	10.3	-38.7, 59.4	0.66	10.8	-40.6, 62.2	0.66
ETIO	462.9 ± 509†	487.7 ± 566†	447.1 ± 324.8	478.5 ± 356†	-7.7	-127.6, 112.3	0.90	-15.9	-136.8, 105.0	0.78
11b-OH-ETIO	151.0 ± 91.3†	121.5 ± 105.2	85.8 ± 64.8	109.5 ± 104†	-16.7	-77.1, 43.7	0.57	-29.7	-89.8, 30.5	0.31
11-OXO-Et	151.0 ± 91.3	157.9 ± 78.3	128.9 ± 106.0	136.3 ± 95.0	7.2	-46.4, 60.7	0.78	-6.7	-54.6, 41.1	0.77

Steroid	**Sham CPAP**		**Continued CPAP**		**Unadjusted analysis**			**Adjusted analysis**		
	Baseline	**Follow-up**	**Baseline**	**Follow-up**						
	Mean ± SD or median (IQR)	**Mean ± SD or median (IQR)**	**Mean ± SD or median (IQR)**	**Mean ± SD or median (IQR)**	**Treatment effect**	**95% CI**	**p value**	**Treatment effect**	**95% CI**	**p value**
Glucocorticoid pathway										
PD	61.8 ± 34.1	76.1 ± 49.5†)	69.8 ± 54.3	65.5 ± 39.8	16.8	-8.8, 42.4	0.19	14.9	-14.4, 44.2	0.30
PT	309 ± 398†	358 ± 528†	180.4 ± 123.6	191.0 ± 112.5	3.2	-59.5, 66.0	0.92	-3.7	-74.0, 66.6	0.91
17-HP	69.9 ± 58.9	75.3 ± 78.5†	51.4 ± 38.6	58.3 ± 38.7	-3.3	-30.4, 23.8	0.80	-3.6	-33.3, 26.0	0.80

Steroid	**Sham CPAP**		**Continued CPAP**		**Unadjusted analysis**			**Adjusted analysis**		
	Baseline	**Follow-up**	**Baseline**	**Follow-up**						
	Mean ± SD or median (IQR)	**Mean ± SD or median (IQR)**	**Mean ± SD or median (IQR)**	**Mean ± SD or median (IQR)**	**Treatment effect**	**95% CI**	**p value**	**Treatment effect**	**95% CI**	**p value**
3a5a 17HP	7.61 ± 7.81†	9.13 ± 12.3†	7.1 ± 5.6	8.1 ± 5.6†	0.4	-3.3, 4.0	0.83	0.6	-3.2, 4.5	0.72
PT'ONE	77.7 ± 217†	99.9 ± 290†	6.7 ± 5.9†	6.1 ±4.3	-0.9	-5.4, 3.6	0.68	-1.6	-6.7, 3.4	0.50
THS	43.0 ± 26.2	43.3 ±20.0	28.9 ± 19.2	29.1 ± 14.2	4.9	-3.4, 13.1	0.23	4.7	-4.6, 14.0	0.30
Cortisol	26.2 ± 14.6	28.5 ±13.0	23.1 ± 12.0	25.9 ± 8.9	0.4	-4.8, 5.5	0.89	0.4	-5.4, 6.2	0.89

Steroid	**Sham CPAP**		**Continued CPAP**		**Unadjusted analysis**			**Adjusted analysis**		
	Baseline	**Follow-up**	**Baseline**	**Follow-up**						
	Mean ± SD or median (IQR)	**Mean ± SD or median (IQR)**	**Mean ± SD or median (IQR)**	**Mean ± SD or median (IQR)**	**Treatment effect**	**95% CI**	**p value**	**Treatment effect**	**95% CI**	**p value**
6b-OH-Cortisol	41.0 ± 20.6	37.0 ±18.1	34.8 ± 16.6	34.1 ± 14.8†	-1.3	-10.9, 8.3	0.78	-1.3	-11.9, 9.3	0.80
THF	709.8 ± 291.5	778.5 ± 230.1	510.7 ± 299.1	500.0 ± 176.4	175.7	42.7, 308.8	0.01*	177.0	31.1, 322.9	0.02*
5a-THF	524.0 ± 305.5	574.0 ± 285.3	619.6 ± 455.0	579.7 ± 274.0	51.3	-94.5, 197.0	0.47	70.0	-94.7, 234.7	0.38
a-cortol	129.5 ± 64.1	149.1 ± 76.1	125.5 ± 71.2	119.2 ± 43.9	26.9	-6.2, 60.0	0.11	30.0	-6.6, 66.6	0.10

Steroid	**Sham CPAP**		**Continued CPAP**		**Unadjusted analysis**			**Adjusted analysis**		
	Baseline	**Follow-up**	**Baseline**	**Follow-up**						
	Mean ± SD or median (IQR)	**Mean ± SD or median (IQR)**	**Mean ± SD or median (IQR)**	**Mean ± SD or median (IQR)**	**Treatment effect**	**95% CI**	**p value**	**Treatment effect**	**95% CI**	**p value**
b-cortol	218.6 ± 112.9	204.3 ± 90.3	198.0 (66.0, 260.0)	227.7 ± 136.3	-11.2	-69.7, 47.4	0.70	-14.4	-80.7, 51.8	0.65
Cortisone	33.6 ±18.1	35.6 ± 12.1	29.1 ± 14.9	32.9 ± 11.6	0.1	-6.3, 6.5	0.97	0.7	-5.9, 7.3	0.83
THE	1257.9 ± 580.5	1432.1 ± 478.3	998.0 ± 589.6	972.5 ± 399.3	299.2	61.9, 536.5	0.02*	310.5	74.1, 546.8	0.01*

Steroid	**Sham CPAP**		**Continued CPAP**		**Unadjusted analysis**			**Adjusted analysis**		
	Baseline	**Follow-up**	**Baseline**	**Follow-up**						
	Mean ± SD or median (IQR)	**Mean ± SD or median (IQR)**	**Mean ± SD or median (IQR)**	**Mean ± SD or median (IQR)**	**Treatment effect**	**95% CI**	**p value**	**Treatment effect**	**95% CI**	**p value**
a-cortolone	449.4 ± 218.6	510.4 ± 246.0	411.3 ± 224.8	397.2 ± 163.4	82.6	-17.4, 182.5	0.10	85.7	-30.5, 201.8	0.14
b-cortolone	315.2 ± 114.2	327.5 ± 152.9	250.3 ± 132.2	253.5 ± 111.6	26.1	-55.5, 107.8	0.51	13.4	-79.4, 106.2	0.76
Mineralocorticoid pathway										
TH-DOC	5.5 ± 3.0	5.5 ± 2.8†	4.4 ± 2.6	4.6 ±2.3	0.1	-1.3, 1.5	0.90	-0.1	-1.6, 1.4	0.87
5α-TH-DOC	1.4 ± 0.8	1.8 ± 1.1	1.4 ± 0.9	1.7 ± 1.2	0.1	-0.7, 0.9	0.77	0.2	-0.7, 1.1	0.67

Steroid	**Sham CPAP**		**Continued CPAP**		**Unadjusted analysis**			**Adjusted analysis**		
	Baseline	**Follow-up**	**Baseline**	**Follow-up**						
	Mean ± SD or median (IQR)	**Mean ± SD or median (IQR)**	**Mean ± SD or median (IQR)**	**Mean ± SD or median (IQR)**	**Treatment effect**	**95% CI**	**p value**	**Treatment effect**	**95% CI**	**p value**
THA	52.0 ± 31.4	54.3 ± 25.7	30.2 ± 17.1	31.1 ±13.6	8.5	-3.0, 20.1	0.14	6.7	-6.4, 19.8	0.30
5a-THA	33.0 ± 16.0	36.6 ± 11.5	30.2 ± 16.3	29.2 ± 10.6†	5.8	0.2, 11.4	0.04*	5.9	-0.6, 12.4	0.07
THB	51.1 ± 34.0	49.5 ± 25.5	32.2 ± 19.4	31.5 ±15.5	6.0	-5.2, 17.3	0.28	3.3	-9.2, 15.9	0.58
5a-THB	85.4 ± 67.7	89.2 ± 69.2†	81.8 ± 44.4	77.4 ±29.1	9.1	-18.1, 36.4	0.49	6.3	-23.9, 36.5	0.67

Steroid	**Sham CPAP**		**Continued CPAP**		**Unadjusted analysis**			**Adjusted analysis**		
	Baseline	**Follow-up**	**Baseline**	**Follow-up**						
	Mean ± SD or median (IQR)	**Mean ± SD or median (IQR)**	**Mean ± SD or median (IQR)**	**Mean ± SD or median (IQR)**	**Treatment effect**	**95% CI**	**p value**	**Treatment effect**	**95% CI**	**p value**
18 OH THA	29.5 ± 16.5	29.8 ± 11.6	23.5 ± 13.8	20.2 ± 8.5	6.7	0.1, 13.3	0.05*	7.1	0.1, 14.2	0.05*
3a5bTHALDO	16.2 ± 9.1	21.9 ± 9.0	15.3 ± 6.8	16.2 ±8.5	4.9	-0.6, 10.4	0.08	5.2	-1.0, 11.3	0.09

Table 3-6 The effect of sham CPAP on the urinary steroid ratios of patients with OSA. Statistically significant values are highlighted in grey. Where data is normally distributed it is expressed as mean ± standard deviation. Where data is not normally distributed it is marked as†.

Ratio name	Sham CPAP		Continued CPAP		Unadjusted analysis			Adjusted analysis		
	Baseline	Follow-up	Baseline	Follow-up						
	Mean ± SD or median (IQR)	Mean ± SD or median (IQR)	Mean ± SD or median (IQR)	Mean ± SD or median (IQR)	Treatment effect	95% CI	p value	Treatment effect	95% CI	p value
Androgen pathways										
(Andros+Etio)/(17HP+PT)	3.01 ± 1.81	3.03 ± 1.64	4.42 ± 1.53	4.65 ±1.79	-0.28	-0.90, 0.35	0.36	-0.23	-0.85, 0.39	0.45
DHEA/(THE+THF+5aTHF)	0.02 ± 0.03†	0.03± 0.05†	0.05 ± 0.09†	0.04 ± 0.04†	0.01	-0.03, 0.04	0.74	0.01	-0.03, 0.04	0.70
ETIO/ANDRO	1.70 ± 2.3†	1.75 ± 2.5†	0.86 ± 0.4†	0.82 ± 0.28	0.03	-0.11, 0.16	0.66	0.03	-0.09, 0.16	0.58

Ratio name	Sham CPAP		Continued CPAP		Unadjusted analysis			Adjusted analysis		
	Baseline	Follow-up	Baseline	Follow-up						
	Mean ± SD or median (IQR)	Mean ± SD or median (IQR)	Mean ± SD or median (IQR)	Mean ± SD or median (IQR)	Treatment effect	95% CI	p value	Treatment effect	95% CI	p value
Glucocorticoid pathways										
F/E	0.77 ± 0.11	0.78 ± 0.17†	0.82± 0.17†	0.86 ± 0.37†	-0.01	-0.23, 0.21	0.93	-0.02	-0.28, 0.24	0.89
(THF+5aTHF)/THE	1.06 ± 0.47	1.0 ±0.40	1.24 ± 0.48†	1.25 ± 0.45	-0.07	-0.16, 0.03	0.15	-0.07	-0.17, 0.03	0.16
cortols/cortolones	0.47 ± 0.15	0.43 ± 0.13†	0.55 ± 0.18†	0.56 ± 0.19†	-0.04	-0.09, 0.02	0.20	-0.02	-0.08, 0.03	0.36

Ratio name	Sham CPAP		Continued CPAP		Unadjusted analysis			Adjusted analysis		
	Baseline	Follow-up	Baseline	Follow-up						
	Mean ± SD or median (IQR)	Mean ± SD or median (IQR)	Mean ± SD or median (IQR)	Mean ± SD or median (IQR)	Treatment effect	95% CI	p value	Treatment effect	95% CI	p value
(F+E)/(THF+5aTHF+THE)	0.02 ± 0.01	0.02 ±0.01	0.03 ±0.01	0.04 ± 0.03†	-0.01	-0.02, 0.01	0.33	-0.01	-0.02, 0.01	0.35
(17HP+PT)/(THE+THF+5aTHF)	0.16 ± 0.18†	0.15 ± 0.2†	0.11 ± 0.05	0.12 ± 0.05	-0.01	-0.03, 0.01	0.26	-0.01	-0.04, 0.01	0.24
(PTONE*100)/ (THE+THF+5aTHF)	3.18 ± 8.99†	3.34 ± 9.6†	0.34 ± 0.20	0.29 ± 0.16†	0.02	-0.10, 0.13	0.75	-0.00	-0.12, 0.12	0.99
PD/(THE+THF+5aTHF)	0.03 ± 0.01	0.03 ± 0.02	0.03 ± 0.02	0.03 ± 0.01	0.00	-0.01, 0.01	0.60	0.00	-0.01, 0.01	0.67

Ratio name	Sham CPAP		Continued CPAP		Unadjusted analysis			Adjusted analysis		
	Baseline	Follow-up	Baseline	Follow-up						
	Mean ± SD or median (IQR)	Mean ± SD or median (IQR)	Mean ± SD or median (IQR)	Mean ± SD or median (IQR)	Treatment effect	95% CI	p value	Treatment effect	95% CI	p value
5PD/(THE+THF+5aTHF)	0.07 ±0.04	0.06 ± 0.04†	0.07 ± 0.03	0.08 ± 0.03	-0.01	-0.03, 0.00	0.10	-0.01	-0.03, 0.00	0.05
PT/(THE+THF+5aTHF)	0.13 ± 0.16†	0.13 ± 0.17†	0.09 ± 0.03	0.09 ± 0.04	-0.01	-0.02, 0.01	0.33	-0.01	-0.02, 0.01	0.21
5PT/(THE+THF+5aTHF)	0.02 ± 0.01	0.02 ± 0.02†	0.03 ± 0.02	0.03 ± 0.01	-0.00	-0.01, 0.00	0.52	-0.00	-0.01, 0.01	0.49
THF/5a THF	5.07 ± 12.2†	5.9 ± 14.8†	0.97 ± 0.48†	0.95 ± 0.35	-0.11	-0.33, 0.12	0.33	-0.06	-0.24, 0.12	0.50

Ratio name	Sham CPAP		Continued CPAP		Unadjusted analysis			Adjusted analysis		
	Baseline	Follow-up	Baseline	Follow-up						
	Mean ± SD or median (IQR)	Mean ± SD or median (IQR)	Mean ± SD or median (IQR)	Mean ± SD or median (IQR)	Treatment effect	95% CI	p value	Treatment effect	95% CI	p value
Total F metabolites	3664.2 ± 1456.9	4040.1 ± 1104.6	3206.4 ± 1824.8	3108.6 ± 1117.0	678.0	94.0, 1262.0	0.03*	720.9	46.1, 1395.6	0.04*
Mineralocorticoid pathways										
(THA+5aTHA+THB+5aTHB)/ (THE+THF+5aTHF)	0.08 ± 0.03	0.08 ± 0.07†	0.09 ±0.02	0.09± 0.03†	0.00	-0.02, 0.02	0.98	-0.00	-0.02, 0.02	0.80
18 OH THA/3a5b-THALDO	1.94 ± 0.66	1.43 ± 0.41	1.54 ± 0.58	1.48 ± 0.60	-0.24	-0.64, 0.16	0.22	-0.25	0.70, 0.20	0.25

3.3.3a Androgen metabolites

Of the 10 steroid metabolites and 3 steroid ratios specific to androgen steroidogenesis, none were altered significantly in either the unadjusted or adjusted models comparing the effect of CPAP withdrawal versus continued CPAP therapy.

3.3.3b Cortisol metabolites

Of the glucocorticoid specific steroid metabolites measured, both tetrahydrocortisol (THF) and tetrahydrocortisone (THE) increased in response to the withdrawal of CPAP therapy (**Table 3-5**). These two biologically inactive metabolites of cortisol (THF) and cortisone (THE) were the most abundant glucocorticoid metabolites found in the urine. All the data within this and the following paragraph refers to µg of steroid metabolite excreted/12 hours. THF increased in response to sham CPAP (sham: 709.8±291.5 to 778.5±230.6; continued CPAP 510.7±299.1 to 500.0±176.4 µg/12 hours; p=0.01, adjusted p=0.02). THE also increased in response to sham CPAP (sham: 1257.9±580.5 to 1432.1±478.3; continued CPAP 998±589.6 to 972.5±399.3 µg/12 hours; p=0.02; adjusted p=0.01). In addition, the combined cortisol metabolites (total F) increased in the sham CPAP group (**Table 3-6**) (sham: 3664.2±1456.9 to 4040.1±1104.7; continued CPAP 3206.4±1824.8 to 3108.6±1117.0 µg/12 hours; p=0.03, adjusted p=0.04).

3.3.3c Mineralocorticoid metabolites

The 5α-tetrahydrocorticosterone (5αTHA) increased in response to sham CPAP (sham: 33±16 to 36.6±11.5; continued CPAP: 30.2±16.3 to 33 (25, 37) µg/12 hours; p=04, adjusted p=0.07). The immediate precursor to aldosterone synthesis 18-hydroxycorticosterone (18OH THA) also increased (sham: 29.5±16.5 to 29.8±11.6; continued CPAP: 23.5±13.8 to 20.2±8.5 µg/12 hours; p=0.05, adjusted p=0.05). The urinary metabolite of aldosterone also increased in response to sham CPAP although this was not statistically significant in either unadjusted or adjusted model (3α5β-

tetrahydroaldosterone (3α5β THALDO) sham: 16.2±9.1 to 21.9±9; continued CPAP 15.3±6.8 to 16.2±8.5 µg/12 hours; p=0.08; adjusted p=0.09).

3.3.4 The effect of CPAP withdrawal on the plasma steroid profile

Plasma cortisol and aldosterone measured early morning in the fasted state were unchanged by 2 weeks of sham CPAP (**Table 3-7**).

Table 3-7 The effect of sham CPAP therapy on early morning fasted plasma aldosterone (pg/ml) and cortisol (ng/ml). This was a retrospectively planned analysis and not all patients had available plasma (n, numbers as presented). Where data is not normally distributed it is marked as†.

	Sham CPAP n=8 Aldo n=9 Cortisol		Continued CPAP n=11 Aldo n=10 CPAP		Unadjusted analysis			Adjusted analysis		
	Baseline	Follow-up	Baseline	Follow-up						
	Mean ± SD or median (IQR)	Mean ± SD or median (IQR)	Mean ± SD or median (IQR)	Mean ± SD or median (IQR)	Treatment effect	95% CI	p value	Treatment effect	95% CI	p value
Aldosterone	140.4 ± 79.7	145.2 ± 75.3	200.3 ± 95.0	177.0 ± 91.9	16.3	-34.3, 66.8	0.51	16.0	-41.6, 73.7	0.56
Cortisol	75.0 ± 24.0	70.1 ± 19.6†	67.7 ± 29.9†	66.2 ± 15.7	0.49	-12.2, 13.2	0.94	-0.35	-14.2, 13.5	0.96

3.3.5 The effect of CPAP withdrawal on adipose tissue gene expression profile

The results from the Fluidigm™ analysis are displayed below (**Table 3-8**). CPAP withdrawal did not result in a significant change in subcutaneous abdominal adipose tissue gene transcription. Several genes appeared to change significantly after continued CPAP however all significance was lost when the data was corrected for multiple comparisons.

Table 3-8. The effect of CPAP withdrawal on the gene expression of subcutaneous abdominal adipose tissue. Data is presented in arbitrary units ± standard deviation. The significant values are highlighted in grey. (*P<0.05)

	Sham CPAP n=10			**Continued CPAP n=7**		
	Baseline	**Follow up**	***P* value**	**Baseline**	**Follow up**	***P* value**
Lipid Metabolism						
ABHD5	0.89±0.39	0.98±0.19	0.52	1.03±0.29	0.95±0.31	0.59
ACACA	0.94±0.39	0.97±0.29	0.75	0.78±0.24	0.94±0.33	0.19
ADIPOQ	1.20±0.19	1.18±0.16	0.84	0.90±0.29	1.13±0.17	0.11
CIDEC	1.32±0.49	1.25±0.24	0.74	0.98±0.37	1.35±0.33	0.09
DGAT1	1.23±0.23	1.25±0.29	0.86	1.13±0.17	1.22±0.16	0.40
FABP3	0.81±0.59	0.54±0.15	0.14	0.58±0.47	0.68±0.37	0.33
FABP4	1.22±0.46	1.16±0.23	0.77	1.02±0.57	1.21±0.33	0.26
FABP5	0.79±0.36	0.92±0.32	0.37	0.75±0.52	1.23±0.55	0.00*
FASN	0.85±0.22	1.09±0.88	0.34	0.82±0.61	0.91±0.25	0.77
LIPE	1.27±0.54	1.06±0.45	0.38	0.86±0.26	1.07±0.20	0.08
LEP	0.61±0.25	0.60±0.24	0.90	0.48±0.19	0.69±0.33	0.17

	Sham CPAP n=10			**Continued CPAP n=7**		
	Baseline	**Follow up**	***P* value**	**Baseline**	**Follow up**	***P* value**
LPL	1.14±0.51	1.22±0.22	0.65	0.91±0.47	1.17±0.58	0.10
MGLL	1.33±0.47	1.14±0.43	0.23	0.94±0.50	1.13±0.38	0.15
PER1	1.42±0.68	1.02±0.18	0.08	0.99±0.22	1.18±0.25	0.20
PER2	1.30±0.37	1.05±0.15	0.09	1.01±0.24	1.06±0.19	0.59
PLIN1	1.71±0.96	1.12±0.35	0.11	0.99±0.26	1.23±0.19	0.04*
PLIN2	1.22±0.57	1.01±0.16	0.23	0.94±0.34	1.21±0.24	0.08
PNPLA	1.24±0.52	0.96±0.30	0.19	0.89±0.20	1.09±0.17	0.04*
PPARA	1.07±0.26	1.10±0.14	0.78	1.03±0.13	1.07±0.21	0.62
Cell Metabolism						
AKT2	1.12±0.37	1.24±0.24	0.29	1.03±0.25	1.17±0.14	0.19
AQP7	1.04±0.37	1.08±0.30	0.73	0.73±0.23	0.90±0.27	0.22
CLOCK	0.68±0.25	0.66±0.13	0.83	0.55±0.16	0.71±0.28	0.22
CREB1	1.06±0.31	1.15±0.20	0.38	1.25±0.47	1.04±0.24	0.25
G6PD	0.81±0.23	0.84±0.12	0.65	1.31±0.85	0.92±0.25	0.29
GAPDH	1.31±0.31	1.19±0.13	0.24	1.21±0.08	1.23±0.26	0.89
GLUL	1.16±0.34	1.19±0.27	0.88	1.14±0.22	1.30±0.42	0.26
IRS1	1.24±0.49	1.09±0.36	0.26	0.85±0.35	0.99±0.25	0.34
IRS2	0.90±0.32	1.05±0.19	0.18	0.88±0.27	1.05±0.28	0.24
JAK2	0.94±0.53	1.33±0.56	0.18	1.23±0.70	0.96±0.39	0.20

	Sham CPAP n=10			**Continued CPAP n=7**		
	Baseline	**Follow up**	***P* value**	**Baseline**	**Follow up**	***P* value**
MAPK1	1.09±0.42	1.25±0.17	0.25	1.53±0.71	1.22±0.20	0.27
NPR3	1.28±0.57	1.11±0.46	0.43	0.84±0.28	0.98±0.24	0.17
PGK1	1.19±0.43	1.25±0.23	0.69	1.17±0.23	1.14±0.16	0.76
PDHA1	1.07±0.38	1.21±0.29	0.17	0.92±0.20	1.06±0.21	0.22
PDK4	0.84±0.40	0.95±0.16	0.46	0.95±0.42	1.12±0.50	0.57
PDP1	1.13±0.52	1.14±0.36	0.99	1.08±0.24	0.95±0.20	0.13
PIK3CA	0.97±0.49	1.15±0.30	0.41	0.96±0.48	1.04±0.43	0.39
PPARG	1.52±0.55	1.29±0.22	0.30	1.09±0.59	1.41±0.57	0.18
PRKA1	1.30±0.36	1.36±0.20	0.28	1.18±0.29	1.17±0.24	0.94
SLC2A1	0.73±0.45	1.01±0.45	0.21	1.10±0.64	0.62±0.18	0.07
SLC2A4	1.08±0.37	1.14±0.28	0.46	0.93±0.45	1.20±0.33	0.23
WNT5A	1.03±0.53	0.97±0.43	0.77	0.79±0.37	0.85±0.26	0.76
Cell remodelling						
BMP4	1.29±0.39	1.05±0.34	0.13	0.84±0.35	1.02±0.29	0.34
BMP7	0.80±0.47	0.55±0.40	0.39	0.50±0.44	0.85±0.64	0.22
COL1A1	0.33±0.29	0.37±0.35	0.73	0.15±0.09	0.23±0.14	0.06
COL3A1	1.00±0.51	1.16±0.64	0.23	0.71±0.33	0.92±0.34	0.14
CTNNB1	0.95±0.32	1.15±0.06	0.08	0.95±0.20	1.08±0.23	0.11
FGFR1	1.54±1.10	1.19±0.20	0.33	1.07±0.18	1.29±0.17	0.06

	Sham CPAP n=10			**Continued CPAP n=7**		
	Baseline	**Follow up**	***P* value**	**Baseline**	**Follow up**	***P* value**
ICAM1	1.32±0.27	1.38±0.31	0.72	1.59±0.64	1.15±0.21	0.18
LOX	1.15±0.58	1.05±0.28	0.54	0.65±0.27	0.92±0.12	0.03
MMP1	0.58±0.64	0.76±0.74	0.53	0.51±0.45	0.27±0.13	0.10
MMP2	0.82±0.25	0.79±0.22	0.66	0.63±0.34	0.80±0.30	0.16
MMP3	0.44±0.31	0.77±0.73	0.20	0.68±0.55	0.34±0.19	0.38
MMP9	0.39±0.24	0.60±0.42	0.09	0.60±0.28	0.51±0.42	0.68
PLAT	0.98±0.57	0.74±0.24	0.19	0.73±0.33	0.71±0.28	0.87
SERPINE1	0.45±0.31	0.47±0.15	0.80	0.56±0.50	0.72±0.73	0.37
Steroid Metabolism and action						
ADRB2	1.34±0.15	1.37±0.27	0.65	1.26±0.41	1.30±0.40	0.65
ARNT	1.23±0.33	1.13±0.13	0.48	1.02±0.09	1.08±0.14	0.34
DUSP1	1.28±0.36	1.06±0.36	0.05	1.30±0.88	1.00±0.21	0.34
HSD11B1	1.10±0.77	0.89±0.21	0.38	0.87±0.55	0.99±0.17	0.55
NR3C1	1.17±0.32	1.21±0.17	0.67	1.04±0.40	1.06±0.29	0.86
SGK1	1.12±0.52	1.27±0.42	0.29	1.38±0.53	1.32±0.55	0.75
SRD5A1	0.97±0.47	1.21±0.35	0.26	1.07±0.36	0.93±0.24	0.23
TSC22D3	1.23±0.48	1.06±0.27	0.23	1.50±0.95	1.03±0.29	0.15

	Sham CPAP n=10			**Continued CPAP n=7**		
	Baseline	**Follow up**	***P* value**	**Baseline**	**Follow up**	***P* value**
Oxidative stress						
ANGPTL4	1.05±0.60	0.88±0.37	0.43	0.78±0.35	1.05±0.37	0.02*
CAT	1.22±0.32	1.12±0.21	0.45	0.93±0.40	0.99±0.30	0.57
GPX1	0.95±0.36	0.94±0.28	0.96	0.83±0.23	1.00±0.26	0.20
GPX3	1.10±0.64	1.11±0.60	0.94	0.70±0.32	0.92±0.33	0.09
HIF1A	1.31±0.51	1.38±0.26	0.68	1.41±0.41	1.25±0.31	0.30
MTOR	0.84±0.37	1.12±0.23	0.02*	1.03±0.26	0.97±0.23	0.56
NOX4	0.66±0.28	0.71±0.24	0.70	0.48±0.29	0.68±0.30	0.06
SIRT1	1.20±0.35	1.22±0.23	0.86	1.13±0.23	1.15±0.27	0.88
SOD1	1.26±0.45	1.22±0.28	0.83	1.04±0.61	1.20±0.32	0.39
UCP2	0.63±0.24	0.80±0.23	0.16	0.76±0.23	0.76±0.35	0.98
VEGFA	1.11±0.46	1.05±0.26	0.66	0.90±0.14	1.07±0.19	0.04*
ER stress						
ATF6	1.08±0.42	1.18±0.16	0.49	1.33±0.35	1.08±0.17	0.12
EIF2AK3	1.49±0.48	1.31±0.24	0.36	1.29±0.15	1.24±0.12	0.41
ERN1	0.50±0.17	0.54±0.15	0.68	1.12±1.23	0.44±0.07	0.20
Inflammation						
CCL2	0.67±0.43	0.59±0.16	0.60	0.67±0.75	0.80±0.70	0.40
CCL28	1.27±0.50	0.90±0.25	0.12	0.80±0.27	0.83±0.25	0.72

	Sham CPAP n=10			**Continued CPAP n=7**		
	Baseline	**Follow up**	***P* value**	**Baseline**	**Follow up**	***P* value**
CD36	1.14±0.43	1.19±0.17	0.63	1.02±0.49	1.18±0.44	0.25
IFNG	0.30±0.19	0.48±0.45	0.05	0.68±1.26	0.38±0.34	0.58
IL10	0.94±0.64	0.88±0.36	0.86	0.88±0.48	1.06±0.52	0.16
IL6	0.55±0.43	0.53±0.38	0.80	0.32±0.21	0.28±0.09	0.45
IL8	0.74±0.85	1.07±1.09	0.47	0.91±0.77	0.43±0.21	0.08
NFKB1	1.20±0.47	1.22±0.15	0.90	1.48±0.69	1.18±0.11	0.30
TNF	0.94±0.41	1.21±0.66	0.16	1.74±0.96	0.96±0.33	0.07

3.4 Discussion

The CPAP withdrawal model employed in the current study was well tolerated and led to a clear "unmasking" of OSA measured by increased ODI. Advantages of this CPAP withdrawal model have been discussed previously (203) and include (i) its comparative efficiency compared to time consuming CPAP studies, (ii) negating variable CPAP compliance in previously CPAP naïve patients and (iii) the rapid return of OSA upon CPAP withdrawal. The samples that form part of this study represent a sub-study of a larger study published previously (204).

In the current work 2 weeks of sham CPAP was associated with an increase in key urinary glucocorticoid metabolites including THF, THE and the total cortisol metabolites. This demonstrates that CPAP withdrawal is associated with activation of the HPA axis.

The key advantage of the methodology used here are that urinary steroid profiling identified changes in steroidogenesis as well as the metabolism of steroids which is directly relevant to HPA axis activation and steroid action.

There are some discordant findings in previously published studies as identified by the authors of a meta-analysis of 7 studies which showed no apparent difference in cortisol levels between controls and patients with OSA (179). The authors in particular comment on the heterogeneity of cortisol assessment methods. Many of the studies compare only morning cortisol levels which may not be fully reflective of any changes seen as a result of OSA where it could be feasibly argued that the physiological disturbance of OSA may cause an early morning surge in cortisol or lead to a persistently elevated cortisol across the night. It is therefore important to note that in the only study employing 24 hour levels of cortisol, the levels were significant higher in those with OSA than in matched controls and as hypothesised the levels were higher over-night (173). The same study showed that 2 months of effective CPAP resulted in a reduction in cortisol levels (173). This study is a useful basis for the present work which employs a more detailed assessment of glucocorticoid metabolism by assessing the urinary steroid profile and further supports the decision to undertake an overnight urinary collection. The precise driver of elevated cortisol in patients with OSA is not known however it may be partly due to disturbed sleep since in healthy individuals micro arousals during sleep were well correlated with cortisol levels (205).

Although previous studies have shown a reduction in cortisol levels with 3 months of CPAP therapy (173, 175, 176) only one study has examined the effect of CPAP withdrawal (185). This study was limited by its acute nature (1 night off CPAP) and by the assessment used (morning ACTH and cortisol) and failed to show any effect (185).

Whether changes in the urinary steroid profile are reflective of the underlying disease state or are potentially causative is debated. Urinary Total F metabolites are increased in NAFLD compared to control patients (206) and I and others have shown experimentally that glucocorticoids drive lipogenesis (163). Furthermore, in a longitudinal analysis, total glucocorticoid production was associated with increasing BMI and worsening glucose tolerance (207). It is plausible therefore that the increased cortisol production seen with CPAP withdrawal may contribute to hepatic lipid accumulation.

In this study, 2 weeks of sham CPAP was sufficient to increase the overnight urinary steroid profiles of several key mineralocorticoid metabolites including the precursors 5αTHA, 18OH THA and the major metabolite of aldosterone 3α5β THALDO (not significant). However, plasma morning levels of aldosterone were not altered. In previously published studies and in those patients without established hypertension, isolated morning measurement of plasma aldosterone was not different between those with OSA and controls (135, 136). However, in a meta-analysis of 9 studies reporting plasma aldosterone concentrations in those with OSA, aldosterone was elevated in those with OSA and hypertension versus those with OSA and no hypertension. In the same study, after excluding a small study, aldosterone was significantly higher in patients with OSA compared to controls (137). Furthermore, when hypertensive patients with and without OSA where compared it was shown that plasma aldosterone concentrations were higher in those with OSA (137). Therefore, given the differences in the prevalence of treated hypertension in the current study (64% in the sham group and 27% in the continued CPAP group) it is possible that any subtle differences to mineralocorticoid steroidogenesis may be masked. Furthermore, assessment of mineralocorticoid pathways may be further

complicated in this setting by the presence of antihypertensive therapy as well as hypertension itself.

No study has previously examined CPAP withdrawal on aldosterone levels. The previously published meta-analysis showed no effect of CPAP of at least 1 month on plasma morning aldosterone (141).Whilst a separate meta-analysis that excluded patients with resistant hypertension treatment with CPAP was associated with a reduction in plasma aldosterone (142). Given the previously reported increases in blood pressure in CPAP withdrawal studies (208) it is plausible given the changes in mineralocorticoids that this may be a causative mechanism.

CPAP withdrawal did not significantly affect subcutaneous abdominal adipose gene expression. This finding was supported by two recent publications (62, 63). In the first such paper adipose tissue oxygenation was measured in 16 men with OSA pre and post 4 months of CPAP as well as in BMI-matched controls using a Clarke-type electrode as well as in mixed blood in adipose tissue microcirculation. It should be noted that these experiments were conducted in the morning following an overnight fast. Tissue oxygenation by either method was unchanged between controls and patients and CPAP had no effect (62). Post-prandial adipose tissue blood flow was unchanged between patients with OSA and controls although resting blood flow was increased in patients (62). This may explain the finding that of the panel of genes studied there were only modest differences between patients and controls and that CPAP therapy effected only 1 of the 18 genes reported (62). These observations were supported by another recent study (63). This was a study of people with obesity (BMI>35) and it is possible that the degree of obesity may have masked any possible differences in gene expression between patients with OSA and controls. Although in this study CPAP did have an effect on the transcriptional profile

those in the CPAP group lost more weight as part of the weight loss intervention that ran in parallel to CPAP (63).

A clear limitation of the present work is that CPAP was only withdrawn for 2 weeks which may be insufficient to detect more modest changes. As this work was part of a larger study (204) we were not involved in the initial study design as a result there were several unavoidable limitations. Namely, although the cohort was mixed gender it was heavily male dominated, secondly those with diabetes were all randomised to continue CPAP and thirdly there was a higher prevalence of hypertension in the group randomised to sham CPAP. Furthermore, as outlined in the relevant sections not all samples were available for every patient (**Table 3-3**).

The plasma steroid data presented here is limited by comparatively small numbers as well as samples taken at a single time point. Furthermore, the assays used had a relatively high co-efficient of variation. This may have contributed to the fact that the plasma steroid data did not accurately mirror the urine data discussed above.

Additional limitations related specifically to the adipose transcription data were: (1) adipose biopsies (as with previously published studies (62)) were taken in the morning which may mask transient changes in transcriptional profile as the tissue may have had sufficient time to "re-oxygenise," (2) the data involved comparatively small numbers of patients, and (3) the diabetic patients were all randomised to continue CPAP.

In conclusion, we have shown that CPAP withdrawal is associated with discrete changes in the HPA axis as well as in mineralocorticoid secretion. It remains to be seen in patients with OSA if this is a cause of consequence of the disease and to what extent these changes may influence the development of metabolic disease including hypertension. In

adipose tissue, CPAP withdrawal had no real effect on gene expression profiles which may reflect either that the adipose is not exposed to sufficient hypoxia or that the adipose is comparatively insensitive to hypoxia. This will be addressed in the following chapter. Furthermore, in this chapter we have not assessed the effect of OSA or hypoxia on the local bioavailability of cortisol as a result of 11βHSD1 activity and I will try to address this in a later chapter.

4. Adipocytes are sensitive to hypoxic exposure

4.1 Introduction

In the previous chapter we saw that subcutaneous abdominal adipose tissue was comparatively insensitive to "unmasking" OSA with CPAP withdrawal. We saw that despite a clear return of overnight oxygen desaturations there was no discernible effect on adipose tissue gene expression. I discussed above whether this might be related to changes in blood flow or secondary to the comparatively low oxygen consumption however what is less clear is the innate ability of adipocytes to respond to different oxygen tensions. Traditional cell culture models culture cells in 21% oxygen and 5% carbon dioxide with the balance gas nitrogen. This is hypercapnic relative to the air which contains only trace elements of CO_2 and although 21% is the FiO_2 of air it is likely to be hyperoxic compared to the *in vivo* exposure of human adipose tissue. 21% equates to a partial pressure of oxygen of 160 mmHg whilst the pO_2 of adipose tissue in individuals with obesity with and without OSA is likely to be around 50 mmHg (59, 62) whilst that of lean individuals may be marginally higher 55 mmHg (59). It is not unreasonable therefore to consider a tissue culture FiO_2 of 5% to be more physiologically relevant. Many of the tissue culture experiments studying hypoxia compare the effects of 1% and 21% where 21% is considered as the control conditions. Based on the above data it may be that previously published works are therefore comparing comparatively modest hypoxia with hyperoxia. Despite these limitations we will test the hypotheses that adipocytes are directly responsive to hypoxic exposure and that glucocorticoid sensitive genes may be oxygen sensitive which we will assess using cultured mature adipocytes exposed to different oxygen tensions for 24 hours.

4.2 Materials and Methods

4.2.1 Research strategy

In this chapter, we will examine the effect of different oxygen tensions on the transcriptional profile of mature human culture subcutaneous abdominal adipocytes. We will achieve this by differentiating pre-adipocytes until they reach maturity as detailed below prior to 24 hours of exposure to different oxygen tensions (0.1%, 1%, 5% and 21%).

The aims of this chapter are (1) to examine the gene expression profile of primary subcutaneous abdominal adipocytes cultured in different oxygen tensions to determine whether adipocytes are oxygen sensitive at a range of physiological oxygen tensions and (2) to determine whether the expression of genes known to be modulated by glucocorticoids are sensitive to changes in oxygen exposure.

4.2.2 Primary adipocyte tissue culture and hypoxic exposure

Primary human pre-adipocytes were derived from subcutaneous abdominal adipose tissue from healthy male volunteers. Adipocytes from 3 separate donors were used for experiments with 2 of the donor samples further passaged for subsequent experiments (n=5). Adipocytes were isolated by digestion in collagenase (1mg/ml) and re-suspended in Hanks Buffered Salt Solution (HBSS) and then further filtered and re-suspended in growth media (DMEM/Ham's F12 (1:1,v/v), foetal calf serum (10%), Penicillin-Streptomycin (100U/ml and 100µg/ml), glutamine (2mM), fibroblast growth factor (0.25ng/ml)) and cultured to a density required to trypsinise and plate for experiments. Pre-adipocytes were plated at a density of 2 x 10^5 cells/well and maintained using growth media (as detailed above). The media was changed every 3 days and plates were incubated at 37°C, 5% CO2, 21% O2. Fully confluent preadipocytes were treated with an adipogenic differentiation media containing DMEM/Ham's F12, 100U/ml penicillin, 100µg/ml streptomycin, 2mM

L-glutamine, 17μM pantothenate, 100nM human insulin, 10nM triiodothyronine, 33μM biotin, 130nM transferrin, 1μM dexamethasone, 250μM 3- isobutyl-1-methylxanthine (IBMX) and 4μM troglitazone. Differentiation media was changed on day 2 and switched to a basal differentiation media not containing IBMX and troglitazone on day 4. The media was then changed every 3 days, until the cells exhibited the morphology of mature adipocytes (day 15). Prior to hypoxic exposure, cells were serum starved to ensure no steroids were present within the media.

Hypoxic incubations were performed using the In vivo2 400 hypoxic workstation (Ruskin Technologies). Cells were cultured for 24 hours at 37˚C in 5% CO_2 with an oxygen tension of 0.1%, 1% and 5% with the balance made up of nitrogen. Gene expression methodology and western blotting is covered in the general methods section (**Chapter 2**).

Gene expression was compared with one-way ANOVA with a Tukey test for multiple comparisons using GraphPad Prism. Data was presented as mean ± standard error of mean.

4.3 Results

4.3.1 Adipocyte sensitivity to hypoxia

In the first instance genes known to be sensitive to hypoxia were analysed (**Figure 4-1**). These included vascular endothelial growth factor A (VEGFA), glucose transporter 1 (GLUT1), interleukin 6 (IL6) and hypoxia inducible factor 1α (HIF1A). VEGFA and GLUT1 were sensitive across the titration of oxygen tensions studied with expression increased in response to 0.1% and 1% oxygen compared to the more physiological 5% and the traditionally studied 21%. The mRNA expression pattern of HIF1A was (non-significantly) decreased in hypoxic conditions. However, the anticipated pattern of expression was seen at protein level when assessed using Western blotting (Figure 4-2).

To further define the interaction between glucocorticoid signalling and hypoxia, we examined target genes known to be regulated by glucocorticoids. Of the genes studied only dual specificity phosphatase 1 (DUSP1) was shown to be oxygen sensitive and only when exposed to severe hypoxia (0.1%). serum/glucocorticoid regulated kinase 1 (SGK1), glucocorticoid-induced leucine zipper protein (GILZ) and the NR3C1 (glucocorticoid receptor) were all unchanged by hypoxic exposure (**Figure 4-3**).

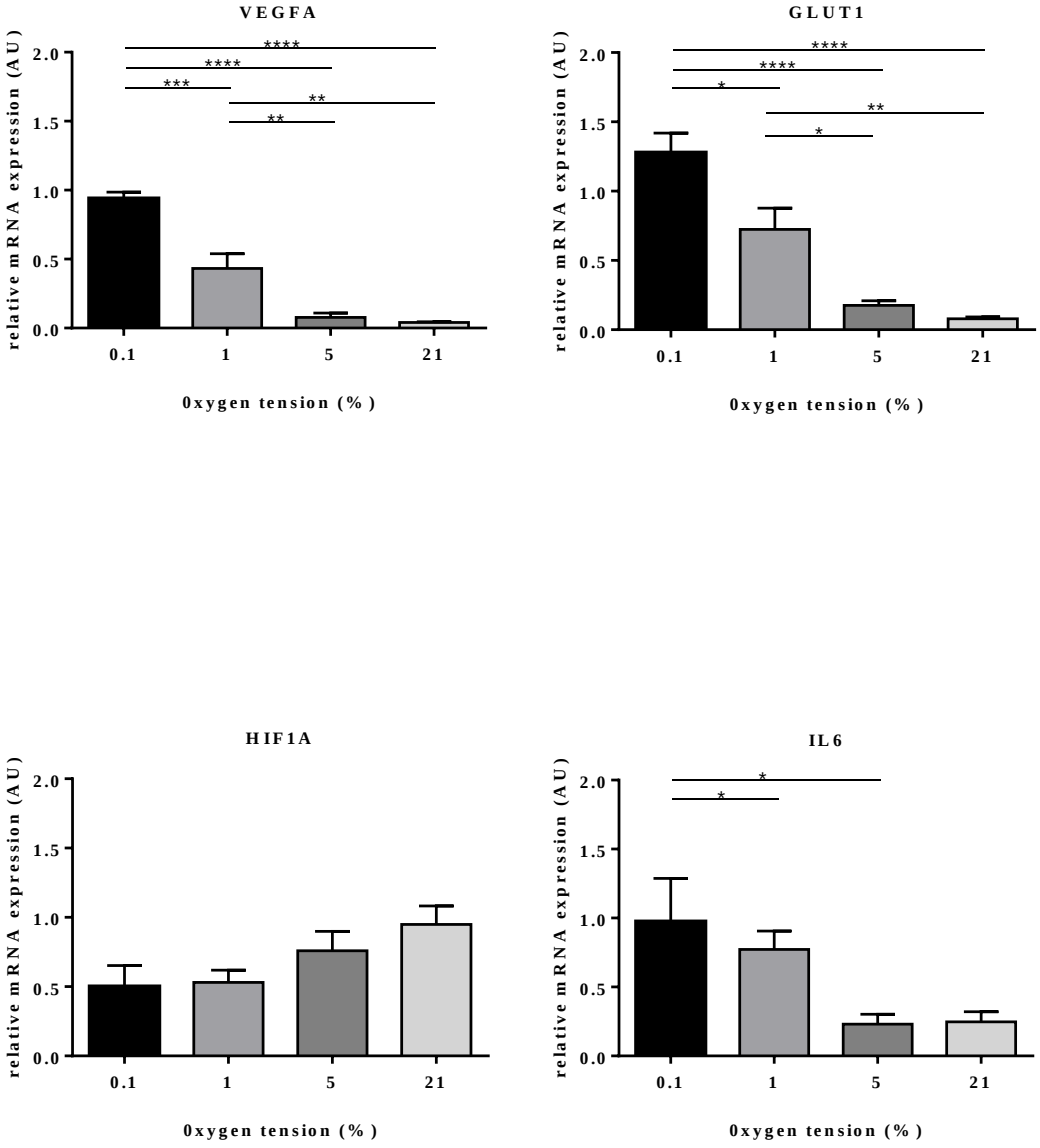


Figure 4- 1 The effect of hypoxia on adipose gene expression of genes known to be oxygen sensitive. Data is presented as arbitrary units (AU) (mean ± SE).

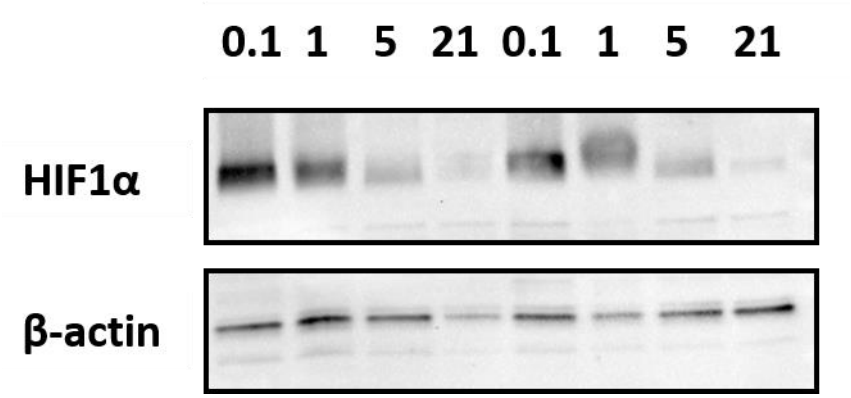


Figure 4- 2 The effect of hypoxia on adipose protein expression of HIF1a protein in response to different oxygen tensions (0.1, 1, 5 and 21%). Data shown for adipocytes from two different primary adipose sources.

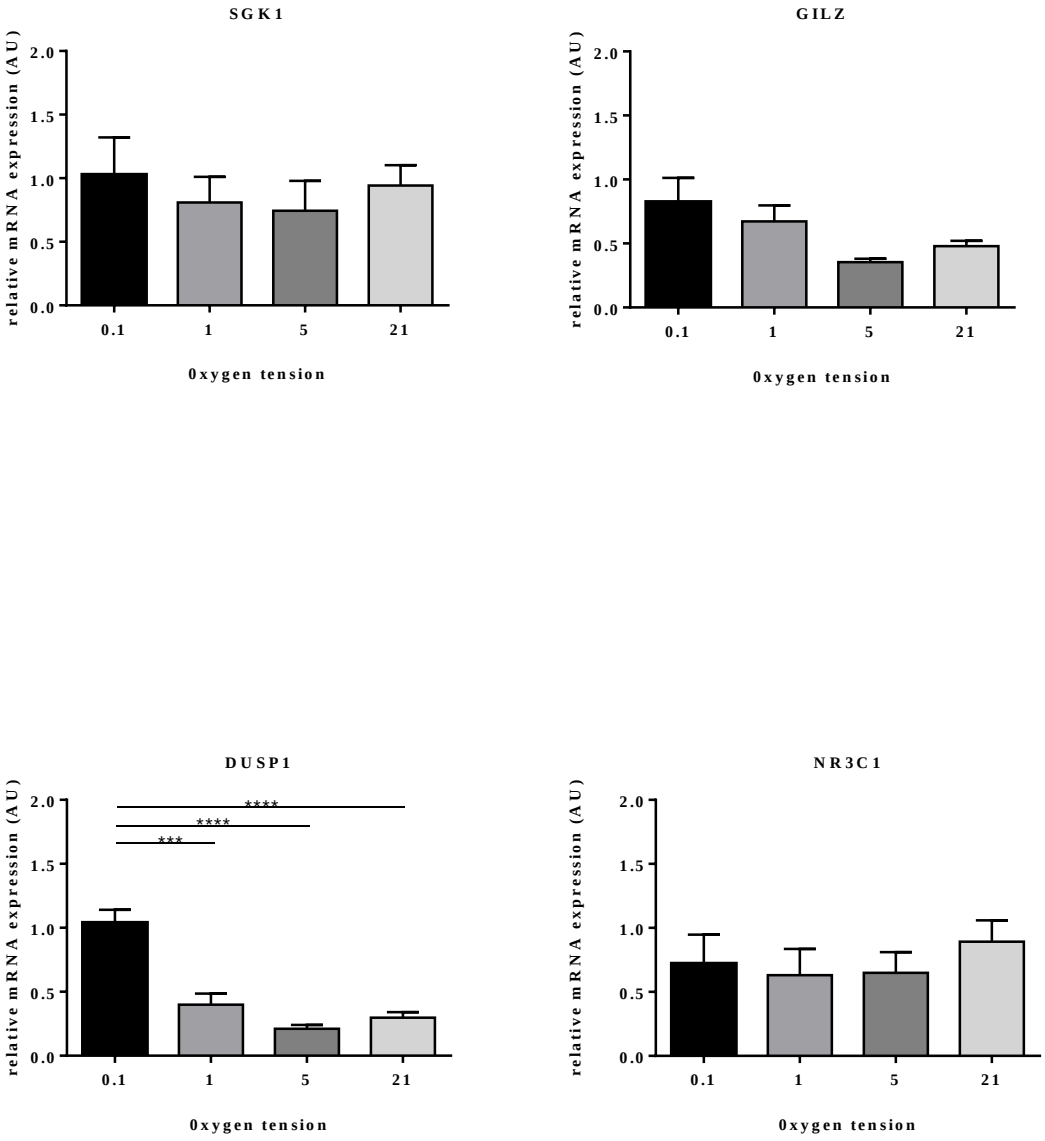


Figure 4- 3 The effect of hypoxia on adipose gene expression of genes known to be glucocorticoid sensitive. Data is presented as arbitrary units (AU) (mean ± SE).

4.4 Discussion

In this chapter we have demonstrated that human pre-adipocytes differentiated to mature adipocytes are capable of sensing and responding to hypoxia at a gene and protein level. Therefore, the lack of an effect of OSA on adipose tissue gene expression seen in Chapter 3 is not secondary to an innate insensitivity of adipose tissue to hypoxia.

However, these dose titration experiments performed in this chapter demonstrate that comparatively severe hypoxia (0.1%) is required to see significant effects when either compared to the "traditional" 21% oxygen or the more physiologically relevant 5% oxygen. It is therefore likely that the degree of relative tissue hypoxia in the CPAP withdrawal study is likely to be insufficient to elicit transcriptional effects.

There are no previously published oxygen dose titration experiments in cultured differentiated subcutaneous human adipocytes. VEGFA is a known regulator of the adipose tissue response to hypoxia and has been shown to be an important signal for adipose tissue derived stem cells in tissue culture (209). The finding here that VEGFA expression is sensitive to even small changes in oxygen tension (1% vs 5%) is therefore not surprising. Whether this translates *in vivo* is less certain since in a previous study in which obese adipose tissue was found to be hypoxic there was no apparent effect on VEGFA expression (59). As outlined above the oxygen tension of adipose tissue in individuals with obesity with and without OSA is likely to correspond to around 50mmHg (59, 62) whilst that of lean individuals is only marginally higher at 55mmHg (59). The measurements in these studies were taken in the morning which may mean genuine tissue hypoxia has been missed as it is more likely to occur during sleep when OSA is most physiologically significant. In an experimental rodent model of intermittent hypoxia significant desaturations down to SaO_2 of 60% were required to reduce the epididymal fat oxygen tension from ≈50mmHg to ≈30mmHg (210). This is far more hypoxic than the nadir oxygen saturations typically seen in OSA. It seems likely therefore, that the kind of tissue oxygen tensions achieved *in vivo* in man in those with obesity ± OSA are far less hypoxic than the oxygen tensions used *in* vitro to elicit gene transcription changes.

Furthermore, whether cells are differentiating or mature adipocytes may affect their response to hypoxia. In one such study it was shown that pre-adipocytes differentiated in 5 or 10% were more responsive to isoproterenol induced lipolysis suggesting a more physiological phenotype than those differentiated in 21% (51). Similar findings are seen when the 3T3L1 adipocyte rodent cell line is differentiated in hypoxic conditions as it becomes more lipid laden than when differentiated in normoxia (55). This is contrasted by the findings that mature adipocytes cultured in hypoxic conditions have reduced levels of TG and droplet size (54). Clearly human adipose tissue *in vivo* includes adipocytes at different stages of maturity as well as additional cell types including immune cells. This synthesised data further questions the extrapolations that can be made to the *in vivo* state from tissue culture experiments.

The impact of systemic *in vivo* hypoxia on glucocorticoid regulated genes in adipose may be mediated via either 1) activation of the HPA axis causing increased systemic glucocorticoids 2) increased local tissue availability of glucocorticoids via changes in pre-receptor metabolism of glucocorticoids or 3) a direct effect of hypoxia on the glucocorticoid receptor (GR). In this series of experiments, we cultured cells in a steroid free environment to try and elucidate an effect of hypoxia on the GR however there may be a contribution to intracellular steroid metabolism. The genes selected are known to be expressed in adipose tissue and are well known to be responsive to glucocorticoids. In the experimental setup cells were serum starved prior to exposure to the different oxygen tensions to ensure the absence of glucocorticoids within the media to assess whether hypoxia could have a ligand independent effect on the GR. SGK1 and GILZ expression were unchanged across different oxygen tensions. Whilst the mRNA expression of the GR (NR3C1) was unchanged by hypoxia there was an effect on DUSP1 (dual specificity

phosphatase 1) although this was only apparent at 0.1% oxygen. The effect seen on DUSP1 may partly explain the transcription pattern seen for HIF1A since it has previously been shown to negatively regulate HIF1A in tumour cells (211).

The potential functional impact of changes to gene expression in adipocyte gene expression in response to hypoxia has not been studied here. GLUT1 expression varied across the oxygen tensions studied, a finding supported by data showing increased glucose uptake and expression of GLUT1 in adipose derived stem cells cultured in 1% oxygen (212). This potential finding of increased glucose uptake by adipose in hypoxia supported by the present data may in part explain why obesity does not correlate with a clear metabolic signal of tissue hypoxia (57). In this study whilst adipose was shown to be glycolytic the relationship between BMI and lactate-pyruvate ratio (a marker of anaerobic metabolism) was actually inversely proportional (57). The inference from the above, is that in conditions of relative hypoxia, biological adaptations (such as increased glucose uptake) may protect against oxidative stress. It is unclear how long such adaptations take to develop and to what extent they may be metabolically protective over time.

Given therefore that adipose tissue *in vivo* even in the context of OSA is not particularly hypoxic compared to well-matched controls (62) and is a low comparative consumer of oxygen (57) the data presented here further supports the data presented in Chapter 3 that there was no significant transcription signal on withdrawal of CPAP.

5. Glucocorticoid receptor antagonism offers metabolic benefit in man

5.1 Introduction

Glucocorticoid excess, as seen in Cushing's disease or as a result of prescribed steroids, is associated with a significant burden of metabolic disease. This includes cardiovascular disease, diabetes, NAFLD, dyslipidaemia and sarcopenia (213, 214). Whilst in Cushing's disease, treatment is associated with an improvement in symptoms and metabolic state it has been shown that cardiovascular risk may persist despite curative treatment (215). In those patients who are prescribed steroids the main strategy is to ensure patients are on the lowest dose possible or to change them to steroid sparing medications.

Whether antagonism of GR signalling in health could be metabolically advantageous is unknown. The GR antagonist used in the present work is RU486 which is also known as Mifepristone. This is a non-selective competitive inhibitor of several steroid receptors including the glucocorticoid receptor, mineralocorticoid receptor, progesterone receptor and androgen receptor. It was chosen because it is usually well tolerated and is available as a medicinal preparation (EXELGYN, France). RU486 has been studied in those with persistent Cushing's despite previously attempted surgical and medical management and was shown to reduce weight, blood pressure and HbA1c (216). It has also been studied in post-menopausal women who were randomised to either placebo or RU486 600mg od for 6 weeks. In this study there was a reduction in total cholesterol and HOMA-IR however there was also a reduction in HDL cholesterol and HDL particle concentration, despite these reductions the functional effect on HDL's ability to carry cholesterol was modest (191). RU486 has also been used to try to prevent metabolic complications in patients treated with antipsychotic agents (risperidone and olanzapine) with some improvement in lipid profile, glycaemic control and weight (192, 193). In the first study healthy young male patients were randomised to receive either RU486,

olanzapine plus placebo or olanzapine plus RU486 for 2 weeks in an institutional setting (192, 193). Those on olanzapine gained significantly more weight than those randomised to olanzapine plus RU486 however those only on RU486 also gained some weight across the study period. There was a modest deterioration in fasting lipid profiles that was not protected by RU486 (179). In the second study healthy young men were randomised to receive either Risperidone, Risperidone plus RU486 or RU486 alone (180). RU486 was able to protect against the weight gain and deterioration in fasting TG and HOMA-IR seen in those patients randomised to receive Risperidone without RU486 (180).

In this chapter we will examine the fasting lipid profile and additional measures of metabolism to address the hypothesis that even in metabolically healthy volunteers GR antagonism has a beneficial effect on lipid metabolism and insulin sensitivity.

5.2 Materials and Methods

5.2.1 Research strategy

In this chapter we will examine the metabolic effect of GR antagonism in male volunteers. This study was part of the larger MEHASS study (Metabolic effect of hypoxia and steroid signalling) (Chapter 6a and 6b). In those chapters we will assess the relationship between GR antagonism and the metabolic effect of intermittent hypoxia. However, here we will examine the metabolic effect of GR antagonism outside of hypoxia. We will test the hypothesis that (1) GR antagonism reduced circulating lipids and that (2) GR antagonism improves insulin sensitivity. We will achieve this via a randomised open label study conducted in healthy male volunteers.

5.2.2 Statement of contributions

I designed and implemented the following study with the support of my supervisors Prof. Tomlinson and Dr Hodson. I processed the samples with additional laboratory support and advice from Catriona Charlton and Thomas Cornfield. I undertook all of the analyses.

5.2.3 Clinical Protocol

The following study was approved by the East Midlands Leicester South Research Ethics Committee (15/EM/0308). This was a prospective, randomised, open label study in 18 healthy male volunteers; 8 in the RU486 (600mg once a day) group and 10 in the control group (**Figure 5-1**). The *a priori* power calculation had necessitated 15 participants in each arm however because of the side effect profile the study was discontinued early. Further details are below. RU486 was obtained from Oxford University Trust pharmacy and is supplied by EXELGYN, 216, Boulevard Saint-Germain, 75007, Paris, France. It is supplied as 200mg capsules therefore the participants randomised to RU486 took 3 capsules of 200mg each to make up the 600mg dose. Patients were randomised at their screening appointment via computer randomisation. The randomisation schedule was kept in the site file and updated manually.

Participants underwent detailed metabolic phenotyping in the fasting state prior to randomisation to either no drug or to take the study drug (RU486 600mg once a day) for 7 days before then repeating the metabolic phenotyping.

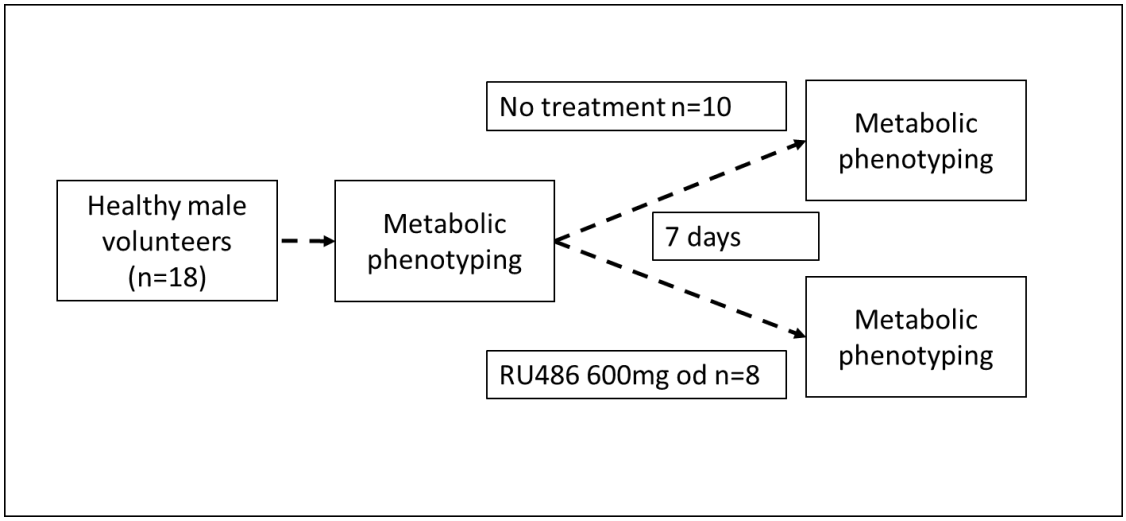


Figure 5- 1 The timeline and work flow of the GR antagonism study.

5.2.4 Inclusion and exclusion criteria

Inclusion

1. Participant is willing and able to give informed consent for participation in the study.
2. Male
3. Age 18-65 years
4. BMI 20-35 kg/m^2

Exclusion Criteria

1. Obstructive sleep apnoea identified with STOP-BANG questionnaire or overnight oximetry (ApneaLink^{TM} Plus).
2. Glucocorticoid use within the last 3 months
3. Drugs that impact upon glucocorticoid metabolism

4. Anticoagulant use (warfarin, novel oral anticoagulants, low molecular weight heparin (aspirin use is not an exclusion criteria)).
5. Smoking
6. Uncontrolled hypertension (BP >160/100mmHg)
7. Significant co-morbidities including (Diabetes, Respiratory disease – including the use of inhaled therapy, cardiac disease, renal disease and hepatic disease)
8. Significant travel sickness
9. BMI > 35 kg/m^2

5.2.5 Recruitment

Recruitment was via local physical and electronic advertisement across the University of Oxford, Oxford Brookes University and The Oxford University Foundation Trust. Interested participants who then contacted us were then provided with an electronic copy of the patient information sheet before being invited to attend for a screening and consent visit.

5.2.6 Metabolic assessment

This GR antagonism study was designed chiefly to assess the effect on lipid metabolism in the fasted state. All measurements were taken as single time points in the fasted state. As such the variables measured included insulin, TAG, HDL, Cholesterol, ApoB, Adipo-IR and hydroxybutyrate as well as other laboratory variables measured chiefly to ensure pharmacological tolerability. The methods used to measure the above variables are covered within Chapter 2. *De novo lipogenesis* (DNL) was assessed by the incorporation of deuterated water into newly synthesised TAG palmitate or VLDL-TG

palmitate (Chapter 2). Participants all underwent body composition scanning and assessment of basal metabolic rate (TANITA®,Amsterdam-Zuidoost, Netherlands). Insulin resistance was assessed using the homeostatic model of assessment 2 (HOMA2) (217). Adipose tissue insulin resistance (Adipo-IR) was calculated by multiplication of fasting non-esterified fatty acids (mM) and fasting insulin (pM) (218).

5.2.6 Statistical analysis

Data was assessed for normality using the D'Agostino and Pearson omnibus normality tests. Data is presented as mean ± SD where normally distributed otherwise it is presented as median (IQR). Baseline data was compared using an unpaired t-test where normally distributed and otherwise was compared using Mann-Whitney tests. Effect of drug compared to baseline was compared using paired t-tests with no adjustment for baseline values. Prism GraphPad was used for statistical analyses of this data. Statistical significance was defined as a $p<0.05$.

5.3 Results

5.3.1 Patient demographics

The patients were all male. There were 10 patients in the control group and 8 patients who had been randomised to RU486. The total cohort had a mean age of 25.3 ± 5.5 and was normotensive (systolic BP 121±10 mmHg) and not overweight (BMI 24.08±1.7 kg/m^2). The control and RU486 groups were well matched with no differences in demographic, anthropometric or metabolic values at baseline (**Table 5-1**).

Table 5-1 The demographics and biochemical profiles of the participants. Data marked† is not normally distributed.

	Controls (n=10)	**RU486 (n=8)**	***P* value**
Age (years)	26.1 ±6.5	24.13 ±3.6	0.7441
Weight (kg)	82.65 ±4.6	80.94 ±6.4	0.5175
Height (cm)	186 ± 7.5	182 ± 6.1	0.1641
BMI (kg/m^2)	23.8 ±1.7	24.5 ± 1.6	0.3910
BMR (kJ)	8542 ± 621	8535 ± 544	0.9811
Fat (%)	15.6 ± 4.5	14.3 ± 4.5	0.5382
Systolic BP (mmHg)	126 ± 10	118.8 ± 10.7†	0.2437
Diastolic BP (mmHg)	68.7 ± 11	65.6 ± 11	0.5724
Glucose (mmol/L)	5.1 ± 0.34	4.9 ± 0.41	0.5348
HOMA2	1.2 ± 0.7†	1.1 ± 0.3	0.4964
TAG (µmol/L)	1023 ± 338	894.4 ± 63.5†	0.1011
Chol (mmol/L)	3.91 ± 0.78	3.82 ± 0.89	0.8079
HDL (mmol/L)	1.32 ± 0.26	1.36 ± 0.38	0.7649
Cortisol (nmol/L)	415 ± 90	372 ± 96	0.3401

5.3.2 Safety and tolerability

All the patients who were randomised to take RU486 were compliant with treatment as shown by the consistent elevation in plasma glucocorticoid levels at their 2nd metabolic assessment visit. No patients reported any side effects of RU486 when on the medication. However, 4/8 patients who were randomised to receive RU486 developed a self-limiting non-pruritic rash on their arms and chest 2-3 days after finishing the medication. This led us to discontinue the study prematurely as this side effect of rash was higher than in the previous literature (192, 193). All the patients with a rash felt

systemically well and were offered additional clinical review. All the rashes settled within a week. As this was an anticipated adverse event, we were not obliged to report to MHRA but we did report to the sponsor and ethics committee.

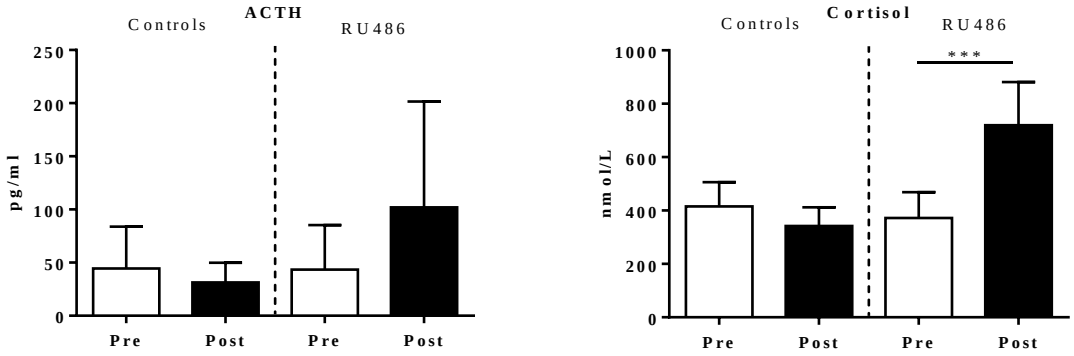


Figure 5- 2 The plasma ACTH and Cortisol of patients randomised to either no treatment or RU486 600mg od for 7 days. (ACTH=adrenocorticotrophin; ***P<0.001). Data presented as mean±SD. Pre refers to pre-randomisation to either no treatment or RU486 and post refers to after 1 week of either no treatment or RU486.

As part of the study we measured full blood counts, creatinine and electrolytes as well as measures of liver function as part of our metabolic assessment as well as safety monitoring. RU486 treatment was associated with a reduction in ALT (P=0.034). Haemoglobin concentration fell in the RU486 and control group in a manner consistent with significant venesection as part of the study protocol (**Figure 5-3)**.

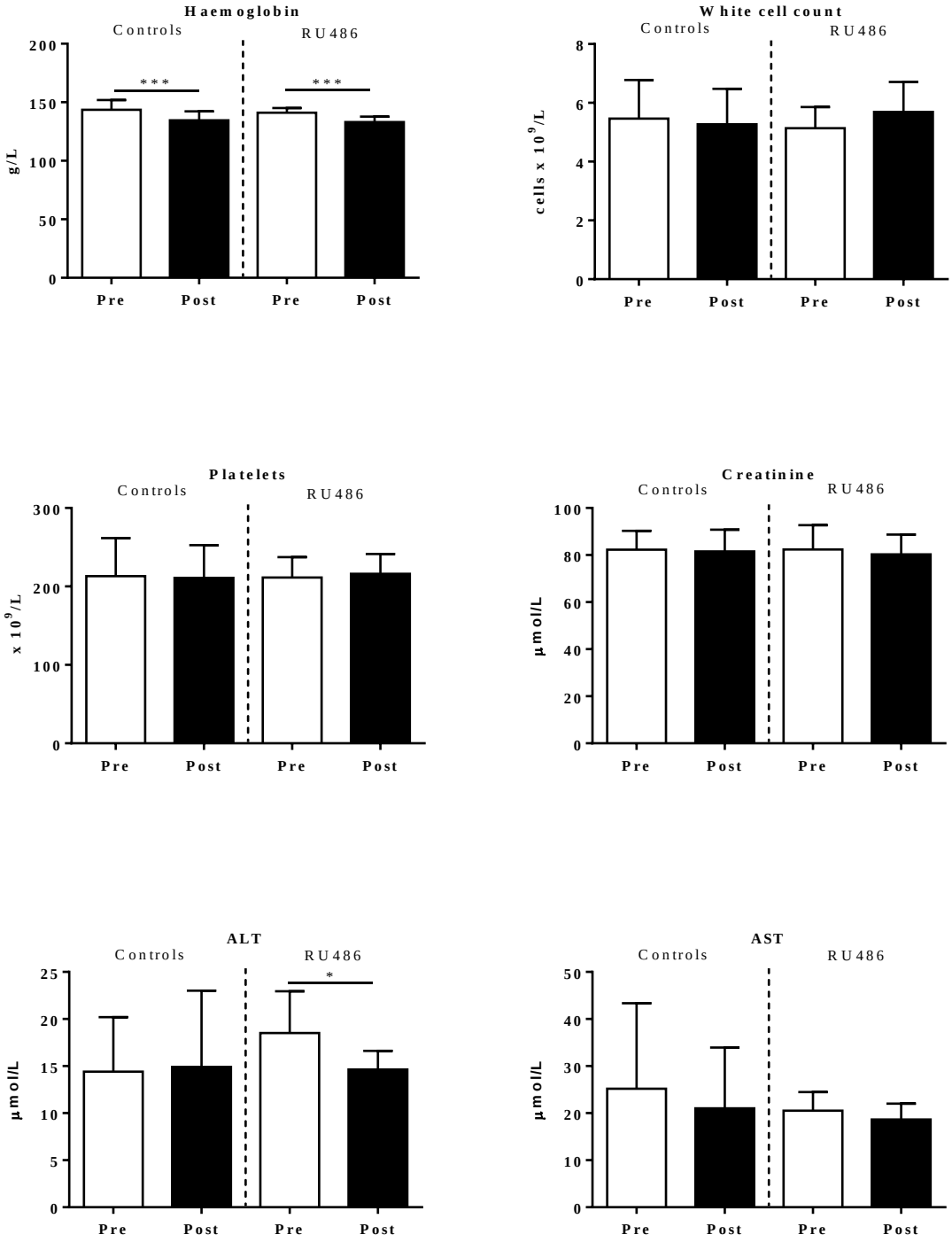


Figure 5- 3 Safety monitoring bloods of patients randomised to either no treatment of RU486 600mg od for 7 days (ALT: alanine aminotransferase; AST: aspartate transaminase; *P<0.05, ***P<0.001). Data presented as mean±SD. Pre refers to pre-randomisation to either no treatment or RU486 and post refers to after 1 week of either no treatment or RU486.

Both control patients and those randomised to RU486 had a reduction in plasma cholesterol (P=0.03 controls; P=0.03 RU486) across the study period and control patients also had a reduction in HDL cholesterol concentrations (**Figure 5-4**). (P=0.04 controls; P=0.09 RU486).

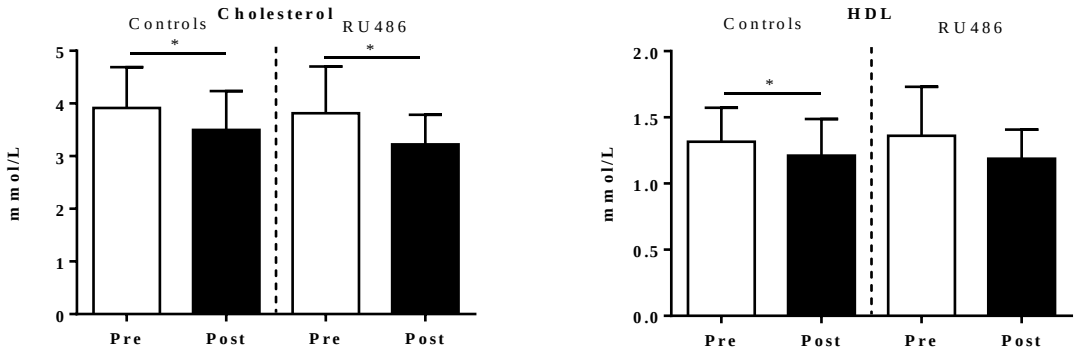


Figure 5- 4 The effect of RU486 on cholesterol and HDL cholesterol. (*P<0.05). Data presented as mean±SD. Pre refers to pre-randomisation to either no treatment or RU486 and post refers to after 1 week of either no treatment or RU486.

5.3.3 Lipid metabolism

We assessed the effect of glucocorticoid receptor antagonism on lipid metabolism in the fasted state. RU486 was associated with increased *de novo lipogenesis* measured within the plasma TAG pool (p=0.014) and the VLDL TAG fraction (p=0.053) without changes to the total TAG or VLDL TAG concentrations.

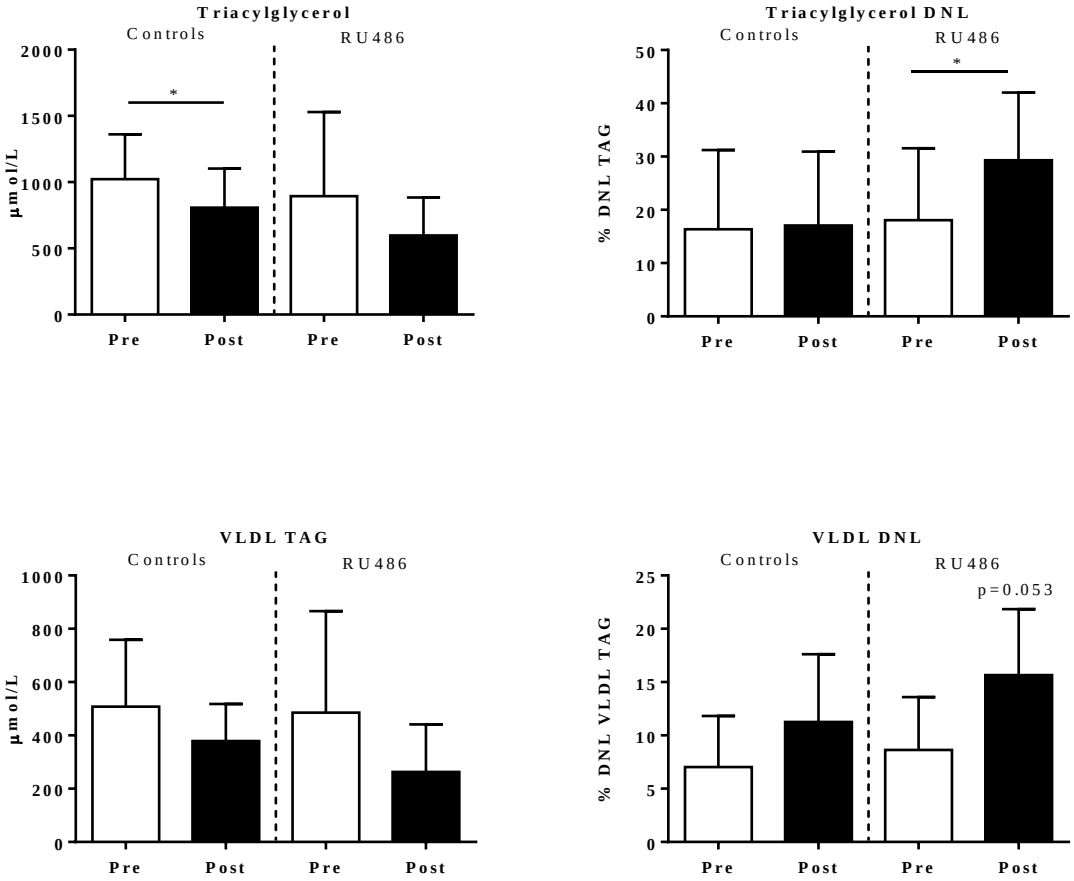


Figure 5- 5 The effect of RU486 on triacylglycerol (TAG) and very low density lipoprotein (VLDL) TAG and de novo lipogenesis within the plasma TAG and VLDL TAG fraction (*P<0.05). Data presented as mean±SD. Pre refers to pre-randomisation to either no treatment or RU486 and post refers to after 1 week of either no treatment or RU486.

We assessed the effect of glucocorticoid receptor antagonism on measures of lipolysis including NEFA, glycerol and adipose tissue insulin resistance (Adipo-IR). RU486 was associated with a reduction in measures of lipolysis (NEFA, P=0.006; Glycerol, P=0.037) as well as an increase in the sensitivity of adipose tissue to insulin (Adipo-IR, P=0.0011). We also demonstrated a reduction in β-hydroxybutyrate (OHB) (which is a measure of hepatic fatty acid oxidation) with RU486 (P=0.006).

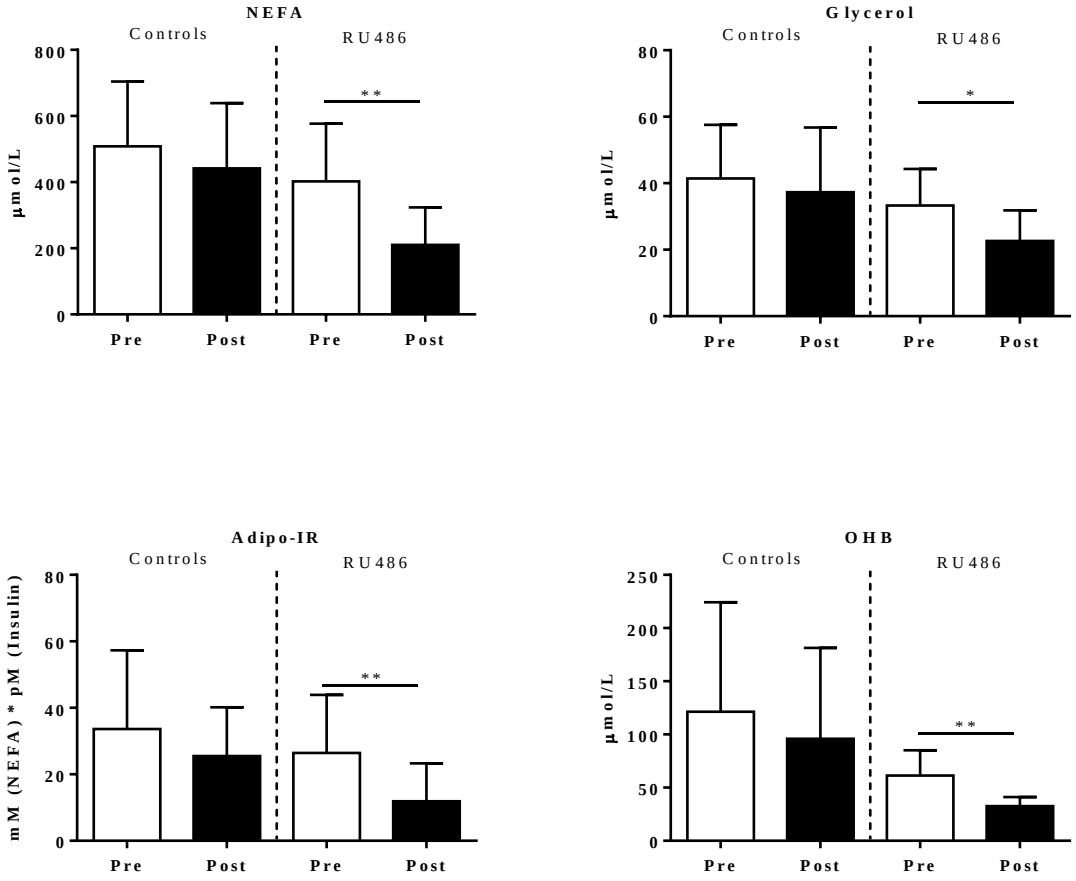


Figure 5- 6 The effect of RU486 on measures of lipolysis and adipose insulin resistance (Adipo-IR). As well as fatty acid oxidation measured by OHB (NEFA=non-esterified fatty acids; OHB=β-hydroxybutyrate; *P<0.05; **P<0.01). Data is presented as mean±SD. Pre refers to pre-randomisation to either no treatment or RU486 and post refers to after 1 week of either no treatment or RU486.

5.3.4 Insulin resistance

We assessed the effect of glucocorticoid receptor antagonism on measures of insulin resistance including fasting plasma glucose, HOMA2 and Adipo-IR. RU486 had no effect on plasma glucose but was associated with a reduction in plasma insulin (P=0.04), Adipo-IR (P=0.001) and HOMA2 (P=0.049).

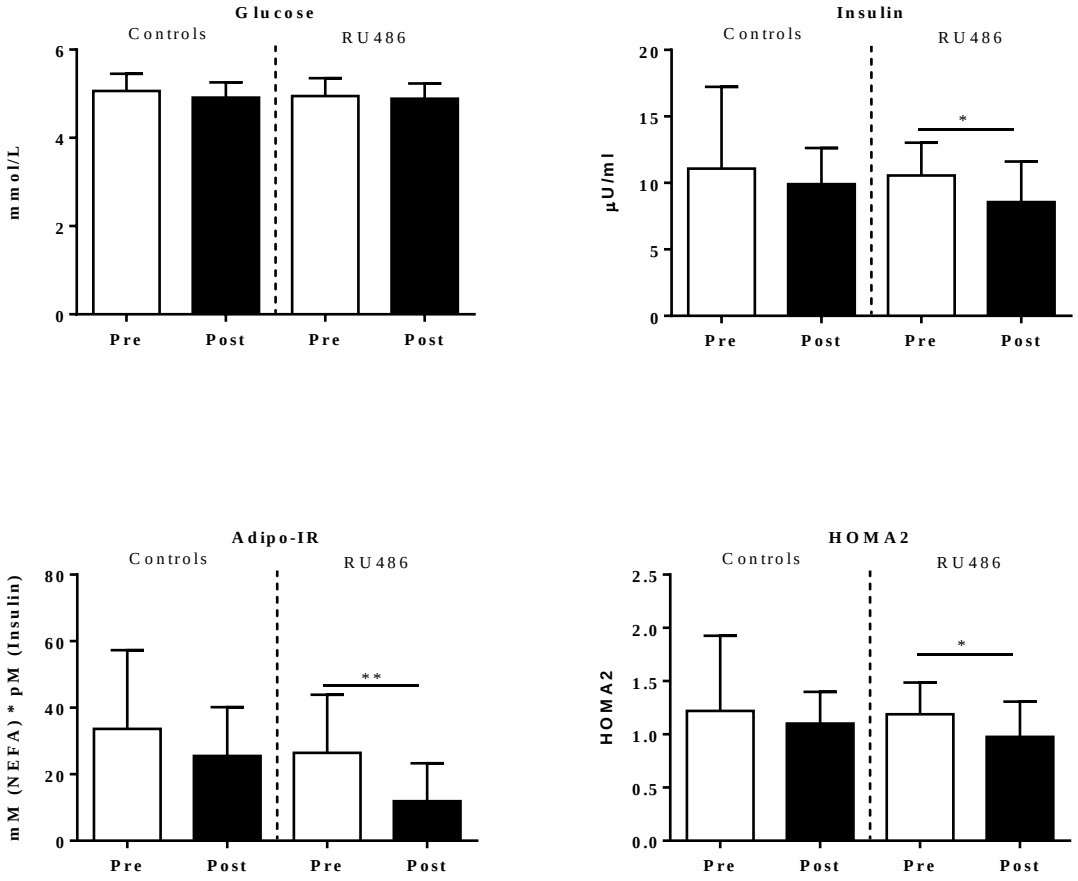


Figure 5- 7 The effect of RU486 on fasting plasma glucose, insulin, adipose-insulin resistance (Adipo-IR) and HOMA2 (homeostatic model of assessment of insulin sensitivity 2). (*P<0.05, **P<0.01). Data presented as mean±SD. Pre refers to pre-randomisation to either no treatment or RU486 and post refers to after 1 week of either no treatment or RU486.

5.4 Discussion

In this study, glucocorticoid receptor antagonism was well tolerated by participants whilst they were on therapy. Safety bloods were also reassuring. Despite this, after stopping the medication 4/8 patients developed self-limiting non-pruritic rashes that settled within a few days. We therefore stopped the study prematurely because this side effect profile was higher than was anticipated from the previously published literature (192, 193).

In the present study RU486 was associated with an increase in *de novo lipogenesis* measured in the plasma and VLDL TAG fractions. Despite this increase there was no change in TAG or VLDL TAG concentrations. RU486 resulted in a reduction in measures of lipolysis with reduced NEFA and glycerol as well as a reduction in Adipo-IR. Additional measures of improved insulin sensitiviy included a reduction in plasma insulin and HOMA2. These findings demonstrate that RU486 treatment is associated with a reduction in lipid mobilisation and an increase in lipid synthesis in the fasted state.

The effect of RU486 on *de novo lipogenesis* (DNL) has not been previously studied. Here we showed that RU486 increased DNL. However in contrast to this finding, mice with a liver specific deletion of the glucocorticoid receptor did not develop hepatic steatosis (219, 220). Furthermore, in a separate rodent study using adenovirus to deliver a GR silencing siRNA, db/db (obese) mice were actually protected from hepatic steatosis which seemed to be mediated by increased fatty acid oxidation (221). However, in the present study we saw a reduction in hydroxybutyrate with RU486 suggesting that the mechanisms may be different in this human model. Given that we observed a reduction in plasma NEFA and glycerol with RU486 as well as a reduction in hydroxybutyrate, it may be that the observed increase in DNL contributes to the maintenance of the plasma TAG levels. Due to the design of the study we were unable to assess the contribution from esterification of labelled NEFA into TAG to further assess this.

The reduction in NEFA and glycerol that we observed is supported by findings in our previously published work demonstrating that glucocorticoids are associated with elevated plasma NEFA (163). This has also been seen in cultured adipocytes and is antagonised with RU486 (222). Glucocorticoids are known to cause significant upregulation of the major lipases adipose triglyceride lipase (ATGL) and hormone

sensitive lipase (HSL) (222) and therefore the effects seen here with RU486 would be anticipated to be mediated by the GR.

In a rodent study using a liver specific GR antagonist there was an improvement in hepatic and global insulin sensitivity demonstrated by a reduction in hepatic glucose production as well as an increase in glucose disposal and glucose infusion rates across a euglycaemic clamp (223). This corresponds to the reduction in plasma insulin and HOMA2 seen in the current work and is supported by a previous human study in which a single dose of RU486 was sufficient to reduce hepatic glucose production. A mouse study has shown that the reduced gluconeogenesis associated with RU486 treatment may be mediated by altered glucose-6-phosphatase (G6Pase) (and phosphoenolpyruvate carboxykinase (PEPCK) (224) key enzymes in the gluconeogenesis pathway.

The major limitation of the current study was that RU486 (Mifepristone) is a non-selective antagonist of the GR. It is also an antagonist of the mineralocorticoid receptor, progesterone receptor and androgen receptor. The wide-ranging action of RU486 is well highlighted by a systematic review that identified 47 different targets relating to its potential anti-tumorigenic action alone (225).

Additional limitations include that the data only involves the comparison of fasted metabolites with no assessment of the impact of insulin action on the changes seen. This is likely to be of particular relevance given that we have shown there are likely to be metabolic differences in the action of glucocorticoid signaling in the fed and fasted state (163). A further limitation is the comparatively small sample size. We had *a priori* intended to recruit 15 participants into each arm of this open label study however given the number of participants who developed a rash we made the decision to discontinue the

study early. With GR antagonism we saw increased insulin sensitivity and a reduction in circulating free fatty acids and glycerol. However, the increase in *de novo lipogenesis* that we saw are likely to limit the usefulness of GR receptor modulation in managing metabolic syndrome. Furthermore as this was an assessment only in the fasted state it is unclear to what extent the changes we saw in lipolysis are metabolically protective .

6a. The metabolic effects of intermittent hypoxia in man

6a.1 Introduction

OSA, as discussed, is a complex physiological problem of which nocturnal intermittent hypoxia is only one component. OSA is well known to be associated with dyslipidaemia and poor glycaemic control as outlined extensively in Chapter 1 (section 1.2.4).

Intermittent hypoxia (IH) occurring during sleep is only one component of OSA though given the metabolic effects of IH seen in animal studies it seems to be a major contributor to the metabolic disease associated with OSA. Certainly in terms of blood pressure regulation, supplementary oxygen therapy has been shown to be sufficient to negate the blood pressure rise seen following CPAP withdrawal (226). Additional support for the pathogenic role of intermittent hypoxia in OSA is drawn from the finding that nocturnal hypoxaemia is associated with elevated risk of developing diabetes (227, 228). Previous studies investigating the role for supplemental oxygen in OSA have not investigated the impact on glycaemic control or lipid metabolism (226, 229); therefore further extrapolation of the role of hypoxia in the metabolic disease associated with OSA has not been well defined. As this chapter focusses on human data, evidence from animal studies will not be further reviewed and will be discussed in Chapters 1 and 7.

The two previous studies examining the metabolic effect of IH have only studied glucose metabolism (36, 37). In the first study 13 healthy adult volunteers were randomised and blinded to either IH or normoxia in a cross-over design with the two visits separated by 1 week (36). During IH participants were exposed to 5% O_2 with the balance N_2 as well as air to induce 25 desaturations per hour down to nadir oxyhaemoglobin saturation of 85%. Then, after 5 hours an intravenous glucose tolerance test (IVGTT) with frequent sampling was performed for 3 hours, with the intermittent hypoxia protocol

continuing over the course of the IVGTT. During the normoxia visit cylinders of air were used to ensure blinding. Mathematical modelling was employed to assess the effect of IH on insulin secretion, insulin sensitivity, and the effect of glucose on its own disposal independent of insulin response to the IVGTT (either adjusted for basal insulin or as a direct result of hyperglycaemia). Although there was no reduction in insulin secretion there was a reduction in insulin sensitivity and the different indices of glucose disposal (36). In a separate study employing the same IH exposure protocol 3 hours of IH was sufficient to increase plasma glucose levels, although no differences were seen in an OGTT performed after the exposure (37). Therefore, as previous studies have not addressed the role of IH on lipid metabolism we sought to investigate this using a combination of stable isotopes and a hyperinsulinaemic-euglycaemic clamp. Our aim was to test the hypotheses that acute IH drives increased hepatic lipid accumulation by increased hepatic *de novo lipogenesis* and that acute IH causes insulin resistance measured across a hyperinsulinaemic-euglycaemic clamp.

6a.2 Materials and Methods

6a.2.1 Research strategy

In this chapter we will assess the metabolic effect of acute IH in healthy male volunteers. Nine healthy male volunteers underwent a detailed metabolic assessment in air prior to repeating this assessment 1 week later in conditions of IH. Nine participants were those included in Chapter 5 that did not receive RU486 and we were able to desaturate. The other participant of the control group in chapter 5 did not desaturate and was not included here. After the experience of that participant we obtained a major amendment to the study design that allowed us to use a more hypoxic gas mix (as detailed below) such that we could therafter readily and reproducibly desaturate our participants. The metabolic assessment included: 1) measuring hepatic *de novo lipogenesis* (using deuterated water); 2)

a hyperinsulinaemic-euglycaemic clamp to study insulin resistance as well as the effect of insulin on the metabolic variables studied; 3) glucose production and disposal and fatty acid incorporation into triglyceride, fatty acid appearance and disposal as well as fatty acid oxidation (through use of stable isotopes). The detailed clinical protocol to deliver this metabolic assessment is included below.

The patients within this study are the same as those included in Chapter 5 and the inclusion and exclusion criteria are therefore included in the previous chapter.

6a.2.2 Clinical Protocol

At visits 3 and 5 volunteers underwent detailed metabolic assessments (**Figure 6-1**). This included drinking deuterated water the night before (3g/kg of total body water in two divided doses) to assess hepatic *de novo lipogenesis.* Body water was calculated using TANITIA® body composition scales (Amsterdam-Zuidoost, Netherlands). During visits 3 and 5 volunteers drank water enriched with deuterated water throughout the day according to thirst. On arrival in the research unit having fasted overnight volunteers had a microdialysis catheter inserted into their abdominal adipose tissue. Volunteers were then cannulated twice in right arm to allow infusions of stable isotopes and a dextrose/insulin infusion. An additional cannula was placed distally in the patients' left hand. This cannula was kept patent by placing the hand in a warmed blanket and by the slow infusion of sodium chloride (0.9% Sodium Chloride). The study days then proceeded as follows: after baseline bloods were taken, infusions began (stable isotopes [^{2}H]-glucose to measure endogenous glucose production rate and glucose disposal, [U^{13}C]-palmitate to measure rates of lipolysis and lipid oxidation). For the first 4 hours 3 sets of blood samples were taken every 2 hours, each set was separated by 15 minutes. Breath collection allowed the quantification of fatty acid oxidation by measuring the incorporation of the labelled carbon

from the [U^{13}C]-palmitate into exhaled CO_2. Breath samples were collected once every hour (Exetainer tubes, Labco Ltd, Bucks, UK). In addition to these samples the blood glucose was checked every 15 minutes by taking samples from the cannula (HemoCue Glucose 201+ Analyser, Radiometer, Crawley, UK). After the initial 4-hour basal period the insulin and dextrose solution infusions began. This is the hyperinsulinaemic-euglycaemic clamp and this period lasted 2 hours. The hyperinsulinaemic-euglycaemic clamp allows both the quantification of insulin resistance/sensitivity as well as to study the effect of insulin on the other metabolic processes examined. The aim here was to keep the blood glucose constant despite the insulin which is achieved by altering the rate of infusion of the dextrose. To do this we closely monitored the blood glucose by measuring it every 5 mins from a small sample of blood taken from the peripheral cannula. We then used an algorithm to calculate the infusion rate of the dextrose needed to maintain the blood glucose (163, 231). As well as the glucose monitoring we continued to collect a sample of breath every hour and to take 3 sets of blood every 2 hours as described above. At the end of the study protocol the infusions were stopped, volunteers were fed a high carbohydrate meal and their blood glucose levels were monitored for 1-2 hours to ensure they were stable prior to them leaving the department. This study day was then repeated in 7 days in

conditions of IH.

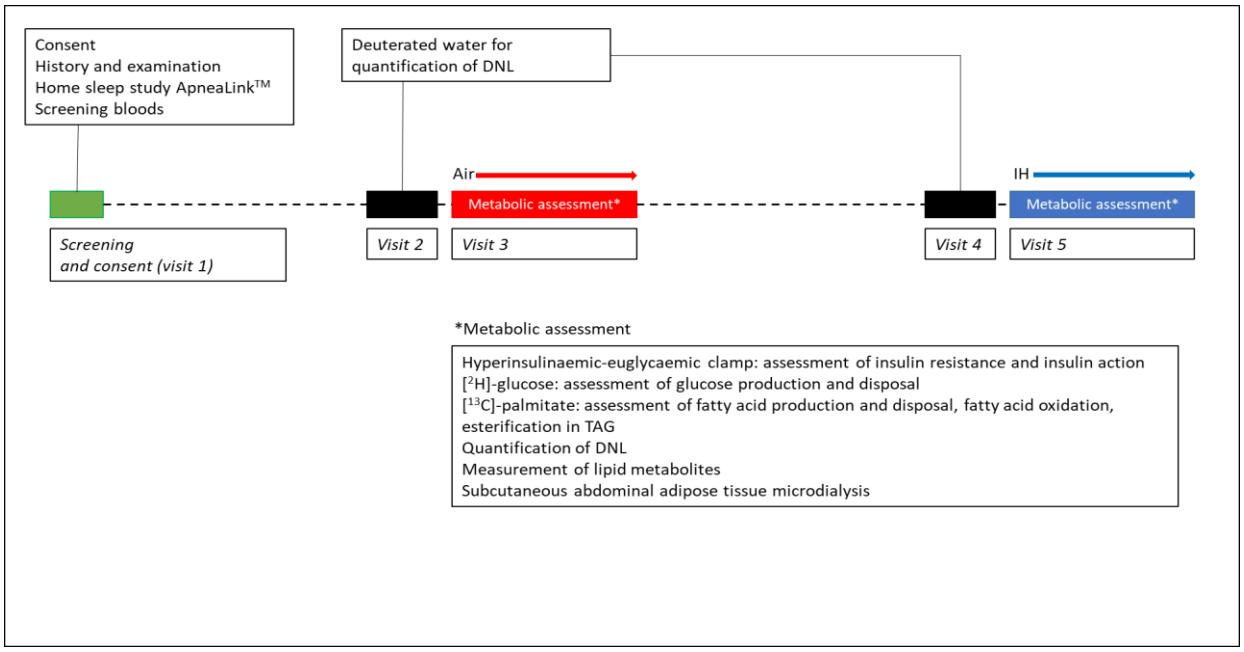


Figure 6a-1 Schematic overview of the intermittent hypoxia study. (DNL=de novo lipogenesis; TAG=triacylglycerol; IH=intermittent hypoxia).

6a.2.3 ACTH and Cortisol ELISA

Plasma ACTH was measured by commercially available enzyme-linked immunosorbent assay ELISAs (Enzo, Exeter, UK). In brief, plates coated with streptavidin are loaded with sample and standard and anti ACTH enzymes conjugated to HRP-peroxidase or biotin are added. After incubation and washing TMB substrate was added and after a further incubation stop solution was added and the plate was read using a spectrophotometer at 450 nm. The concentration of samples is then calculated from a standard curve with a linear x-axis of the concentrations of the standards and a linear y-axis of the absorbance. The intra-assay co-efficient of variation of the ACTH ELISA was 8.18% with an inter-assay co-efficient of variation of 2.67%.

Details of the cortisol ELISA has been covered in Chapter 3, section 2.6. The intra-assay co-efficient of variation was 3.39% with an inter-assay co-efficient of variation of 15.74%.

6a.2.4 Intermittent hypoxia protocol

IH was achieved by controlling the FiO_2 of the inspired gas. Volunteers wore a standard non-rebreathe mask with a T junction inlet connected to medical air (BOC, UK) and 5% oxygen; balance nitrogen (BOC Special Gases, UK). Volunteers were then intermittently exposed to the hypoxic gas mix to achieve 12 desaturations/hour to 85-91% for 6 hours. Full recovery to normal oxygen saturations were achieved between desaturations by exposing the participants to medical air and subsequently room air prior to the next desaturation.

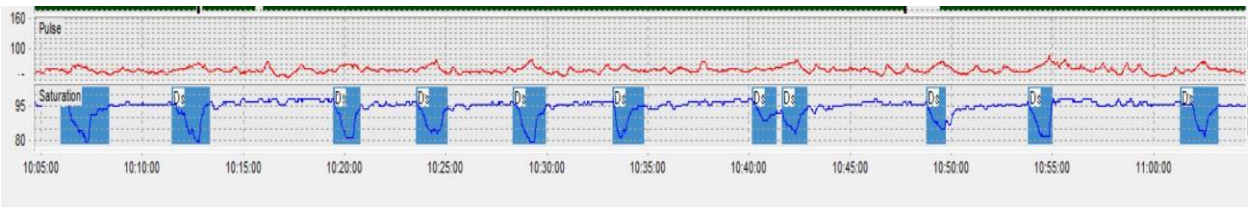


Figure 6a-2 A trace showing the intermittent desaturations achieved using the intermittent hypoxia protocol. The time shown is an hour interval.

6a.2.5 Statistical analyses

Data is presented as mean ± SD. Area under the curve analysis (AUC) was performed using the trapezoidal method. AUC 1 (Pre-insulin) represents the half an hour at the end of the basal phase of the hyperinsulinaemic clamp (i.e. before the insulin) and AUC 2 (Post-insulin) represents the half an hour at the end of the insulin phase of the hyperinsulinaemic clamp. The AUC analysis involved unpaired and paired t-tests where

appropriate. Prism GraphPad was used for statistical analyses of this data. Statistical significance was defined as a $p<0.05$.

6a.3 Results

6a.3.1 Acute intermittent hypoxia

The acute IH protocol was well tolerated by participants with no adverse events. The protocol reliably resulted in a rapid reduction and resolution in the arterial saturations (**Figure 6a-2**) with 11.3±0.2 desaturations per hr to nadir saturations of 86.7±0.7 %.

6a.3.2 Insulin resistance

The effect of IH on insulin resistance was assessed using a hyperinsulinaemic-euglycaemic clamp. The rate of glucose infusion (adjusted for participant weight) required to maintain euglycaemia during the infusion of insulin (M-value) was unchanged (7.7±3.8 vs 8.5±4.7 mg/kg/min, air vs IH respectively, P=0.102). The M/I value which is the M-value adjusted for insulin concentrations was also unchanged (8.7±3.9 vs 9.2±5.0 mg/kg/min/μU/ml, air vs IH respectively, P=0.541). Glucose production (measured after 4 hours of the study protocol) (15.8±4.6 vs 15.5±3.2 μmol/kg/min, air vs IH respectively, P=0.906) as well as glucose disposal (measured at the end of the hyperinsulinaemic phase of the clamp) were also unchanged (79.0±89.6 vs 72.0±58.2 μmol/kg/min, air vs IH respectively, P=0.639) (**Figure 6a-3**).

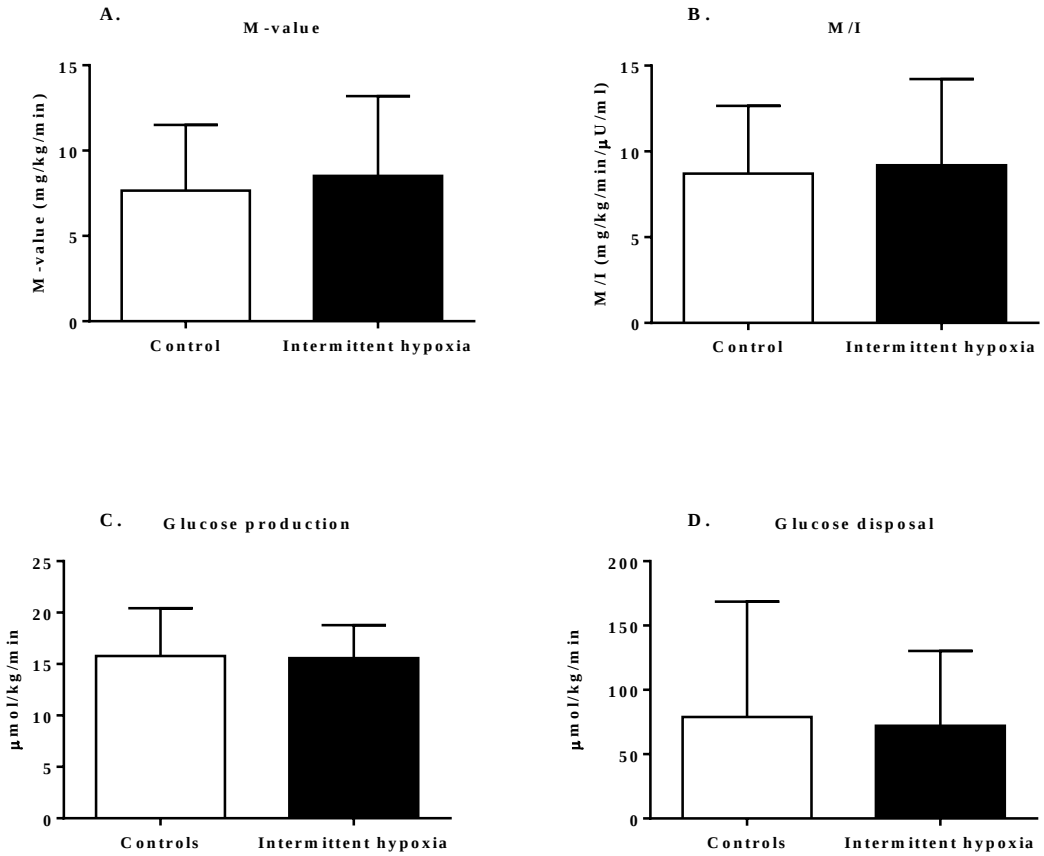


Figure 6a-3 The effect of intermittent hypoxia on measure of insulin sensitivity assessed across a hyperinsulinaemic-euglycaemic clamp. A. M-value relates to the rate of glucose infusion required to maintain euglycaemia in hyperinsulinaemic conditions. B. M/I shows the M-value adjusted for measured plasma insulin. C. Glucose production was quantified using the appearance of isotopically labelled glucose ([^{2}H]-glucose) measured prior to insulin infusion. D. Glucose disposal was quantified isotopically following the infusion of insulin at the completion of the hyperinsulinaemic-euglycaemic clamp. Data is presented as mean±SD.

6a.3.3 Fatty acid production and disposal

The effect of IH on fatty acid turnover was assessed across a hyperinsulinaemic-clamp using ^{13}C-palmitate. The data shown represents the effect of 4 hours of hypoxia/air (AUC 1 (Pre-insulin)) and the effect of hypoxia/air as well as insulin (measured at the end of the hyperinsulinaemic phase of clamp (AUC 2 (Post-insulin)). Insulin suppressed NEFA appearance and increased NEFA disposal as anticipated. These effects did not appear to be modulated by the acute IH exposure (NEFA production: (pre-insulin) 661±353 vs

598±245; (post-insulin) 158±54 vs 254±241 (air vs IH, AUC Ra NEFA whole body µmol/min.hr). NEFA disposal: (pre-insulin) 1.4±0.67 vs 1.5±0.84; (post-insulin) 25±24 vs 39±69 (air vs IH, AUC Rd NEFA whole body µmol/min.hr).

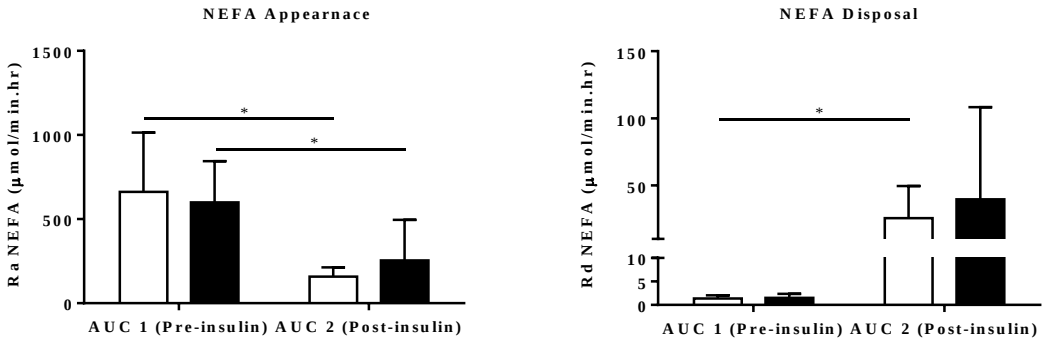


Figure 6a-4 The effect of intermittent hypoxia on NEFA appearance and disposal. This was quantified by measuring the appearance and disposal of isotopically labelled palmitate ([U^{13}C]-palmitate) within the NEFA total palmitate isolated from the plasma fraction measured using gas chromatography mass spectrometry. Data displayed includes the time periods of the hyperinsulinaemic-euglycaemic clamp immediately prior to insulin infusion (labelled pre-insulin) and immediately prior to the cessation of insulin infusion (labelled post-insulin). (NEFA=non-esterified fatty acids; AUC=area under the curve; open bars=air; closed bars=intermittent hypoxia. P<0.05*). Data is presented as mean±SD.

6a.3.4 Fatty acid mobilisation

The effect of IH on fatty acid mobilisation from adipose tissue was assessed across a hyperinsulinaemic-clamp using measurements of plasma NEFA and glycerol and the microdialysis measurement of the appearance of glycerol within the subcutaneous abdominal adipose tissue interstitial fluid. The insulin-mediated suppression of lipolysis was not affected by IH, nor did IH effect adipose tissue lipolysis prior to insulin (**Figure 6a-5**).

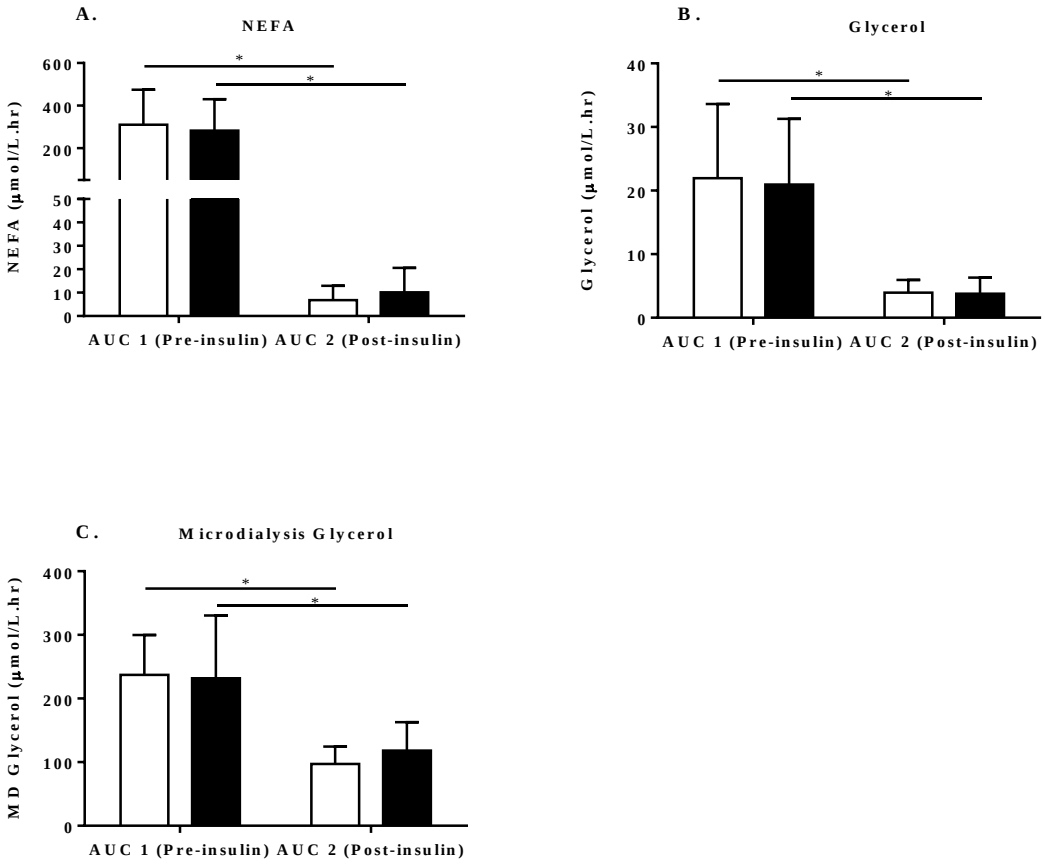


Figure 6a-5 The effect of intermittent hypoxia on lipolysis expressed as plasma NEFA (A), glycerol (B) and subcutaneous abdominal adipose interstitial fluid glycerol (C). Data displayed includes the time periods of the hyperinsulinaemic-euglycaemic clamp immediately prior to insulin infusion (labelled pre-insulin) and immediately prior to the cessation of insulin infusion (labelled post-insulin) (NEFA=non-esterified fatty acids; AUC=area under the curve; open bars=air; closed bars=intermittent hypoxia. P<0.05*). Data is presented as mean±SD.

6a.3.5 Fatty acid oxidation

Fatty acid oxidation was assessed by the incorporation of ^{13}C, from ^{13}C-palmitate into exhaled CO_2 which was corrected for lean mass as well as the plasma availability of ^{13}C-palmitate (corrected for tracer:tracee ratio (TTR)). Hepatic fatty acid oxidation was also quantified by the measurement of plasma β-hydroxybutyrate (OHB). Insulin had a

suppressive effect on fatty acid oxidation, although this was not altered in conditions of IH (**Figure 6a-6**).

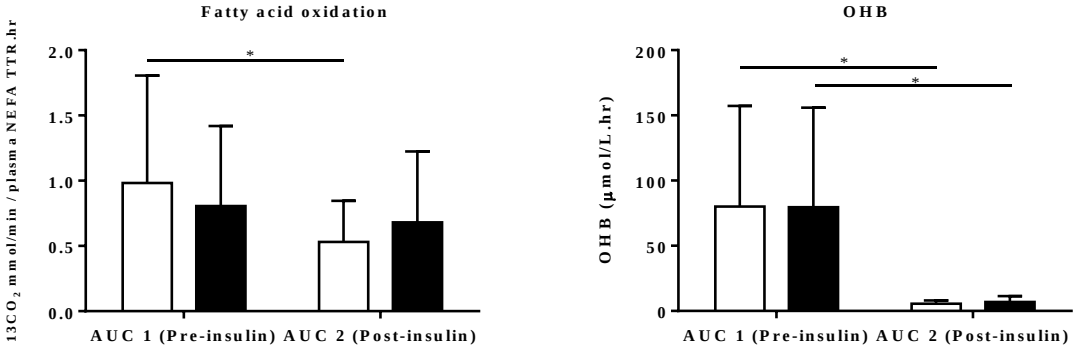


Figure 6a-6 The effect of intermittent hypoxia on fatty acid oxidation measured as the incorporation of ^{13}C, from ^{13}C-palmitate into CO_2 and the plasma concentration of β-hydroxybutyrate. Data displayed includes the time periods of the hyperinsulinaemic-euglycaemic clamp immediately prior to insulin infusion (labelled pre-insulin) and immediately prior to the cessation of insulin infusion (labelled post-insulin). (NEFA=non-esterified fatty acids; AUC=area under the curve; OHB= β-hydroxybutyrate; open bars=air; closed bars=intermittent hypoxia. P<0.05*). Data is presented as mean±SD.

6a.3.6 Fatty acid incorporation into VLDL TAG

Hepatic esterification of fatty acids into VLDL-TAG was assessed by quantification of the relative incorporation of ^{13}C-palmitate into VLDL-TAG. Measurement of this hepatic process relies on the analysis of the VLDL TAG fraction. IH had no apparent effect on the incorporation of palmitate into plasma VLDL-TAG (**Figure 6a-7**).

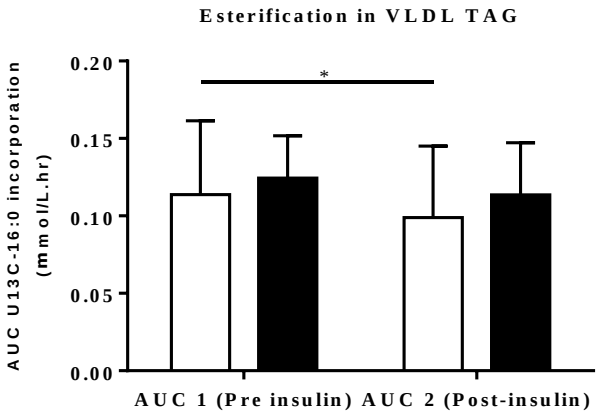


Figure 6a-7 The esterification of ^{13}C-palmitate into VLDL TAG. This was measured via quantification of the incorporation of [U^{13}C]-palmitate into the total palmitate isolated from the VLDL TAG fraction using gas chromatrography mass spectrometry. Data displayed includes the time periods of the hyperinsulinaemic-euglycaemic clamp immediately prior to insulin infusion (labelled pre-insulin) and immediately prior to the cessation of insulin infusion (labelled post-insulin) (AUC=area under the curve; VLDL=very low density lipoprotein; TAG=triacylglycerol; open bars=air; closed bars=intermittent hypoxia. P<0.05*). Data is presented as mean±SD.

6a.3.7 De novo lipogenesis

De novo lipogenesis was assessed by quantification of the incorporation of $^{2}H_2O$ into plasma TAG and VLDL-TAG palmitate. Insulin had a suppressive effect on plasma and VLDL TAG concentrations as a result of the known effect of insulin suppressing VLDL export from the liver (232). IH increased DNL both prior to and post insulin infusion, measured in VLDL, although in the total plasma TAG this only reached significance post-insulin (VLDL DNL: (pre-insulin) 1.69±0.72 vs 2.54±1.38, P=0.041; (post-insulin) 0.91±0.54 vs 2.57±1.50, P=0.005 (air vs IH, VLDL DNL AUC (% DNL/hr). Total TAG DNL: (pre-insulin) 4.08±2.80 vs 5.42±4.28, P=0.247; (post-insulin) 2.96±2.15 vs 5.44±3.45, P=0.011 (air vs IH, Total TAG DNL AUC (% DNL/hr) (**Figure 6a-8**).

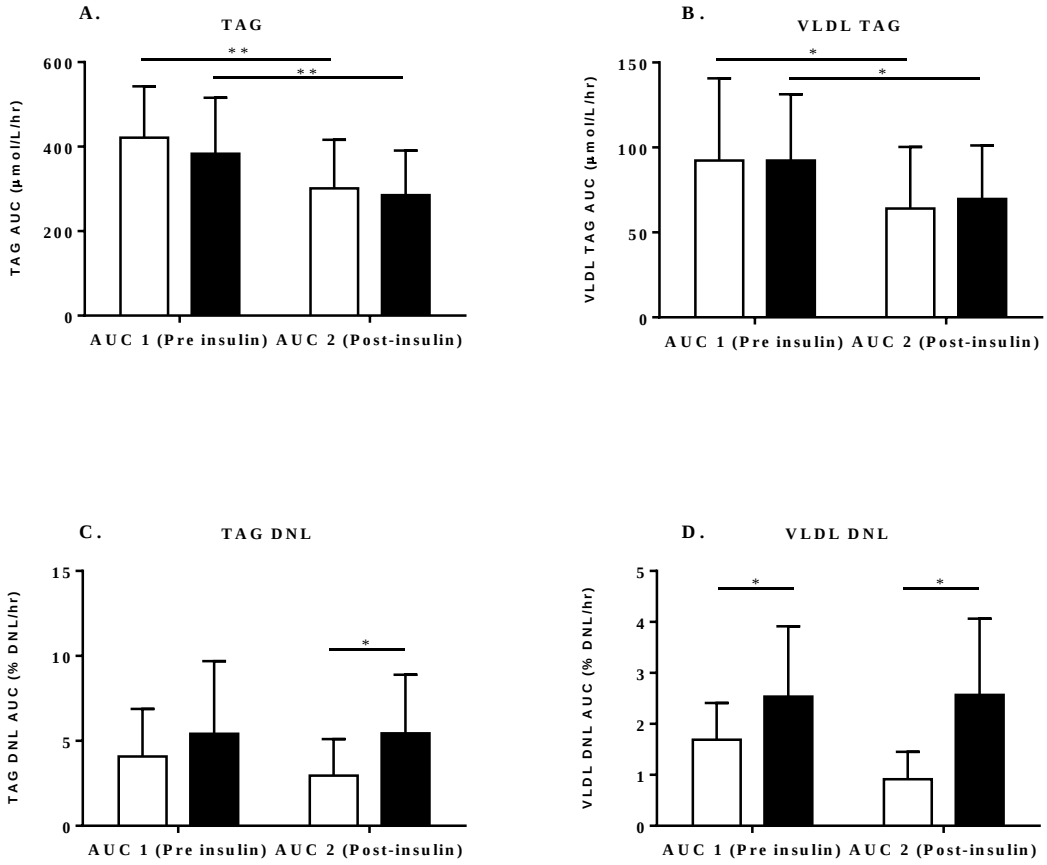


Figure 6a-8 The effect of intermittent hypoxia on plasma TAG, VLDL TAG and DNL measured in the plasma and VLDL TAG fractions. (A) TAG was measured within the plasma and (B) isolated VLDL fractions. Similarly, DNL was measured in the plasma TAG (C) and VLDL TAG fractions (D). DNL was measured via quantification of deuterated water into the isolated palmitate TAG fraction either from whole plasma (C) or the liver specific VLDL fraction (D). (AUC=area under the curve; VLDL=very low-density lipoprotein; TAG=triacylglycerol; DNL=*de novo lipogenesis*; open bars=air; closed bars=intermittent hypoxia. P<0.05*, P<0.001). Data is presented as mean±SD.**

6a.3.8 Cortisol and ACTH

Cortisol and ACTH decreased over the course of the study visits in keeping with the diurnal variation. IH had no effect on plasma ACTH or cortisol

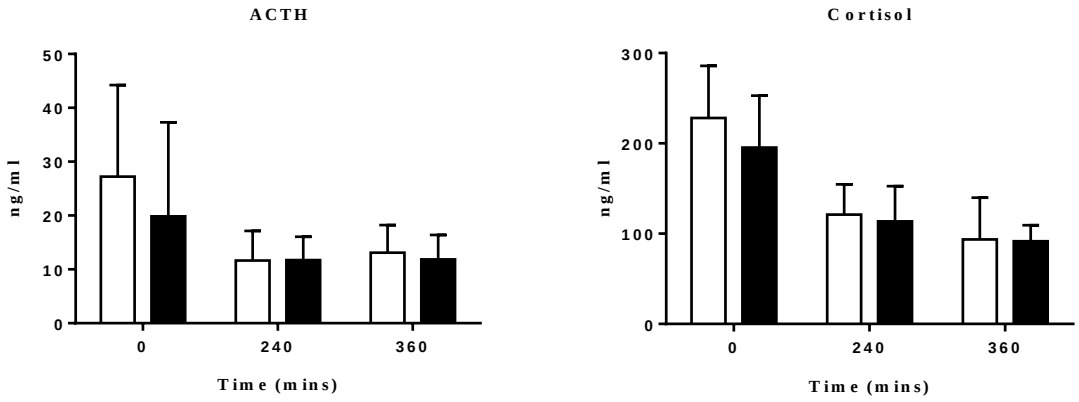


Figure 6a-9 The effect of intermittent hypoxia on plasma ACTH and cortisol (ACTH=adrenocorticotropic hormone; open bars=air; closed bars=intermittent hypoxia). ACTH and cortisol were measured using commercially available ELISA at the beginning of the study protocol T=0, prior to the insulin infusion T=240 minutes and at the end of the insulin infusion T=360 minutes. Data is presented as mean±SD.

6a.4 Discussion

This is the first study undertaking a detailed assessment of carbohydrate and lipid metabolism in AIH in man and we found the acute intermittent hypoxia (AIH) protocol was reproducible and well tolerated by all the participants. The main positive finding from this study was that AIH was associated with increased rates of *de novo lipogenesis* (DNL). DNL is thought to contribute 25% of the hepatic TAG in patients with NAFLD (233). Whilst this is an acute protocol it provides some evidence linking hypoxia and hepatic lipid accumulation more widely. Evidence from rodent studies shows that under conditions of chronic IH, rodents develop significantly more hepatic steatosis than control animals (81, 82). Because of the difficulties in accurately diagnosing and staging NAFLD, as well as the associations between obesity and NAFLD and obesity and OSA it is difficult to draw conclusive conclusions as to the association between OSA and NAFLD. However, in a meta-analysis (over 2000 patients drawn from 18 studies) OSA was found to be

associated with an increased odds ratio of NAFLD, including advanced fibrosis (126). Given, the current findings and those in previous rodent studies (81, 82) as well as my own (**Chapter 7**) it seems likely that the IH component of OSA could be considered to be a major driver of hepatic lipid accumulation.

In this robust assessment of the effect of IH on glucose metabolism we found no effect on M-value, M/I-value or isotopic measurement of glucose production or disposal. No previous studies have assessed the effect of AIH across a hyerpinsulinaemic-euglycaemic clamp or used stable isotopes to measure glucose production and disposal. However, two previous studies did assess the effect of AIH on several indices of insulin action and glucose metabolism (36, 37). In the first study although AIH had no effect on insulin secretion insulin sensitivity and glucose disposal were reduced (36). In a separate study employing the same IH exposure protocol 3 hours of IH was sufficient to increase plasma glucose levels, although no differences were seen in an OGTT performed after the exposure (37). These studies employed severe models of AIH with 25 desaturations per hour achieved rather than 12 per hour as in the current work. The milder desaturation protocol employed in the current work may have explained some of these differences in findings between studies.

In the current work we also examined the effect on fatty acid turnover including appearance, disposal, oxidation, and esterification in TAG and from direct measurement within the subcutaneous abdominal adipose tissue interstitial fluid. We saw no effect on any of these indices. The only effects we saw were the anticipated effect on insulin suppressing lipolysis. The major tissue contributing to the NEFA pool is adipose tissue and the lack of an effect seen is reflective of the modest effect seen at a transcriptional

level seen within my own *in vitro* work (**Chapter 3**) and the lack of a transcriptional effect on adipose from patients with OSA (**Chapter 4**).

The limitations of the current chapter include: firstly participants were metabolically healthy and comparatively young (**Table 5-1**), whilst an older more metabolically unhealthy group may have responded differently to AIH; secondly the protocol occurred during daylight hours rather than during sleep which would be a more accurate model of OSA; thirdly the protocol itself was relatively acute (6 hours) and relatively mild (12 desaturations/hour to 85%) whilst more severe protocols (36, 37) had previously shown effects on glucose metabolism; and finally this protocol employed only hypoxia without inducing hypercapnia principally because of concerns about tolerability and monitoring a combined protocol may have better reflected the changes seen in OSA and therefore the effects seen may have differed.

Despite these limitations we did see clear differences in DNL which may well be clinically relevant in determining a causal mechanism linking OSA and NAFLD. This will be further explored in a murine mode (**Chapter 7**).

6b. Glucocorticoid receptor antagonism fails to protect against the metabolic effect of intermittent hypoxia

6b.1 Introduction

Given the association between OSA and NAFLD as well as our finding that IH is associated with increased DNL observed in **Chapter 6a** it is biologically plausible that the mechanism linking OSA and NAFLD is through increased glucocorticoid signalling. This is particularly relevant given that we have already demonstrated, in Chapter 3 increased levels of glucocorticoid metabolites in patients with OSA. We therefore hypothesised that hypoxia mediated increased glucocorticoids drive increased hepatic lipid accumulation via increased rates of DNL as well as on the other key parts of the glucocorticoid regulated steatosis pathway, as outlined below. We have previously reviewed the potential role for glucocorticoids in the pathogenesis of NAFLD (165). These are likely to be mediated by increased hepatic lipid uptake (166) undergoing increased esterification to TAG (167) and reduced hepatic export (163). Glucorticoids may well also have an additional effect driving hepatic DNL in the presence of insulin (163, 168) whilst increased gluconeogenesis (169) may provide additional substrate. This may be exacerbated by a reduction in β-oxidation of lipid within the liver (170, 171), as outlined in **Figure 1-4**.

In Chapter 5 we demonstrated that glucocorticoid antagonism is associated with an improvement in indices of insulin resistance in the fasted state including Adipo-IR, HOMA-2 and plasma insulin levels as well as a reduction in measures of lipolysis including NEFA and glycerol. Therefore in this chapter we will test the hypothesis that glucocorticoid receptor antagonism offers metabolic protection to the effects of AIH.

6b.2 Materials and Methods

6b.2.1 Research strategy

In this chapter we will assess the role of glucocorticoid receptor (GR) antagonism in conditions of intermittent hypoxia. In particular we will look to assess whether GR antagonism is metabolically protective. We will do this via comparison of the metabolic effects seen in those exposed to intermittent hypoxia (**Chapter 6a**) and comparing these effects to those volunteers who were randomised to receive RU486 600mg once a day for 1 week prior and on the day of intermittent hypoxia exposure. This chapter therefore compares the effect of intermittent hypoxia between control patients (**Chapter 6a**) and those treated with RU486. We have already demonstrated the effects of RU486 in air in the fasted state (**Chapter 5**). The variables measured and methods used are already covered within **Chapter 6a**. The data includes 9 control patients exposed to intermittent hypoxia and 8 patients randomised to RU496 exposed to intermittent hypoxia.

6b.2.2 Statistical analysis

Data is presented as mean ± SD. One-way ANOVA was used for multiple comparisons between conditions (baseline in air, IH without drug, IH with RU486) with Tukey correction for multiple comparisons. Data was analysed using GraphPad Prism 6. Statistical significance was defined as a $p<0.05$

6b.3 Results

6b.3.1 Acute intermittent hypoxia

Individuals randomised to RU486 tolerated the IH exposure protocol well (desaturations/hour: 11.3±0.2 (controls) vs 11.6±0.3 (RU486). nadir saturations (%): 86.7±0.7 (controls) vs 86.5±0.7 (RU486)).

6b.3.2 Insulin resistance

Insulin resistance was studied across a hyperinsulaemic-euglycaemic clamp, as described in chapter 6a, where we did not show an effect of IH alone on the measured indices. Similar to the control patients, RU486 also had no effect on the M-value, M/I value, glucose production (measured after 4 hours of the study protocol) or glucose disposal (measured in response to hyperinsulinaemia) (**Figure 6b-1**).

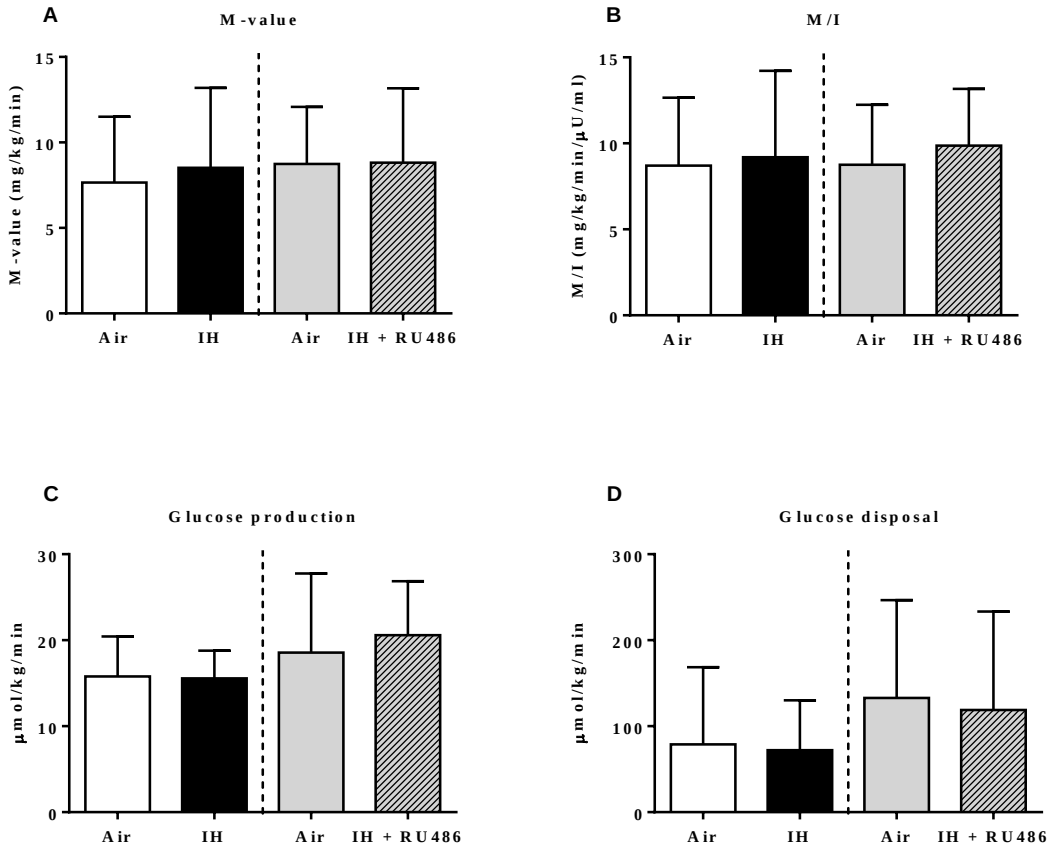


Figure 6b- 1 The effect of intermittent hypoxia and intermittent hypoxia and RU486 on measures of insulin sensitivity measured across a hyperinsulinaemic-euglycaemic clamp. A. M-value relates to the rate of glucose infusion required to maintain euglycaemia in hyperinsulinaemic conditions. B. M/I shows the M-value adjusted for measured plasma insulin. C. Glucose production was quantified using the appearance of isotopically labelled glucose ([^{2}H]-glucose) measured prior to insulin infusion. D.

Glucose disposal was quantified isotopically following the infusion of insulin at the completion of the hyperinsulinaemic-euglycaemic clamp.

6b.3.3 Lipid metabolism

In Chapter 6a, we found that IH did not significantly alter lipid metabolism, across the range of measured indices: IH and RU486 also had no effect on a range of lipid metabolites, being no different than IH alone (**Table 6b-1**).

Table 6b 1 A comparison of the effect of intermittent hypoxia (IH) and IH + RU486 on lipid metabolism (NEFA=non-esterified fatty acids; TTR=tracer:tracee ratio; AUC=area under the curve)

	Participants randomised to no drug				***Participants randomised to RU486***			
	Pre-insulin (AUC 1)		**Post-insulin (AUC 2)**		**Pre-insulin (AUC 1)**		**Post-insulin (AUC 2)**	
	Air	**IH**	**Air**	**IH**	**Air**	**IH + RU486**	**Air**	**IH + RU486**
Assessments of fatty acid metabolism								
NEFA production (µmol/min.hr)	661±353	599±245	158±54.7	254±241	372±193	594±449	189±206	207±182
NEFA disposal (µmol/min.hr)	1.39±0.672	1.52±0.842	25.6±24.0	39.5±68.8	0.901±0.424	1.53±1.02	65.7±98.9	59.9±100.5
NEFA (µmol/L.hr)	310±165	283±148	6.79±6.17	10.1±10.4	223±77.2	223±105	3.19±1.86	4.04±2.73
Glycerol (µmol/L.hr)	22±11.7	20.9±10.3	3.96±1.98	3.78±2.54	17±4.75	17.6±7.23	2.19±1.05	2.80±2.02
Adipose interstitial glycerol (µmol/L.hr)	237±62.4	232±98.5	97.1±27.4	118±44.6	221±80.4	199±54.1	92.3±15.5	121±68.3
NEFA oxidation (mmol/min/plasma NEFA TTR.hr)	0.983±0.822	0.806±0.613	0.531±0.314	0.680±0.543	0.840±0.442	0.908±0.429	0.627±0.557	0.591±0.359
Hydroxybutyrate (µmol/L.hr)	80.1±77.2	79.5±76.5	5.65±2.40	6.86±4.51	48.9±37.2	45.7±43.2	5.13±1.65	6.00±1.43
Esterification into VLDL of ^{13}C-palmitate (mmol/L/hr)	0.114±0.048	0.124±0.023	0.099±0.046	0.113±0.035	0.106±0.057	0.106±0.07	0.083±0.061	0.090±0.078

6b.3.4 Hepatic de novo lipogenesis

In line with Chapter 6a, insulin had a suppressive effect on plasma and VLDL TAG concentrations. In Chapter 6a, IH increased DNL however, there was no effect of RU486 and IH compared to IH alone (**Figure 6b-2**).

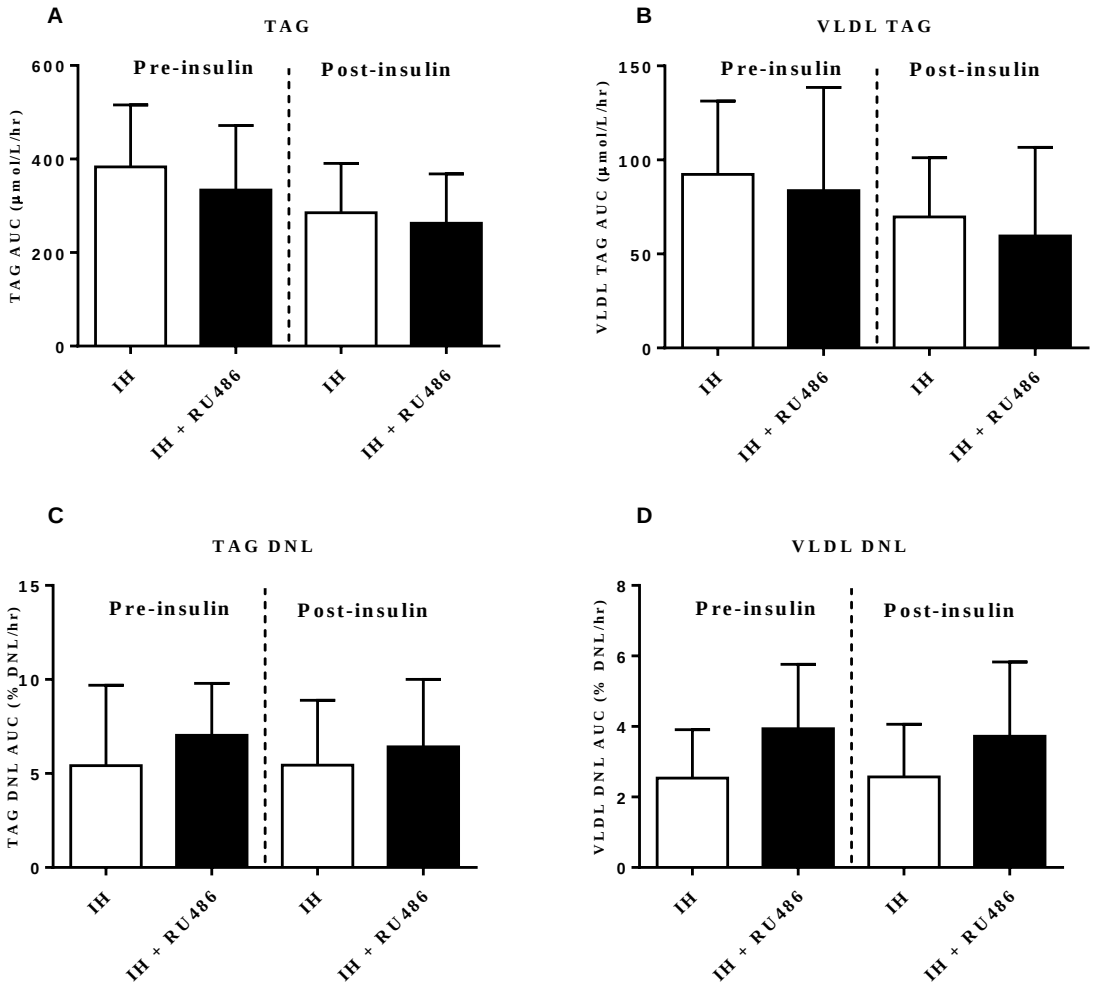


Figure 6b- 2 The effect of intermittent hypoxia and RU486 compared to the effect of intermittent hypoxia alone on TAG, VLDL TAG and DNL measured in the plasma and VLDL TAG fractions. (A) TAG was measured within the plasma and (B) isolated VLDL fractions. Similarly, DNL was measured in the plasma TAG (C) and VLDL fractions TAG (D). DNL was measured via quantification of deuterated water into the isolated palmitate TAG fraction either from whole plasma (C) or the liver specific VLDL fraction (D). (AUC=area under the curve; VLDL=very low-density lipoprotein; TAG=triacylglycerol; DNL=*de novo lipogenesis*; open bars=intermittent hypoxia; closed bars=intermittent hypoxia and RU486.) Data is presented as mean±SD.

6b.4 Discussion

In this chapter we assessed whether RU486 had a protective effect on the metabolic effects of IH as part of an AIH protocol. In Chapter 6a, we demonstrated that IH in isolation increased hepatic *de novo lipogenesis*. Given the potential association between hepatic steatosis in OSA as well as the relationship between glucocorticoids and hepatic steatosis (165) and the findings in Chapter 3, of increased glucocorticoids in OSA, whether glucocorticoid signalling mechanistically links OSA and hepatic steatosis is a clinically salient question.

In a previous study we showed a non-significant reduction in DNL *in vivo* in the fasted state in participants given glucocorticoids which mirrors cellular studies wherein glucocorticoid treatment of hepatocytes is associated with a reduction in DNL (163, 234). This is supported by our findings that RU486 is associated with an increase in DNL (**Chapter 5**). However, the effect of glucocorticoids on DNL seems to be dependent on the presence of insulin since in these conditions glucocorticoids drive DNL in cellular studies (163, 234). Given the significance of the presence of insulin in modulating the effect of glucocorticoids it is perhaps not surprising that i) GR signalling does not seem to have a major role in the regulation of DNL in IH and that ii) the effects of IH on DNL do not appear to be GR mediated.

Here we show that glucocorticoid receptor antagonism with RU486 was not protective against the increased rates of *DNL* seen in IH. Whether this is a feature of the acute nature of this protocol, remains unclear. In this healthy volunteer study, the current AIH protocol alone did not increase plasma ACTH or cortisol (**Chapter 6a**) and whilst we

have not assessed the local tissue bio-availability of glucocorticoids, which are highly regulated by pre-receptor metabolism, it is perhaps therefore not surprising that RU486 had no antagonistic effect on the actions of IH. This was a proof of principle study with the ultimate aim of investigating a role for glucocorticoid receptor antagonism in patients with OSA. Given the lack of a useful physiological effect of RU486 in IH as well as the increased rates of self-limiting rash seen (discussed in **Chapter 5**) it is difficult to justify such a study. Whether more specific glucocorticoid receptor (GR) antagonists may be useful is a possibility but given GR knock-out animals are not protected from hepatic steatosis (220) this is not likely to be clinically useful outside of those with conditions associated with glucocorticoid excess. What we are unable to assess here is the regulation of 11βHSD1 by IH which may yet contribute to the increased DNL seen in IH. Such an assessment would require a rodent study to directly measure 11βHSD1 in response to IH.

7. Chronic intermittent hypoxia model in rats

7.1. Introduction

The mechanism linking obstructive sleep apnoea to NAFLD remains uncertain. Whilst intermittent hypoxia is only one component of OSA we have already seen in Chapter 6 that in a human model of acute intermittent hypoxia there is an increase in *de novo lipogenesis* (DNL). DNL contributes approximately 25% of the hepatic lipid content seen in patient with NAFLD (233). Previous animal models of CIH (chronic intermittent hypoxia) have demonstrated an increase in hepatic TAG accumulation (81, 82). These studies have demonstrated increased hepatic accumulation of TAG as well as increases in key genes of DNL including SREBF1 and ACC1 (76, 77). *In vitro* work has also showed that hepatocytes cultured in hypoxic conditions accumulate lipid though mechanistically this appeared to be via reduced fatty acid β-oxidation rather than increased DNL (65). No previous studies have examined the effect of CIH on DNL by anything other than gene expression and TAG accumulation assays.

The relationship between OSA or CIH and 11βHSD1 activity has not been studied. Previous studies have suggested that 11βHSD1 activity may be reduced in obesity (235) and that baseline 11βHSD1 activity is not predictive of metabolic complications of obesity (207). However, these studies are all reliant on urinary steroid ratios as surrogate markers of 11βHSD1 activity and whilst useful such ratios are often dependant on multiple steroid metabolising enzymes. In the only study that measured hepatic 11βHSD1 activity directly in *ex vivo* tissue from patients with NAFLD, activity was shown to be reduced in those with simple steatosis but increased in those with steatohepatitis (206). The authors of that study suggested that this may be a protective mechanism to minimise hepatic glucocorticoid exposure in simple steatosis to preserve the metabolic phenotype (206). This theory is supported by the findings that pharmacological 11βHSD1 inhibition (236)

and global 11βHSD1 knock-out (237) are both protective of hepatic steatosis. Whether downregulation of hepatic 11βHSD1 activity in the liver in response to hypoxia may represent a protective mechanism in humans is unknown. CIH in rodents was found to increase 11βHSD2 activity and expression in the myocardium but liver was not studied. Of interest plasma corticosterone increased in this study suggestive of HPA axis activation (188) .

In this chapter we will examine the effect of CIH on hepatic lipid accumulation using a combination of direct hepatic lipid measurement, histology, gene expression and deuterated water to examine DNL. We will also examine whether 11βHSD1 activity is downregulated in response to CIH by gene expression and an *ex vivo* assay of enzyme activity.

7.2. Materials and Methods

7.2.1 Research strategy

In this chapter we will assess whether CIH in rodents drives hepatic lipid accumulation in lean male rodents on normal chow. As well as expanding on the methodology used in previous studies we will for the first time directly assess DNL using deuterated water to measure the incorporation directly into hepatic tissue. This not only provides a robust assessment of DNL but also circumvents the reliance on assessing DNL via plasma measurements which are subject to the small amount of DNL that occurs in adipose tissue as well as to changes in lipid uptake and secretion. This will test the hypothesis that CIH drives hepatic lipid accumulation via increased DNL.

We will also use this experimental model to assess the effect of CIH on hepatic 111βHSD1 activity. By using an *ex vivo* 11βHSD1 activity assay we can directly quantify

enzymatic activity in hepatic tissue without the reliance on urinary steroid ratios as a proxy for enzyme activity.

7.2.2 Statement of contributions

I undertook these rodent experiments under the supervision of Professor Tyler, Professor Carr and Dr Heather within the Department of Human Physiology, Anatomy and Genetics (DPAG). I processed and analysed all the samples. This group had an established protocol working on chronic hypoxia that I was able to adapt to study chronic intermittent hypoxia as a model of OSA. I received technical electronics support from Dr Jack Miller who designed the electronic controls to automate the CIH protocol which was crucial for reproducibility. I received additional support harvesting tissue from Drs. Ahmad Moolla, Nantia Othonos, Niall Dempster and Laura Gathercole. Maria da Luz Sousa Fialho and Matthew Keller (from Dr Heather's group) assisted by performing the schedule 1 killing. Vicky Ball provided essential high quality daily support and supervision to the project.

7.2.3 Protocol

Male Wistar rats were exposed to chronic intermittent hypoxia (CIH) or normal air for 14 days. During weekends animals were all housed in ambient air. 16 rats were used in total with 8 exposed to CIH and 8 to normal ambient air. Animals were housed in groups of 4 males. Animals were purchased via BioMedical Services, University of Oxford and were approximately 250g on arrival. Animals were allowed to acclimatize in the research facility for 6 days (Department of Human Physiology, Anatomy and Genetics (DPAG), University of Oxford). After 6 days of acclimatization and before any exposure to CIH, all animals underwent fasting bloods under isoflurane anaesthesia from the saphenous vein. The CIH took the form of 12 exposures/hour to a hypoxic gas mix for 6 hours per day during the animals' sleep period. The design was to mirror the intermittent hypoxia which

is a feature of obstructive sleep apnoea. The hypoxic gas mix was achieved by housing the animals in modified individually ventilated cages (IVCs) with inlet gases of nitrogen and oxygen. 32 seconds of nitrogen (0.5 bar pressure; ¼" internal diameter tubing) was sufficient to reduce the FiO2 in the cages to 10% O_2 before the FiO_2 was restored to 21% (FiO_2 of air) by 4 seconds of oxygen (0.5 bar pressure; ¼" internal diameter tubing). The gases were controlled by a series of valves controlled electronically by means of Linux code run through a Raspberry Pi (RS Components, UK). The concentrations of O_2, CO_2, and N_2 within the modified IVCs was monitored using Normocap 200 Oxy (Datex Ohmeda, UK). These were calibrated daily with Quick CalTM Calibration Gas (GE Healthcare, UK). Gases were supplied by BOC, UK. Gas flow through the IVC was aided by a small axial fan (40mm x 40mm x 10mm). CO_2 was removed using CarboLime (Allied Health Products, UK). Animals were fed normal chow. The drinking water was enriched to 3% with deuterated water (CK Isotopes, UK) so we could assess *de novo lipogenesis*. A schematic of the exposures is shown below (CIH Rat protocol; Methods figure 2). To ensure tolerability of the CIH exposures animals were exposed to 2 hours on day 1 of CIH; 4 hours on day 2; and then 6 hours for the following 14 days. Animals were harvested after a minimum IH exposure on the day of harvest of 2 hours and no more than the 6-hour protocol that the licence allowed. Animals were harvested in the fasted state.

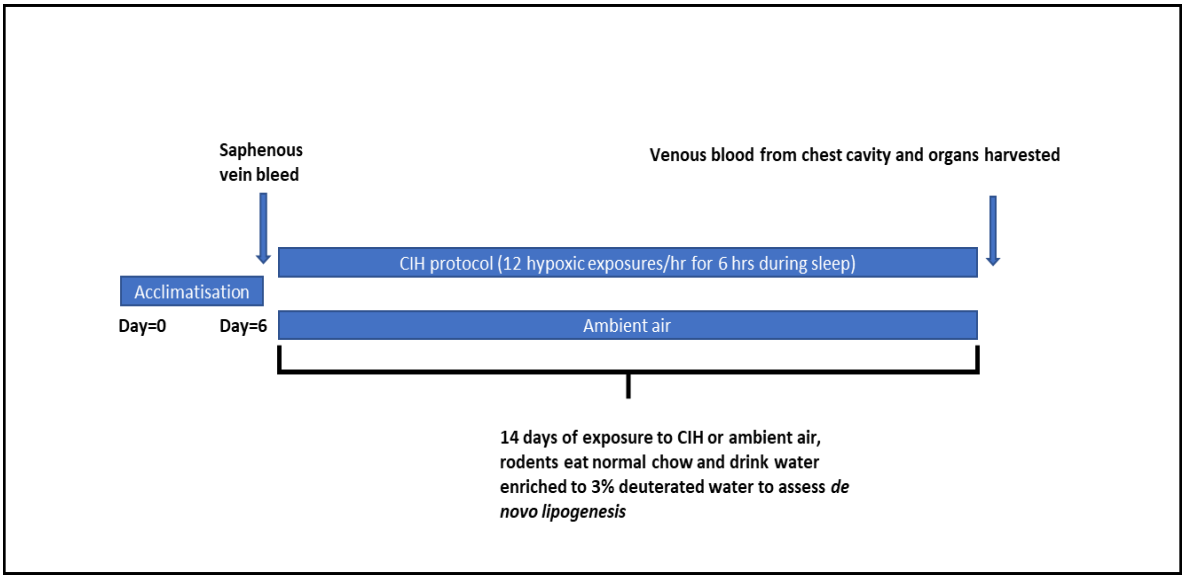


Figure 7- 1The experimental design of the rodent chronic intermittent hypoxia (CIH) exposure.

7.2.4 Tissue weights and venous blood glucose

On completion of the study protocol, the animals were terminally anaesthetised with isoflurane and then weighed prior to tissue harvest. After this the liver was dissected prior to removal of the pancreas, kidneys, adrenals, tibialis anterior, subcutaneous adipose and gonadal adipose tissue. All tissues were weighed including total subcutaneous and gonadal adipose tissue depots. When two organs were removed (e.g. kidneys, adrenal and tibialis anterior) the left organ was weighed for consistency.

7.2.5 Liver histology

Sections were prepared from excised liver tissue. The livers were removed whole from the peritoneal cavity having divided the blood vessels and ligamentous tissues above and below the liver. Having weighed the livers, they were then divided anatomically with a portion retained in 4% formalin (Sigma-Aldrich, Dorset, UK) for subsequent histology. Tissues were fixed in formalin for 48 hours before being stored in 70% ethanol (Fisher, Loughborough, UK) prior to placing in a histological cassette and washing in deionised water and dehydrated through a series of graded industrial methylated spirit (75, 90 and

100%). The tissues were then cleared in xylene and impregnated in paraffin wax. The samples were transferred to a tissue embedding processor (Leica TP1020, Milton Keynes, UK) in which samples were embedded in a fresh paraffin block prior to being left to solidify. The paraffin blocked samples were then sectioned to 5µm thickness using a rotary microtome (Leica, Milton Keynes, UK) with an S35 coated microtome blade (Leica, Milton Keynes, UK). Blocked samples were sectioned in ice to permit clean efficient sectioning. The cut sections were placed onto deionised water heated to 50°C to float and subsequently manoeuvred onto a poly-L-lysine coated glass slide (VWR International, Leicestershire, UK). Slides were left to dry in an oven at 50°C overnight. Slides were then subsequently stained using the established Harris haematoxylin and eosin method.

In brief, sections were deparaffinised in xylene and subsequently rehydrated in reducing concentrations of alcohol. Having washed the sections, they were stained using Harris haematoxylin solution and then washed under a running tap. Having been then rinsed in alcohol the sections were counterstained in eosin and subsequently dehydrated in alcohol. After immersion in xylene the cover slip was fixed to the slide and the slides were allowed to dry overnight prior to subsequent imaging with an upright light microscope (Olympus BH2-RFCA, Southend-on-Sea, UK) at 4x and 20x magnification and images were captured (Canon EOS 700D with a 1.6X additional magnification, Canon, Surrey UK).

7.2.6 Liver gene expression

Sections of 100 mg of liver were weighed and processed for RNA extraction as described in the general methods section. The genes measured included β-actin (ACTB), HIF1A, HIF2A, VEGFA, tumour necrosis factor α (TNFA), fatty acid synthase (FASN), Acetyl-CoA Carboxylase (ACC1) and carnitine palmitoyltransferase 1A (CPT1A).

7.2.7 Measurement of liver TAG

100 mg of liver tissue was weighed and dissolved in 1.5 ml of NP40 Substitute Assay Reagent as per protocol (Triglyceride Colorimetric Assay kit, Cayman, Ann Arbor, USA). The tissue was then homogenised and transferred to a new tube and centrifuged at 10,000g for 10 minutes at 4°C. The assay then proceeded as per the manufacturer's instructions. The liver TAG content was normalised both to the mg of tissue and the mg of protein.

7.2.8 Measurement of liver and plasma DNL

Liver tissue

The rats drank water enriched to 3% with deuterated water (CK Isotopes, UK). The livers of the rats were excised on termination and weighed and further dissected. Additional control livers provided by Dr Heather from male rats were also processed to serve as controls since these animals had only drunk normal water. A section of the liver of 10mg was weighed. 1.5 ml of methanol was added to the liver tissues. This was then sonicated for 5 minutes. 3 ml of chloroform was then added to each tube. To a blank tube to the same suspension 500 µl of 0.9% NaCl was added. 20 µl of the NEFA and phospholipid internal standard was added to each tube. The protocol was then followed to separate out the lipid fractions as described in the general methods.

Plasma

100 µl of plasma was aliquoted from each rat. Samples were taken at the beginning and end of the protocol. 200 µl of 0.9% NaCl was added. 3ml of 2:1 chloroform:methanol solution was added. 10 µl of the TAG standard was added. The samples were then centrifuged as per the standard protocol covered in general methods but this time rather

than continue through the column stages to extract the separate lipid layers the total sample was methylated. This was because of the low rodent sample volume.

7.2.9 Measurement of liver 11βHSD1 activity

In addition to quantification of liver 11βHSD1 gene expression, an 11βHSD1 activity assay was performed on explanted liver tissue in accordance with the following method. 10^{-2} 11 dehydrocorticosterone (11DHC) stock was made up in 100% ethanol. 0.5ml of 250nM solution was added to a 24 well plate and warmed in the incubator (37 ˚C). The diluent used was DMEM, 1000mg glucose/L without the addition of phenol red. At sacrifice of the animal a section of the liver was weighed and placed in warmed DMEM, 1000mg glucose/L (without 11DHC). To 3 wells of the 24 well plate small subsections of liver were added. 3-4 subsections of tissue were added per well. In 1 well no tissue was added (no tissue control (NTC)). The liver explants were incubated in the 11DHC media for 30 minutes at 37˚C. The media from these wells as well as the NTC well was removed, placed on ice and centrifuged to remove any cellular debris. This procedure was repeated for all the experimental animals.

A corticosterone assay was then performed on the pooled media for each experimental animal as well as the NTC wells according to manufacturer's instructions (Enzo life sciences). The corticosterone production was then corrected for the weight of the assayed tissue and the duration of the incubation (expressed as nmol/mg/hr). The corticosterone production could then be corrected for the NTC wells. Corticosterone production is a measure of the 11βHSD1 activity on the DHC within the media.

7.2.10 Statistical Analysis

Data was assessed for normality using the D'Agostino and Pearson omnibus normality tests. Data is presented as mean ± SD. Inter group data was compared using an

unpaired t-test where normally distributed and otherwise was compared using a Mann-Whitney tests. Prism GraphPad was used for statistical analyses of this data.

7.3 Results

7.3.1 Tissue weights and animal behavioural monitoring

The rodents were weighed daily throughout the protocol to ensure safety. These male Wistar rats tolerated the experimental protocol well with no issues identified from behavioural monitoring or the daily weights. One of the rodent livers (hypoxia animal group 1 animal 1) was abnormally small and this animal had a high blood glucose. Whilst there were no macroscopic abnormalities on dissection of this animal given these results this animal was discounted from the rest of the analysis. Removing this animal from the statistical analysis did not alter any of the patterns or statistical significances seen. This left 8 control animals and 7 in the CIH group. The automated gas system was able to reliably reduce the FiO_2 to 10±1% without deviation in the CO_2 or N_2 in accordance with the protocol and animal licence.

Table 7-1 The animal and tissue weights for all animals following completion of the study protocol. Data is presented as mean±SD. SC=subcutaneous.

	Controls (n=8)	**Intermittent hypoxia (n=8)**	***P* value**
Animal weight (g)	327 ± 36	314 ± 30	0.235
Liver (g)	8.25 ± 0.43	7.44 ± 1.37	0.130
SC Adipose (g)	2.65 ± 0.42	2.74 ± 1.12	0.845
Gonadal adipose (g)	6.69 ± 1.5	6.82 ± 1.7	0.876
Pancreas (g)	0.85 ± 0.2	0.85 ± 0.2	0.969
Kidney (g)	1.04 ± 0.08	0.96 ± 0.10	0.104

Adrenal (mg)	55 ± 21.8	57 ± 20.0	0.825
Tibialis anterior (g)	0.981 ± 0.08	0.950 ± 0.12	0.557

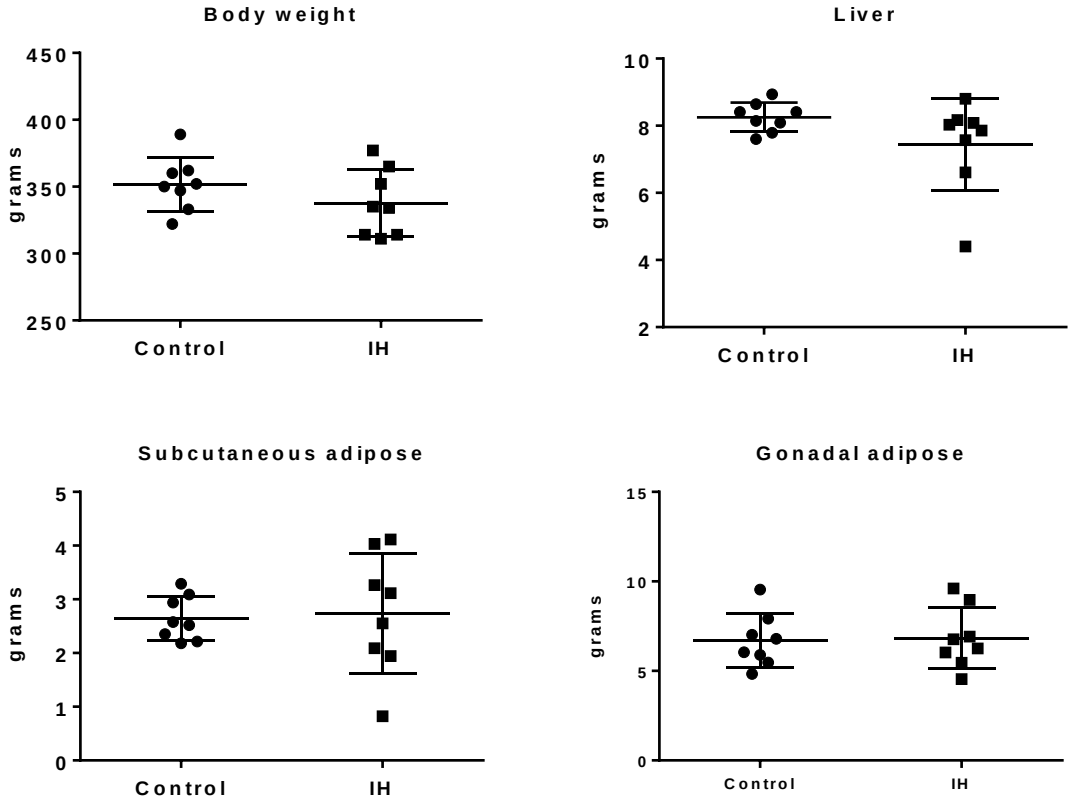


Figure 7- 2 Body weights and tissue weights from adult male Wistar rats exposed to room air (n=8) or chronic intermittent hypoxia (IH) (n=8).

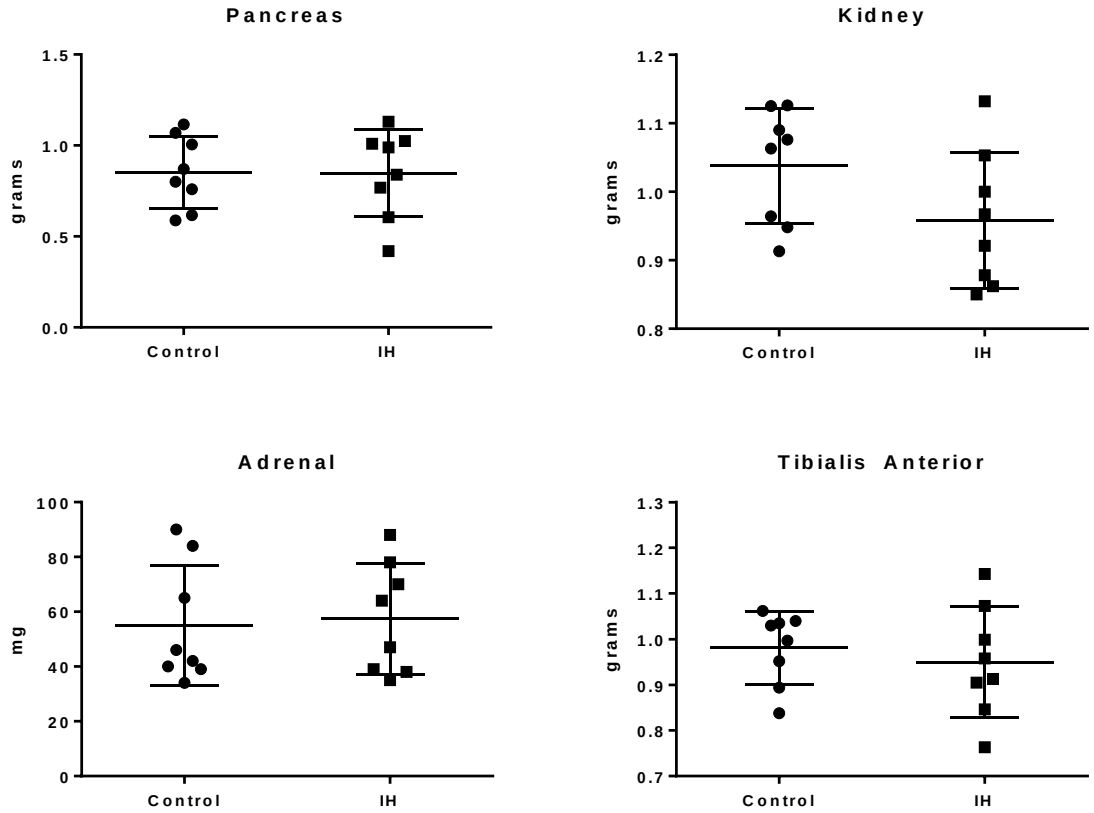


Figure 7- 3 Body weights and tissue weights from adult male Wistar rats exposed to room air (n=8) or chronic intermittent hypoxia (IH) (n=8).

7.3.2 Venous glucose

There was no difference in fasting blood glucose between either the control or intermittent hypoxia groups (6.04 ± 1.06 vs 7.27 ± 2.31 mmol/L respectively, P=0.205) or intermittent hypoxia groups (**Figure 7-4**).

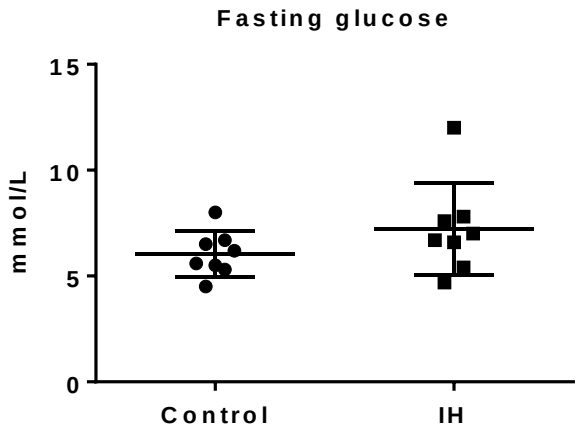


Figure 7- 4 The fasting venous glucose at completion of protocol. IH=intermittent hypoxia

7.3.3 Liver histology

Sections of the rodents' livers were imaged at 4x and 20x magnification principally to detect changes in macro-steatosis. No differences were identified between the control and intermittent hypoxia livers (**Figure 7-5**).

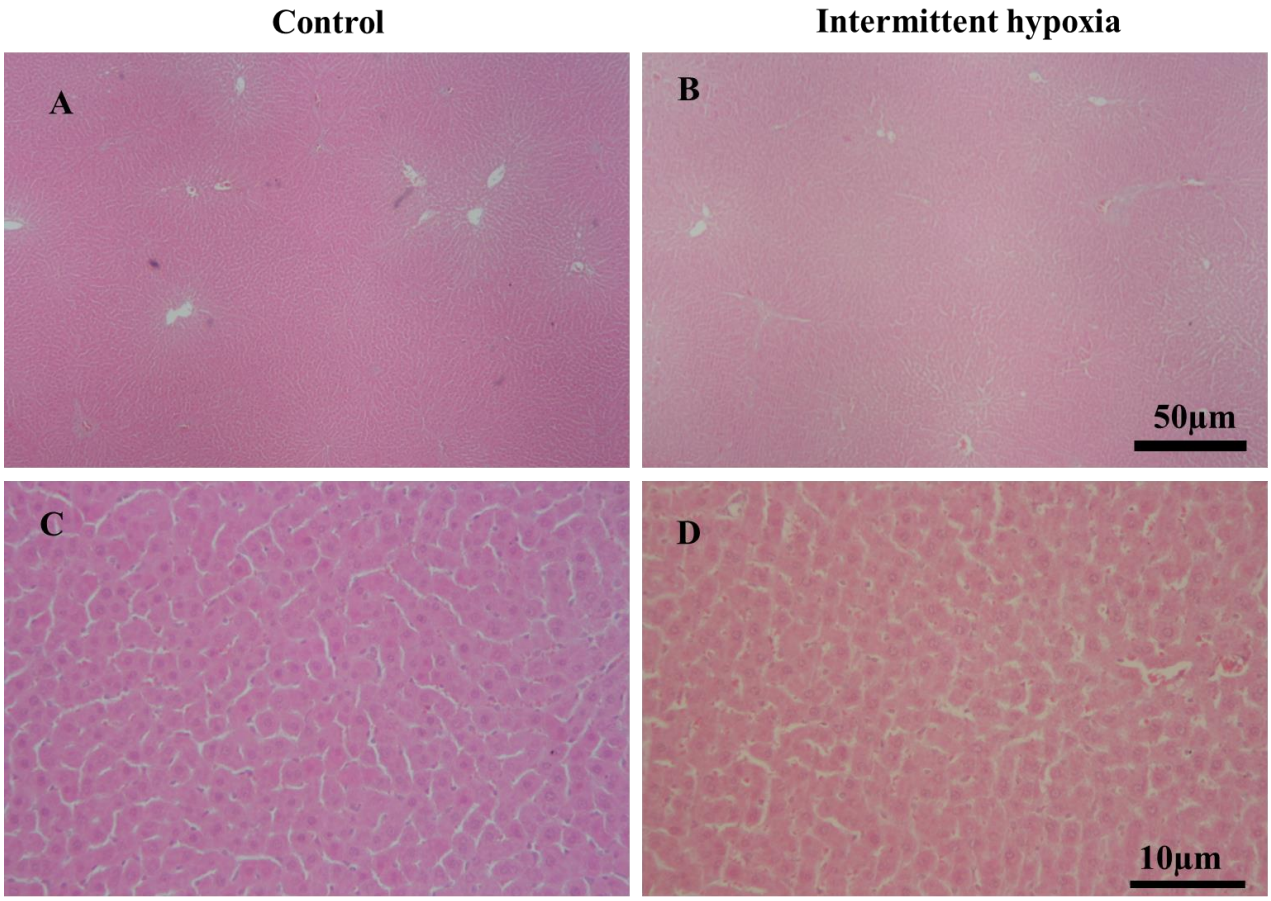


Figure 7- 5 No histological changes were observed between livers section from control (A 4x magnification; C 20x magnification) and intermittent hypoxia exposed rats (B 4x magnification; D 20x magnification).

7.3.4 Liver gene expression

The liver expression of genes known to be oxygen sensitive was quantified. There were no significant differences in liver mRNA expression of HIF1A, HIF2A, VEGFA and TNFA under conditions of intermittent hypoxia (**Figure 7-6**).

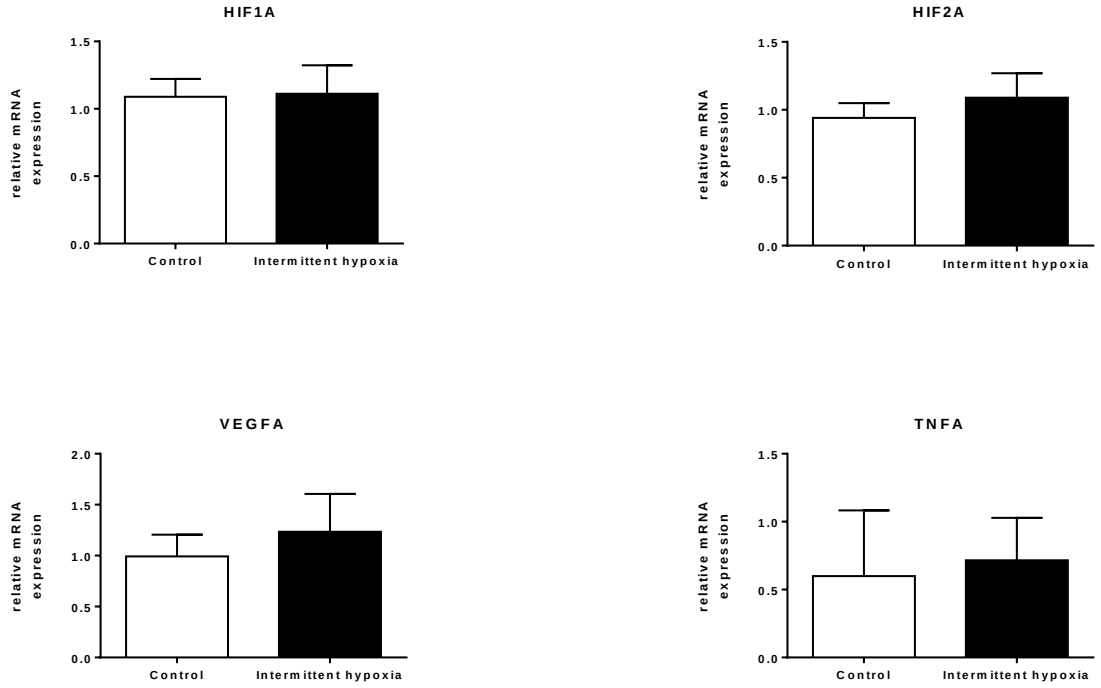


Figure 7- 6 Liver mRNA expression of genes known to be oxygen sensitive (n=8 controls; n=7 intermittent hypoxia). Data is expressed as mean±SD. (*P<0.05)

The liver mRNA expression of fatty acid synthase (FASN) and acetyl-CoA carboxylase (ACC1) increased in the animals exposed to intermittent hypoxia (*P=0.02, P=0.01* respectively). The expression of carnitine palmitoyltransferase 1A (CPT1A) was unchanged between the control and intermittent hypoxia groups (*P*=0.968).

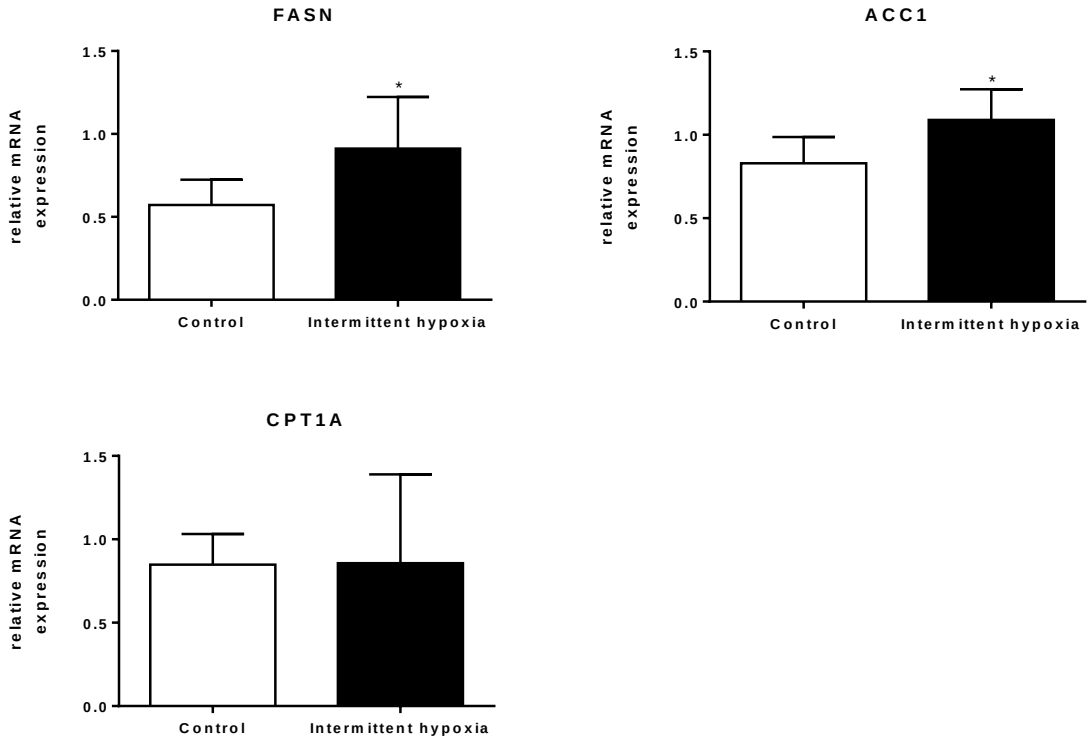


Figure 7- 7 Liver mRNA expression of key genes of liver lipid metabolism. (n=8 controls; n=7 intermittent hypoxia). Data is expressed as mean±SD. (*P<0.05)

7.3.5 Liver triacylglycerol

Liver triacylglycerol (TAG) was measured from 100mg sections of liver tissue and corrected for mg tissue (**Figure 7.7**). Despite the changes seen at gene expression of the lipogenic enzymes ACC1 and FASN there was no increase in liver TAG accumulation instead there was a reduction in TAG content.

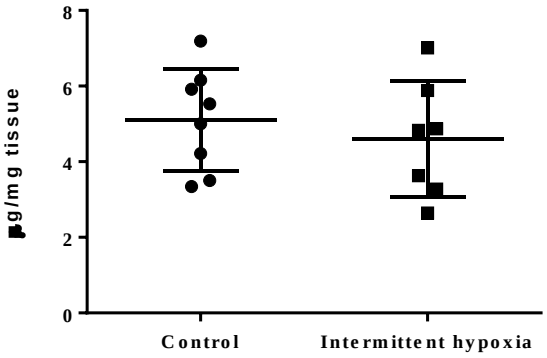


Figure 7- 8 Liver TAG content normalised to mg of tissue. TAG=triacylglycerol. (n=8 controls; n=7 intermittent hypoxia)

7.3.6 Liver and plasma assessment of *de novo lipogenesis*

De novo lipogenesis (DNL) was measured by assessing the incorporation of deuterated water into TAG extracted directly from the liver tissue as well as from TAG extracted from the plasma (expressed here as a GC/MS derived tracer: tracee ratio (271/270)). Liver DNL increased in conditions of intermittent hypoxia with borderline significance (p=0.05). Plasma DNL did not increase in intermittent hypoxia

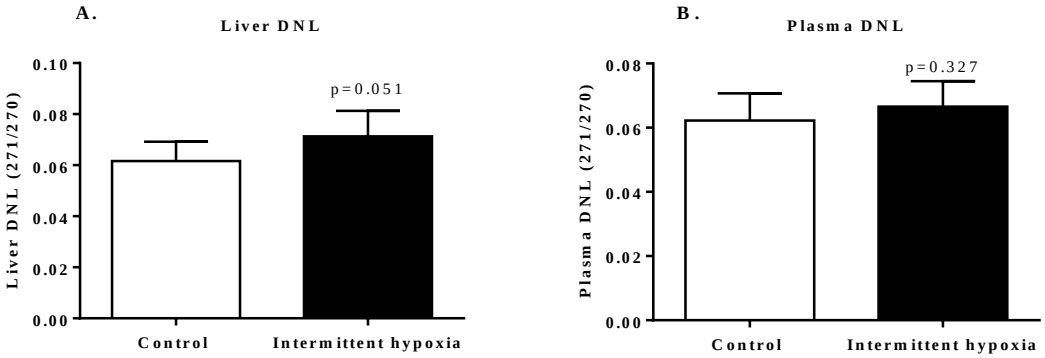


Figure 7- 9Liver and plasma assessment of de novo lipogenesis. DNL was measured by the ratio of palmitate labelled with deuterated water to unlabelled palmitate within the liver tissue (A) and within plasma total lipid fraction (B). This was measured using gas chromatography mass spectrometry (DNL=de novo lipogenesis; 271/270 is the incorporation of deuterated water in triacylglycerol. (n=8 controls; n=7 intermittent hypoxia)) Data is expressed as mean±SD.

7.3.7 Liver 11βHSD1 expression and activity

The liver mRNA expression of 11β-HSD1 was quantified by real-time PCR. Expression increased significantly in the livers of animals exposed to intermittent hypoxia (*P*=0.024). 11β-HSD1 activity was quantified in explanted liver tissue via measurement of the production of corticosterone from 11-dehydrocorticosterone. The inverse relationship was seen with activity reducing in livers of animals exposed to intermittent hypoxia (*P*=0.07).

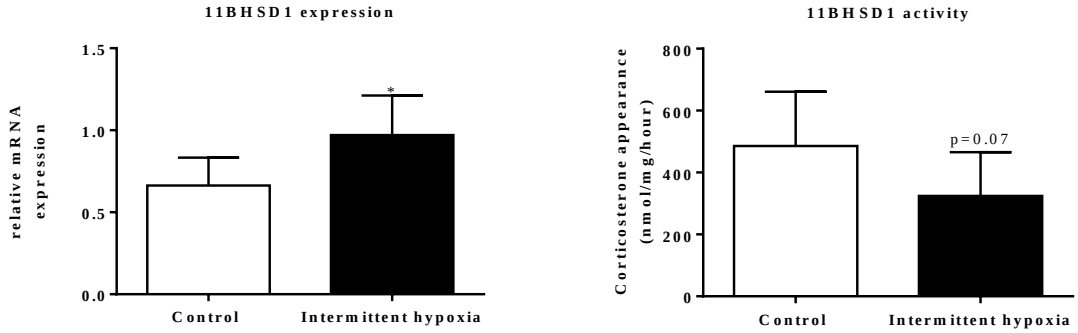


Figure 7- 10 Liver mRNA expression and explant activity of 11β-hydroxysteroid dehydrogenase (11β-HSD1). (n=8 controls; n=7 intermittent hypoxia). Data is expressed as mean±SD. (*P<0.05)

7.4 Discussion

In this chapter we have seen that exposure to chronic intermittent hypoxia is associated with increased hepatic expression of lipogenic genes as well as an increase in hepatic *de novo lipogenesis*. These findings are consistent with intermittent hypoxia linking OSA and hepatic steatosis via increased lipogenesis. However, in the current work an increase in hepatic TAG was not seen.

Hepatic gene expression of acetyl-coA carboxylase (ACC1) and fatty acid synthase (FASN) were increased in animals exposed to CIH, whilst the expression of carnitine palmitoyltransferase 1A (CPT1A) was unchanged between the control and intermittent hypoxia groups. CPT1A is an essential step in the mitochondrial uptake of long chain fatty acids prior to β-oxidation. These findings coupled with the deuterated water assessment of DNL suggests that the mechanism linking intermittent hypoxia to hepatic steatosis is dependent on altered DNL. Previous studies have relied on the quantification of hepatic TAG and gene expression and this is the first study using stable isotope methodology to directly quantify DNL in conditions of intermittent hypoxia.

Hepatic gene expression was examined to look for evidence of tissue specific hypoxia and there was no change seen in hypoxia inducible factors 1α or 2α (HIF1A, HIF2A) or vascular endothelial growth factor α (VEGFA) or tumour necrosis factor α (TNFA). Hepatic HIF1A has been shown to be increased in animal models of CIH previously (74) and the failure to identify that in the recent work may have been a result of measurement only at the gene expression level. Previous over expression studies have suggested a role for HIF1A (100) and HIF2A (67). There is some heterogeneity in the published literature regarding whether the action of HIF2A on hepatic lipid metabolism is a result of either lipogenesis or changes in β-oxidation (67, 101).

In this relatively short hypoxia exposure (2 week) protocol we did not see a change in either hepatic TAG or hepatic histology. However, the gene expression profile was mirrored by the DNL quantification measured within the liver tissue. When we assessed the incorporation of deuterated water into the plasma palmitate pool we did not see the

difference that we observed within the liver. We felt that methodologically that this was likely due to saturation of the plasma palmitate pool with the deuterium label given that the rodents drank the deuterated water across the study period rather than just prior to the end of the study protocol.

As I have outlined, 11βHSD1 activity is part of the regulatory control for tissue availability of active glucocorticoid. In rodents this is corticosterone. Cultured hepatocytes exposed to glucocorticoids and insulin undergo increased DNL though we have not demonstrated this convincingly in a previous human study in fasting conditions (163). In the fed state the presence of GCs drives DNL which may well be an insulin-mediated effect (163, 168). It has been hypothesised previously that reduced 11βHSD1 may be a protective mechanism in patients with simple steatosis (206). Here we saw that although the gene expression of 11βHSD1 was increased in the livers of animals in the CIH group the activity of 11βHSD1 was in fact downregulated by CIH. Although it is plausible that reduced 11βHSD1 activity may be protecting these rodents from further GC driven hepatic lipid accumulation (particularly since it appears the rodent HPA axis is activated by CIH (188)) we have insufficient evidence from the current work to conclude this. This would require a similar series of experiments in rodents which have a liver specific deletion of 11βHSD1. However, a major contributory role of 11βHSD1 seems unlikely given knockout animals are not protected from diet induced hepatic steatosis (238).

The limitations of the current work were principally that the exposure to intermittent hypoxia was relatively short at 14 days in total and that the animals were housed in normoxic conditions at weekends. This may have contributed to the finding that hepatic TAG was no different between the groups. Furthermore, the animals studied were non-obese, non-diabetic rodents therefore the full metabolic potential of intermittent

hypoxia may have been missed. This limitation is echoed by a previous study in which the metabolic impact of CIH was only seen in obese animals (85). Furthermore, the only way to currently measure 11βHSD1 activity is via an explant assay. Although the assay used was standardised between control and hypoxic animals whether there is an effect on cell death or other enzyme pathways manipulating these results is unclear.

In conclusion, this is the first study employing deuterated water to make a functional assessment of *de novo lipogenesis*. The DNL data here is supported by the hepatic gene expression and is supportive of previously published papers which have been reliant on hepatic TAG assays and gene expression. Whilst we have shown that 11βHSD1 activity is reduced in the liver of CIH rodents we are not able to conclude that this represents a protective mechanism though it may be an interesting avenue for further work.

8. Final conclusions and future directions

8.1 Final conclusions

8.1.1 Adipose tissue plays a comparatively minor role in the metabolic response to hypoxia and OSA

OSA is a complex heterogenous condition that is often undiagnosed and is associated with a significant burden of metabolic disease. Whilst the pathogenesis of OSA is complex this thesis has focused mostly on the effect of hypoxia. Lipid toxicity is a popular hypothesis in which metabolic disease including type 2 diabetes and non-alcoholic fatty liver disease are driven by inflammatory adipose tissue which is unable to act as a lipid reservoir such that lipids accumulate in the liver and pancreas (239). Given the associated between OSA and type 2 diabetes (31–34) and OSA and NAFLD (124–126) a role for dysfunctional adipose in the pathogenesis of OSA complications is attractive.

We have shown here that at a transcriptional and protein level that subcutaneous abdominal adipose tissue is able to sense and respond to hypoxia in a dose-dependent manner (**Chapter 4**). However, the transcriptional effects seen are reliant on comparatively extreme hypoxia exposures. When we looked at the subcutaneous abdominal adipose tissue gene expression in patients with OSA who were randomised to sham CPAP we saw no transcriptional effect (**Chapter 3**) mirroring our *in vitro* finding that severe hypoxia is required to elicit significant effect. Whilst, it could be argued that two weeks of sham CPAP was insufficient to cause a significant effect our findings echo recent studies comparing patients with OSA to well-matched controls as well as studying the effect of 4 months of CPAP on adipose gene expression (62, 63).

Furthermore, in our AIH study we did not see a significant effect of hypoxia across multiple measures of fatty acid metabolism including: production and disposal, the effect of insulin on lipolysis suppression, oxidation and esterification in TAG. Though the

protocol we used was acute the lack of an effect seen is supportive of the previously discussed cell culture and patient studies.

8.1.2 Intermittent hypoxia increases hepatic *de novo lipogenesis*

In our acute intermittent hypoxia protocol, we saw a significant increase in DNL. This was echoed by the findings in our rodent protocol which employed a more sustained intermittent hypoxia exposure. These are the first studies to formally assess the effect of IH on DNL using stable isotopes (deuterated water) in rodents or man. The functional increase we saw in DNL in man and rodent were supported by the findings of increased hepatic gene expression of the key enzymes of DNL in the rodent study. In our study (unlike previous studies (81, 82)) we did not see an accompanying increase in hepatic TAG (as measured in the rodent study) or in plasma TAG (as measured in the human study). This may be reflective of either the comparatively short hypoxia protocols used in these studies (6 hours in the human studies, 14 days in the rodent study) or it may reflect the relative metabolic health of the human participants or rodents (young active research participants, young adult rats fed normal chow). This conclusion is supported by a previous study in which the full metabolic impact of chronic IH was only seen in obese rodents (85).

DNL is suggested to contribute approximately 25% of the lipid seen in patients with NAFLD (233). Therefore, the importance of the current finding should not be over emphasised. In the AIH human study in which we were also able to assess fatty acid oxidation and esterification as well as formal assessment of lipolysis both within plasma and the adipose interstitial fluid we did not see an effect. The lack of an effect on these pathways, accepting that this was an acute hypoxia protocol, may well explain that we did not see an increase in hepatic TAG (rodent study) or plasma TAG (human study).

8.1.3 OSA is associated with changes in steroid levels though the functional consequences of this are not clear

Patients with OSA randomised to sham CPAP had increased urinary concentrations of glucocorticoid metabolites (THF) and tetrahydrocortisone (THE) as well as total glucocorticoid metabolites (Total F). This however had no effect on a widespread panel of genes known to be glucocorticoid sensitive (**Chapter 3**). Furthermore, in a cell system (**Chapter 4**) hypoxia did not consistently drive expression of genes known to be glucocorticoid sensitive.

In our AIH study, we assessed whether glucocorticoid receptor (GR) antagonism may be metabolically protective (**Chapter 6b**). Despite our previous findings of comparative glucocorticoid excess in OSA (**Chapter 3**) we found no protective effect of antagonising the GR in acute intermittent hypoxia. This was despite our finding that in conditions of air GR antagonism was associated with a reduction in fasting insulin and other measures of insulin resistance as well as in circulating NEFA and glycerol (**Chapter 5**).

Although from our OSA patients' urines we had been able to study the effect of CPAP withdrawal on steroid levels we were keen to undertake an assessment of the effect of hypoxia on functional steroidogenesis. In our rodent study (**Chapter 7**) we performed an *ex vivo* assessment of glucocorticoid synthesis (11β-HSD1 activity assay) and found that although hepatic gene expression of 11β-HSD1 increased functional activity reduced. Whilst these experiments could be expanded upon it does not support a role for the increase tissue bioavailability of glucocorticoids in response to hypoxia driving local metabolic pathways. It has been hypothesised previously that a reduction in 11β-HSD1 activity may be a protective mechanism in patients with NAFLD (206) and whilst this may

be relevant here there is insufficient evidence to confirm this based on the current rodent study (**Chapter 7**).

In the current CPAP withdrawal study (**Chapter 3**) we saw increased urinary mineralocorticoid metabolites. This could be highly relevant in terms of blood pressure pharmacotherapy in patient with OSA since it has been shown that hypertension in OSA responds favourably to mineralocorticoid antagonists (144, 145). Interestingly we now know that supplemental oxygen is sufficient to negate the increase in blood pressure typically seen on CPAP withdrawal (226) and it is possible that this may be a result in mineralocorticoid regulation.

8.2 Future thoughts

OSA is associated with hypertension and cardiovascular disease. Whilst the mainstay of treatment for OSA remains weight loss and CPAP therapy many patients find weight loss difficult to achieve and struggle to tolerate CPAP because of noise or sensation of claustrophobia. By increasing our understanding of the mechanisms linking OSA to its metabolic consequences we may be able to develop new treatments for these patients. Collaborators in Oxford have recently demonstrated that supplemental oxygen is sufficient to negate the increase in blood pressure typically seen in CPAP withdrawal studies (226). It should be noted that this would not be an optimum treatment as it would not have the same benefits to day time sleepiness as CPAP. That said we are intending to study the urinary steroid profiles of these patients to determine whether the protection in terms of blood pressure control offered by oxygen is regulated by mineralocorticoids.

The increase in DNL seen was consistent across my human and animal models in response to IH. DNL and the contribution it makes to hepatic steatosis in OSA has not

been studied. Whether DNL is more significant in patients with both OSA and NAFLD compared to patients with NAFLD but not OSA is not known. Medications that limit DNL for example diabetes agents that lower the carbohydrate substrate for DNL may be of use in patients with OSA and NAFLD though their uptake outside of patients with co-existent diabetes would require a significant further body of work. In particular, I would be keen to study the contribution of DNL to hepatic steatosis in patients with OSA both on and off CPAP to validate the murine and human *in vivo* physiology data generated in this study. The mechanistic finding of increased DNL in intermittent hypoxia adds further biological plausibility for OSA as an independent risk factor for metabolic disease and supports the prompt recognition and treatment of OSA that should form part of a patient's metabolic assessment.

9. References

1. Epstein LJ, et al. (2009) Clinical guideline for the evaluation, management and long-term care of obstructive sleep apnea in adults. *J Clin Sleep Med* 5(3):263–76.

2. Eckert DJ, Younes MK (2014) Arousal from sleep: implications for obstructive sleep apnea pathogenesis and treatment. *J Appl Physiol* 116(3):302–313.

3. Eckert DJ, Malhotra A (2008) Pathophysiology of adult obstructive sleep apnea. *Proc Am Thorac Soc* 5(2):144–53.

4. Eckert DJ (2018) Phenotypic approaches to obstructive sleep apnoea – New pathways for targeted therapy. *Sleep Med Rev* 37:45–59.

5. Neelapu BC, et al. (2017) Craniofacial and upper airway morphology in adult obstructive sleep apnea patients: A systematic review and meta-analysis of cephalometric studies. *Sleep Med Rev* 31:79–90.

6. Krimsky WR, Leiter JC (2005) Physiology of breathing and respiratory control during sleep. *Semin Respir Crit Care Med* 26(1):5–12.

7. Appelberg J, Sundström G (1997) Ventilatory response to CO2 in patients with snoring, obstructive hypopnoea and obstructive apnoea. *Clin Physiol* 17(5):497–507.

8. Wellman A, et al. (2004) Ventilatory control and airway anatomy in obstructive sleep apnea. *Am J Respir Crit Care Med* 170(11):1225–32.

9. Lee RWW, et al. (2017) Differences in respiratory arousal threshold in Caucasian and Chinese patients with obstructive sleep apnoea. *Respirology* 22(5):1015–1021.

10. Alzoubaidi M, Mokhlesi B (2016) Obstructive sleep apnea during rapid eye movement sleep: clinical relevance and therapeutic implications. *Curr Opin Pulm Med* 22(6):545–54.

11. Senaratna C V., et al. (2017) Prevalence of obstructive sleep apnea in the general population: A systematic review. *Sleep Med Rev* 34:70–81.

12. Pamidi S, et al. (2012) Obstructive sleep apnea in young lean men: impact on insulin sensitivity and secretion. *Diabetes Care* 35(11):2384–9.

13. Kapur VK, et al. (2017) Clinical Practice Guideline for Diagnostic Testing for Adult Obstructive Sleep Apnea: An American Academy of Sleep Medicine Clinical Practice Guideline. *J Clin Sleep Med* 13(03):479–504.

14. NICE (2008) Continuous positive airway pressure for the treatment of obstructive sleep apnoea/hypopnoea syndrome. Available at: https://www.nice.org.uk/guidance/ta139/resources/continuous-positive-airway-pressure-for-the-treatment-of-obstructive-sleep-apnoeahypopnoea-syndrome-pdf-82598202209221 [Accessed March 13, 2018].

15. Hung J, Whitford EG, Parsons RW, Hillman DR (1990) Association of sleep apnoea with myocardial infarction in men. *Lancet* 336(8710):261–4.

16. Garbarino S, Guglielmi O, Sanna A, Mancardi GL, Magnavita N (2016) Risk of Occupational Accidents in Workers with Obstructive Sleep Apnea: Systematic Review and Meta-analysis. *Sleep* 39(6):1211–8.

17. Tregear S, Reston J, Schoelles K, Phillips B (2009) Obstructive sleep apnea and risk of motor vehicle crash: systematic review and meta-analysis. *J Clin Sleep Med* 5(6):573–81.

18. Steier J, et al. (2014) Predicted relative prevalence estimates for obstructive sleep apnoea and the associated healthcare provision across the UK. *Thorax* 69:390–392.

19. Carlos Rejón-Parrilla J, Garau M, Sussex J (2014) Obstructive Sleep Apnoea Health Economics Report Obstructive Sleep Apnoea Health Economics Report Consulting Report for the British Lung Foundation. Available at: https://www.blf.org.uk/sites/default/files/OHE-OSA-health-economics-report---FINAL---v2.pdf [Accessed February 12, 2018].

20. Wolkove N, Baltzan M, Kamel H, Dabrusin R, Palayew M (2008) Long-term compliance with continuous positive airway pressure in patients with obstructive sleep apnea. *Can Respir J* 15(7):365–9.

21. Baratta F, et al. (2018) Long-term prediction of adherence to continuous positive air pressure therapy for the treatment of moderate/severe obstructive sleep apnea syndrome. *Sleep Med* 43:66–70.

22. Toyama Y, et al. (2013) Association between sleep apnea, sleep duration, and serum lipid profile in an urban, male, working population in Japan. *Chest* 143(3):720–8.

23. Togeiro SM, et al. (2013) Consequences of obstructive sleep apnea on metabolic profile: a Population-Based Survey. *Obesity (Silver Spring)* 21(4):847–51.

24. Nadeem R, et al. (2014) Effect of obstructive sleep apnea hypopnea syndrome on lipid profile: a meta-regression analysis. *J Clin Sleep Med* 10(5):475–89.

25. Nadeem R, et al. (2014) Effect of CPAP treatment for obstructive sleep apnea hypopnea syndrome on lipid profile: a meta-regression analysis. *J Clin Sleep Med* 10(12):1295–302.

26. Monneret D, et al. (2016) Glucose tolerance and cardiovascular risk biomarkers in non-diabetic non-obese obstructive sleep apnea patients: Effects of long-term continuous positive airway pressure. *Respir Med* 112:119–125.

27. Iftikhar IH, Hoyos CM, Phillips CL, Magalang UJ (2015) Meta-analyses of the Association of Sleep Apnea with Insulin Resistance, and the Effects of CPAP on HOMA-IR, Adiponectin, and Visceral Adipose Fat. *J Clin Sleep Med* 11(4):475–85.

28. Mokhlesi B, Grimaldi D, Beccuti G, Van Cauter E (2017) Effect of one week of CPAP treatment of obstructive sleep apnoea on 24-hour profiles of glucose, insulin and counter-regulatory hormones in type 2 diabetes. *Diabetes Obes Metab* 19(3):452–456.

29. West SD, Nicoll DJ, Wallace TM, Matthews DR, Stradling JR (2007) Effect of CPAP on insulin resistance and HbA1c in men with obstructive sleep apnoea and type 2 diabetes. *Thorax* 62(11):969–74.

30. Shaw JE, et al. (2016) The Effect of Treatment of Obstructive Sleep Apnea on Glycemic Control in Type 2 Diabetes. *Am J Respir Crit Care Med* 194(4):486–92.

31. Pillai A, Warren G, Gunathilake W, Idris I (2011) Effects of sleep apnea severity on glycemic control in patients with type 2 diabetes prior to continuous positive airway pressure treatment. *Diabetes Technol Ther* 13(9):945–9.

32. Aronsohn RS, Whitmore H, Van Cauter E, Tasali E (2010) Impact of untreated

obstructive sleep apnea on glucose control in type 2 diabetes. *Am J Respir Crit Care Med* 181(5):507–13.

33. Grimaldi D, Beccuti G, Touma C, Van Cauter E, Mokhlesi B (2014) Association of Obstructive Sleep Apnea in Rapid Eye Movement Sleep With Reduced Glycemic Control in Type 2 Diabetes: Therapeutic Implications. *Diabetes Care* 37(2):355–363.

34. Papanas N, et al. (2009) HbA1c is associated with severity of obstructive sleep apnea hypopnea syndrome in nondiabetic men. *Vasc Health Risk Manag* 5:751–6.

35. Siwasaranond N, et al. (2018) The Relationship between Diabetes-Related Complications and Obstructive Sleep Apnea in Type 2 Diabetes. *J Diabetes Res* 2018:1–9.

36. Louis M, Punjabi NM (2009) Effects of acute intermittent hypoxia on glucose metabolism in awake healthy volunteers. *J Appl Physiol* 106(5):1538–44.

37. Newhouse LP, et al. (2017) Three hours of intermittent hypoxia increases circulating glucose levels in healthy adults. *Physiol Rep* 5(1):e13106.

38. Yaggi HK, et al. (2005) Obstructive sleep apnea as a risk factor for stroke and death. *N Engl J Med* 353(19):2034–41.

39. Marin JM, Carrizo SJ, Vicente E, Agusti AGN (2005) Long-term cardiovascular outcomes in men with obstructive sleep apnoea-hypopnoea with or without treatment with continuous positive airway pressure: an observational study. *Lancet (London, England)* 365(9464):1046–53.

40. Sahlin C, et al. (2008) Obstructive sleep apnea is a risk factor for death in patients with stroke: a 10-year follow-up. *Arch Intern Med* 168(3):297–301.

41. Xie J, et al. (2016) Nocturnal Hypoxemia Due to Obstructive Sleep Apnea Is an Independent Predictor of Poor Prognosis After Myocardial Infarction. *J Am Heart Assoc* 5(8):e003162.

42. Zhao Y, Yu BY-M, Liu Y, Liu Y (2017) Meta-Analysis of the Effect of Obstructive Sleep Apnea on Cardiovascular Events After Percutaneous Coronary Intervention. *Am J Cardiol* 120(6):1026–1030.

43. Marshall NS, Wong KKH, Cullen SRJ, Knuiman MW, Grunstein RR (2014) Sleep Apnea and 20-Year Follow-Up for All-Cause Mortality, Stroke, and Cancer Incidence and Mortality in the Busselton Health Study Cohort. *J Clin Sleep Med* 10(4):355–62.

44. Yu J, et al. (2017) Association of Positive Airway Pressure With Cardiovascular Events and Death in Adults With Sleep Apnea: A Systematic Review and Meta-analysis. *JAMA* 318(2):156–166.

45. Javaheri S, Campos-Rodriguez F (2017) Outcomes of Positive Airway Pressure for Sleep Apnea. *JAMA* 318(20):2042.

46. Martínez-García MÁ, et al. (2009) Continuous Positive Airway Pressure Treatment Reduces Mortality in Patients with Ischemic Stroke and Obstructive Sleep Apnea. *Am J Respir Crit Care Med* 180(1):36–41.

47. Garcia-Rio F, et al. (2013) CPAP effect on recurrent episodes in patients with sleep apnea and myocardial infarction. *Int J Cardiol* 168(2):1328–1335.

48. McEvoy RD, et al. (2016) CPAP for Prevention of Cardiovascular Events in Obstructive Sleep Apnea. *N Engl J Med* 375(10):919–931.

49. Rosen ED, MacDougald OA (2006) Adipocyte differentiation from the inside out. *Nat Rev Mol Cell Biol* 7(12):885–896.

50. Jiang C, et al. (2015) HIF-1A and C/EBPs transcriptionally regulate adipogenic differentiation of bone marrow-derived MSCs in hypoxia. *Stem Cell Res Ther* 6(1):21.

51. Famulla S, Schlich R, Sell H, Eckel J (2012) Differentiation of human adipocytes at physiological oxygen levels results in increased adiponectin secretion and isoproterenol-stimulated lipolysis. *Adipocyte* 1(3):132–181.

52. Oliva-Olivera W, et al. (2017) Different response to hypoxia of adipose-derived multipotent cells from obese subjects with and without metabolic syndrome. *PLoS One* 12(11):e0188324.

53. Morrison S, McGee SL (2015) 3T3-L1 adipocytes display phenotypic characteristics of multiple adipocyte lineages. *Adipocyte* 4(4):295–302.

54. Hashimoto T, et al. (2013) Modest hypoxia significantly reduces triglyceride content and lipid droplet size in 3T3-L1 adipocytes. *Biochem Biophys Res Commun* 440(1):43–49.

55. Weiszenstein M, et al. (2016) Adipogenesis, lipogenesis and lipolysis is stimulated by mild but not severe hypoxia in 3T3-L1 cells. *Biochem Biophys Res Commun* 478(2):727–32.

56. Trayhurn P, Wood IS (2004) Adipokines: inflammation and the pleiotropic role of white adipose tissue. *Br J Nutr* 92(3):347–55.

57. Hodson L, Humphreys SM, Karpe F, Frayn KN (2013) Metabolic Signatures of Human Adipose Tissue Hypoxia in Obesity. *Diabetes* 62(5):1417–1425.

58. Goossens GH, et al. (2011) Increased adipose tissue oxygen tension in obese compared with lean men is accompanied by insulin resistance, impaired adipose tissue capillarization, and inflammation. *Circulation* 124(1):67–76.

59. Pasarica M, et al. (2009) Reduced adipose tissue oxygenation in human obesity: evidence for rarefaction, macrophage chemotaxis, and inflammation without an angiogenic response. *Diabetes* 58(3):718–25.

60. Corvera S, Czech MP (2011) Tensions rise and blood flows over dysfunctional fat. *Circulation* 124(1):13–6.

61. Plihalova A, et al. (2016) The effect of hypoxia and re-oxygenation on adipose tissue lipolysis in COPD patients. *Eur Respir J* 48(4):1218–1220.

62. Thorn CE, et al. (2017) Adipose tissue is influenced by hypoxia of obstructive sleep apnea syndrome independent of obesity. *Diabetes Metab* 43(3):240–247.

63. Perrini S, et al. (2017) Correction of intermittent hypoxia reduces inflammation in obese subjects with obstructive sleep apnea. *JCI insight* 2(17). doi:10.1172/jci.insight.94379.

64. Mahat B, Chassé É, Mauger J-F, Imbeault P (2016) Effects of acute hypoxia on human adipose tissue lipoprotein lipase activity and lipolysis. *J Transl Med*

14(1):212.

65. Liu Y, et al. (2014) HIF-1α and HIF-2α are critically involved in hypoxia-induced lipid accumulation in hepatocytes through reducing PGC-1α-mediated fatty acid β-oxidation. *Toxicol Lett* 226(2):117–123.

66. Cao R, et al. (2014) Hypoxia induces dysregulation of lipid metabolism in HepG2 cells via activation of HIF-2α. *Cell Physiol Biochem* 34(5):1427–41.

67. Rankin EB, et al. (2009) Hypoxia-Inducible Factor 2 Regulates Hepatic Lipid Metabolism. *Mol Cell Biol* 29(16):4527–4538.

68. Anavi S, Harmelin NB, Madar Z, Tirosh O (2012) Oxidative stress impairs HIF1α activation: a novel mechanism for increased vulnerability of steatotic hepatocytes to hypoxic stress. *Free Radic Biol Med* 52(9):1531–1542.

69. Gu CJ, et al. (2018) Intermittent Hypoxia Disrupts Glucose Homeostasis in Liver Cells in an Insulin-Dependent and Independent Manner. *Cell Physiol Biochem* 47(3):1042–1050.

70. Wilson GK, Tennant DA, McKeating JA (2014) Hypoxia inducible factors in liver disease and hepatocellular carcinoma: current understanding and future directions. *J Hepatol* 61(6):1397–406.

71. Guzmán M, Castro J (1989) Zonation of fatty acid metabolism in rat liver. *Biochem J* 264(1):107–13.

72. Bruder ED, Lee PC, Raff H (2005) Lipid and fatty acid profiles in the brain, liver, and stomach contents of neonatal rats: effects of hypoxia. *Am J Physiol Endocrinol*

Metab 288(2):E314-20.

73. Wang Y, et al. (2017) Chronic intermittent hypoxia disturbs insulin secretion and causes pancreatic injury via MAPK signaling pathway. *Biochem Cell Biol* 95(3):415–420.

74. Sacramento JF, et al. (2016) Insulin resistance is associated with tissue-specific regulation of HIF-1α and HIF-2α during mild chronic intermittent hypoxia. *Respir Physiol Neurobiol* 228:30–8.

75. Thomas A, et al. (2017) Chronic Intermittent Hypoxia Impairs Insulin Sensitivity but Improves Whole-Body Glucose Tolerance by Activating Skeletal Muscle AMPK. *Diabetes* 66(12):2942–2951.

76. Tian Y-M, et al. (2016) Anti-diabetes effect of chronic intermittent hypobaric hypoxia through improving liver insulin resistance in diabetic rats. *Life Sci* 150:1–7.

77. Schobersberger W, et al. (2003) Austrian Moderate Altitude Study 2000 (AMAS 2000). The effects of moderate altitude (1,700 m) on cardiovascular and metabolic variables in patients with metabolic syndrome. *Eur J Appl Physiol* 88(6):506–14.

78. Li P, Wu J, Zhao L, Feng X-W (2016) Effects and relationship of intermittent hypoxia on serum lipid levels, hepatic low-density lipoprotein receptor-related protein 1, and hypoxia-inducible factor 1α. *Sleep Breath* 20(1):167–73.

79. Yao Q, et al. (2013) Effect of chronic intermittent hypoxia on triglyceride uptake in different tissues. *J Lipid Res* 54(4):1058–1065.

80. Jun JC, et al. (2012) Acute hypoxia induces hypertriglyceridemia by decreasing

plasma triglyceride clearance in mice. *Am J Physiol Endocrinol Metab* 303(3):E377-88.

81. Li J, et al. (2005) Chronic intermittent hypoxia upregulates genes of lipid biosynthesis in obese mice. *J Appl Physiol* 99(5):1643–8.

82. Li J, et al. (2005) Intermittent hypoxia induces hyperlipidemia in lean mice. *Circ Res* 97(7):698–706.

83. Conotte S, et al. (2018) Metabonomic profiling of chronic intermittent hypoxia in a mouse model. *Respir Physiol Neurobiol* 256:157–173.

84. Corbin KD, Zeisel SH (2012) Choline metabolism provides novel insights into nonalcoholic fatty liver disease and its progression. *Curr Opin Gastroenterol* 28(2):159–165.

85. Briançon-Marjollet A, et al. (2016) Intermittent hypoxia in obese Zucker rats: cardiometabolic and inflammatory effects. *Exp Physiol* 101(11):1432–1442.

86. Quintero M, et al. (2013) The effects of intermittent hypoxia on redox status, NF-κB activation, and plasma lipid levels are dependent on the lowest oxygen saturation. *Free Radic Biol Med* 65:1143–54.

87. Fu C, et al. (2015) Chronic intermittent hypoxia leads to insulin resistance and impaired glucose tolerance through dysregulation of adipokines in non-obese rats. *Sleep Breath* 19(4):1467–73.

88. Shin M-K, et al. (2017) Effect of adrenal medullectomy on metabolic responses to chronic intermittent hypoxia in the frequently sampled intravenous glucose

tolerance test. *J Appl Physiol* 122(4):767–774.

89. Chen X, et al. (2016) Intermittent hypoxia maintains glycemia in streptozotocin-induced diabetic rats. *Cell Stress Chaperones* 21(3):515–22.

90. Lu W, et al. (2017) The role of the Nox4-derived ROS-mediated RhoA/Rho kinase pathway in rat hypertension induced by chronic intermittent hypoxia. *Sleep Breath* 21(3):667–677.

91. Savransky V, et al. (2007) Chronic intermittent hypoxia causes hepatitis in a mouse model of diet-induced fatty liver. *AJP Gastrointest Liver Physiol* 293(4):G871–G877.

92. Cai C, Aranda J V, Valencia GB, Xu J, Beharry KD (2017) Chronic Intermittent Hypoxia Causes Lipid Peroxidation and Altered Phase 1 Drug Metabolizing Enzymes in the Neonatal Rat Liver. *React Oxyg species (Apex, NC)* 3(9):218–236.

93. Olea E, et al. (2014) Intermittent hypoxia and diet-induced obesity: effects on oxidative status, sympathetic tone, plasma glucose and insulin levels, and arterial pressure. *J Appl Physiol* 117(7):706–19.

94. Hernández-Guerra M, et al. (2013) Chronic intermittent hypoxia aggravates intrahepatic endothelial dysfunction in cirrhotic rats. *Hepatology* 57(4):1564–1574.

95. Nishiyama Y, et al. (2012) HIF-1α induction suppresses excessive lipid accumulation in alcoholic fatty liver in mice. *J Hepatol* 56(2):441–447.

96. Nath B, et al. (2011) Hepatocyte-specific hypoxia-inducible factor-1α is a determinant of lipid accumulation and liver injury in alcohol-induced steatosis in

mice. *Hepatology* 53(5):1526–1537.

97. Mesarwi OA, et al. (2016) Hepatocyte Hypoxia Inducible Factor-1 Mediates the Development of Liver Fibrosis in a Mouse Model of Nonalcoholic Fatty Liver Disease. *PLoS One* 11(12):e0168572.

98. Buzzetti E, Pinzani M, Tsochatzis EA (2016) The multiple-hit pathogenesis of non-alcoholic fatty liver disease (NAFLD). *Metabolism* 65(8):1038–1048.

99. Yoo W, et al. (2014) HIF-1α expression as a protective strategy of HepG2 cells against fatty acid-induced toxicity. *J Cell Biochem* 115(6):1147–58.

100. Kim WY, et al. (2006) Failure to prolyl hydroxylate hypoxia-inducible factor alpha phenocopies VHL inactivation in vivo. *EMBO J* 25(19):4650–62.

101. Qu A, et al. (2011) Hypoxia-inducible transcription factor 2α promotes steatohepatitis through augmenting lipid accumulation, inflammation, and fibrosis. *Hepatology* 54(2):472–483.

102. Handa P, et al. (2017) Differences in hepatic expression of iron, inflammation and stress-related genes in patients with nonalcoholic steatohepatitis. *Ann Hepatol* 16(1):77–85.

103. Csak T, et al. (2015) microRNA-122 regulates hypoxia-inducible factor-1 and vimentin in hepatocytes and correlates with fibrosis in diet-induced steatohepatitis. *Liver Int* 35(2):532–41.

104. Shen WD, Zhang W, Xu QH, Liu PF (2016) [Effect of targeted inhibition of hypoxia-inducible factor-1α by 3-(5'-hydroxymethyl-2'-furyl)-1-benzylindazole on

the progression of non-alcoholic fatty liver disease in rats]. *Zhonghua Gan Zang Bing Za Zhi* 24(10):749–754.

105. Shin M-K, et al. (2012) Metabolic consequences of high-fat diet are attenuated by suppression of HIF-1α. *PLoS One* 7(10):e46562.

106. Thomas A, et al. (2016) Hypoxia-inducible factor prolyl hydroxylase 1 (PHD1) deficiency promotes hepatic steatosis and liver-specific insulin resistance in mice. *Sci Rep* 6(1):24618.

107. Rahtu-Korpela L, et al. (2014) HIF prolyl 4-hydroxylase-2 inhibition improves glucose and lipid metabolism and protects against obesity and metabolic dysfunction. *Diabetes* 63(10):3324–33.

108. Wei K, et al. (2013) A liver Hif-2α-Irs2 pathway sensitizes hepatic insulin signaling and is modulated by Vegf inhibition. *Nat Med* 19(10):1331–7.

109. Kurabayashi A, et al. (2013) Conditional VHL gene deletion causes hypoglycemic death associated with disproportionately increased glucose uptake by hepatocytes through an upregulated IGF-I receptor. *PLoS One* 8(7):e69139.

110. Park S-K, Haase VH, Johnson RS (2007) von Hippel Lindau tumor suppressor regulates hepatic glucose metabolism by controlling expression of glucose transporter 2 and glucose 6-phosphatase. *Int J Oncol* 30(2):341–8.

111. Dongiovanni P, et al. (2008) Iron depletion by deferoxamine up-regulates glucose uptake and insulin signaling in hepatoma cells and in rat liver. *Am J Pathol* 172(3):738–47.

112. Rahtu-Korpela L, et al. (2014) HIF Prolyl 4-Hydroxylase-2 Inhibition Improves Glucose and Lipid Metabolism and Protects Against Obesity and Metabolic Dysfunction. *Diabetes* 63(10):3324–3333.

113. Morello E, et al. (2017) Hypoxia-inducible factor 2α drives nonalcoholic fatty liver progression by triggering hepatocyte release of histidine rich glycoprotein. *Hepatology*. doi:10.1002/hep.29754.

114. Qu A, et al. (2011) Hypoxia-inducible transcription factor 2α promotes steatohepatitis through augmenting lipid accumulation, inflammation, and fibrosis. *Hepatology* 54(2):472–483.

115. Xie C, et al. (2017) Activation of intestinal hypoxia-inducible factor 2α during obesity contributes to hepatic steatosis. *Nat Med* 23(11):1298–1308.

116. Minamishima YA, et al. (2009) A feedback loop involving the Phd3 prolyl hydroxylase tunes the mammalian hypoxic response in vivo. *Mol Cell Biol* 29(21):5729–41.

117. Scott C, et al. (2015) Hepatocyte- Specific Deletion of ARNT (Aryl Hydrocarbon Receptor Nuclear Translocator) Results in Altered Fibrotic Gene Expression in the Thioacetamide Model of Liver Injury. *PLoS One* 10(3):e0121650.

118. Hang L-W, et al. (2016) The association between continuous positive airway pressure therapy and liver disease development in obstructive sleep apnea/hypopnea syndrome patients: a nationwide population-based cohort study in Taiwan. *Sleep Breath*. doi:10.1007/s11325-016-1439-4.

119. Cakmak E, et al. (2015) Association Between the Severity of Nocturnal Hypoxia in

Obstructive Sleep Apnea and Non-Alcoholic Fatty Liver Damage. *Hepat Mon* 15(11):e32655.

120. Petta S, et al. (2015) Obstructive Sleep Apnea Is Associated with Liver Damage and Atherosclerosis in Patients with Non-Alcoholic Fatty Liver Disease. *PLoS One* 10(12):e0142210.

121. Benotti P, et al. (2016) The impact of obstructive sleep apnea on nonalcoholic fatty liver disease in patients with severe obesity. *Obesity (Silver Spring)* 24(4):871–7.

122. Corey KE, et al. (2015) Obstructive Sleep Apnea Is Associated with Nonalcoholic Steatohepatitis and Advanced Liver Histology. *Dig Dis Sci* 60(8):2523–8.

123. Chen X, et al. (2016) Obstructive sleep apnea is associated with fatty liver index, the index of nonalcoholic fatty liver disease. *Eur J Gastroenterol Hepatol* 28(6):650–5.

124. Qi J-C, et al. (2016) Relationship between obstructive sleep apnea and nonalcoholic fatty liver disease in nonobese adults. *Sleep Breath* 20(2):529–35.

125. Sundaram SS, et al. (2016) Nocturnal hypoxia-induced oxidative stress promotes progression of pediatric non-alcoholic fatty liver disease. *J Hepatol* 65(3):560–9.

126. Musso G, et al. (2013) Association of obstructive sleep apnoea with the presence and severity of non-alcoholic fatty liver disease. A systematic review and meta-analysis. *Obes Rev* 14(5):417–431.

127. Munteanu M, et al. (2008) Noninvasive Biomarkers for the Screening of Fibrosis, Steatosis and Steatohepatitis in Patients with Metabolic Risk Factors: FibroTest-

FibroMax™ Experience. *J Gastrointestin Liver Dis June* 17(2):187–191.

128. Jullian-Desayes I, et al. (2016) Impact of effective versus sham continuous positive airway pressure on liver injury in obstructive sleep apnoea: Data from randomized trials. *Respirology* 21(2):378–85.

129. Chen L-D, et al. (2016) Effect of continuous positive airway pressure on liver enzymes in obstructive sleep apnea: A meta-analysis. *Clin Respir J*. doi:10.1111/crj.12554.

130. Kim D, Ahmed A, Kushida C (2018) Continuous Positive Airway Pressure Therapy on Nonalcoholic Fatty Liver Disease in Patients With Obstructive Sleep Apnea. *J Clin Sleep Med* 14(08):1315–1322.

131. Sundaram SS, et al. (2018) Treating Obstructive Sleep Apnea and Chronic Intermittent Hypoxia Improves the Severity of Nonalcoholic Fatty Liver Disease in Children. *J Pediatr* 198:67–75.e1.

132. Krone N, et al. (2010) Gas chromatography/mass spectrometry (GC/MS) remains a pre-eminent discovery tool in clinical steroid investigations even in the era of fast liquid chromatography tandem mass spectrometry (LC/MS/MS). *J Steroid Biochem Mol Biol* 121(3–5):496–504.

133. Connell JMC, Davies E (2005) The new biology of aldosterone. *J Endocrinol* 186(1):1–20.

134. Vecchiola A, Lagos CF, Carvajal CA, Baudrand R, Fardella CE (2016) Aldosterone Production and Signaling Dysregulation in Obesity. *Curr Hypertens Rep* 18(3):20.

135. Lykouras D, et al. (2015) The impact of obstructive sleep apnea syndrome on renin and aldosterone. *Eur Rev Med Pharmacol Sci* 19(21):4164–70.

136. Svatikova A, et al. (2009) Obstructive sleep apnea and aldosterone. *Sleep* 32(12):1589–92.

137. Jin Z-N, Wei Y-X (2016) Meta-analysis of effects of obstructive sleep apnea on the renin-angiotensin-aldosterone system. *J Geriatr Cardiol* 13(4):333–43.

138. Gonzaga CC, et al. (2010) Severity of obstructive sleep apnea is related to aldosterone status in subjects with resistant hypertension. *J Clin Sleep Med* 6(4):363–8.

139. Di Murro A, et al. (2010) Renin-angiotensin-aldosterone system in patients with sleep apnoea: prevalence of primary aldosteronism. *J Renin Angiotensin Aldosterone Syst* 11(3):165–72.

140. Wolley MJ, et al. (2017) Treatment of primary aldosteronism is associated with a reduction in the severity of obstructive sleep apnoea. *J Hum Hypertens*. doi:10.1038/jhh.2017.28.

141. Deng G, Qiu Z-D, Li D-Y, Fang Y, Zhang S-M (2016) Effects of continuous positive airway pressure therapy on plasma aldosterone levels in patients with obstructive sleep apnea: A meta-analysis. *J Huazhong Univ Sci Technolog Med Sci* 36(5):619–625.

142. Yang S, Jiang X-T, Zhang X-B, Yin X-W, Deng W-X (2016) Does continuous positive airway pressure reduce aldosterone levels in patients with obstructive sleep apnea? *Sleep Breath* 20(3):921–928.

143. de Souza F, et al. (2017) Effects of continuous positive airway pressure treatment on aldosterone excretion in patients with obstructive sleep apnoea and resistant hypertension: a randomized controlled trial. *J Hypertens* 35(4):837–844.

144. Yang L, et al. (2016) Effect of spironolactone on patients with resistant hypertension and obstructive sleep apnea. *Clin Exp Hypertens* 38(5):464–8.

145. Krasińska B, et al. (2016) Effect of eplerenone on the severity of obstructive sleep apnea and arterial stiffness in patients with resistant arterial hypertension. *Pol Arch Med Wewn* 126(5):330–9.

146. Zhang W-D, et al. (2017) Effect of aldosterone antagonists on obstructive sleep apnea in patients with resistant hypertension: a systematic review and meta-analysis. *J Hum Hypertens* 31(12):855–856.

147. Sim JJ, et al. (2011) Positive relationship of sleep apnea to hyperaldosteronism in an ethnically diverse population. *J Hypertens* 29(8):1553–1559.

148. Friedman O, Bradley TD, Chan CT, Parkes R, Logan AG (2010) Relationship Between Overnight Rostral Fluid Shift and Obstructive Sleep Apnea in Drug-Resistant Hypertension. *Hypertension* 56(6):1077–1082.

149. Jenq W, Rabb H, Wahe M, Ramirez G (1996) Hypoxic effects on the expression of mineralocorticoid and glucocorticoid receptors in human renal cortex epithelial cells. *Biochem Biophys Res Commun* 218(2):444–8.

150. Ghiciuc CM, et al. (2016) Imbalance in the diurnal salivary testosterone/cortisol ratio in men with severe obstructive sleep apnea: an observational study. *Braz J Otorhinolaryngol* 82(5):529–35.

151. Luboshitzky R, Lavie L, Shen-Orr Z, Herer P (2005) Altered Luteinizing Hormone and Testosterone Secretion in Middle-Aged Obese Men with Obstructive Sleep Apnea. *Obes Res* 13(4):780–786.

152. Luboshitzky R, et al. (2002) Decreased pituitary-gonadal secretion in men with obstructive sleep apnea. *J Clin Endocrinol Metab* 87(7):3394–8.

153. Gambineri A, Pelusi C, Pasquali R (2003) Testosterone levels in obese male patients with obstructive sleep apnea syndrome: Relation to oxygen desaturation, body weight, fat distribution and the metabolic parameters. *J Endocrinol Invest* 26(6):493–498.

154. Barrett-Connor E, et al. (2008) The Association of Testosterone Levels with Overall Sleep Quality, Sleep Architecture, and Sleep-Disordered Breathing. *J Clin Endocrinol Metab* 93(7):2602–2609.

155. Zhang X-B, et al. (2016) Erectile Dysfunction and Sexual Hormone Levels in Men With Obstructive Sleep Apnea: Efficacy of Continuous Positive Airway Pressure. *Arch Sex Behav* 45(1):235–40.

156. Zhang X-B, Jiang X-T, Du Y-P, Yuan Y-T, Chen B (2014) Efficacy of continuous positive airway pressure on testosterone in men with obstructive sleep apnea: a meta-analysis. *PLoS One* 9(12):e115033.

157. Knapp A, et al. (2014) Effect of continuous positive airway pressure therapy on sexual function and serum testosterone in males with type 2 diabetes and obstructive sleep apnoea. *Clin Endocrinol (Oxf)* 81(2):254–8.

158. Hoyos CM, Killick R, Yee BJ, Grunstein RR, Liu PY (2012) Effects of testosterone

therapy on sleep and breathing in obese men with severe obstructive sleep apnoea: a randomized placebo-controlled trial. *Clin Endocrinol (Oxf)* 77(4):599–607.

159. Killick R, et al. (2013) The effects of testosterone on ventilatory responses in men with obstructive sleep apnea: a randomised, placebo-controlled trial. *J Sleep Res* 22(3):331–6.

160. Cole AP, et al. (2018) Impact of testosterone replacement therapy on thromboembolism, heart disease and obstructive sleep apnoea in men. *BJU Int* 121(5):811–818.

161. Melehan KL, et al. (2016) Increased sexual desire with exogenous testosterone administration in men with obstructive sleep apnea: a randomized placebo-controlled study. *Andrology* 4(1):55–61.

162. Liu PY, et al. (2003) The Short-Term Effects of High-Dose Testosterone on Sleep, Breathing, and Function in Older Men. *J Clin Endocrinol Metab* 88(8):3605–3613.

163. Hazlehurst JM, et al. (2013) Glucocorticoids fail to cause insulin resistance in human subcutaneous adipose tissue in vivo. *J Clin Endocrinol Metab* 98(4):1631–40.

164. Gathercole LL, et al. (2011) Regulation of lipogenesis by glucocorticoids and insulin in human adipose tissue. *PLoS One* 6(10):e26223.

165. Woods CP, Hazlehurst JM, Tomlinson JW (2015) Glucocorticoids and non-alcoholic fatty liver disease. *J Steroid Biochem Mol Biol* 154:94–103.

166. Morgan SA, et al. (2014) 11β-HSD1 is the major regulator of the tissue-specific

effects of circulating glucocorticoid excess. *Proc Natl Acad Sci U S A* 111(24):E2482-91.

167. Mendoza-Figueroa T, Hernandez A, De Lourdes Lopez M, Kuri-Harcuch W (1988) Intracytoplasmic triglyceride accumulation produced by dexamethasone in adult rat hepatocytes cultivated on 3T3 cells. *Toxicology* 52(3):273–86.

168. Amatruda JM, Danahy SA, Chang CL (1983) The effects of glucocorticoids on insulin-stimulated lipogenesis in primary cultures of rat hepatocytes. *Biochem J* 212(1):135–41.

169. Mueller KM, et al. (2012) Hepatic growth hormone and glucocorticoid receptor signaling in body growth, steatosis and metabolic liver cancer development. *Mol Cell Endocrinol* 361(1–2):1–11.

170. Lettéron P, et al. (1997) Glucocorticoids inhibit mitochondrial matrix acyl-CoA dehydrogenases and fatty acid beta-oxidation. *Am J Physiol* 272(5 Pt 1):G1141-50.

171. Berthiaume M, et al. (2007) Depot-specific modulation of rat intraabdominal adipose tissue lipid metabolism by pharmacological inhibition of 11beta-hydroxysteroid dehydrogenase type 1. *Endocrinology* 148(5):2391–7.

172. Bozic J, et al. (2016) Morning cortisol levels and glucose metabolism parameters in moderate and severe obstructive sleep apnea patients. *Endocrine* 53(3):730–739.

173. Kritikou I, et al. (2016) Sleep apnoea and the hypothalamic-pituitary-adrenal axis in men and women: effects of continuous positive airway pressure. *Eur Respir J* 47(2):531–40.

174. Raff H, Ettema SL, Eastwood DC, Woodson BT (2011) Salivary cortisol in obstructive sleep apnea: the effect of CPAP. *Endocrine* 40(1):137–9.

175. Henley DE, et al. (2009) Hypothalamic-pituitary-adrenal axis activation in obstructive sleep apnea: the effect of continuous positive airway pressure therapy. *J Clin Endocrinol Metab* 94(11):4234–42.

176. Schmoller A, et al. (2009) Continuous positive airway pressure therapy decreases evening cortisol concentrations in patients with severe obstructive sleep apnea. *Metabolism* 58(6):848–53.

177. Patacchioli FR, et al. (2014) Salivary biomarkers of obstructive sleep apnea syndrome in children. *Pediatr Pulmonol* 49(11):1145–52.

178. Karaca Z, et al. (2013) Obstructive sleep apnoea syndrome is associated with relative hypocortisolemia and decreased hypothalamo-pituitary-adrenal axis response to 1 and 250μg ACTH and glucagon stimulation tests. *Sleep Med* 14(2):160–4.

179. Tomfohr LM, Edwards KM, Dimsdale JE (2012) Is obstructive sleep apnea associated with cortisol levels? A systematic review of the research evidence. *Sleep Med Rev* 16(3):243–9.

180. Hwang G-S, et al. (2017) Stimulatory Effect of Intermittent Hypoxia on the Production of Corticosterone by Zona Fasciculata-Reticularis Cells in Rats. *Sci Rep* 7(1):9035.

181. Wang L-U, et al. (2017) Risk of obstructive sleep apnea among patients with Cushing's syndrome: a nationwide longitudinal study. *Sleep Med* 36:44–47.

182. Gokosmanog˘lu F, Güzel A, Kan EK, Atmaca H (2017) Increased prevalence of obstructive sleep apnea in patients with Cushing's syndrome compared with weight- and age-matched controls. *Eur J Endocrinol* 176(3):267–272.

183. Tamada D, et al. (2013) Obstructive sleep apnea syndrome causes a pseudo-Cushing's state in Japanese obese patients with type 2 diabetes mellitus. *Endocr J* 60(12):1289–94.

184. Carneiro G, et al. (2008) Effect of continuous positive airway pressure therapy on hypothalamic-pituitary-adrenal axis function and 24-h blood pressure profile in obese men with obstructive sleep apnea syndrome. *Am J Physiol Endocrinol Metab* 295(2):E380-4.

185. Grunstein RR, et al. (1996) Acute withdrawal of nasal CPAP in obstructive sleep apnea does not cause a rise in stress hormones. *Sleep* 19(10):774–82.

186. Kamiya Y, et al. (2003) Modulation by steroid receptor coactivator-1 of target-tissue responsiveness in resistance to thyroid hormone. *Endocrinology* 144(9):4144–53.

187. Michailidou Z, et al. (2012) Increased angiogenesis protects against adipose hypoxia and fibrosis in metabolic disease-resistant 11β-hydroxysteroid dehydrogenase type 1 (HSD1)-deficient mice. *J Biol Chem* 287(6):4188–97.

188. Klusonová P, et al. (2009) Chronic intermittent hypoxia induces 11beta-hydroxysteroid dehydrogenase in rat heart. *Endocrinology* 150(9):4270–7.

189. Leonard MO, Godson C, Brady HR, Taylor CT (2005) Potentiation of glucocorticoid activity in hypoxia through induction of the glucocorticoid receptor.

J Immunol 174(4):2250–7.

190. Macfarlane DP, et al. (2014) Effects of acute glucocorticoid blockade on metabolic dysfunction in patients with Type 2 diabetes with and without fatty liver. *Am J Physiol Gastrointest Liver Physiol* 307(7):G760-8.

191. Page ST, et al. (2012) Impact of mifepristone, a glucocorticoid/progesterone antagonist, on HDL cholesterol, HDL particle concentration, and HDL function. *J Clin Endocrinol Metab* 97(5):1598–605.

192. Gross C, et al. (2009) Mifepristone treatment of olanzapine-induced weight gain in healthy men. *Adv Ther* 26(10):959–69.

193. Gross C, Blasey CM, Roe RL, Belanoff JK (2010) Mifepristone reduces weight gain and improves metabolic abnormalities associated with risperidone treatment in normal men. *Obesity (Silver Spring)* 18(12):2295–300.

194. Wang B, Wood IS, Trayhurn P (2008) Hypoxia induces leptin gene expression and secretion in human preadipocytes: differential effects of hypoxia on adipokine expression by preadipocytes. *J Endocrinol* 198(1):127–134.

195. Pramfalk C, et al. (2016) Fasting Plasma Insulin Concentrations Are Associated With Changes in Hepatic Fatty Acid Synthesis and Partitioning Prior to Changes in Liver Fat Content in Healthy Adults. *Diabetes* 65(7):1858–1867.

196. Steele R, Wall JS, de Bodo RC, Altszuler N (1956) Measurement of Size and Turnover Rate of Body Glucose Pool by the Isotope Dilution Method. *Am J Physiol Content* 187(1):15–24.

197. Chong MF-F, Fielding BA, Frayn KN (2007) Mechanisms for the acute effect of fructose on postprandial lipemia. *Am J Clin Nutr* 85(6):1511–1520.

198. Elia M, Livesey G (1992) Energy expenditure and fuel selection in biological systems: the theory and practice of calculations based on indirect calorimetry and tracer methods. *World Rev Nutr Diet* 70:68–131.

199. Armstrong MJ, et al. (2014) Abdominal subcutaneous adipose tissue insulin resistance and lipolysis in patients with non-alcoholic steatohepatitis. *Diabetes Obes Metab* 16(7):651–60.

200. Turnbull CD, et al. (2017) Effect of OSA on hypoxic and inflammatory markers during CPAP withdrawal: Further evidence from three randomized control trials. *Respirology* 22(4):793–799.

201. Kohler M, et al. (2011) Effects of Continuous Positive Airway Pressure Therapy Withdrawal in Patients with Obstructive Sleep Apnea. *Am J Respir Crit Care Med* 184(10):1192–1199.

202. Shackleton CHL, Marcos J (2011) GC/MS steroid profiling. *The Encyclopedia of Mass Spectrometry.*, eds Gross M, Caprioli R (Elsevier), pp 789–813. Vol 8 Amst.

203. Schwarz EI, Stradling JR, Kohler M (2018) Physiological consequences of CPAP therapy withdrawal in patients with obstructive sleep apnoea-an opportunity for an efficient experimental model. *J Thorac Dis* 10(Suppl 1):S24–S32.

204. Stradling JR, et al. (2015) Biomarkers of oxidative stress following continuous positive airway pressure withdrawal: data from two randomised trials. *Eur Respir J* 46(4):1065–71.

205. Ekstedt M, Åkerstedt T, Söderström M (2004) Microarousals During Sleep Are Associated With Increased Levels of Lipids, Cortisol, and Blood Pressure. *Psychosom Med* 66(6):925–931.

206. Ahmed A, et al. (2012) A switch in hepatic cortisol metabolism across the spectrum of non alcoholic fatty liver disease. *PLoS One* 7(2):e29531.

207. Crowley RK, et al. (2014) Longitudinal changes in glucocorticoid metabolism are associated with later development of adverse metabolic phenotype. *Eur J Endocrinol* 171(4):433–42.

208. Schwarz EI, Schlatzer C, Rossi VA, Stradling JR, Kohler M (2016) Effect of CPAP Withdrawal on BP in OSA: Data from Three Randomized Controlled Trials. *Chest* 150(6):1202–1210.

209. Song S-Y, Chung H-M, Sung J-H (2010) The pivotal role of VEGF in adipose-derived-stem-cell-mediated regeneration. *Expert Opin Biol Ther* 10(11):1529–1537.

210. Reinke C, Bevans-Fonti S, Drager LF, Shin M-K, Polotsky VY (2011) Effects of different acute hypoxic regimens on tissue oxygen profiles and metabolic outcomes. *J Appl Physiol* 111(3):881–890.

211. Liu C, et al. (2005) Dual-specificity phosphatase DUSP1 protects overactivation of hypoxia-inducible factor 1 through inactivating ERK MAPK. *Exp Cell Res* 309(2):410–418.

212. Park HS, et al. (2016) Hypoxia induces glucose uptake and metabolism of adipose-derived stem cells. *Mol Med Rep* 14(5):4706–4714.

213. Arnaldi G, et al. (2003) Diagnosis and Complications of Cushing's Syndrome: A Consensus Statement. *J Clin Endocrinol Metab* 88(12):5593–5602.

214. Wei L, MacDonald TM, Walker BR (2004) Taking glucocorticoids by prescription is associated with subsequent cardiovascular disease. *Ann Intern Med* 141(10):764–70.

215. Colao A, et al. (1999) Persistence of Increased Cardiovascular Risk in Patients with Cushing's Disease after Five Years of Successful Cure. *J Clin Endocrinol Metab* 84(8):2664–2672.

216. Fleseriu M, et al. (2012) Mifepristone, a glucocorticoid receptor antagonist, produces clinical and metabolic benefits in patients with Cushing's syndrome. *J Clin Endocrinol Metab* 97(6):2039–49.

217. Levy JC, Matthews DR, Hermans MP (1998) Correct homeostasis model assessment (HOMA) evaluation uses the computer program. *Diabetes Care* 21(12):2191–2.

218. Bell LN, et al. (2012) Relationship between adipose tissue insulin resistance and liver histology in nonalcoholic steatohepatitis: a pioglitazone versus vitamin E versus placebo for the treatment of nondiabetic patients with nonalcoholic steatohepatitis trial follow-up study. *Hepatology* 56(4):1311–8.

219. Bose SK, Hutson I, Harris CA (2016) Hepatic Glucocorticoid Receptor Plays a Greater Role Than Adipose GR in Metabolic Syndrome Despite Renal Compensation. *Endocrinology* 157(12):4943–4960.

220. Mueller KM, et al. (2011) Impairment of hepatic growth hormone and

glucocorticoid receptor signaling causes steatosis and hepatocellular carcinoma in mice. *Hepatology* 54(4):1398–409.

221. Lemke U, et al. (2008) The glucocorticoid receptor controls hepatic dyslipidemia through Hes1. *Cell Metab* 8(3):212–23.

222. Xu C, et al. (2009) Direct effect of glucocorticoids on lipolysis in adipocytes. *Mol Endocrinol* 23(8):1161–70.

223. Zinker B, et al. (2007) Liver-selective glucocorticoid receptor antagonism decreases glucose production and increases glucose disposal, ameliorating insulin resistance. *Metabolism* 56(3):380–7.

224. Taylor AI, Frizzell N, McKillop AM, Flatt PR, Gault VA (2009) Effect of RU486 on hepatic and adipocyte gene expression improves diabetes control in obesity-type 2 diabetes. *Horm Metab Res = Horm und Stoffwechselforsch = Horm métabolisme* 41(12):899–904.

225. Yu S, et al. (2015) Systems pharmacology of mifepristone (RU486) reveals its 47 hub targets and network: Comprehensive analysis and pharmacological focus on FAK-Src-Paxillin complex. *Sci Rep* 5(1):7830.

226. Turnbull CD, Sen D, Kohler M, Petousi N, Stradling JR (2018) Effect of Supplemental Oxygen on Blood Pressure in Obstructive Sleep Apnea (SOX): A Randomised, CPAP Withdrawal Trial. *Am J Respir Crit Care Med*:rccm.201802-0240OC.

227. Muraki I, et al. (2010) Nocturnal intermittent hypoxia and the development of type 2 diabetes: the Circulatory Risk in Communities Study (CIRCS). *Diabetologia*

53(3):481–488.

228. Appleton SL, et al. (2016) The association of obstructive sleep apnea (OSA) and nocturnal hypoxemia with the development of abnormal HbA1c in a population cohort of men without diabetes. *Diabetes Res Clin Pract* 114:151–9.

229. Lewis EF, et al. (2017) Impact of continuous positive airway pressure and oxygen on health status in patients with coronary heart disease, cardiovascular risk factors, and obstructive sleep apnea: A Heart Biomarker Evaluation in Apnea Treatment (HEARTBEAT) analysis. *Am Heart J* 189:59–67.

230. Newhouse LP, et al. (2017) Three hours of intermittent hypoxia increases circulating glucose levels in healthy adults. *Physiol Rep* 5(1):e13106.

231. Steele R (1959) Influences of glucose loading and of injected insulin on hepatic glucose output. *Ann N Y Acad Sci* 82:420–30.

232. Choi SH, Ginsberg HN (2011) Increased very low density lipoprotein (VLDL) secretion, hepatic steatosis, and insulin resistance. *Trends Endocrinol Metab* 22(9):353–63.

233. Donnelly KL, et al. (2005) Sources of fatty acids stored in liver and secreted via lipoproteins in patients with nonalcoholic fatty liver disease. *J Clin Invest* 115(5):1343–51.

234. Nasiri M, et al. (2015) 5α-Reductase Type 2 Regulates Glucocorticoid Action and Metabolic Phenotype in Human Hepatocytes. *Endocrinology* 156(8):2863–71.

235. Rask E, Simonyte K, Lönn L, Axelson M (2013) Cortisol metabolism after weight

loss: associations with 11 β-HSD type 1 and markers of obesity in women. *Clin Endocrinol (Oxf)* 78(5):700–5.

236. Yuan X, et al. (2016) The 11β-hydroxysteroid dehydrogenase type 1 inhibitor protects against the insulin resistance and hepatic steatosis in db/db mice. *Eur J Pharmacol* 788:140–151.

237. Morgan SA, et al. (2014) 11 -HSD1 is the major regulator of the tissue-specific effects of circulating glucocorticoid excess. *Proc Natl Acad Sci* 111(24):E2482–E2491.

238. Larner DP, et al. (2016) Male 11β-HSD1 Knockout Mice Fed Trans-Fats and Fructose Are Not Protected From Metabolic Syndrome or Nonalcoholic Fatty Liver Disease. *Endocrinology* 157(9):3493–3504.

239. Cusi K (2009) Role of insulin resistance and lipotoxicity in non-alcoholic steatohepatitis. *Clin Liver Dis* 13(4):545–63.